UCL
Université
catholique
de Louvain

Mobilisation of lipophilic pollutants from adipose tissue during periods of lipolysis by *in vitro* and *in vivo* approaches

Thèse présentée par **Caroline Louis** en vue de l'obtention
du grade de docteur en sciences agronomiques et ingénierie biologique

Promoteur :	Pr Cathy Debier
Membres du jury :	Pr Adrian Covaci Pr Yvan Larondelle Pr Claude Remacle Pr Jean-Pierre Thomé
Président du jury :	Pr Yves-Jacques Schneider

Acknowledgments

Nous y voilà! La fin d'une longue et belle aventure. Beaucoup de souvenirs, de rencontres et de découvertes. Par ces quelques lignes, je tiens à remercier toutes les personnes qui m'ont permis d'atteindre cet objectif. C'est grâce à vous si j'y suis arrivée !

Tout d'abord, merci à ma promotrice, Cathy Debier, qui m'a offert un sujet de mémoire qui m'a rapidement passionnée. Tu m'as ensuite permis de continuer mes recherches sur les PCBs et les adipocytes durant ce doctorat. Merci pour ta disponibilité et tes paroles toujours motivantes. Grâce à toi, j'ai aussi eu la chance de voyager et de travailler dans d'autres labos. Ce sont des expériences scientifiques et humaines inoubliables ! Un merci tout particulier pour m'avoir permis de vivre quelques mois aux US. Finalement, une excellente façon de joindre l'utile à l'agréable... *I think that I am falling in love with SC.*

Je remercie également Yvan Larondelle pour son regard critique et lucide sur mes expériences. Tu as toujours été de bon conseil pour moi. Mes remerciements vont également à Yves-Jacques Schneider, Claude Remacle, Adrian Covaci et Jean-Pierre Thomé avec qui j'ai eu la chance de travailler. Merci de m'avoir accueillie dans vos laboratoires, de m'avoir appris les techniques de la culture cellulaire et l'analyse des polluants organiques. Je vous remercie également de m'avoir fait l'honneur de participer à mon jury de thèse et d'avoir contribué à l'amélioration de ce travail. Je tiens également à remercier nos collaborateurs américains, Dan Crocker, Don Smith et Dan Costa, pour m'avoir ouvert les portes de leur labo. J'ai découvert avec vous la joie et les exigences des missions de terrain.

En écrivant ces lignes, je pense aussi à mes mémorants, Stéphanie, Marie, Stéphanie, Gilles et Laurent. Du fond du cœur, merci à tous pour votre contribution à ce travail. Même si tout ne s'est pas déroulé comme on l'avait prévu, avec un peu de persévérance et beaucoup de bonne humeur, on a réussi à produire de chouettes résultats. Vous pouvez être fières !

Je tiens également à remercier toute l'équipe de BNTE, ce cher labo *so girly*, dans lequel il fait bon travailler. Merci pour votre soutien et les bons moments passés ensemble ! Faites perdurer l'ouverture de banane Louis© ☺. Un merci tout particulier à ma chère Sophie, qui m'a mis le pied à l'étrier, m'a transmis sa passion de la recherche et m'a motivée lors de mes débuts un peu difficiles. Un tout grand merci aussi à Carine qui m'a aidée dans la mise au point de la lipolyse et avec qui je partage l'amour des voyages. C'était vraiment très chouette de bosser avec toi ! Merci Eric d'avoir tant travailler sur la mise au point du dosage des PCBs dans notre labo. On est passé par toutes les couleurs avec ce GC/MS ! Un clin d'œil un peu spécial à Stéphanie (vive le vin!). Merci d'avoir (re)décoré mon mur. Grâce à toi, j'ai beaucoup appris sur les croisements des BBB. Je garderai longtemps le souvenir de ta chaise qui vient s'écraser contre mon bureau. Ineke, merci de m'avoir soutenue et écoutée pendant ces quelques mois de rédaction de thèse. Tu es un sacré petit bout de femme ! Vous avez tous été des collègues exceptionnels.

Merci à Marie-Thérèse, André, Daniel, Willy, Coralie et Philippe de l'ISV pour leur soutien technique. Je voudrais également remercier les différentes équipes avec lesquelles j'ai eu le plaisir de travailler en dehors de notre institut : le Laboratoire d'écologie animale et d'écotoxicologie de l'ULg, le Department of Pharmaceutical Sciences de l'Universiteit Antwerpen, le Service d'Anatomie Pathologique de l'UCL-Woluwé et le Earth and Life Institut de l'UCL. Avec un merci tout particulier à Murielle et Arnaud de l'ULg, Alin et Malar de l'Universiteit Antwerpen, Yves Guiot et Rose-Marie de l'UCL-Woluwé et Céline et Stéphanie de l'UCL (les filles, merci aussi pour le papotage !).

Mes séjours en Californie n'auraient pas été aussi enrichissants sans ces chouettes rencontres. Merci à Sarah pour notre inoubliable colocation durant mon premier séjour. Merci à Brett et Jen, sans oublié Kona. Vous avez égaillez mon second séjour et m'avez appris à fabriquer de la bière. Un comble pour une petite Belge ! Un énorme merci à Kenneth, Susan et la petite Maggy. Votre philosophie de vie m'a énormément apporté. Comme Susan a l'habitude de dire : « Great ! ». Merci à toute l'équipe de METX-UCSC et plus spécialement à David pour tes conseils en culture cellulaire et

ton dynamisme, à Walter pour ton grand sourire et ton célèbre « Walter can fly, Sarah can walk, Caro can drive », à Will (alias Reagent Man) et à Miles (alias Kilometers) pour leur disponibilité et bien plus encore. Quelle belle aventure ! Merci aussi à toute l'équipe d'Año Nuevo : Betsy, Segal, Cory, Melinda, Luis, Josh, Sarah et Jeff. Un énorme merci à Mike-Sugar et Stephen. Vous êtes uniques. Passionnés par votre travail, vous avez tout donné pour que mes missions soient couronnées de succès. Je vous dois énormément !

Je voudrais remercier la « vieille » équipe de l'Activ (Pauline, Julie, Bertrand, Mathieu et Didier), de même que la fine équipe des Nutris (Virg, Véro, Alex, Lou et Kevin). Mon doctorat a pris une couleur plus agréable et plus festive grâce à vous. C'était top !

Un énorme MERCI à mes parents et à ma petite Sabi. Même si vous n'avez pas toujours compris ce qui occupait mes journées, merci de m'avoir poussée jusque-là et d'y avoir cru, avec moi (« tu sais, on ... » : vous connaissez la suite !). Bien évidemment, une petite pensée pour les tables de conjugaison ☺.

Enfin, MERCI à Guillaume d'avoir été présent et patient, d'une incroyable patience. Merci pour tes précieux conseils, en informatique le plus souvent. Eps, drive, CMU Serif, crop et crop-crop, mais quel charabia. Tu as assuré ! Et pourquoi ? Parce qu'on est quand même des sacrés L !

Summary

Since several decades, a specific attention has been focused on a class of molecules called persistent organic pollutants (POPs). All of them present a lipophilic character, they resist to degradation and they can be transported far away from the production sites, contaminating biota until remote locations. Highly toxic for humans and wildlife, they biomagnify through the food chain. The adipose tissue is the main reservoir of POPs. However, it can become a source of POPs through their release into the circulation during periods of negative energy balance. To date, little is known regarding the factors that govern the mobilisation of POPs from adipose tissue.

The present study aimed at investigating the toxicokinetics of POPs during periods of adipose tissue lipolysis through *in vivo* and *in vitro* approaches. The selected *in vivo* model was the weaned northern elephant seal (NES) pup. Concentrations of POPs increased within blubber over the NES fast, despite a mobilisation into the circulation. The rise was more pronounced in the inner blubber layer compared to the outer blubber layer, which suggests a more efficient release of lipids than POPs, especially from the inner layer. The POP release mainly depended on their degree of lipophilicity. The retention of the more lipophilic POPs and the discharge of the less lipophilic POPs were highlighted. This selective mobilisation might be linked to the one of fatty acids (FAs), which was also in favour of the less lipophilic FAs, leading to an enrichment of adipocytes with more lipophilic FAs at late fast. Concurrently to the *in vivo* study, we set up an efficient *in vitro* lipolytic model of primary cell cultures of differentiated rat adipocytes by using isoproterenol, a well-known catecholamine, and a regular renewal of the lipolytic culture medium. We used this model to follow the mobilisation of three POPs (PCB-28, -118 and -153), which differed by their lipophilicity and bulk. The results showed that PCB-153, the more lipophilic and bulky POP, was preferentially retained within adipocytes, confirming the *in vivo* data. This work brings additional information regarding the parameters that govern the dynamics of POPs released from the adipose tissue and points out the complementarity of the *in vivo* and *in vitro* models in such research.

List of abbreviations

ABHD5	Alpha/beta-hydrolase domain-containing protein 5
AC	Adenylate cyclase
ACBP	Acyl-CoA binding protein
ACS	Acyl-CoA synthase
ADD1	Adipocyte determination and differentiation factor-1
AhR	Aryl hydrocarbon receptor
ANP	Atrial natriuretic peptide
aP2	Adipocyte fatty acid binding protein
AQP	Aquaporin
ARNt	Aryl hydrocarbon receptor nuclear translocator
ATGL	Adipose triglyceride lipase
BAT	Brown adipose tissue
BFR	Brominated flame retardant
bHLH	Basic helix-loop-helix
BMI	Body mass index
BNP	Brain natriuretic peptide
BSA	Bovine serum albumin
C/EBP	CCAAT/enhancer binding protein
cAMP	Cyclic adenosine monophosphate
CAR	Constitutive androstan receptor
CD36	Cluster of differentiation 36
CGI58	Comparative gene identification-58
cGMP	Guanosine 3',5'-cyclic monophosphate
CYP	Cytochrome P450 enzyme
DDA	2,2-*bis*(*p*-chlorophenyl) acetic acid
DDD	Dichlorodiphenyldichloroethane
DDE	Dichlorodiphenyldichloroethylene
DDT	Dichlorodiphenyltrichloroethane
DG	Diglyceride
DHAP	Dihydroxyacetone phosphate
DNA	Deoxyribonucleic acid
DRE	Dioxin response element
EDTA	Ethylenediaminetetraacetic acid
EPA	Environmental protection agency
FA	Fatty acid
FABP	Fatty acid binding protein

FA-CoA	Fatty acid-CoA
FAME	Fatty acid methyl ester
FAS	Fatty acid synthase
FAT	Fatty acid translocase
FATP	Fatty acid transport protein
FBS	Foetal bovine serum
FM	Fractional mobilisation
G3P	Glycerol-3-phosphate
GC	Guanylyl cyclase
G_i	Inhibitory GTP-binding protein
GLUT	Glucose transporter
G_s	Stimulatory GTP-binding protein
GST	Glutathione-S-transferase
GTP	Guanosine triphosphate
Gyk	Glycerol kinase
HBCD	Hexabromocyclododecane
HCB	Hexachlorobenzene
HCH	Hexachlorocyclohexane
HSL	Hormone sensitive lipase
Hsp90	Heat shock protein 90
IBMX	3-Isobutyl-1-methylxanthine
IL-6	Interleukin-6
IR	Insulin receptor
IRS1	Insulin receptor substrate 1
Iso	Isoproterenol
LC-MUFA	Long-chain monounsatured fatty acid
LD	Lipid droplet
LDH	Lactate dehydrogenase
LM	Lipolytic medium
LOQ	Limit of quantification
LPL	Lipoprotein lipase
M	Gene-stability value
MAP	Mitogen activated protein
MC-MUFA	Medium-chain monounsaturated fatty acid
MeO-PBDE	Methoxylated polybrominated diphenyl ether
$MeSO_2$ -	Methylsulfone metabolite
MG	Monoglyceride
MGL	Monoglyceride lipase
MUFA	Monounsatured fatty acid

NES	Northern elephant seal
NL	Neutral lipid
NPR-A	Natriuretic peptide receptor-A
NRQ	Normalised relative quantity
OCP	Organochlorine pesticide
ORO	Oil Red O
PBDE	Polybrominated diphenyl ether
PBS	Phosphate buffered saline
PCB	Polychlorinated biphenyl
PCP	Pentachlorophenol
PDE	Phosphodiesterase
PEPCK	Phosphoenolpyruvate carboxykinase
PI3K	Phosphatidylinositol-3-kinase
PKA	Protein kinase A
PKG	Protein kinase G
POP	Persistent organic pollutant
PPAR	Peroxisome proliferator-activated receptor
PPRE	PPARγ response element
PUFA	Polyunsaturated fatty acid
PXR	Pregnane X receptor
RPL8	Ribosomal protein L8
RXR	Retinoid X receptor
SDHA	Succinate dehydrogenase complex subunit A
SEM	Standard error of the mean
SFA	Saturated fatty acid
SREBP-1c	Sterol regulatory element binding protein 1c
SULT	Sulfotransferase
T_4	Thyroxine
TBBP-A	Tetrabromobisphenol-A
TCDD	2,6,7,8-tetrachlorinated dibenzo-*p*-dioxin
TEF	Toxic equivalency factor
TG	Triglyceride
TNFR-1	Tumor necrosis factor receptor 1
TNF-α	Tumor necrosis factor α
TTR	Transthyretin
TZD	Thiazolidinedione
UGT	Uridine 5'-diphospho-glucuronosyltransferase
VLDL	Very low-density protein
WAT	White adipose tissue

Table of content

Chapter 1

Introduction

1.1. The adipose tissue

1.1.1. Generalities

The adipose tissue is a loose connective tissue that develops in humans and animals. This tissue is classified in two types according to its colour, the white adipose tissue (WAT) and the brown adipose tissue (BAT). WAT and BAT also differ from each other by their localisation, structure and roles (Cinti, 2006). In this chapter, we will essentially describe the histology of WAT and its functions during situations of positive and negative energy balance.

In addition to its roles of isolation and mechanical support, the WAT is specialised in the storage of energetic surplus in the form of triglycerides (TGs) in periods of positive energy balance. Lipid reserves may then be released to comply with the energy requirements (Sethi and Vidal-Puig, 2007). Although the WAT was considered as an inert tissue, studies from the last decade evidence that WAT possesses an active secretory system, whose the function is to release various proteins, which are referred to as adipokines (Harwood Jr, 2012). These adipokines act as endocrine and paracrine factors on neighbouring adipocytes and other cell types contained in the WAT but also on central and peripheral organs such as liver, skeletal muscles, brain and pancreas. Adipokines thus control the energy metabolism of the overall organism through diverse metabolic processes (e.g. feeding behaviour, lipid metabolism, blood pressure and inflammation) (Harwood Jr, 2012). Adipokines are produced either by the adipocytes (e.g. leptin and

adiponectin) or macrophages (e.g. tumor necrosis factor α (TNF-α) and interleukin-6 (IL-6)) (Fonseca-Alaniz et al., 2007). The secretions of many adipokines are subject to variations according to the fat distribution, the fat mass and the physiological status of the individual (Dusserre et al., 2000; Lafontan and Berlan, 2003; Skurk et al., 2007).

In humans, the WAT is one of the largest tissues. It represents 9 – 18 % of body weight in males and 14 – 28% of body weight in females, with a normal body mass index (BMI) (i.e. BMI range: 18.5 – 25 kg/m^2). The fat mass can range from 60 to 70% of body weight in massively obese individuals (i.e. BMI $>$ 35 kg/m^2) (Hausman et al., 2001). Its distribution varies according to sex and age (Foufelle and Ferre, 2013). The main fat deposits are the subcutaneous (i.e. in the femerogluteal regions and in the back and anterior abdominal wall) and visceral (i.e. in the mesentery and omentum) areas. About 80% of all fat are in the subcutaneous area (Ibrahim, 2010; Wajchenberg, 2000). The two deposits show some different characteristics in terms of anatomy, cellularity and physiology. The visceral WAT is characterised by a greater number of large adipocytes, which are widely innervated and vascularised compared to subcutaneous WAT. The secretory and metabolic activities as well as the expression of developmental genes also vary according to the fat distribution. The visceral WAT is more metabolically active and shows a higher expression level of some receptors (Gesta et al., 2006; Giorgino et al., 2005; Ibrahim, 2010).

The WAT is organised into lobules mainly formed by adipocytes, which are surrounded by a connective tissue matrix such as collagen fibres (Figure 1.1) (Tordjman, 2013). The non-fat cell fraction of WAT is composed by endothelial cells, fibroblasts, preadipocytes, macrophages, mast cells, etc. and is called the stromal-vascular fraction (Ibrahim, 2010; Tordjman, 2013). These cells play different roles in the adipose tissue such as the endothelial cells that provide the vascularisation of the tissue or the macrophages that are able to clear the necrotic adipocytes (Harwood Jr, 2012).

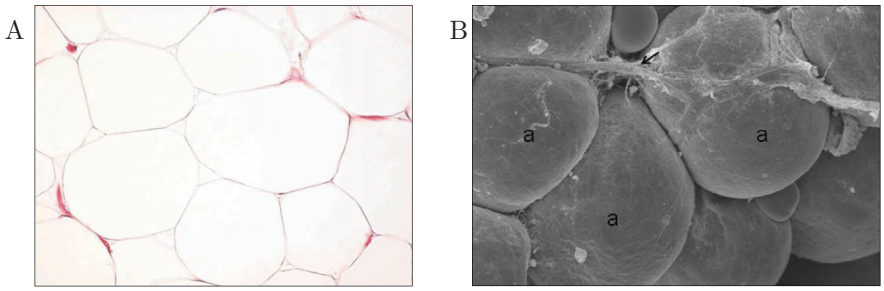

Figure 1.1 – Human subcutaneous white adipose tissue made up of adipocytes. A. light microscopy 550x (Cinti, 2006) and B. scanning electron microscopy (Sbarbati et al., 2010).

Mature adipocytes are specialised in the storage and the mobilisation of TGs within the WAT. During their development, young adipocytes contain multiple small lipid droplets (LDs) that accumulate TGs and merge then together. The morphological aspect of mature adipocytes consists of spherical cells whose more than 90% of volume are occupied by a unique LD surrounded by a thin rim of cytoplasm. The nucleus is rejected at the periphery of the cell (Cinti, 2006). Cells are thus called "unilocular". The diameter of the LD may vary from 10 to 150 µm and the one of mature adipocyte from 30 to 160 µm (Cinti, 2007, 2012). The LD is a dynamic organelle with a lipophilic core formed by TGs and cholesterol esters and surrounded by a monolayer of phospholipids, which is coated by several proteins such as perilipin, involved in the control of the size of LDs (Ahmadian et al., 2010; Bartz et al., 2007; Tordjman, 2013; Walther and Farese Jr, 2012).

1.1.2. Adipogenesis

During the embryonic development of adipose tissue, the fate of pluripotent precursor stem cells is limited to multipotent mesenchymal stem cells by mechanisms that are still unknown. These cells of mesodermal origin have the capacity to differentiate into adipocytes, chondroblasts, osteoblasts, fibroblasts or myoblasts (Avram et al., 2007; Feve and Mercier, 2007). In

humans, the formation of fat cells begins at the middle of gestation (Stillaert et al., 2007). There is a rapid extension of adipose tissue after birth. The cellularity of the adipose tissue continues to change throughout the life of individuals to respond to the normal cell turnover and to be able to store the dietary energy exceeding the nutritional needs. This involves hypertrophy (i.e. increase in size of the existing adipocytes) and hyperplasia (i.e. increase of number of cells by the production of new adipocytes). Hypertrophy is widely influenced by dietary factors and results in an accumulation of TGs, whereas hyperplasia corresponds to a recruitment of new adipocytes from precursor cells in adipose tissue. Both events occur in concert, even if hyperplasia is predominant during the development of obesity.

The first step of adipogenesis is the "proliferation" of mesenchymal stem cells, which is followed by the differentiation of these cells into preadipocytes (Figure 1.2). This stage corresponds to the "determination". These partially differentiated cells, called preadipocytes, are still capable of replication. They are present throughout the life in the adipose tissue, which allows an expansion of the adipose tissue even in adulthood (Prins and O'rahilly, 1997). They are also used for *in vitro* studies by isolation from the stromal-vascular fraction of various species in order to obtain primary cultures of adipocytes. *In vivo*, the next step of adipogenesis is called "differentiation" and corresponds to the transition from undifferentiated fibroblast-like preadipocytes into mature lipid-filled adipocytes (Figure 1.2) (Hausman et al., 2001). The differentiation into adipocytes represents a complex process depending on stimulatory and inhibitory factors. The early differentiation stage is characterised by a morphological change. Cells become spherical and begin to accumulate TGs within small LDs. In addition, expression of genes involved in glucose and lipid metabolism increases (e.g. insulin receptor, insulin-dependent glucose transporter 4 (GLUT4) and β-adrenergic receptors). Cells also acquire the ability to secrete adipokines (e.g. adiponectin and leptin), which makes adipocytes specialised in energy homeostasis (Avram et al., 2007; Gregoire et al., 1998; Hausman et al., 2001). The differentiation ends in mature adipocytes, filled with an unilocular LD, which express all the genes of adipocytes, allowing them answering to future stimuli of lipogenesis and lipolysis

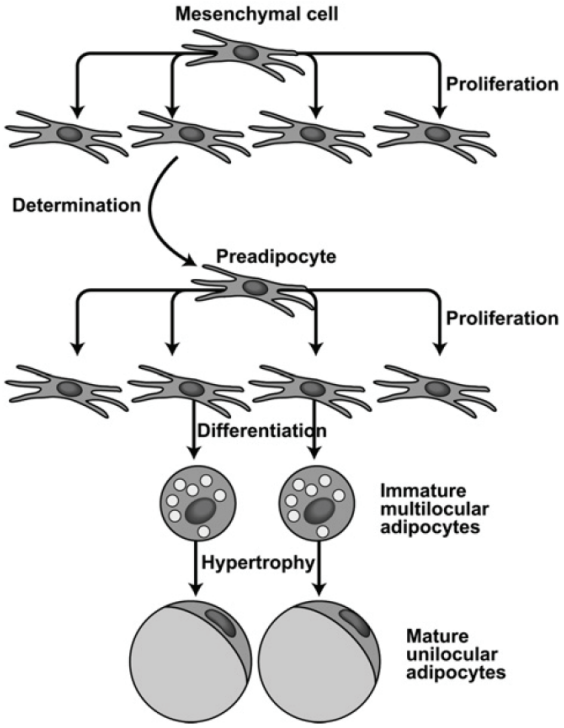

Figure 1.2 – Proliferation and differentiation of cells in adipogenesis (Avram et al., 2007).

The transition from preadipocyte to adipocyte appears to be tightly regulated by hormones, cytokines and nutrients that change the expression of transcription factors involved in the differentation. This is the balance between the stimulating (e.g. insulin, glucose and fatty acids (FAs)) and inhibiting (e.g. IL-6 and TNF-α) factors that determines if preadipocytes undergo adipogenesis (Feve, 2005).

Peroxisome proliferator-activated receptor-gamma (PPARγ), adipocyte determination and differentiation factor-1/sterol regulatory element binding protein-1c (ADD1/SREBP-1c) and CCAAT/enhancer binding protein (C/EBP) are the key factors of the complex cascade of adipogenesis (Fonseca-Alaniz et al., 2007). PPARγ is part of the superfamily of nuclear

receptors. There are two isoforms: PPARγ1 and PPARγ2. PPARγ1 is highly expressed in the adipose tissue, and to a lesser extent in other cell types (e.g. macrophages and pneumocytes), whereas PPARγ2 is exclusively expressed in the adipose tissue (Feve and Mercier, 2007). Several candidates were mentioned as endogenous ligands for PPARγ such as FAs, eicosanoids and prostaglandins (Khan and Vanden Heuvel, 2003). SREBP-1c is a transcription factor of basic helix-loop-helix (bHLH) type that contains a leucine-zipper motif in humans. ADD1 is its homologous in murine (Tontonoz et al., 1993). Both form a heterodimer. Expression of ADD1/SREBP-1c occurs predominantly in the adipose tissue, but also in the liver, skeletal muscle and adrenal gland. C/EBPα, β, δ are three isoforms of proteins that are part of basic DNA binding domain family. They also contain the leucine zipper structural motif necessary for their dimerization. The three isoforms are highly expressed in the adipose tissue (Farmer, 2006; Feve and Mercier, 2007).

We have to consider the adipocyte differentiation programme as a continuum of genetic and molecular events. Following the adipogenic stimuli (e.g. glucocorticoids and prostaglandins (Feve, 2005)), C/EBPβ and C/EBPδ are first induced and subsequently, activate the expression of PPARγ2 and C/EBPα. They undergo a cross-activation on the expression of each other and thus, reinforce the state of differentiation. C/EBPα and the heterodimer formed by PPARγ2 and retinoid X receptor (RXR) bind DNA at the consensus sequence corresponding to CCAAT and PPARγ response element (PPRE), respectively (Figure 1.3). This leads to the activation of genes specific to WAT (e.g. lipoprotein lipase (LPL) and adipocyte FA binding protein (aP2)) (Chandra et al., 2008; Kersten et al., 2000; Ramji and Foka, 2002). Moreover, it seems that ADD1/SREBP-1c could produce an endogenous ligand of PPARγ and/or act directly on the gene promotor of PPARγ (Feve and Mercier, 2007).

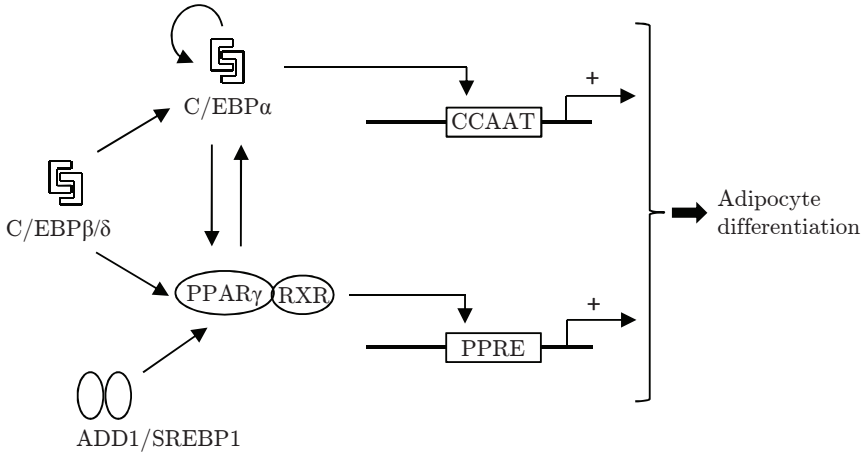

Figure 1.3 – Outline of interactions between the major transcriptional factor of adipogenesis. The activation of C/EBPβ and C/EBPδ stimulates the expression of C/EBPα and PPARγ, which stimulate mutually. This results in the activation of target genes involved in the development of adipocytes. ADD1, adipocyte determination and differentiation factor-1; C/EBP, CCAAT/enhancer binding protein; PPARγ, peroxisome proliferator-activated receptor γ; PPRE, PPARγ response element; RXR, retinoid X receptor; SREBP-1c, sterol regulatory element binding protein 1c (adapted from Feve and Mercier (2007)).

1.1.3. The metabolism of adipocytes

The principal action of adipose tissue can be divided into two components: the lipogenic action that corresponds to the biosynthesis, the incorporation and the storage of TGs, and the lipolytic action that corresponds to the mobilisation of TGs and subsequently, the release of FAs and glycerol. Thus, the adipose tissue plays a role of buffer zone in the organism, being able to store energy when the dietary uptake exceeds the needs and to release this energy when it is missing.

1.1.3.1. Origins of lipids

Lipids are an important source of energy for mammals. The form of storage in the adipose tissue is TGs that are formed by glycerol and three FAs. The origin of FAs in adipocytes may come either from the diet or *de novo* synthesis.

In humans, the origin of FAs stored as TGs in adipocytes is mainly from the diet. Once ingested, the dietary TGs are hydrolysed in the intestinal lumen, leading to the release of FAs, which enter into enterocytes and are activated in acyl-CoA by the acyl-CoA synthetase in order to enable their reesterification into TGs. TGs then leave enterocytes with chylomicrons in the lymphatic ducts and thereafter, in the bloodstream (Ferre, 2007). The rest of their path until adipocytes is explained in the 1.1.3.2 section.

The *de novo* synthesis of FAs involves the conversion of glucose excess from the diet into lipids. Two organs are able to modulate their lipogenic capacity according to the nutritional conditions: the liver and the adipose tissue (Girard et al., 1997). The relative contribution of these two tissues differs between species. In humans, the FA synthesis seems to be mainly hepatic, although the adipose tissue also plays this role after a hyperglucidic diet (Aarsland et al., 1997; Hellerstein et al., 1991). In rodents, the FA synthesis is one of the major pathways leading to TG accumulation in the adipose tissue. It is active in the liver and WAT and depends on the feeding status of the animal. The FA synthesis is low in the adipose tissue when rodents fast or receive a high fat diet. On the contrary, the FA synthesis is high in the adipose tissue when rodents receive a carbohydrate-rich diet (Ballard, 1972; Ferre, 2007). Thereafter, we will focus essentially on the FA synthesis in adipocytes.

At elevated glucose level in blood, glucose enters into adipocytes by adipocyte glucose transporters. Adipocytes express mainly GLUT4, and to a lower extent, GLUT1. The stimulation of insulin, which is produced during the prandial period, allows the translocation of the GLUT4 transporters to the cell surface. GLUT4 is thus inserted in the cell membrane and is able to participate to the glucose transport (Figure 1.4) (Huang and Czech, 2007;

Rowland et al., 2011). Once in the adipocytes, glucose is transformed into glucose-6-phosphate and undergoes the glycolysis pathway that ends up by the formation of pyruvate. In mitochondria, pyruvate dehydrogenase generates the production of acetyl-CoA from pyruvate. Acetyl-CoA is then exported to cytosol via the formation of a citrate intermediate catalysed by citrate synthase, which is splitted in the cytoplasm by citrate lyase in oxaloacetate and acetyl-CoA. Acetyl-CoA carboxylase catalyses the production of malonyl-CoA from acetyl-CoA. Malonyl-CoA enters then in the FA synthesis catalysed by the FA synthase (FAS). The assembly of long carbon chains of FAs occurs in a repeating four-step sequence by addition of two carbons at each sequence. It begins with the condensation between acetyl-CoA and malonyl-CoA, with the elimination of CO_2. It leads to the formation of a β-keto group. The three next steps are reactions of reduction, dehydration and reduction leading to the formation of butyryl (4C). The length of the chain can be extended by sequential addition of malonyl-CoA on the existing FA. FAS mainly produces palmitate (C16:0). For longer chain and polyunsaturated FA, the intervention of elongases and desaturases, localised in the endoplasmic reticulum, is required (Dinel et al., 2010; Nelson and Cox, 2008c).

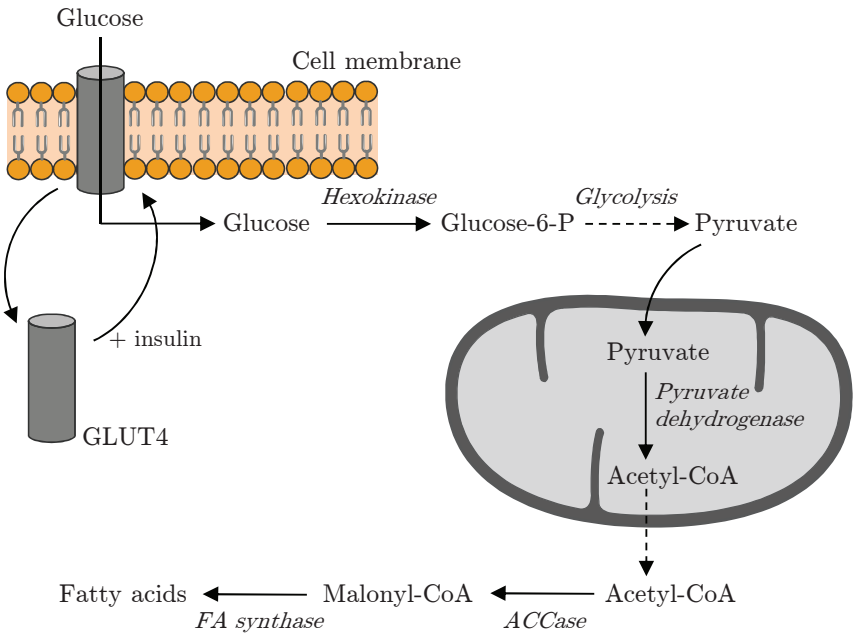

Figure 1.4 – Schema of the fatty acid (FA) synthesis in adipocyte. In the presence of insulin, the glucose transporter 4 (GLUT4) migrates to the cell membrane and glucose enters into the adipocytes. After phosphorylation into glucose-6-phosphate (glucose-6-P), it enters glycolysis to produce pyruvate, which is transported inside the mitochondria and converted to acetyl-CoA by pyruvate dehydrogenase. Acetyl-CoA leaves the mitochondria and is transformed in the cytoplasm into malonyl-CoA by acetyl-CoA carboxylase (ACCase). Malonyl-CoA is the substrate for FA synthase that produces FAs (adapted from Foufelle and Ferre (2013)).

1.1.3.2. Absorption of fatty acids from the circulation

Whatever their origin (diet or *de novo* synthesis in the liver), FAs are transported in the blood as TGs by lipoproteins (chylomicrons originating from the intestine or very low-density lipoproteins (VLDLs) originating mainly from the liver) or as complexes with albumin. Since TGs cannot enter into adipocytes as it is, they have to be hydrolysed by LPL. This results in the release of FAs, 2-monoacylglycerol and lipoprotein remnants. LPL is

produced by adipocytes and translocated at the luminal face of capillary endothelium (Fielding and Frayn, 1998; Wang and Eckel, 2009). It is also subject to regulation. Insulin has an important role in the activation of LPL during the postprandial states, while the decrease of insulin level and the increase of catecholamines during the post-absorptive or fasting periods reduce the LPL activity.

FAs liberated from lipoproteins or dissociated from albumin enter into adipocytes either by flip-flop diffusion (but this process is slow) (Zakim, 1996) or by a facilitated transport with membrane transport proteins. The complete mechanism is not fully understood but a number of FA transporters are known to be involved in this process, such as the FA transport proteins (FATP), the human cluster of differentiation 36 (CD36) proteins (the murine homolog is FA translocase (FAT)) and the plasma membrane FA binding proteins (FABPpm) (Figure 1.5) (Gimeno et al., 2003; Kazantzis and Stahl, 2012; Silverstein and Febbraio, 2009). The influx of FAs is determined by the gradient of FA concentration. In lipolytic period, the generation of FAs from TGs reduces the gradient of FA uptake. In postprandial period, insulin stimulates the esterification of FAs into TGs that promotes the gradient maintenance. In addition, FATP, which translocates from the cytosol to the cell membrane under insulin stimulation (Wu et al. 2006), facilitates the uptake of FAs by transforming them into their acyl-CoA derivatives, fatty acyl-CoA (FA-CoA), that is an irreversible reaction (Chmurzynska, 2006; Dinel et al., 2010). Intracellular FAs are then transported by specific cytosolic proteins. Cytosolic FABP (FABPc) transports the free FAs and acyl-CoA binding protein (ACBP) transports the FA-CoA, which are obtained either by FATP or by the action of acyl-CoA synthase (ACS) in the cytosol (Dinel et al., 2010; Storch and McDermott, 2009).

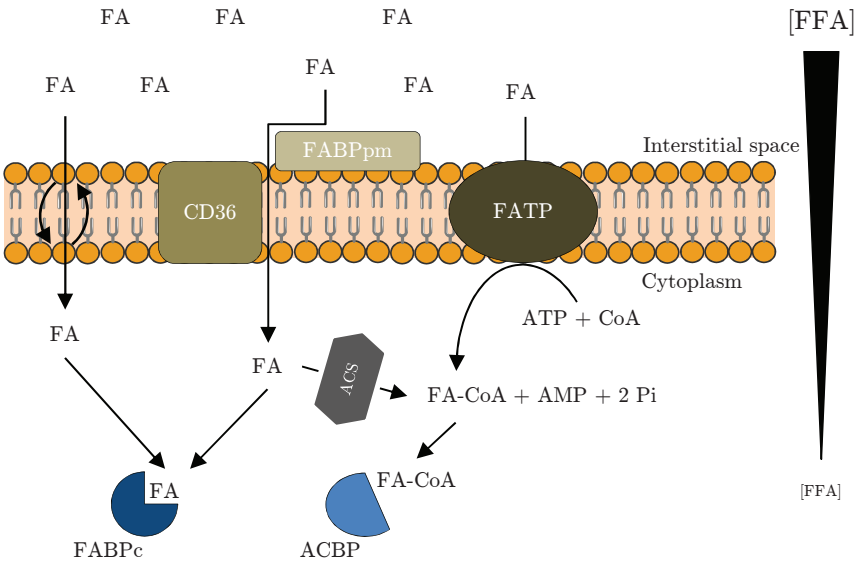

Figure 1.5 – Schematic representation of fatty acid (FA) transport across the plasma membranes. FAs released from hydrolysis of triglycerides (TGs) by lipoprotein lipase or dissociated from albumin may enter into adipocytes through either a diffusional flip-flop process or a facilitated-transporter system involving cluster of differentiation 36 (CD36), FA transport protein (FATP) and plasma membrane FA binding protein (FABPpm). The exact mechanisms by which these proteins operate to translocate FAs across the phospholipid bilayer are still under debate. In the absence of active transport, FA influx into adipocytes is governed by concentration gradients that are maintained by coordinated reduction of the intracellular FA pool through esterification into TGs and/or activation into fatty acyl-CoA (FA-CoA). Once in the cytoplasm, free FAs bind cytosolic FA binding proteins (FABPc), or undergo activation into FA-CoA by intracellular acyl-CoA synthetases (ACS). FA-CoA resulting from the action of ACS and FATP bind to acyl-CoA-binding protein (ACBP) before entering other metabolic pathways (adapted from Dinel et al. (2010)).

1.1.3.3. Fatty acid esterification

The formation of TGs within adipocytes results from the successive esterification of FA-CoA on three alcoholic functions of glycerol-3-phosphate (G3P). The first stage is the synthesis of phosphatidic acid by the acylation of two hydroxyl groups of G3P by two FA-CoA. This involves two acyl transferases (G3P acyltransferase and 1-acyl-G3P acyltransferase). Phosphatidic acid is then hydrolysed into 1,2-diacylglycerol by the phosphatidic acid phosphatase. Eventually, the esterification of a third FA-CoA by diacylglycerol acyltransferase leads to the formation of TG. The synthetised TGs are then stored in the cytosolic LDs (Dinel et al., 2010; Nelson and Cox, 2008c).

G3P required for the esterification cannot come from the glycerol since the glycerol kinase (Gyk) activity in the adipose tissue is low. G3P can derive either from an intermediate of glycolysis, dihydroxyacetone phosphate (DHAP), by the action of G3P dehydrogenase, or by the glyceroneogenesis pathway from substrates such as pyruvate, lactate and alanine (Beale et al., 2002). The contribution of one pathway rather than the other one depends on the plasma insulin and thus, the nutritional status of the individual. Under postprandial conditions, the formation of G3P from DHAP is preferred, whereas under fasting or glucose-depleted conditions, the major source of G3P is the glyceroneogenesis (Reshef et al., 2003).

The regulation of TG synthesis is relatively complex since numerous controls are involved. The TG synthesis is the final step of a cascade of reactions that are subtly regulated such as the LPL activation, the crossing of FAs through the cell membrane and the stimulation of the *de novo* FA synthesis. Two main factors, linked to the nutritional status of the individual, control the metabolism of adipocytes: the catecholamines and insulin. This latter one leads to the TG synthesis, whereas catecholamines inhibit the FA synthesis as well as the synthesis and activity of LPL (Foufelle and Ferre, 2013).

1.1.3.4. Lipolysis

The principle

The energy stored in adipocytes under the form of TGs can be released in case of energy shortage for the needs of other organs such as skeletal muscles, heart, kidney and liver. This catabolic process called lipolysis leads to the breakdown of TGs stored in the LDs into FAs and glycerol. Firstly, TGs are hydrolysed into diglycerides (DGs), then into monoglycerides (MGs) and finally, into glycerol. At each step, one FA is released under the sequential activity of three adipocyte lipases: adipose triglyceride lipase (ATGL), hormone sensitive lipase (HSL) and monoglyceride lipase (MGL). ATGL is the limiting enzyme and is substrate-specific, with a 10-fold higher affinity for TGs than DGs (Zimmermann et al., 2009). Its activity is thus crucial for the lipolysis. Indeed, mice deficient in ATGL show a potent reduction of FA release and an accumulation of TGs in adipocytes (Haemmerle et al., 2006). Similarly, its over-expression in human adipocytes increases the lipolysis (Bezaire and Langin, 2009). HSL is the second enzyme involved in the lipolytic pathway. It is also able to hydrolyse TGs into DGs, acting essentially on the esters on sn-1 and sn-3 positions. However, HSL shows a 10-fold higher affinity for DGs than for TGs. Since mice deficient in HSL show an accumulation of DGs, HSL is responsible for DG hydrolysis in adipocytes (Haemmerle et al., 2002). Eventually, MGL, an abundant and non-hormonally regulated enzyme, is the last enzyme required for the entire hydrolysis of TGs. This enzyme allows the hydrolysis of sn-1, -2 and -3 ester bonds (Karlsson et al., 2000).

The selective mobilisation of fatty acids

A wide range of FAs constitutes the TGs of the LDs. They are different by their molecular structure such as the chain length and the degree of unsaturation. Several studies highlighted a relationship between the molecular structure of FAs and their metabolic fate in humans and animals (Raclot, 2003).

The mobilisation of FAs from adipocytes appears to be selective and this selectivity does not seem to depend on the FA composition of adipose tissue

(Raclot et al., 1997). The proportions of FAs released from adipocytes differ greatly from the composition of TGs. The relative mobilisation of FAs increases with the degree of unsaturation for a given chain length and decreases with the chain length for a given number of unsaturation, whatever the FA composition of adipose tissue (Figure 1.6). This means that short and unsaturated FAs are more readily mobilised. These rules seem to be applied to humans (i.e. in isolated adipocytes stimulated *in vitro* with isoprenaline), rats (i.e. in adipocytes isolated from rats fed with fish-oil and *in vitro* stimulated with norepinephrine, and in *in vivo* rats fed with fish-oil and undergoing prolonged periods of fast), and rabbits (i.e. in *in vivo* rabbits fed with enriched-oil diet and after an injection of adrenocorticotropic hormone) and lead to a remodelling of the FA composition of adipose tissue (Conner et al., 1996; Raclot and Groscolas, 1993, 1995; Raclot et al., 1997; Raclot, 2003).

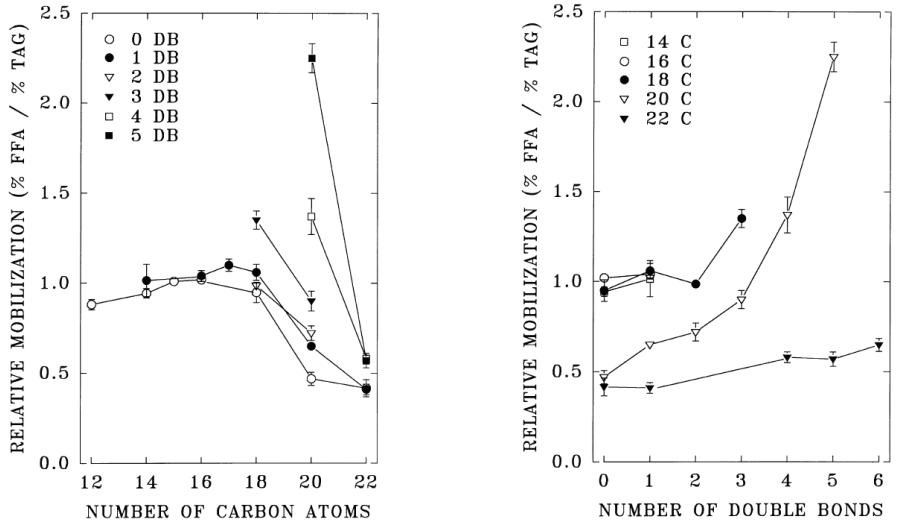

Figure 1.6 – Relationships between (i) the chain length and the relative mobilisation of fatty acids from human adipocytes at given degrees of unsaturation (on left), and (ii) the degree of unsaturation and the relative mobilisation of fatty acids from human adipocytes at given chain lengths (on right). C, carbon atoms; DB, double bond(s); FFA, free fatty acids; TAG, triglycerides (Raclot et al., 1997).

To date, no evidence shows that the selectivity of mobilisation of FAs is governed by specific demands of tissue, but the selective mobilisation could affect their supply. For example, C20:5n-3 and C20:4n-6, which are readily mobilised, are both precursors of eicosanoids and thus have many biological effects on the organism such as on inflammation, lipolysis and adipocyte differentiation (Raclot et al., 1997; Russell and Tisdale, 2005; Tisdale and Beck, 1991). As the lipolysis takes place at the water-lipid interface between cytoplasm and LD, the selective mobilisation of FAs may be related to their selective accessibility and availability to the lipases according to the differential solubility of FAs. The physico-chemical properties of FAs may thus govern their mobilisation (Raclot and Groscolas, 1995; Raclot et al., 1997).

The end-products of lipolysis

The action of the three lipases (ATGL, HSL and MGL) leads eventually to the formation of lipolytic end-products, three FAs and one glycerol. Once hydrolysed, FAs bind FABP and are excreted to the blood circulation by passive diffusion and by transport proteins. The accurate mechanisms involved are not completely elucidated yet (Su and Abumrad, 2009). FAs are then transported by albumin to reach the target tissues. They are β-oxidised in the muscle and the liver. They can also be reesterified into TGs in the liver to be excreted as VLDLs (Large et al., 2004). Some FAs newly released can be reabsorbed by the adicpoyte itself or by the neighbouring adipocytes in order to synthesise new TGs (Zimmermann et al., 2004).

The glycerol generated during lipolysis is poorly used by adipocytes since Gyk activity is low in the adipose tissue. Glycerol is released through adipose aquaporins (AQP) and transported to the other tissues (and specially, the liver) to be metabolised. Thanks to AQP7-knockout mice, it was demonstrated that AQP7, an AQP abundantly expressed in the adipose tissue, serves as an adipose glycerol channel *in vivo* (Hibuse et al., 2005). It was shown that a treatment of murine 3T3-L1 adipocytes by thiazolidinedione (TZD), which is an exogenous ligand of PPARγ, upregulates the expression of Gyk, and thereby may accentuate the reesterification of FAs. Therefore, the incorporation of glycerol into TGs is

promoted and reduces the release of FAs (Guan et al., 2002). The process seems to be different between species since the stimulation of human preadipocytes and type-2 diabetic patients with TZD did not stimulated the Gyk expression (Mazzucotelli et al., 2007; Tan et al., 2003).

The stimulation of lipolysis

In a normal-weight man, the mean turnover of TGs in the total mass is 100 – 300 g per day (Lafontan et al., 2008). However, the hydrolysis of TGs and the release of FAs are tightly regulated by numerous signals of nervous, endocrine and paracrine origins. Catecholamines, natriuretic peptides and insulin are considered as the major lipolytic regulators in human adipocytes. The first two agents are lipolytic agents and the last one has an antilipolytic action. This is therefore the balance between the lipolytic and antilipolytic pathways that conditions the adipocyte response.

Two kinds of receptors with seven transmembrane domains are found in the adipocyte membranes: the α_2-adrenergic receptors and β-adrenergic receptors. They are respectively coupled with inhibitory guanosine triphosphate (GTP)-binding proteins (G_i) and stimulatory GTP-binding proteins (G_s). The relative contribution of adrenergic receptors depends on the species. The α_2-adrenergic receptors are poorly or even not present in rodents, whereas they are considerably expressed in humans. Regarding the β-adrenergic receptors, there are three subtypes of receptors: β_1, β_2 and β_3. The β_3-adrenergic receptors are dominant in rodents, whereas the β_1- and β_2-adrenergic receptors are more abundant in humans (Feve and Mercier, 2007). Catecholamines such as noradrenaline and adrenaline act through the binding and the subsequent activation of adenylate cyclase (AC) via G_s (Dodt et al., 2003). AC catalyses then the conversion of adenosine triphosphate (ATP) into cyclic adenosine monophosphate (cAMP) that actives in turn the protein kinase A (PKA) (Figure 1.7). This latter promotes the phosphorylation of HSL and perilipin A. In unstimulated stage, HSL is distributed in the cytosol of adipocytes. Under stimulation, the phosphorylation of HSL on serine residues (649 and 650) leads to the activation of HSL by exposing the catalytic site. Furthermore, this phosphorylation allows its translocation from cytosol to LD surface that is

coated by perilipins. The phosphorylation of perilipins promotes access of phosphorylated HSL to lipid substrates of the LD (Figure 1.7) (Feve and Mercier, 2007). However, catecholamines also bind α_2-adrenergic receptors, which inhibit lipolysis. The net effect depends on the balance between the stimulation of β-adrenergic receptors and the inhibition of α_2-adrenergic receptors. It seems that the predominance of β-adrenergic receptors against α_2-adrenergic receptors is dependent on endocrine and paracrine mechanisms, but this is not clarified yet. In addition, there are some regional variations in the adipose tissue regarding the lipolytic and antilipolytic activities of receptors. Indeed, α_2-adrenergic receptors have been reported to be most active in subcutaneous fat cells compared to visceral depots (Dodt et al., 2003). A decrease of α_2-adrenergic receptor number was observed with a reduction of the cell size (Lafontan and Berlan, 1995).

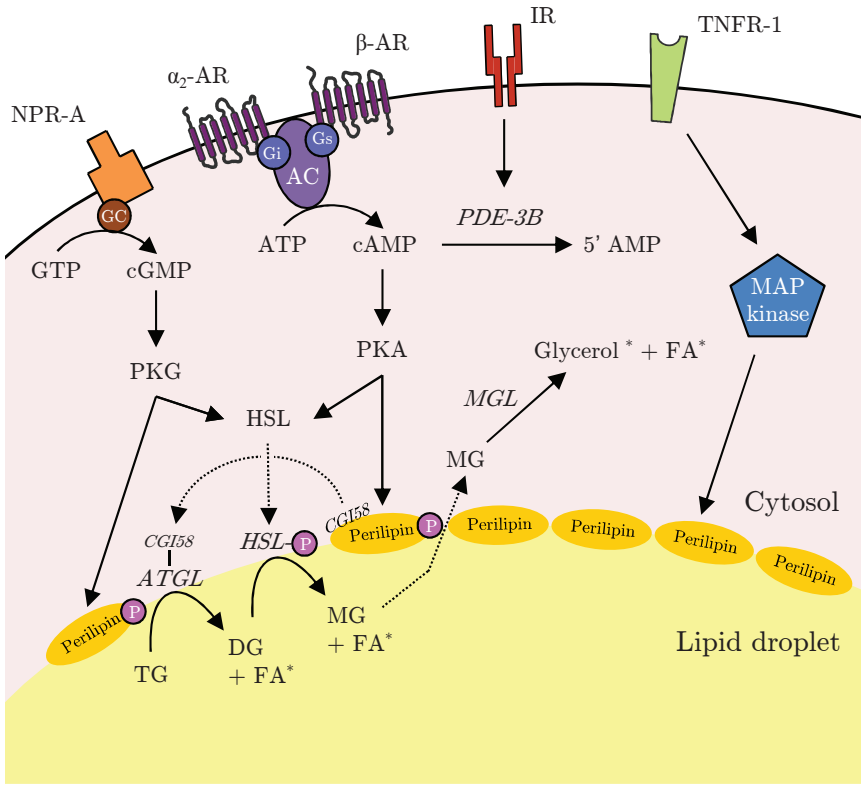

Figure 1.7 – Illustration of the lipolytic pathway in adipocytes. The products of lipolysis marked with a star (*) are released from adipocytes. For more details refer to the text. AC, adenylate cyclase; cAMP, cyclic adenosine monophosphate; α_2-AR, α_2-adrenergic receptor; ATGL, adipose triglyceride lipase; ATP, adenosine triphosphate; β-AR, β-adrenergic receptor; CGI58, comparative gene identification-58; DG, diglyceride; FA, fatty acid; GC, guanylyl cyclase; G_i, inhibitory GTP-binding protein; cGMP, cyclic guanosine monophosphate; G_s, stimulatory GTP-binding protein; GTP, guanosine triphosphate; HSL, hormone sensitive lipase; IR, insulin receptor; MAP kinase, mitogen activated protein kinase; MG, monoglyceride; MGL, monoacylglycerol lipase; NPR-A, natriuretic peptide receptor A; P, phosphate; PDE-3B, phosphodiesterase 3B; PKA, protein kinase A; PKG, protein kinase G; TNFR-1, tumor necrosis factor receptor 1; TG, triglyceride; 5'AMP, 5'-adenosine monophosphate (adapted from Frayn et al. (2006) and Lafontan et al. (2008)).

The atrial and brain natriuretic peptides (ANP and BNP, respectively) exert a lipolytic activity in the human and primate adipocytes, but not in the rodent cells (Sengenes et al., 2000). These endogenous peptides are synthesised by thymus and macrophages and can be stored in myocytes (Lafontan et al., 2008). They are released during stress states and exercise, and operate via a natriuretic peptide receptor-A (NPR-A) present in adipocyte membrane. Its activation promotes the production of intracellular guanosine 3',5'-cyclic monophosphate (cGMP) by the guanylyl cyclase (GC) intermediate. The signal is then mediated by protein kinase G (PKG) that phosphorylates HSL and perilipins (Figure 1.7) (Lafontan et al., 2008; Sengenes et al., 2000). PDE-5A, a phosphodiesterase (PDE) hydrolysing cGMP, was identified in the adipocytes but its impact on the lipolysis is weak (Moro et al., 2007).

TNF-α is able to stimulate lipolysis by different mechanisms. Firstly, it indirectly counteracts the antilipolytic action of insulin and G_i protein by inhibiting the signal of receptors. This leads to an increase of phosphorylated HSL and perilipins. Secondly, the link of TNF-α to its receptor (TNF-α receptor 1 (TNFR-1)) promotes the activation of two mitogen activated protein (MAP) kinases (p44/42 and Jun kinase) that modulate the lipolytic pathway by the phosphorylation of perilipin and by a decrease of its expression in humans and mice (Ryden et al., 2002; Souza et al., 2003).

In addition to HSL and perilipins, the ATGL activation is also regulated. Current data indicate that ATGL is indirectly controlled by hormonal stimulation. Nevertheless, the precise mechanisms by which ATGL responds to hormonal stimulation are incompletely known (Yang et al., 2013). Altough this enzyme can be phosphorylated, it is not the target of PKA and PKG (Zechner et al., 2009; Zimmermann et al., 2004). ATGL is localised on LD whatever the stimulation. Under unstimulated conditions, perilipin is associated with the phospholipid monolayer coating LDs and thus, limits the acces of ATGL to underlying TGs (Miyoshi et al., 2007; Yang et al., 2013). Under β-adrenergic stimulation, perilipin acts to facilite the LD redistribution of ATGL and thus, enhances ATGL-mediated lipolysis. In addition, the comparative gene identification-58 (CGI58) is a LD protein that acts as a cofactor to activate ATGL. Under unstimulated conditions,

CGI58 is sequestered by perilipin at the surface of LD and is not able to activate ATGL. Concomitant to the phosphorylation of perilipin, CGI58 dissociates from perilipin and becomes cytosolic (Figure 1.7). It then interacts with ATGL and activates TG hydrolysis (Granneman et al., 2007; Granneman et al., 2009). Moreover, other proteins associated to LDs are also involved in the regulation of ATGL. Pigment epithelium-derived factor is an adipocyte-secreted factor that regulates the TG metabolism through ATGL. It promotes lipolysis in an ATGL-dependent manner (Borg et al., 2011). To date, the molecular mechanisms remain however elusive (Yang et al., 2013). Fat-specific protein 27 is one of the additional proteins discovered to be colocalized with LDs. In contrast with perilipin, fat-specific protein 27 does not directly affect the activity of ATGL or its activation by CGI58 but acts as a lipolytic barrier by limiting the presence of ATGL as the LD surface. The nutritional status of the individual seems to influence the ATGL mRNA. The mRNA levels increase with fasting periods and decrease with feeding periods (Lake et al., 2005; Zimmermann et al., 2004).

The inhibition of lipolysis

The link of insulin to its receptor (insulin receptor (IR)) leads to an antilipolytic effect in adipocytes. IR undergoes a tyrosine phosphorylation thanks to its tyrosine-kinase activity. It is followed by a phosphorylation of insulin receptor substrate 1 (IRS1) that is then able to activate phosphatidylinositol-3-kinase (PI3K), which in turn, activates PDE-3B that degrades cAMP into 5'AMP (Ferre, 2007). Thereby, it negatively modulates the lipolysis by a reduction of activated HSL and perilipins. An insulin treatment has no impact on the natriuretic peptide pathway and it seems that insulin does not regulate the activity of PDE-5A (Conti and Beavo, 2007).

Other factors are known to have a negative impact on the lipolysis, but their physiological relevance is still uncertain (Large et al., 2004). Insulin-like growth factor-1 inhibits the lipolytic pathway in humans, maybe through the PDE-3B, similarly to insulin (Boulware et al., 1992). Adenosine has been shown to locally regulate the lipolysis in humans as a paracrine and autocrine agent by inhibition of AC mediated by G_i proteins and

subsequently, by inhibition of the lipolytic activity of HSL and the activation of perilipins (Arner, 1993). Similarly to adenosine, the prostaglandins E1 and E2 act on AC via G_i proteins in *in vitro* human adipocytes but their biological levels are too low to assess an *in vivo* lipolytic inhibition (Richelsen, 1992). Neuropeptide Y has an antilipolytic action in murine adipocytes in a similar manner than prostaglandins (Bradley et al., 2005).

The regulation of the lipolytic pathway is thus a complex process that involves many factors depending on food status as well as gender, age, physical activity and adipose region (Arner, 2005).

1.1.3.5. The concept of fasting

All animals depend on food in order to match the energy needs for basal metabolism, thermoregulation, physical activities, immunity, growth and reproduction. Many animals undergo periods of fast during their life cycle due to the fluctuation of food availability, seasonal changes in temperature, migration activity, moulting and care of eggs or youngs. The ability of animals to survive when energy sources are not available is based on their capacity to store energy. The onset of fasting is obviously the creation of large energy storages (Wang et al., 2006). A distinction has to be done between fasting and starvation. The fasting animal maintains the metabolic homeostasis and thus, the critical functions are conserved, whereas the starved animal does not control its homeostasis and the critical functions are compromised (Castellini and Rea, 1992). The fast has been more widely studied in birds and mammals than in other vertebrates and invertebrates. In the present section, we are focusing on the phases of fasting in mammals.

During the period of fast, mammals exhibit adaptive biochemical and physiological responses to the lack of food. The metabolism of food deprivation can be divided in three phases. These phases are defined according to the progressive metabolic changes. In other words, they are based on the primary fuel available for use.

Phase I

Fasting is thus defined as the absence of food and fluid intake. Nevertheless, it is not clearly defined when the fast may be considered to begin after the last intake. The duration of the post-prandial period may indeed last for several hours and depend on the type and amount of food ingested (Maughan et al., 2010). The first stage of fasting begins after this post-prandial period and lasts for a few hours (Wang et al., 2006). During that period, the hepatic glycogen is progressively hydrolysed in order to maintain a constant blood glucose level and a proper glucose supply to the central nervous system, brain, erythrocytes, testes and renal medulla. The breakdown of hepatic glycogen produces glucose-1-phosphate that is converted into glucose-6-phosphate and finally into free glucose (Nelson and Cox, 2008a). Moreover, energy demand is met by an increased rate of fat oxidation. The substantial reserves of TGs contained within adipose tissue begin to be mobilised, leading to an increase of FAs in the circulation and thus, to an increase of the FA availability for muscles for oxidation (Maughan et al., 2010; Wang et al., 2006). There is also an increase of released glycerol from adipose tissue that can undergo gluconeogenesis in the liver in order to contribute to the pool of available carbohydrate. Moreover, amino acids from the breakdown of proteins may also form glucose through this same pathway (Wang et al., 2006).

Phase II

The stores of glycogen being depleted, the phase II of fasting begins. In humans, this period can last for up to three months for normal-weight individual and for more than one year for a very obese adult (Nelson and Cox, 2008b; Wang et al., 2006). Lipids represent the main energy source through their mobilisation and oxidation, especially for the skeletal muscles (Bertile et al., 2003). As glucose is the sole or the major fuel source for certain tissues, the organism needs to synthetise glucose through gluconeogenesis in the liver. This pathway, which is in part the opposite of glycolysis, uses as substrates glycerol from the hydrolysis of TGs in adipose tissue and certain amino acids from the proteolysis of muscle and liver proteins. The proteins that are not essential for survival are degraded first.

After approximately one week of fasting, the brain is able to use ketone bodies as energy source. They are produced by the liver from FAs exported from adipose tissue.

Phase III

This stage is considered as the terminal starvation. When the lipid stores are completely depleted, the use of protein increases and becomes the major energy source. Proteins from muscles, which are the largest source of proteins in the body, are rapidly degraded by gluconeogenesis. At the end of this phase, proteins that are essential for cellular functions are depleted leading to a cell degeneration and even, to the animal death.

The example of the northern elephant seal

Some mammals such seals are adapted to extremely long periods of fast without food and water. Northern elephant seals (NES) (*Mirounga angustirostris*) undergo spontaneous and voluntary long-term fasting during their natural history. For example, the reproduction period requires a stay on land. After to give birth, females have a short but intensive lactation during which they completely fast. They are relatively unmoving during that period but have considerable energetic demands through milk production. They may lose 50% of their initial reserves during lactation (Castellini and Rea, 1992; Champagne et al., 2012; Noren et al., 2003). After the 25-day nursing period, NES pups are abruptly weaned and undergo a long post-weaning fast (2 – 3 months) (Le Boeuf and Laws, 1994). During this period, pups gather into small groups and stay on the beach during the first weeks. Later on, they start making short daily trips to the sea. They lose 25% of their body mass over the entire fast. During the reproduction period, males may remain on the colony and fast for up to 90 days. Males undertake violent fights between each others in order to constitute their harem. When the females get into oestrus, the males (especially, the alpha bulls) try to mate with a maximum of them. Males lose over a third of their initial body mass throughout the breeding season (Le Boeuf and Laws, 1994).

During such periods of fast, seals minimise the loss of lean body mass, even with the energy expenditure in absence of food intake. An extended

phase II fast period with a sparing of protein is the key to endure prolonged periods of fast (Castellini and Rea, 1992). Indeed, an estimation of protein catabolism was carried out in NES pups during the post-weaning fast. The protein catabolism was evaluated to contribute to less than 4% of their metabolic rate. Similar levels of catabolism were found in suckled NES pups. This confirms that NES pups are adapted to fast (Houser and Costa, 2001). The study of Noren et al. (2003) in weaned NES pups specified that protein contributed for $\leq$ 6% to total metabolism for weaned pups with $>$ 38% lipid, and for 12 – 15% to total metabolism for weaned pups with $<$ 38% lipid. These findings indicate that fatter weaned NES pups use proportionally more fat and spare more protein compared to leaner animals. This may occur because NES are characterised by a large adipose tissue depot and are able to promote high rates of lipolysis in response to energy needs. The levels of FAs in blood are greater in fasted NES than in fed NES and these concentrations increase over the fast periods (Houser et al., 2007). Animals generate the majority of ATP through lipid oxidation. Indeed, from 80 to 95 % of the energetic demand are met by lipids (Champagne et al., 2012). Moreover, ketone bodies may contribute to the energy metabolism of NES during long-term fast since they accumulate in NES undergoing a post-weaning fast. It is however important to point out that the levels of ketone bodies in NES are significantly lower than in species that are not adapted to fast. NES seem thus to continuously exhibit the metabolic characteristics of Phase II fasting, that contribute to the success of their fast (Champagne et al., 2012). Paradoxically, levels of glucose in the circulation appear elevated in fasting NES (Fowler et al., 2008; Viscarra et al., 2011). The high rate of lipolysis suggested that glycerol from the hydrolysis of TGs, would partly contribuate to an endogeneous production of glucose as a recycling pathway (Champagne et al., 2012).

1.2. Persistent organic pollutants (POPs)

Over the last decades, an increasing focus has been paid on a group of organic chemicals called persistent organic pollutants (POPs). They have mostly an anthropogenic origin resulting from intentional or unintentional production (Harrad, 2009). Even if the levels vary between molecules, all share four properties:

- They are resistant to environmental degradation (chemical, biological and photolytic processes), lasting for years or even decades before degrading;
- They persist in the environment and travel long distances through the air and water;
- They bioaccumulate in the human and animal fatty tissues and biomagnify through the food web;
- They are highly toxic and can cause serious health problems (Gevao et al., 2009; Harrad, 2009).

The Stockholm Convention is an international treaty that targets twelve particularly toxic POPs. It aims at restricting and ultimately, eliminating their production, use, release and storage. The Convention gathers some pesticides (e.g. dichlorodiphenyltrichloroethane (DDT) and Mirex), industrial chemicals (e.g. hexachlorobenzene (HCB) and polychlorinated biphenyls (PCBs)) and unintentional chemical by-products (polychlorinated dioxins and furans). It was adopted on 22 May 2001 and entered into force on 17 May 2004. Being aware that POPs pose major threats to environment, it sets up a system for tackling additional chemicals identified as unacceptably hazardous. This is why nine new POPs were added to the Convention as of 2009 (Table 1.1).

The properties, production, legislation in USA and European Union as well as the toxicity of some targeted families of POPs (PCBs, polybrominated diphenyl ethers (PBDEs), DDT and HCB) are developed in the subsequent sections.

Table 1.1 – List of persistent organic pollutants targeted by the Stockholm Convention with the year of their addition

Classification in 2004
Aldrin
Chlordane
Dibenzofurans
Dichlorodiphenyltrichloroethane
Dieldrin
Endrin
Heptachlor
Hexachlorobenzene
Mirex
Polychlorinated biphenyls
Polychlorinated dibenzo-*p*-dioxins
Toxaphene
Classification in 2009
Alpha-hexachlorohexane
Beta-hexachlorocyclohexane
Chlordecone
Hexabromobiphenyl
Hexabromodiphenyl ether and heptabromodiphenyl ether
Lindane
Pentachlorobenzene
Perfluorooctane sulfonic acid, its salt and perfluorooctane sulfonyl fluoride
Tetrabromodiphenyl ether and pentabromodiphenyl ether

1.2.1. Polychlorinated biphenyls (PCBs)

1.2.1.1. Chemical structure

PCBs are a group of 209 chlorinated compounds, called congeners, ranging from one to ten chlorine atoms attached to the biphenyl group (Figure 1.8) (Ballschmiter and Zell, 1980). A numbering system that is currently widely used was developed by Ballschmiter and Zell (1980) in which a number from 1 to 209 (i.e. IUPAC number) was given to each congener.

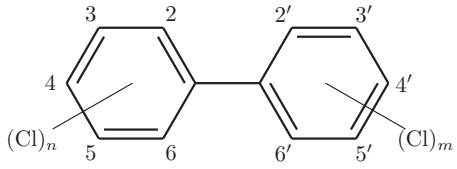

Figure 1.8 – Chemical structure of PCBs

PCBs with the same number of chlorine atoms are referenced under the term "homologue". Homologue PCBs with different patterns of substitution are listed as "isomers". The 2, 2', 6 and 6' positions on the biphenyl group are called *ortho* positions; the 3, 3', 5 and 5' positions, *meta* positions; 4 and 4' positions, *para* positions (Figure 1.8) (Erickson and Kaley II, 2011). Depending on the chlorine substitution, the phenyl rings can rotate and take different configurations with as extreme configurations, the coplanar (two rings in the same plane) and the non-coplanar configurations (two rings forming a 90-degree angle). PCB congeners with a coplanar conformation are either non *ortho*-substituted (i.e. CB-77, -81, -126 and -169) or mono *ortho*-substituted (i.e. CB-105, -114, -118, -123, -156, -157, -167 and -189). The mono *ortho*-substituted PCBs bind weakly to the aryl hydrocarbon receptor (AhR) compared to non *ortho*-substituted PCBs (Erickson and Kaley II, 2011). This coplanar conformation is necessary to link AhR, which is a cellular receptor that leads to various toxic effects (Erickson and Kaley II, 2011; Safe et al., 1985). The four non *ortho*- and eight mono *ortho*-PCBs

have been assigned a toxic equivalency factor (TEF) as compared to 2,3,7,8-tetrachlorinated dibenzo-*p*-dioxin (TCDD), which is the reference chemical to which the toxicity of other dioxins and coplanar PCBs are compared. TCDD has a TEF of 1.0. The TEF is reflected by the relative potencies to bind AhR (Van den Berg et al., 2006). Consequently, these PCB congeners are frequently called "dioxin-like" PCBs.

1.2.1.2. Sources and legislation

There are no known natural sources of PCBs in the environment (ATSDR, 2014). PCBs have been extensively manufactured since 1920s in the form of mixtures with industrial trade names such as Aroclor (USA), Clophen (Germany), Fenclor (Italy), Kanechlor (Japan), and Phenoclor (France) (De Voogt and Brinkman, 1989).

PCBs have interesting physico-chemical properties. Among others, they have a high chemical and thermal stability and an electrical resistance. In addition, PCBs have low water solubility (experimental log K_{ow} are comprised approximately between 4 and 8), which decreases with increased chlorination degree (Hansen et al., 1999). Because of these characteristics, they were widely used both for closed applications (e.g. dielectric fluids in transformers and capacitors, heat transfer fluids, and lubricants) and in open-end applications (e.g. flame retardants, inks, paints and adhesives) (ATSDR, 2014; Safe and Hutzinger, 1984).

Following strong evidence on the toxic effects of PCB exposure as well as their persistence in the environment, their production in USA was banned in 1976 pursuant to the Toxic Substances Control Act. Their use was regulated and their discharge was prohibited (EPA, 1977, 1979a, b). It was also since 1970s that European Union evaluated the use of PCBs and restricted it to closed-system equipment (EC, 1985, 2002). According to the Stockholm Convention, PCBs Elimination Network (PEN) invite the stakeholders from different sectors to eliminate equipment and oils containing PCBs from use by 2025 and bring these under environmentally sound waste management by 2028 (PEN, 2009).

1.2.1.3. Biotransformation and toxic effects

Because of their stability, PCBs do not readily breakdown and remain for long periods of time in the environment. They can bioaccumulate in the tissues of humans and wildlife and biomagnify (i.e. increase of concentrations of a substance with the trophic level) over the food chain. Once PCBs have entered the body, they tend to accumulate in lipid-rich tissues due to their lipophilic character, but they can be enzymatically converted to more hydrophilic species in order to increase the rate of clearance. This process is called biotransformation and occurs in two major steps. The first pathway is called "functionalization" (or Phase I reactions) and the second one is called "conjugation" (or Phase II reactions). The rate of biotransformation of congeners is influenced by the number and the position of chlorine atoms on the phenyl rings. The *meta-para*-unsubstituted PCB congeners are more easily biotransformed than congeners with *meta-para*-substitution and more than five chlorine atoms (Safe, 1989).

Phase I reactions

The Phase I reactions result in hydroxylated PCBs (HO-PCBs). Their formation occurs by direct insertion of HO-group on a phenyl ring or by the formation of arene oxide intermediate, formed preferentially on unsubstituted *meta* and *para* carbon atoms (Daly et al., 1972; Letcher et al., 2000). The phase I reactions involve essentially a microsomal monooxygenase system catalysed by cytochrome P450 enzyme (CYP) that is found predominantly in the membrane of smooth endoplasmic reticulum of liver, but also in other organs such as intestine, nose epithelia, lung, kidney, ovary, placenta, sertoli cells of the testis and skin (Boelsterli, 2007). CYP are tightly regulated. Dioxin-like PCBs (i.e. PCB congeners with a coplanar conformation) are able to induce the expression of CYP1A and CYP1B by the AhR pathway (Denison et al., 2002; James, 2001). Indeed, the binding of PCB to AhR results in a translocation of complex from cytosol into nucleus where there is a dissociation from heat shock protein 90 (hsp90). AhR is thus available to form a heterodimer with AhR nuclear translocator (ARNt) and bind to the dioxin response element (DRE) on the promoter region of the target gene. It results in transcriptional activation of this gene (i.e. phase I and phase II

enzymes) (Figure 1.9) (Boelsterli, 2007). In addition to AhR, the pregnane X receptor (PXR) may regulate CYP2B expression through the binding to *ortho*- and *para*-PCBs and constitutive androstan receptor (CAR) may regulate CYP3A through the binding to e.g. poly-ortho-PCBs, PCB-47 and PCB-184 (Kretschmer and Baldwin, 2005).

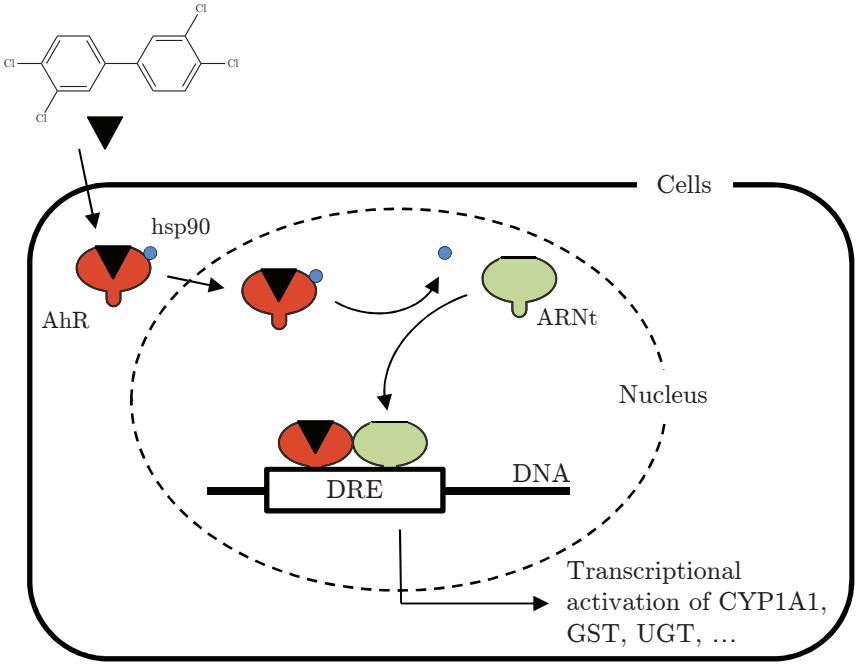

Figure 1.9 – Mechanism of AhR transactivation of selective genes: example of PCB-77. AhR, aryl hydrocarbon receptor; ARNt, AhR nuclear translocator; CYP, cytochrome P450 enzyme; DNA, deoxyribonucleic acid; DRE, dioxin response element; GST, glutathione-S-transferase; hsp90, heat shock protein 90; UGT, uridine 5'-diphospho-glucuronosyltransferase (adapted from Boelsterli (2007)).

Phase II reactions

HO-PCBs from Phase I reactions can then undergo a conjugation of Phase II with a polar molecule such as sulphate, glutathione or glucuronic acid. The transfer of substrate to HO-PCBs is catalysed either by sulfotransferase (SULT), glutathione-S-transferase (GST) or uridine 5'-diphospho-glucuronosyltransferase (UGT), respectively (Figure 1.10) (James, 2001). These second metabolites can undergo additional metabolism and lead to other metabolites such as methylsulfones ($MeSO_2$-PCBs) and mercapturic acids (Figure 1.10) (James, 2001).

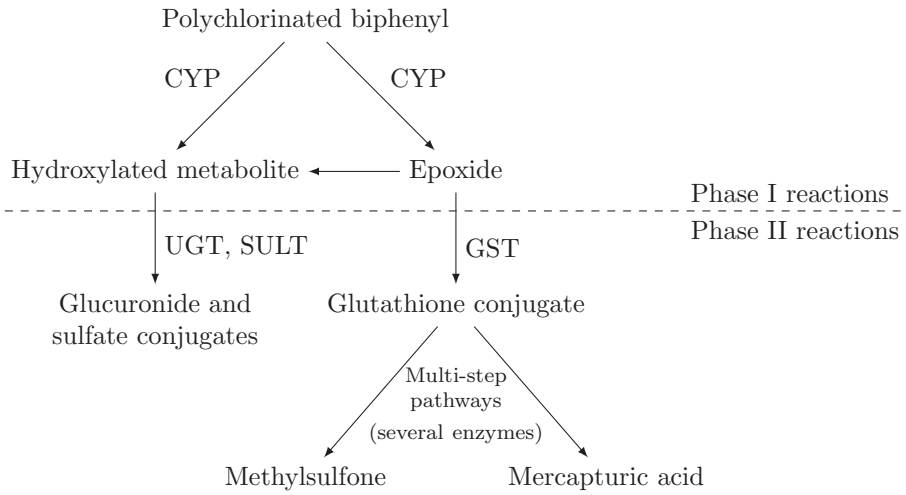

Figure 1.10 – Example of potential pathways for biotransformation of polychlorinated biphenyl. CYP, cytochrome P450; UGT, uridine 5'-diphospho-glucuronosyltransferase; SULT, sulfotransferase; GST, glutathione-S-transferase (adapted from James (2001)).

Although PCB metabolites from Phases I and II are more hydrophilic than the parent compounds, some of them are retained in the tissue of humans and wildlife instead of being excreted (Dirtu et al., 2010; Dirtu et al., 2013; Vanden Berghe et al., 2012). HO-PCBs that persist in blood have a specific structure: an HO-group in *meta* or *para* positions with one or more adjacent chlorine atoms. This structural element gives to the metabolites a

specific structure: an HO-group in *meta* or *para* positions with one or more adjacent chlorine atoms. This structural element gives to the metabolites a similar structure to thyroxine (T_4) (Figure 1.11), the natural substrate of thyroid hormone transport protein, transthyretin (TTR). HO-PCBs bind thus TTR with high affinity and consequently, are poorly excreted (Lans et al., 1993; Letcher et al., 2000). Similarly, $MeSO_2$-PCBs are retained in selected tissue, such as liver and lung. The greater affinity for protein may explain their retention in tissue (Letcher et al., 2000).

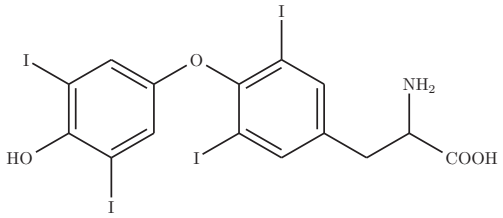

Figure 1.11 – Chemical structure of thyroxine (T_4)

The exposure to PCBs and their metabolites cause various toxic responses. As described above, PCBs induce hepatic Phase I and II enzymes involving AhR mechanisms. PCBs are classified as carcinogenic to humans (Group 1) from 2013 by the International Agency for Research on Cancer (IARC) (IARC, 2014). PCBs and HO-PCBs are endocrine disruptors. They can bind to estrogen receptors and induce estrogenic or anti-estrogenic effects. Similar effects were noted for androgenic receptors. HO-PCBs are also able to inhibit the estrogen conjugation enzymes, leading to an higher availability of estrogens, and to reduce the activity of the enzyme involved in the conversion of testosterone into estrogen (Amaral Mendes, 2002; Portigal et al., 2002; Ulbrich and Stahlmann, 2004). Moreover, HO-PCBs can interfere with the activity of the thyroid stimulating hormone. They are also able to bind to TTR, which is involved in the T_4 transport. It thus leads to a decrease of T_4 levels in the bloodstream. HO-PCBs disturb the blood levels of retinol. The latter forms a large complex with the retinol binding protein and the T_4-TTR heterodimer, which prevents the excretion of retinol. Once

linked to HO-PCBs, TTR separates from retinol binding protein, leading to the decrease of blood retinol levels (ATSDR, 2014).

1.2.2. Polybrominated diphenyl ethers (PBDEs)

1.2.2.1. Chemical structure

PBDEs are a group of brominated flame retardants (BFRs). Their structure is similar to the one of PCBs. They have two phenyl rings carrying from one to ten bromine atoms. Contrary to PCBs, the two phenyl rings are connected by an oxygen atom (Figure 1.12). PBDEs are potentially made up of 209 congeners varying in both number and position of bromine atoms on the phenyl rings (Darnerud et al., 2001). The nomenclature suggested by Ballschmiter and Zell (1980) for PCBs is also used for PBDE congeners (Alaee et al., 2003).

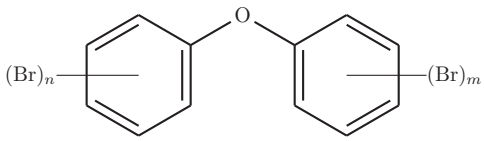

Figure 1.12 – Chemical structure of PBDEs

1.2.2.2. Sources and legislation

PBDEs are major industrial products. The first commercial productions began in 1970s. Three different formulations are available: Penta-BDE, Octa-BDE and Deca-BDE. This classification reflects their average bromine content. The commercial Penta-BDE mixture contains mainly BDE-99 and BDE-47 followed by other congeners in low levels such as BDE-17, -28, -100, -153 and -154. The major congener found in Octa-BDE product is BDE-183. BDE-153 and -154 as well as octa- and nona-BDEs are also present. The formulation of Deca-BDE is relatively pure, consisting mainly of BDE-209 with a small quantity of nona-BDEs (Figure 1.13) (Alaee et al., 2003; Harrad, 2010).

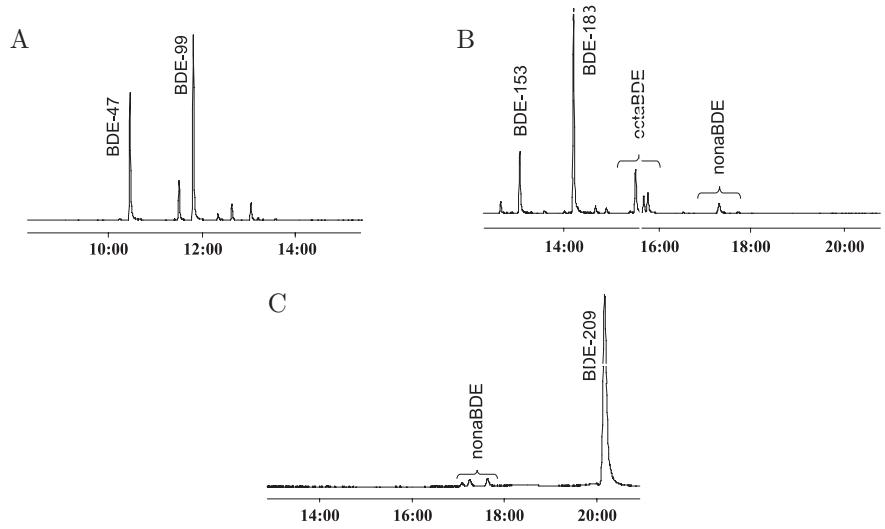

Figure 1.13 – Chromatograms of three PBDE commercial products: Penta-BDE (A), Octa-BDE (B) and Deca-BDE (C) (Alaee et al., 2003)

All PBDEs have a high lipophilicity (log K_{ow} are comprised approximately between 4 and 9) and are persistent and resistant to degradations. They have a relatively low cost of production (Darnerud et al., 2001; Wania and Dugani, 2003). PBDEs are only used as additive flame retardants to reduce the flammability of combustible materials. The Penta-BDE formulation is mainly added to polyurethane foams in household furniture. The Octa-BDE product is used in the hard casings of electrical and electronic equipments and the Deca-BDE, which has the widest industrial use, is added to polystyrene for televisions, computers and other electronic housings (Birnbaum and Staskal, 2004; de Wit, 2002; Harrad, 2010; Law, 2009).

Due to public concern, the United States Environmental Protection Agency (EPA) evaluated the risk of PBDEs. They decided in 2004 to phase out Penta-BDE and Octa-BDE by prohibiting the new manufacture or import of these mixtures (EPA, 2010a). The only North American producer

has voluntarily ceased the production of Penta-BDE and Octa-BDE mixtures since the end of 2004 (Ward et al., 2008). The US producers of Deca-BDE then committed to stop their production, import and sale by the end of 2013 (EPA, 2010b). The European Union has also taken steps towards PBDEs. It brought into effect in 2004 a legislation that prohibits the sale and the use of products containing more than 0.1% of Penta-BDE or Octa-BDE (EU, 2003b). This restriction of use implies that most Deca-BDE mixtures, which contain these congeners in small quantities, are also banned (Ward et al., 2008). Since 2006, all new electronic and electrical equipments cannot contain PBDEs in any concentrations (EU, 2003a). In 2008, Deca-BDE, which was exempted from the restrictions hitherto, was also banned by the European Court of Justice in these kind of equipment (EU, 2008). In 2009, hexa-BDEs and hepta-BDEs, corresponding to the commercial Octa-BDE product, were added to the Annex A of the Stockholm Convention. Even if some measures have been taken to reduce the production and the use of PBDEs, they are still present in much of furnitures and equipments currently used and remain a significant risk of exposure (Ward et al., 2008).

1.2.2.3. Biotransformation and toxic effects

PBDEs can enter the environment through emissions from manufacturing process, volatilization from products containing them or through waste recycling (Harrad, 2010; Streets et al., 2006). Similar to PCBs, they are currently ubiquitous in the environment (de Wit, 2002) and they tend to accumulate into lipophilic tissues because of their high lipophilicity (Covaci et al., 2002; Shaw et al., 2009; She et al., 2002; Vanden Berghe et al., 2012). PBDEs can however be subject to biotransformation through Phase I and II pathways.

Several studies highlighted the impact of PBDEs on Phase I enzymes. For example, PBDE congeners such as BDE-77, -100, -126 and -153 are able to induce *in vitro* CYP1A1, a biomarker for activation of AhR, in hepatocytes of rat, chick, trout or human (Chen et al., 2001). Nevertheless, their affinities for this receptor are weak compared to TCDD or PCB-126, a dioxin-like congener. The affinity of PBDEs with AhR does not seem to be related to the planarity as PCBs, possibly because the large size of the

bromine atoms expands the Ah receptor's binding site (Chen et al., 2001; Sanders et al., 2005). In rodents, BDE-47, -99, -153 and -209 induce CYP2B and CYP3A expression, which are biomarkers for activation of CAR and PXR (Pacyniak et al., 2007; Sanders et al., 2005). These studies suggest that animals are able to biotransform, to some extent, PBDEs by Phase I reactions. Indeed, it has been shown that rats form hydroxylated PBDEs (HO-PBDEs) from BDE-47, -99 and -209 (Chen et al., 2006; Hakk et al., 2002; Hakk and Letcher, 2003). Nevertheless, the metabolism pathway has not been conclusively shown. The biotransformation of PBDEs differs between species and congeners. For example, mouse is more capable to metabolise BDE-47 as compared to rat (Hakk and Letcher, 2003) and BDE-99 appears to be metabolised to a greater extent than BDE-47 or BDE-209 (Chen et al., 2006; Stapleton et al., 2009).

Metabolites of PBDEs, such as HO-PBDEs, have been detected in wildlife (e.g. ringed seals, grey seals, Atlantic salmon and herring) and humans (Athanasiadou et al., 2008; Haglund et al., 1997; Qiu et al., 2009; Routti et al., 2009).

PBDEs may also undergo Phase II reactions. The impact of PBDEs on Phase II enzymes was evaluated in a few studies only. DE-71 (a commercial Penta-BDE mixture) and DE-79 (a commercial Octa-BDE mixture) induce UGT in rats (Zhou et al., 2001). An up-regulation of genes encoding for GST was observed in human hepatocytes *in vitro* (Stapleton et al., 2009). Glutathione conjugate metabolites of BDE-47 and -99 were detected in bile of BDE-47 treated rats and BDE-99 treated rats, whereas glucuronide and sulfate conjugate metabolites were found in the urine (Chen et al., 2006; Sanders et al., 2006). However, the exact pathways are still unknown.

Methoxylated PBDEs (MeO-PBDEs) can be found in biota samples. In the marine environment, their origin is mainly from the bioformation in sponges and algae but they can also come from the methylation of their hydroxylated homologues by microorganisms (Haglund et al., 1997; Marsh et al., 2004; Valters et al., 2005). To date, the biotransformation of PBDEs to MeO-PBDEs has never been reported in laboratory experiments (Marsh et al., 2004). It thus seems that MeO-PBDEs have mainly a natural origin (i.e.

from non-metabolic sources such as sponges and algae) (Munschy et al., 2010).

In addition, PBDEs may undergo debromination. It has been shown in common carp, which appears to be able to debrominate BDE-99 to BDE-47 and BDE-183 to BDE-154 in the intestine and the liver (Benedict et al., 2007; Stapleton et al., 2004). In common sole, BDE-99 debromination produced preferentially BDE-49 (Munschy et al., 2011). BDE-209 undergoes debromination in the environment by photo- and thermal degradation (Costa et al., 2008; Darnerud et al., 2001).

The potential health hazards of PBDEs are significant and depend on the type of product. Studies on humans and rodents have shown several toxicological properties of PBDEs (ATSDR, 2004; Birnbaum and Staskal, 2004; Costa and Giordano, 2007; de Wit, 2002; Legler, 2008; Stoker et al., 2004; Zhou et al., 2002).. Penta-BDE mixture seems to cause negative effects at lower dose than Deca-BDE (Darnerud, 2003). Penta-BDE mixture induces the expression of several CYP enzymes and decreases the levels of circulating T_4 in rats and mice (Zhou et al., 2001; Zhou et al., 2002). BDE-99 and BDE-47, two penta-BDEs, cause neurobehavioural developmental troubles (impaired learning, memory functions and habituation) in mice offspring (Branchi et al., 2002; Eriksson et al., 2001). The toxic effects of Octa-BDE mixture seem primarily to occur at early developmental stages as fetal toxicity and teratogenicity have been reported in rats and rabbits (e.g. weight decrease and reduced ossification) (Breslin et al., 1989; Darnerud, 2003). Exposure to Deca-BDE mixture gives rise to morphological effects in the thyroid, liver and kidney of adult animals (e.g. rat, mice, rainbow trout and Daphnia). Furthermore, IARC classified PBDEs as possible carcinogenic to humans (IARC, 2011). Endocrine-disrupting effects (oestrogen receptor, TTR, retinol) have also been reported for HO-PBDEs (Canton et al., 2006; Cesh et al., 2010).

1.2.3. Organochlorine pesticides (OCP)

1.2.3.1. Hexachlorobenzene (HCB)

HCB was previously used as a fungicide on seed treatment and as a wood-preserving agent (Figure 1.14). It is also a persistent lipophilic compound (log K_{ow} = 5.47), which is able to bioaccumulate in the fat tissues and biomagnify in the food web (Kelly et al., 2007). Its use was banned in the 1970s in Europe and in the 1980s in USA (Courtney, 1979). Otherwise, HCB is still inadvertently generated as a by-product during incomplete combustion of waste incinerations where chlorine is present, during the production of other chlorine-containing chemicals and/or during the magnesium and nickel production. HCB has also been detected as impurity in pesticides (e.g. lindane, hexachlorocyclohexane and pentachlorophenol (PCP)) (Bailey, 2001; Barber et al., 2005).

Once absorbed, hexachlorobenzene is not evenly distributed in the body. Due to its lipophilic nature, it is preferentially stored in adipose tissue, and to a lesser extent, in other lipid-rich tissues (ATSDR, 2013). HCB is slowly metabolised in mammals, but can lead to the formation of major and minor metabolites. The major metabolite is PCP (Figure 1.14), followed by pentachlorobenzene. They result from the HCB biotransformation by hepatic CYP. Indeed, purified HCB induces CYP1A in three avian species *in vitro* (chicken, pheasant and Japanese quail) (Mundy, 2011). The minor metabolites are, among others, tetrachlorobenzene, pentachlorobenzene, hexachlorobenzene and tetrachloro-1,4-hydroquinone (Koss et al., 1976; To-Figueras et al., 1988). The conjugation of PCP with glutathione after the CYP action is an important biotransformation pathway (To-Figueras et al., 1997). The excretion of HCB as unchanged molecules occurs mostly by the feces, and the major metabolites, by urine (ATSDR, 2013).

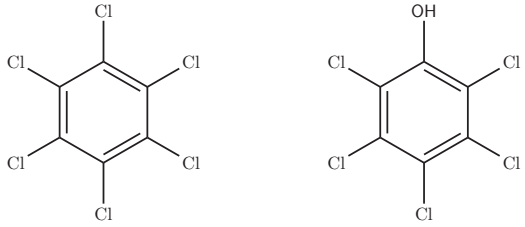

Figure 1.14 – Chemical structure of hexachlorobenzene (on left) and pentachlorophenol (on right)

HCB can induce deleterious effects on health. Porphyria is the major toxic effect of this chemical in animals and humans (Gocmen et al., 1985). As an inducer of CYP1A1 and CYP1A2, HCB can cause liver damage. It has been reported to induce hepatic and thyroid neoplasm and hormonal disruption (Cabral et al., 1977; Cabral et al., 1979), including alterations in progesterone and testosterone concentrations (Foster et al., 1992; Jarrell et al., 1993) and depletion of T_3 and T_4 (Van Raaij et al., 1993). The most notable targets of HCB toxicity are the liver, ovary, and central nervous system (ATSDR, 2013). HCB also leads to impairments of the levels and metabolism of thyroid hormones and retinoids (Addae et al., 2013; Mundy, 2011; Reed et al., 2007). HCB is also listed as a possible human carcinogen (IARC, 1997).

In addition to being the major hydroxylated metabolite of HCB, PCP (Figure 1.14) was also produced for using as wood preservative, biocide and disinfectant (Sandau et al., 2002). Once in the organism, it is mostly stored in the plasma: more than 95% of PCP are bound to plasma protein in rats and humans (Braun et al., 1977; Uhl et al., 1986). In this compartment, PCP binds to TTR, leading to a decrease of circulating T_4 (Beard et al., 1999; Sandau et al., 2002). PCP is reported to be an endocrine disruptor, to affect the thyroid hormone metabolism and is recognized as a carcinogen agent (Orton et al., 2009; Schuur et al., 1999; Zha et al., 2006).

1.2.3.2. Dichlorodiphenyltrichloroethane (DDT)

Dichlorodiphenyltrichloroethane (DDT) is one of the best known pesticides that was widely used from 1939 to control insect pests in agriculture and human health (malaria and typhus control) (Figure 1.15) (Van Metre et al., 1997). DDT is not produced naturally and thus has only an anthropogenic origin. The technical DDT is a mixture of isomers (*p,p'*-DDT, *o,p'*-DDT and *o,o'*-DDT) with dichlorodiphenyldichloroethylene (DDE) and dichlorodiphenyldichloroethane (DDD), which are considered as contaminants (Metcalf, 1995).

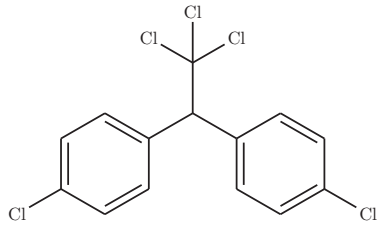

Figure 1.15 – Chemical structure of DDT

The efficiency of DDT, even at low dose, favoured its widespread use. However, some health repercussions for humans and wildlife were recognised (Smith, 2012) and the use of DDT was banned in USA in 1973. Subsequently, similar measures were taken in Western countries. In 1978, European Union decided to prohibit the placing on the market and the use of DDT (EC, 1979). In 2004, the European Parliament allowed the production and the use of DDT as an intermediate of production in a closed system until 2014 (EC, 2004). Currently, DDT is still used in some areas of the world (e.g. South Africa, Swaziland and Madagascar, where malaria is endemic) to control malaria and *o,p'*-DDT is used as a chemotherapy drug for adrenal gland cancer (ATSDR, 2002; Roberts et al., 2000).

Once absorbed by animals or humans, DDT (log K_{ow} = 6.91) is readily distributed to all body tissues with highest concentrations in the fat tissues (ATSDR, 2002). Its metabolism depends on tissues and species (Tebourbi et

al., 2006). A variety of minor metabolites can be produced in mammals, but the pathway leads mostly to the formation of DDE by dehydrochlorination and DDD by reductive dechlorination. DDT and DDD, not DDE, can be further metabolised in 2,2-*bis*(*p*-chlorophenyl) acetic acid (DDA), the major urinary metabolite in mammals (Figure 1.16). The detection of DDE and DDD in the organisms can be explained either by their presence in the DDT mixture or by their bioformation from DDT. Moreover, bacteria, fungi and algae may be able to convert DDT to DDE under both aerobic and anaerobic conditions in the environment, and then be absorbed by animals and humans (ATSDR, 2002). Further metabolism of DDE is apparently slow and therefore, this form is retained in the adipose tissue (ATSDR, 2002; Chen et al., 2009). DDT, DDE and DDD have been shown to induce their own hepatic metabolism in rodents and hamsters by CYP2B and CYP3A, no CYP1A (ATSDR, 2002; Lubet et al., 1998). After reactions of phase I, most of metabolites are excreted in the conjugated form (e.g. glucuronic acid, serine and aspartic acid conjugates). Methylsulfonyl metabolites can also be produced by the microbiota of the large intestine and be reabsorbed (Bakke et al., 1982; Letcher et al., 1998). The excretion in humans and rodents occurs mainly by urine, and to some extent in feces (via biliary excretion) and milk (ATSDR, 2002).

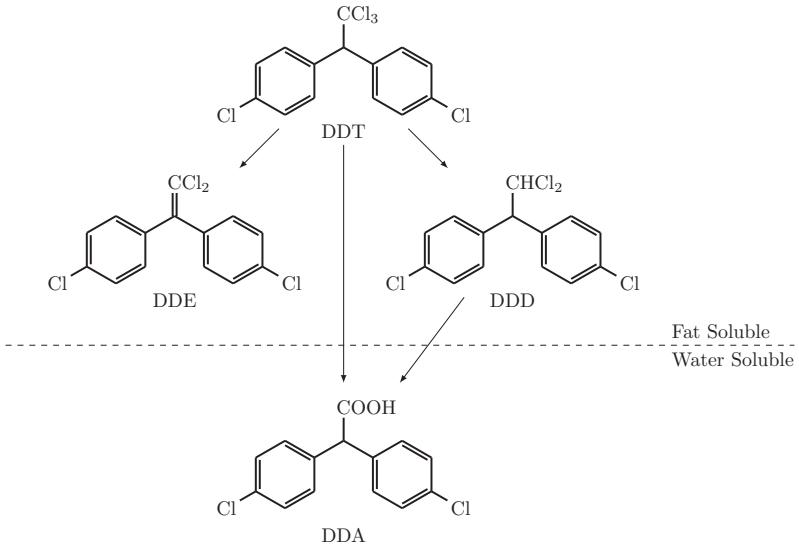

Figure 1.16 – Formation of dichlorodiphenyltrichloroethane (DDT) metabolites. DDA, 2,2-bis(p-chlorophenyl) acetic acid; DDD, dichlorodiphenyldichloroethane; DDE, dichlorodiphenyldichloroethylene (adapted from Chen et al. (2009)).

Health effects of DDT and its metabolites are numerous. The most known effect is an impairment of nerve impulse conduction that was observed in both humans and animals, leading to tremors and convulsions. In addition, DDT is able to induce marked alterations on development and reproduction in animals. DDT has the strongest estrogen-like action, whereas *p,p'*-DDE has antiandrogenic properties. DDT and its metabolites can cause cancer, primarily in the liver. Additional hepatic effects include induction of microsomal enzymes, hypertrophia, hyperplasia and necrosis (ATSDR, 2002; Smith, 2012).

1.3. Adipose tissue as a source of persistent organic pollutants

As described above, POPs share lipophilic and persistent properties. They thus tend to bioaccumulate and distribute into lipophilic compartments, especially within the adipose tissue. Despite the cellular complexity of adipose tissue, the storage of POPs is believed to be mainly in adipocytes (Bourez et al., 2012b). Furthermore, *in vitro* studies evidenced that the amounts of accumulated PCBs in adipocytes were strongly correlated to the amounts of adipocyte TGs (Bourez et al., 2012a; Bourez et al., 2013). During periods of lipolysis, TGs stored within LDs are hydrolysed and the resulting FAs are mainly released in the blood circulation. Several studies evidenced the mobilisation of POPs from adipose tissue during periods of negative energy balance (Debier et al., 2006; Dirtu et al., 2013; Vanden Berghe et al., 2012).

In humans, observations regarding the release of POPs come mainly from studies on drastic weight loss in obese subjects thanks to bariatric surgery and hypocaloric diet. As the total weight of adipose tissue decreases, the concentrations of POPs expressed per unit of lipids increase. Further to weight loss, the concentrations of POPs increase in blood (Hue et al., 2006; Imbeault et al., 2001; Kim et al., 2011). It was indeed demonstrated that the changes of weight are inversely correlated with the POP concentrations in serum (Lim et al., 2011). Moreover, the released POPs may be reabsorbed by the remaining fat. Once mobilised, they can be distributed to other tissues or fluids. Indeed, several studies on breast milk have shown the presence of POPs in milk, which can originate, at least partly from the adipose tissue (Antignac et al., 2009; Kanja et al., 1992; Suzuki et al., 2005; Waliszewski et al., 2001).

An experimental study has shown that weight loss in mice, resulting from a period of fast, involves an increase of HCB concentrations in the adipose tissue. They also noted a redistribution of POPs from adipose tissue to other organs such as the brain and the liver during caloric restriction

(Jandacek et al., 2005). The decrease of mass of adipose tissue may thus lead to a partial redistribution of POPs.

Data from POP mobilisation are also gathered from wildlife and specially, from marine mammals that are known to be highly contaminated. Furthermore, they are characterised by large adipose deposit and undergo extended periods of fast. For example, studies on weaned NES pups as well as lactating grey seal and NES females have shown that fasting was accompanied by an increase of plasma concentrations of POPs, mainly due to a release from contaminated blubber (i.e. the subcutaneous adipose tissue). Their data have also indicated that POP concentrations, expressed per unit of lipids, increased in the blubber. These paradoxical observations are linked to the fact that POPs are not as efficiently mobilised from adipose tissue as lipids and thus, tend to concentrate in the remaining amount of blubber with the progression of the fast (Debier et al., 2003; Debier et al., 2006; Debier et al., 2012; Vanden Berghe et al., 2012). Similar to humans, it has also been suggested that the remaining adipose tissue can take back the released POPs. A consequence of POP release from blubber to blood during periods of fast is the presence of POPs in the milk of lactating grey seal and NES females (Debier et al., 2003; Vanden Berghe et al., 2012). Indeed, females in these species fast entirely during lactation and POPs present in the milk reflect, to some extent, their release from the adipose tissue. POPs appear to be selectively mobilised from blubber to serum according to their physico-chemical properties, which can be reflected, for example, by a coefficient of partition between octanol and water (log K_{ow}). Within PBDE and PCB families, the lipophilic character of congener increases with the number of bromine and chlorine atoms. This involves that the less lipophilic compounds are more readily mobilised from adipose tissue (Vanden Berghe et al., 2012).

To conclude, many studies on humans and animals agree to say that the adipose tissue is a source of POPs for the organism during a period of negative energy balance. The mobilisation appears to be influenced by the lipophilic character of these molecules. It thus seems reasonable to think that the FA composition of adipocyte TGs may also interact with the rate of

mobilisation of POPs. However, to the best of our knowledge, studies investigating this hypothesis are lacking.

A large mixture of POPs contaminates the tissues *in vivo*. A possible interaction can exist between the different molecules during their release from the adipose tissue. Due to the complexity of the *in vivo* situation, the impact of the presence of other lipophilic pollutants on the behaviour of individual POP congeners has never been investigated.

Those different considerations constitute interesting avenues for exploration in order to get a better understanding of the toxicokinetics of pollutants within the adipose tissue.

1.4. References

Aarsland, A., et al., 1997. Hepatic and whole-body fat synthesis in humans during carbohydrate overfeeding. The American Journal of Clinical Nutrition. 65**,** 1774-1782.

Addae, C., et al., 2013. Effect of the environmental pollutant hexachlorobenzene (HCB) on the neuronal differentiation of mouse embryonic stem cells. International Journal of Environmental Research and Public Health. 10**,** 5244-5256.

Ahmadian, M., et al., 2010. Lipolysis in adipocytes. International Journal of Biochemistry & Cell Biology. 42**,** 555-559.

Alaee, M., et al., 2003. An overview of commercially used brominated flame retardants, their applications, their use patterns in different countries/regions and possible modes of release. Environment International. 29**,** 683-689.

Amaral Mendes, J., 2002. The endocrine disrupters: a major medical challenge. Food and Chemical Toxicology. 40**,** 781-788.

Antignac, J.-P., et al., 2009. Exposure assessment of French women and their newborn to brominated flame retardants: determination of tri- to deca-polybromodiphenylethers (PBDE) in maternal adipose tissue, serum, breast milk and cord serum. Environmental Pollution. 157**,** 164-173.

Arner, P., 1993. Adenosine, prostaglandins and phosphodiesterase as targets for obesity pharmacotherapy. International Journal of Obesity. 17**,** S57-S59.

Arner, P., 2005. Human fat cell lipolysis: Biochemistry, regulation and clinical role. Best Practice & Research Clinical Endocrinology & Metabolism. 19**,** 471-482.

Athanasiadou, M., et al., 2008. Polybrominated diphenyl ethers (PBDEs) and bioaccumulative hydroxylated PBDE metabolites in young humans from Managua, Nicaragua. Environmental Health Perspectives. 116**,** 400-408.

ATSDR, 2002. Agency for Toxic Substances and Disease Registry. Toxicological profile for DDT, DDE and DDD. Agency for Toxic Substances and Disease Registry, Public Health Service, U.S. Department of Health and Human Services. 497 pp.

ATSDR, 2004. Agency for Toxic Substances and Disease Registry. Toxicological profile for polybrominated biphenyls and polybrominated diphenyl ethers.

Agency for Toxic Substances and Disease Registry, Public Health Service, U.S. Department of Health and Human Services. 316 pp.

ATSDR, 2013. Agency for Toxic Substances and Disease Registry. Draft toxicological profile for hexachlorobenzene. Agency for Toxic Substances and Disease Registry, Public Health Service, U.S. Department of Health and Human Services. 448 pp.

ATSDR, 2014. Agency for Toxic Substances and Disease Registry. Toxicological profile for polychlorinated biphenyls (PCBs). Agency for Toxic Substances and Disease Registry, Public Health Service, U.S. Department of Health and Human Services. 316 pp.

Avram, M. M., et al., 2007. Subcutaneous fat in normal and diseased states: 3. Adipogenesis: From stem cell to fat cell. Journal of the American Academy of Dermatology. 56**,** 472-492.

Bailey, R. E., 2001. Global hexachlorobenzene emissions. Chemosphere. 43**,** 167-182.

Bakke, J., et al., 1982. Metabolism of 2,4',5-trichlorobiphenyl by the mercapturic acid pathway. Science. 217**,** 645-647.

Ballard, F., 1972. Effects of fasting and refeeding on the concentrations of glycolytic intermediates and the regulation of lipogenesis in rat adipose tissue *in vivo*. Biochimica et Biophysica Acta (BBA). 273**,** 110-118.

Ballschmiter, K., Zell, M., 1980. Analysis of polychlorinated biphenyls (PCB) by glass capillary gas chromatography. Fresenius' Zeitschrift für Analytische Chemie. 302**,** 20-31.

Barber, J. L., et al., 2005. Hexachlorobenzene in the global environment: emissions, levels, distribution, trends and processes. Science of the Total Environment. 349**,** 1-44.

Bartz, R., et al., 2007. Lipidomics reveals that adiposomes store ether lipids and mediate phospholipid traffic. Journal of Lipid Research. 48**,** 837-847.

Beale, E. G., et al., 2002. Glyceroneogenesis comes of age. The FASEB Journal. 16**,** 1695-1696.

Beard, A., et al., 1999. Reproductive and endocrine function in rams exposed to the organochlorine pesticides lindane and pentachlorophenol from conception. Journal of Reproduction and Fertility. 115**,** 303-314.

Benedict, R. T., et al., 2007. Debromination of polybrominated diphenyl ether-99 (BDE-99) in carp (*Cyprinus carpio*) microflora and microsomes. Chemosphere. 69**,** 987-993.

Bertile, F., et al., 2003. Hypothalamic gene expression in long-term fasted rats: relationship with body fat. Biochemical and Biophysical Research Communications. 303, 1106-1113.

Bezaire, V., Langin, D., 2009. Regulation of adipose tissue lipolysis revisited. Proceedings of the Nutrition Society. 68, 350-360.

Birnbaum, L. S., Staskal, D. F., 2004. Brominated flame retardants: cause for concern? Environmental Health Perspectives. 112, 9-17.

Boelsterli, U. A., 2007. Mechanistic toxicology: the molecular basis of how chemicals disrupt biological targets. CRC Press.

Borg, M. L., et al., 2011. Pigment epithelium–derived factor regulates lipid metabolism via adipose triglyceride lipase. Diabetes. 60, 1458-1466.

Boulware, S., et al., 1992. Diverse effects of insulin-like growth factor I on glucose, lipid, and amino acid metabolism. American Journal of Physiology-Endocrinology and Metabolism. 262, E130-E133.

Bourez, S., et al., 2012a. Accumulation capacity of primary cultures of adipocytes for PCB-126: Influence of cell differentiation stage and triglyceride levels. Toxicology Letters. 214, 243-250.

Bourez, S., et al., 2012b. Accumulation of polychlorinated biphenyls in adipocytes: Selective targeting to lipid droplets and role of caveolin-1. PLoS ONE. 7, e31834.

Bourez, S., et al., 2013. The dynamics of accumulation of PCBs in cultured adipocytes vary with the cell lipid content and the lipophilicity of the congener. Toxicology Letters. 216, 40-46.

Bradley, R. L., et al., 2005. Neuropeptides, including neuropeptide Y and melanocortins, mediate lipolysis in murine adipocytes. Obesity Research. 13, 653-661.

Branchi, I., et al., 2002. Effects of perinatal exposure to a polybrominated diphenyl ether (PBDE 99) on mouse neurobehavioural development. Neurotoxicology. 23, 375-384.

Braun, W., et al., 1977. The pharmacokinetics and metabolism of pentachlorophenol in rats. Toxicology and Applied Pharmacology. 41, 395-406.

Breslin, W., et al., 1989. Teratogenic evaluation of a polybromodiphenyl oxide mixture in New Zealand White rabbits following oral exposure. Fundamental and Applied Toxicology. 12, 151-157.

Cabral, J., et al., 1979. Carcinogenesis of hexachlorobenzene in mice. International Journal of Cancer. 23**,** 47-51.

Cabral, J., et al., 1977. Carcinogenic activity of hexacholorobenzene in hamsters.

Canton, R. F., et al., 2006. *In vitro* effects of brominated flame retardants and metabolites on CYP17 catalytic activity: A novel mechanism of action? Toxicology and Applied Pharmacology. 216**,** 274-281.

Castellini, M., Rea, L., 1992. The biochemistry of natural fasting at its limits. Experientia. 48**,** 575-582.

Cesh, L. S., et al., 2010. Polyhalogenated aromatic hydrocarbons and metabolites: relation to circulating thyroid hormone and retinol in nestling bald eagles (*Haliaeetus leucocephalus*). Environmental Toxicology and Chemistry. 29**,** 1301-1310.

Champagne, C. D., et al., Fasting physiology of the pinnipeds: The challenges of fasting while maintaining high energy expenditure and nutrient delivery for lactation. Comparative physiology of fasting, starvation, and food limitation. M. D. McCue, Springer Berlin Heidelberg, 2012, 309-336.

Chandra, V., et al., 2008. Structure of the intact PPAR-gamma – RXR-alpha; nuclear receptor complex on DNA. Nature. 456**,** 350-356.

Chen, G., et al., 2001. Synthesis of polybrominated diphenyl ethers and their capacity to induce CYP1A by the Ah receptor mediated pathway. Environmental Science & Technology. 35**,** 3749-3756.

Chen, L.-J., et al., 2006. Metabolism and disposition of 2,2',4,4',5-pentabromodiphenyl ether (BDE99) following a single or repeated administration to rats or mice. Xenobiotica. 36**,** 515-534.

Chen, Z., et al., 2009. 2,2-bis(4-Chlorophenyl) Acetic Acid (DDA), a water-soluble urine biomarker of DDT metabolism in humans. International Journal of Toxicology. 28**,** 528-533.

Chmurzynska, A., 2006. The multigene family of fatty acid-binding proteins (FABPs): function, structure and polymorphism. Journal of Applied Genetics. 47**,** 39-48.

Cinti, S., Functional anatomy of the adipose organ. In: Cachexia and Wasting: A Modern Approach. Springer, 2006, 3-22.

Cinti, S., The adipose organ. In: Adipose tissue and adipokines in health and disease. Springer, 2007, 3-19.

Cinti, S., 2012. The adipose organ at a glance. Disease Models & Mechanisms. 5, 588-594.

Conner, W., et al., 1996. Differential mobilization of fatty acids from adipose tissue. Journal of Lipid Research. 37, 290-298.

Conti, M., Beavo, J., 2007. Biochemistry and physiology of cyclic nucleotide phosphodiesterases: essential components in cyclic nucleotide signaling. Annual Review of Biochemistry. 76, 481-511.

Costa, L. G., Giordano, G., 2007. Developmental neurotoxicity of polybrominated diphenyl ether (PBDE) flame retardants. Neurotoxicology. 28, 1047-1067.

Costa, L. G., et al., 2008. Polybrominated diphenyl ether (PBDE) flame retardants: environmental contamination, human body burden and potential adverse health effects. Acta Biomed. 79, 172-183.

Courtney, K. D., 1979. Hexachlorobenzene (HCB): A review. Environmental Research. 20, 225-266.

Covaci, A., et al., 2002. Distribution of organobrominated and organochlorinated contaminants in Belgian human adipose tissue. Environmental Research. 88, 210-218.

Daly, J., et al., 1972. Arene oxides and the NIH shift: the metabolism, toxicity and carcinogenicity of aromatic compounds. Experientia. 28, 1129-1149.

Darnerud, P. O., 2003. Toxic effects of brominated flame retardants in man and in wildlife. Environment International. 29, 841-853.

Darnerud, P. O., et al., 2001. Polybrominated diphenyl ethers: occurrence, dietary exposure, and toxicology. Environmental Health Perspectives. 109, 49-68.

De Voogt, P., Brinkman, U., 1989. Production, properties and usage of polychlorinated biphenyls. Halogenated Biphenyls, Terphenyls, Naphthalenes, Dibenzodioxins and Related Products. 3-45.

de Wit, C. A., 2002. An overview of brominated flame retardants in the environment. Chemosphere. 46, 583-624.

Debier, C., et al., 2006. Mobilization of PCBs from blubber to blood in northern elephant seals (*Mirounga angustirostris*) during the post-weaning fast. Aquatic Toxicology. 80, 149-157.

Debier, C., et al., 2012. Differential changes of fat-soluble vitamins and pollutants during lactation in northern elephant seal mother–pup pairs. Comparative Biochemistry and Physiology Part A. 162, 323-330.

Debier, C., et al., 2003. Quantitative dynamics of PCB transfer from mother to pup during lactation in UK grey seals *Halichoerus grypus*. Marine Ecology Progress Series. 247, 237-248.

Denison, M. S., et al., 2002. Ligand binding and activation of the Ah receptor. Chemico-Biological Interactions. 141, 3-24.

Dinel, A., et al., Metabolism of fatty acids in adipocytes. In: Novel insights into adipose cell functions. Springer, 2010, 21-43.

Dirtu, A. C., et al., 2013. Dynamics of organohalogenated contaminants in human serum from obese individuals during one year of weight loss treatment. Environmental Science & Technology. 47, 12441-12449.

Dirtu, A. C., et al., 2010. Distribution of PCBs, their hydroxylated metabolites, and other phenolic contaminants in human serum from two European countries. Environmental Science & Technology. 44, 2876-2883.

Dodt, C., et al., 2003. Sympathetic control of white adipose tissue in lean and obese humans. Acta Physiologica Scandinavica. 177, 351-357.

Dusserre, E., et al., 2000. Differences in mRNA expression of the proteins secreted by the adipocytes in human subcutaneous and visceral adipose tissues. Biochimica et Biophysica Acta (BBA). 1500, 88-96.

EC, 1979. European Commission. Council Directive 79/117/EEC of 21 December 1978 prohibiting the placing on the market and use of plant protection products containing certain active substances. Official Journal of the European Union Legislation. 33, 36-40.

EC, 1985. Council Directive 85/467/EEC of 1 October 1985 amending for the sixth time (PCBs/PCTs) Directive 76/769/EEC on the approximation of the laws, regulations and administrative provisions of the Member States relating to restrictions on the marketing and use of certain dangerous substances and preparations. Official Journal of the European Union Legislation. 269, 56-58.

EC, 2002. European Commission. Council L221/8. Official Journal of the European Communities. 262, 8-36.

EC, 2004. European Commission. Regulation (EC) No 850/2004 of the European Parliament and of the Council of 29 April 2004 on persistent organic pollutants and amending Directive 79/117/EEC. Official Journal of the European Union Legislation. 158, 7-49.

EPA, 1977. U.S. Environmental Protection Agency. Code of Federal Regulations. 40 CFR 129.105.

EPA, 1979a. U.S. Environmental Protection Agency. Code of Federal Regulations. 40 CFR 761.60-761.65.

EPA, 1979b. U.S. Environmental Protection Agency. Polychlorinated biphenyls (PCBs) in manufacturing, processing, distribution in commerce, and use prohibition; Final rule. Federal Register 44:31514-31568.

EPA, 2010a. Office of Pollution Prevention and Toxics (OPPT). Polybrominated Diphenylethers. Online at: http://www.Epa.Gov/oppt/existingchemicals/pubs/actionplans/pbde.html.

EPA, 2010b. US Environmental Protection Agency. DecaBDE phase-out initiative. Online at: http://www.epa.gov/oppt/existingchemicals/pubs/actionplans/deccadbe.html.

Erickson, M. D., Kaley II, R. G., 2011. Applications of polychlorinated biphenyls. Environmental Science and Pollution Research. 18**,** 135-151.

Eriksson, P., et al., 2001. Brominated flame retardants: a novel class of developmental neurotoxicants in our environment? Environmental Health Perspectives. 109**,** 903-908.

EU, 2003a. Directive 2002/95/EC of the European Parliament and of the Council of 27 January 2003 on the restriction of the use of certain hazardous substances in electrical and electronic equipment Official Journal of the European Union Legislation. 37**,** 19-23.

EU, 2003b. Directive 2003/11/EC of the European Parliament and of the Council of 6 February 2003 amending for the 24th time Council Directive 76/769/EEC relating to restrictions on the marketing and use of certain dangerous substances and preparations (pentabromodiphenyl ether, octabromodiphenyl ether). Official Journal of the European Union Legislation. 42**,** 45-46.

EU, 2008. Judgment of the Court (Grand Chamber) of 1 April 2008. Directive 2002/95/EC- Electrical and electronic equipment - Restriction of use of certain hazardous substances - Decabromodiphenyl ether ('DecaBDE') - Commission Decision 2005/717/EC - Exemption of DecaBDE from the prohibition on use - Actions for annulment - Commission's implementing powers - Infringement of the enabling provision. Joined cases C-14/06 and C-295/06. European Court Reports. I-01649

Farmer, S. R., 2006. Transcriptional control of adipocyte formation. Cell Metabolism. 4**,** 263-273.

Ferre, P., Métabolisme énergétique des lipides. In: Traité de nutrition artificielle de l'adulte. Springer, 2007, 93-102.

Feve, B., 2005. Adipogenesis: cellular and molecular aspects. Best Practice & Research Clinical Endocrinology & Metabolism. 19**,** 483-499.

Feve, B., Mercier, N., 2007. Adipocyte, une cellule en devenir. MT Cardio. 3**,** 6-17.

Fielding, B. A., Frayn, K. N., 1998. Lipoprotein lipase and the disposition of dietary fatty acids. British Journal of Nutrition. 80**,** 495-502.

Fonseca-Alaniz, M. H., et al., 2007. Adipose tissue as an endocrine organ: from theory to practice. Jornal de Pediatria. 83**,** S192-S203.

Foster, W. G., et al., 1992. Hexachlorobenzene (HCB) suppresses circulating progesterone concentrations during the luteal phase in the cynomolgus monkey. Journal of Applied Toxicology. 12**,** 13-17.

Foufelle, F., Ferre, P., Mechanism of storage and synthesis of fatty acids and triglycerides in white adipocytes. In: Physiology and physiopathology of adipose tissue. J.-P. Bastard and B. Feve Eds., Springer-Verlag France, 2013, 101-121.

Fowler, M. A., et al., 2008. Hormonal regulation of glucose clearance in lactating northern elephant seals (*Mirounga angustirostris*). The Journal of Experimental Biology. 211**,** 2943-9.

Frayn, K., et al., 2006. Fatty acid metabolism in adipose tissue, muscle and liver in health and disease. Essays in Biochemistry. 42**,** 89-103.

Gesta, S., et al., 2006. Evidence for a role of developmental genes in the origin of obesity and body fat distribution. Proceedings of the National Academy of Sciences. 103**,** 6676-6681.

Gevao, B., et al., 2009. Persistent organic pollutants in the developing world. Persistent Organic Pollutants. 137-169.

Gimeno, R., et al., Fatty acid transport proteins. Google Patents, 2003.

Giorgino, F., et al., 2005. Regional differences of insulin action in adipose tissue: insights from *in vivo* and *in vitro* studies. Acta Physiologica Scandinavica. 183**,** 13-30.

Girard, J., et al., 1997. Mechanisms by which carbohydrates regulate expression of genes for glycolytic and lipogenic enzymes. Annual Review of Nutrition. 17**,** 325-352.

Gocmen, A., et al., 1985. Porphyria turcica: hexachlorobenzene-induced porphyria. IARC Scientific Publications. 567-573.

Granneman, J. G., et al., 2007. Analysis of lipolytic protein trafficking and interactions in adipocytes. Journal of Biological Chemistry. 282**,** 5726-5735.

Granneman, J. G., et al., 2009. Perilipin controls lipolysis by regulating the interactions of AB-hydrolase containing 5 (Abhd5) and adipose triglyceride lipase (Atgl). Journal of Biological Chemistry. 284**,** 34538-34544.

Gregoire, F. M., et al., 1998. Understanding adipocyte differentiation. Physiological Reviews. 78**,** 783-809.

Guan, H.-P., et al., 2002. A futile metabolic cycle activated in adipocytes by antidiabetic agents. Nature Medicine. 8**,** 1122-1128.

Haemmerle, G., et al., 2006. Defective lipolysis and altered energy metabolism in mice lacking adipose triglyceride lipase. Science. 312**,** 734-737.

Haemmerle, G., et al., 2002. Hormone-sensitive lipase deficiency in mice causes diglyceride accumulation in adipose tissue, muscle, and testis. Journal of Biological Chemistry. 277**,** 4806-4815.

Haglund, P. S., et al., 1997. Identification and quantification of polybrominated diphenyl ethers and methoxy-polybrominated diphenyl ethers in Baltic biota. Environmental Science & Technology. 31**,** 3281-3287.

Hakk, H., et al., 2002. Tissue disposition, excretion and metabolism of 2,2',4,4',5-pentabromodiphenyl ether (BDE-99) in the male Sprague-Dawley rat. Xenobiotica. 32**,** 369-382.

Hakk, H., Letcher, R. J., 2003. Metabolism in the toxicokinetics and fate of brominated flame retardants - a review. Environment International. 29**,** 801-828.

Hansen, B. G., et al., 1999. QSARs for K_{OW} and K_{OC} of PCB congeners: A critical examination of data, assumptions and statistical approaches. Chemosphere. 39**,** 2209-2228.

Harrad, S., 2009. Beyond the Stockholm Convention: An introduction to current issues and future challenges in POPs research. Persistent Organic Pollutants. 1-4.

Harrad, S., 2010. Persistent organic pollutants. Wiley Online Library.

Harwood Jr, H. J., 2012. The adipocyte as an endocrine organ in the regulation of metabolic homeostasis. Neuropharmacology. 63**,** 57-75.

Hausman, D., et al., 2001. The biology of white adipocyte proliferation. Obesity Reviews. 2**,** 239-254.

Hellerstein, M., et al., 1991. Measurement of *de novo* hepatic lipogenesis in humans using stable isotopes. Journal of Clinical Investigation. 87**,** 1841-1852.

Hibuse, T., et al., 2005. Aquaporin 7 deficiency is associated with development of obesity through activation of adipose glycerol kinase. Proceedings of the National Academy of Sciences of the United States of America. 102**,** 10993-10998.

Houser, D., Costa, D., 2001. Protein catabolism in suckling and fasting northern elephant seal pups (*Mirounga angustirostris*). Journal of Comparative Physiology B. 171**,** 635-642.

Houser, D. S., et al., 2007. Lipolysis and glycerol gluconeogenesis in simultaneously fasting and lactating northern elephant seals. American Journal of Physiology - Regulatory, Integrative and Comparative Physiology. 293**,** R2376-R2381.

Huang, S., Czech, M. P., 2007. The GLUT4 glucose transporter. Cell Metabolism. 5**,** 237-252.

Hue, O., et al., 2006. Increased plasma levels of toxic pollutants accompanying weight loss induced by hypocaloric diet or by bariatric surgery. Obesity Surgery. 16**,** 1145-1154.

IARC, 1997. Hexachlorobenzene. IARC monographs on the evaluation of carcinogenic risk of chemicals to humans. Lyon: International Agency for Research on Cancer. 79**,** 493-568.

IARC, 2011. World Health Organization International Agency for Research on Cancer. Agents reviewed by the IARC monographs. 1-96.

IARC, 2014. Agents Classified by the IARC Monographs. Online at: http://monographs.iarc.fr/ENG/Classification/.

Ibrahim, M. M., 2010. Subcutaneous and visceral adipose tissue: structural and functional differences. Obesity Reviews. 11**,** 11-18.

Imbeault, P., et al., 2001. Increase in plasma pollutant levels in response to weight loss in humans is related to *in vitro* subcutaneous adipocyte basal lipolysis. International Journal of Obesity and Related Metabolic Disorders. 25**,** 1585-91.

James, M. O., 2001. Polychlorinated biphenyls: metabolism and metabolites. PCBs-Recent Advances in Environmental Toxicology and Health Effects (Robertson LW, Hansen LG, eds). Lexington, KY: University Press of Kentucky. 35-46.

Jandacek, R. J., et al., 2005. Effects of yo-yo diet, caloric restriction, and olestra on tissue distribution of hexachlorobenzene. American Journal of Physiology-Gastrointestinal and Liver Physiology. 288, G292-G299.

Jarrell, J. F., et al., 1993. Hexachlorobenzene toxicity in the monkey primordial germ cell without induced porphyria. Reproductive Toxicology. 7, 41-47.

Kanja, L. W., et al., 1992. A comparison of organochlorine pesticide residues in maternal adipose tissue, maternal blood, cord blood, and human milk from mother/infant pairs. Archives of Environmental Contamination and Toxicology. 22, 21-24.

Kazantzis, M., Stahl, A., 2012. Fatty acid transport proteins, implications in physiology and disease. Biochimica et Biophysica Acta (BBA). 1821, 852-857.

Kelly, B. C., et al., 2007. Food web-specific biomagnification of persistent organic pollutants. Science. 317, 236-239.

Kersten, S., et al., 2000. Roles of PPARs in health and disease. Nature. 405, 421-424.

Khan, S. A., Vanden Heuvel, J. P., 2003. Reviews: current topics: role of nuclear receptors in the regulation of gene expression by dietary fatty acids (review). The Journal of Nutritional Biochemistry. 14, 554-567.

Kim, M. J., et al., 2011. Fate and complex pathogenic effects of dioxins and polychlorinated biphenyls in obese subjects before and after drastic weight loss. Environmental Health Perspectives. 119, 377-383.

Koss, G., et al., 1976. Studies on the toxicology of hexachlorobenzene. Archives of Toxicology. 35, 107-114.

Kretschmer, X. C., Baldwin, W. S., 2005. CAR and PXR: xenosensors of endocrine disrupters? Chemico-Biological Interactions. 155, 111-128.

Lafontan, M., Berlan, M., 1995. Fat cell α_2-adrenoceptors: The regulation of fat cell function and lipolysis. Endocrine Reviews. 16, 716-738.

Lafontan, M., Berlan, M., 2003. Do regional differences in adipocyte biology provide new pathophysiological insights? Trends in Pharmacological Sciences. 24, 276-283.

Lafontan, M., et al., 2008. Control of lipolysis by natriuretic peptides and cyclic GMP. Trends in Endocrinology & Metabolism. 19, 130-137.

Lake, A. C., et al., 2005. Expression, regulation, and triglyceride hydrolase activity of adiponutrin family members. Journal of Lipid Research. 46, 2477-2487.

Lans, M. C., et al., 1993. Structure-dependent, competitive interaction of hydroxy-polychlorobiphenyls, -dibenzo-*p*-dioxins and -dibenzofurans with human transthyretin. Chemico-Biological Interactions. 88**,** 7-21.

Large, V., et al., 2004. Metabolism of lipids in human white adipocyte. Diabetes & Metabolism. 30**,** 294-309.

Law, R., 2009. Brominated flame retardants. John Wiley & Sons, Ltd. pp. 5-24.

Le Boeuf, B. J., Laws, R. M., 1994. Elephant seals: population ecology, behavior, and physiology. Univ of California Press.

Legler, J., 2008. New insights into the endocrine disrupting effects of brominated flame retardants. Chemosphere. 73**,** 216-222.

Letcher, R., et al., Methyl sulfone and hydroxylated metabolites of polychlorinated biphenyls. O. Hutzinger and J. Paasivirta Eds., Springer Berlin / Heidelberg, 2000, 315-359.

Letcher, R. J., et al., 1998. Biotransformation *versus* bioaccumulation: Sources of methyl sulfone PCB and 4,4'-DDE metabolites in the polar bear food chain. Environmental Science & Technology. 32**,** 1656-1661.

Lim, J. S., et al., 2011. Inverse associations between long-term weight change and serum concentrations of persistent organic pollutants. International Journal of Obesity. 35**,** 744-747.

Lubet, R. W. N. R. A., et al., 1998. Comparative pharmacodynamics of CYP2B induction by DDT, DDE, and DDD in male rat liver and cultured rat hepatocytes. Journal of Toxicology and Environmental Health Part A. 53**,** 455-477.

Marsh, G., et al., 2004. Identification of hydroxylated and methoxylated polybrominated diphenyl ethers in Baltic Sea salmon (*Salmo salar*) blood. Environmental Science & Technology. 38**,** 10-18.

Maughan, R., et al., 2010. The effects of fasting on metabolism and performance. British Journal of Sports Medicine. 44**,** 490-494.

Mazzucotelli, A., et al., 2007. The transcriptional coactivator peroxisome proliferator-activated ceceptor (PPAR) γ coactivator-1α and the nuclear receptor PPARα control the expression of glycerol kinase and metabolism genes independently of PPARγ activation in human white adipocytes. Diabetes. 56**,** 2467-2475.

Metcalf, R. L., Insect control technology. In: Kirk-Othmer encyclopedia of chemical technology. John Wiley & Sons, Inc., 1995.

Miyoshi, H., et al., 2007. Control of adipose triglyceride lipase action by serine 517 of perilipin A globally regulates protein kinase A-stimulated lipolysis in adipocytes. Journal of Biological Chemistry. 282**,** 996-1002.

Moro, C., et al., 2007. Phosphodiesterase-5A and neutral endopeptidase activities in human adipocytes do not control atrial natriuretic peptide-mediated lipolysis. British Journal of Pharmacology. 152**,** 1102-1110.

Mundy, L., Cytochrome P4501A induction by highly purified hexachlorobenzene in primary cultures of avian hepatocytes. University of Ottawa, 2011.

Munschy, C., et al., 2011. Dietary exposure of juvenile common sole (*Solea solea* L.) to polybrominated diphenyl ethers (PBDEs): Part 1. Bioaccumulation and elimination kinetics of individual congeners and their debrominated metabolites. Environmental Pollution. 159**,** 229-237.

Munschy, C., et al., 2010. Dietary exposure of juvenile common sole (*Solea solea* L.) to polybrominated diphenyl ethers (PBDEs): Part 2. Formation, bioaccumulation and elimination of hydroxylated metabolites. Environmental Pollution. 158**,** 3527-3533.

Nelson, D. L., Cox, M. M., Glycolysis, gluconeogenesis, and the pentose phosphate pathway. In: Principles of Biochemistry. W. H. Freeman, New-York, 2008a, 527-568.

Nelson, D. L., Cox, M. M., Hormonal regulation and integration of mammalian metabolism. In: Principles of Biochemistry. W. H. Freeman, New-York, 2008b, 901-944.

Nelson, D. L., Cox, M. M., Lipid biosynthesis. In: Principles of Biochemistry. W. H. Freeman, New-York, 2008c, 805-850.

Noren, D. P., et al., 2003. Energy reserve utilization in northern elephant seal (*Mirounga angustirostris*) pups during the postweaning fast: size does matter. Journal of Comparative Physiology B. 173**,** 443-454.

Orton, F., et al., 2009. Endocrine disrupting effects of herbicides and pentachlorophenol: *in vitro* and *in vivo* evidence. Environmental Science & Technology. 43**,** 2144-2150.

Pacyniak, E. K., et al., 2007. The flame retardants, polybrominated diphenyl ethers, are pregnane X receptor activators. Toxicological Sciences. 97**,** 94-102.

PEN, 2009. PCBs Elimination Network. Conference of the Parties to the Stockholm Convention. Decision SC-4/5.

Portigal, C. L., et al., 2002. Polychlorinated biphenyls interfere with androgen-induced transcriptional activation and hormone binding. Toxicology and Applied Pharmacology. 179, 185-194.

Prins, J. B., O'rahilly, S., 1997. Regulation of adipose cell number in man. Clinical Science. 92, 3-11.

Qiu, X., et al., 2009. Hydroxylated metabolites of polybrominated diphenyl ethers in human blood samples from the United States. Environmental Health Perspectives. 117, 93-98.

Raclot, T., 2003. Selective mobilization of fatty acids from adipose tissue triacylglycerols. Progress in Lipid Research. 42, 257-288.

Raclot, T., Groscolas, R., 1993. Differential mobilization of white adipose tissue fatty acids according to chain length, unsaturation, and positional isomerism. Journal of Lipid Research. 34, 1515-1526.

Raclot, T., Groscolas, R., 1995. Selective mobilization of adipose tissue fatty acids during energy depletion in the rat. Journal of Lipid Research. 36, 2164-2173.

Raclot, T., et al., 1997. Selective release of human adipocyte fatty acids according to molecular structure. Biochemical Journal. 324, 911-915.

Ramji, D., Foka, P., 2002. CCAAT/enhancer-binding proteins: structure, function and regulation. Biochemical Journal. 365, 561-575.

Reed, L., et al., 2007. Environmental toxicology and health effects associated with hexachlorobenzene exposure. Reviews on Environmental Health. 22, 213-244.

Reshef, L., et al., 2003. Glyceroneogenesis and the triglyceride/fatty acid cycle. Journal of Biological Chemistry. 278, 30413-30416.

Richelsen, B., 1992. Release and effects of prostaglandins in adipose tissue. Prostaglandins, Leukotrienes and Essential Fatty Acids. 47, 171-182.

Roberts, D. R., et al., 2000. DDT house spraying and re-emerging malaria. The Lancet. 356, 330-332.

Routti, H., et al., 2009. Polybrominated diphenyl ethers and their hydroxylated analogues in ringed seals (*Phoca hispida*) from Svalbard and the Baltic Sea. Environmental Science & Technology. 43, 3494-3499.

Rowland, A. F., et al., 2011. Mapping insulin/GLUT4 circuitry. Traffic. 12, 672-681.

Russell, S., Tisdale, M., 2005. Effect of eicosapentaenoic acid (EPA) on expression of a lipid mobilizing factor in adipose tissue in cancer cachexia. Prostaglandins, Leukotrienes and Essential Fatty Acids. 72, 409-414.

Ryden, M., et al., 2002. Mapping of early signaling events in tumor necrosis factor-α-mediated lipolysis in human fat cells. Journal of Biological Chemistry. 277, 1085-1091.

Safe, S., 1989. Polyhalogenated aromatics: uptake, disposition and metabolism. Halogenated Biphenyls, Terphenyls, Naphthalenes, Dibenzodioxins and Related Products. 131-159.

Safe, S., et al., 1985. PCBs: Structure-function relationships and mechanism of action. Environmental Health Perspectives. 60, 47-56.

Safe, S., Hutzinger, O., 1984. Polychlorinated biphenyls (PCBs) and polybrominated biphenyls (PBBs): Biochemistry, toxicology, and mechanism of action. CRC Critical Reviews in Toxicology. 13, 319-395.

Sandau, C. D., et al., 2002. Pentachlorophenol and hydroxylated polychlorinated biphenyl metabolites in umbilical cord plasma of neonates from coastal populations in Quebec. Environmental Health Perspectives. 110, 411-417.

Sanders, J., et al., 2005. Differential expression of CYP1A, 2B, and 3A genes in the F344 rat following exposure to a polybrominated diphenyl ether mixture or individual components. Toxicological Sciences. 88, 127-133.

Sanders, J., et al., 2006. Metabolism and disposition of 2,2',4,4'-tetrabromodiphenyl ether following administration of single or multiple doses to rats and mice. Xenobiotica. 36, 103-117.

Sbarbati, A., et al., 2010. Subcutaneous adipose tissue classification. European Journal of Histochemistry. 54, e48.

Schuur, A., et al., 1999. Effects of pentachlorophenol and hydroxylated polychlorinated biphenyls on thyroid hormone conjugation in a rat and a human hepatoma cell line. Toxicology *in vitro*. 13, 417-425.

Sengenes, C., et al., 2000. Natriuretic peptides: a new lipolytic pathway in human adipocytes. The FASEB Journal. 14, 1345-1351.

Shaw, S. D., et al., 2009. Bioaccumulation of polybrominated diphenyl ethers and hexabromocyclododecane in the northwest Atlantic marine food web. Science of the Total Environment. 407, 3323-3329.

She, J., et al., 2002. PBDEs in the San Francisco Bay Area: Measurements in harbor seal blubber and human breast adipose tissue. Chemosphere. 46, 697-707.

Silverstein, R. L., Febbraio, M., 2009. CD36, a scavenger receptor involved in immunity, metabolism, angiogenesis, and behavior. Science Signaling. 2, re3.

Skurk, T., et al., 2007. Relationship between adipocyte size and adipokine expression and secretion. Journal of Clinical Endocrinology & Metabolism. 92, 1023-1033.

Smith, A. G., DDT and other chlorinated insecticides. In: Mammalian Toxicology of Insecticides. T. C. Marrs, The Royal Society of Chemistry, 2012, 37-70.

Souza, S. C., et al., 2003. TNF-α induction of lipolysis is mediated through activation of the extracellular signal related kinase pathway in 3T3-L1 adipocytes. Journal of Cellular Biochemistry. 89, 1077-1086.

Stapleton, H. M., et al., 2009. Metabolism of polybrominated diphenyl ethers (PBDEs) by human hepatocytes *in vitro*. Environmental Health Perspectives. 117, 197-202.

Stapleton, H. M., et al., 2004. Debromination of polybrominated diphenyl ether congeners BDE 99 and BDE 183 in the intestinal tract of the common carp (*Cyprinus carpio*). Environmental Science & Technology. 38, 1054-1061.

Stillaert, F. B., et al., Adipose tissue induction *in vivo*. In: Tissue Engineering. Springer, 2007, 403-412.

Stoker, T. E., et al., 2004. Assessment of DE-71, a commercial polybrominated diphenyl ether (PBDE) mixture, in the EDSP male and female pubertal protocols. Toxicological Sciences. 78, 144-155.

Storch, J., McDermott, L., 2009. Structural and functional analysis of fatty acid-binding proteins. Journal of Lipid Research. 50, S126-S131.

Streets, S. S., et al., 2006. Partitioning and bioaccumulation of PBDEs and PCBs in Lake Michigan. Environmental Science & Technology. 40, 7263-7269.

Su, X., Abumrad, N. A., 2009. Cellular fatty acid uptake: a pathway under construction. Trends in Endocrinology & Metabolism. 20, 72-77.

Suzuki, G., et al., 2005. Distribution of PCDDs/PCDFs and Co-PCBs in human maternal blood, cord blood, placenta, milk, and adipose tissue: dioxins showing high toxic equivalency factor accumulate in the placenta. Bioscience, Biotechnology, and Biochemistry. 69, 1836-1847.

Tan, G. D., et al., 2003. A "futile cycle" induced by thiazolidinediones in human adipose tissue? Nature Medicine. 9, 811-812.

Tebourbi, O., et al., 2006. Metabolism of DDT in different tissues of young rats. Journal of Environmental Science and Health Part B. 41, 167-176.

Tisdale, M. J., Beck, S. A., 1991. Inhibition of tumour-induced lipolysis *in vitro* and cachexia and tumour growth *in vivo* by eicosapentaenoic acid. Biochemical Pharmacology. 41, 103-107.

To-Figueras, J., et al., 1988. Mobilization of stored hexachlorobenzene and *p,p'*-dichlorodiphenyldichloroethylene during partial starvation in rats. Toxicology Letters. 42, 79-86.

To-Figueras, J., et al., 1997. Metabolism of hexachlorobenzene in humans: Association between serum levels and urinary metabolites in a highly exposed population. Environmental Health Perspectives. 105, 78-83.

Tontonoz, P., et al., 1993. ADD1: a novel helix-loop-helix transcription factor associated with adipocyte determination and differentiation. Molecular and Cellular Biology. 13, 4753-4759.

Tordjman, J., Histology of adipose tissue. In: Physiology and Physiopathology of Adipose Tissue. J.-P. Bastard and B. Feve Eds., Springer-Verlag France, 2013, 67-75.

Uhl, S., et al., 1986. Pharmacokinetics of pentachlorophenol in man. Archives of Toxicology. 58, 182-186.

Ulbrich, B., Stahlmann, R., 2004. Developmental toxicity of polychlorinated biphenyls (PCBs): a systematic review of experimental data. Archives of Toxicology. 78, 252-268.

Valters, K., et al., 2005. Polybrominated diphenyl ethers and hydroxylated and methoxylated brominated and chlorinated analogues in the plasma of fish from the Detroit River. Environmental Science & Technology. 39, 5612-5619.

Van den Berg, M., et al., 2006. The 2005 World Health Organization reevaluation of human and mammalian toxic equivalency factors for dioxins and dioxin-like compounds. Toxicological Sciences. 93, 223-241.

Van Metre, P. C., et al., 1997. Historical trends in organochlorine compounds in river basins identified using sediment cores from reservoirs. Environmental Science & Technology. 31, 2339-2344.

Van Raaij, J., et al., 1993. Increased glucuronidation of thyroid hormone in hexachlorobenzene-treated rats. Biochemical Pharmacology. 45, 627-631.

Vanden Berghe, M., et al., 2012. Selective transfer of persistent organic pollutants and their metabolites in grey seals during lactation. Environment International. 46, 6-15.

Viscarra, J. A., et al., 2011. Glut4 is upregulated despite decreased insulin signaling during prolonged fasting in northern elephant seal pups. The American Journal of Physiology - Regulatory, Integrative and Comparative Physiology 300, R150-4.

Wajchenberg, B. L., 2000. Subcutaneous and visceral adipose tissue: their relation to the metabolic syndrome. Endocrine Reviews. 21, 697-738.

Waliszewski, S., et al., 2001. Organochlorine pesticide levels in maternal adipose tissue, maternal blood serum, umbilical blood serum, and milk from inhabitants of Veracruz, Mexico. Archives of Environmental Contamination and Toxicology. 40, 432-438.

Walther, T. C., Farese Jr, R. V., 2012. Lipid droplets and cellular lipid metabolism. Annual Review of Biochemistry. 81, 687-714.

Wang, H., Eckel, R. H., 2009. Lipoprotein lipase: from gene to obesity. American Journal of Physiology-Endocrinology and Metabolism. 297, E271-E288.

Wang, T., et al., 2006. The comparative physiology of food deprivation: from feast to famine. Annual Review of Physiology. 68, 223-251.

Wania, F., Dugani, C. B., 2003. Assessing the long-range transport potential of polybrominated diphenyl ethers: A comparison of four multimedia models. Environmental Toxicology and Chemistry. 22, 1252-1261.

Ward, J., et al., 2008. An overview of policies for managing polybrominated diphenyl ethers (PBDEs) in the Great Lakes basin. Environment International. 34, 1148-1156.

Yang, X., et al., 2013. Distinct mechanisms regulate ATGL-mediated adipocyte lipolysis by lipid droplet coat proteins. Molecular Endocrinology. 27, 116-126.

Zakim, D., 1996. Fatty acids enter cells by simple diffusion. Experimental Biology and Medicine. 212, 5-14.

Zechner, R., et al., 2009. Adipose triglyceride lipase and the lipolytic catabolism of cellular fat stores. Journal of Lipid Research. 50, 3-21.

Zha, J., et al., 2006. Effects of pentachlorophenol on the reproduction of Japanese medaka (*Oryzias latipes*). Chemico-Biological Interactions. 161, 26-36.

Zhou, T., et al., 2001. Effects of short-term *in vivo* exposure to polybrominated diphenyl ethers on thyroid hormones and hepatic enzyme activities in weanling rats. Toxicological Sciences. 61, 76-82.

Zhou, T., et al., 2002. Developmental exposure to brominated diphenyl ethers results in thyroid hormone disruption. Toxicological Sciences. 66, 105-116.

Zimmermann, R., et al., 2009. Fate of fat: The role of adipose triglyceride lipase in lipolysis. Biochimica et Biophysica Acta (BBA). 1791, 494-500.

Zimmermann, R., et al., 2004. Fat mobilization in adipose tissue is promoted by adipose triglyceride lipase. Science. 306, 1383-1386.

Chapter 2

Aims of the thesis

The literature widely describes the contamination of humans and wildlife by numerous lipophilic pollutants such as PBDEs, PCBs and organochlorine pesticides (OCPs). All these toxic molecules share the same properties. They tend to bioaccumulate throughout the food chain and resist to the biological degradations. They are highly lipophilic and therefore, are stored within the adipose tissue. Many studies have attempted to better understand the relationships between lipophilic pollutants and the adipose tissue. Among others, it has been reported in *in vitro* studies from our research laboratory that PCBs preferentially accumulate within LDs of adipocytes and their uptake is mainly governed by the TG content of fat cells (Bourez et al., 2012a; Bourez et al., 2012b; Bourez et al., 2013).

During periods of negative energy balance, the adipose tissue is considered as a source of lipophilic pollutants, leading to the release of these pollutants in blood as well as to their concentration in the remaining amount of adipose tissue (Debier et al., 2006; Kim et al., 2011; Vanden Berghe et al., 2013). The release of lipophilic pollutants does not seem to be a homogeneous phenomenon among the congeners. Their dynamics of mobilisation appear to depend on their physico-chemical properties (e.g. log K_{ow}) and to differ from those of adipocyte lipids (Debier et al., 2003; Debier et al., 2006; Vanden Berghe et al., 2013). It has also been suggested that it could be influenced by the differential mobilisation of FAs from the adipose tissue (Debier et al., 2003; Vanden Berghe et al., 2012). Nevertheless, little is known about the parameters that govern the release of such lipophilic pollutants from the adipose tissue during a lipolytic process. In addition,

their fate after being mobilised from the adipose tissue (uptake by other tissues, biotransformation, and excretion) has been poorly studied.

The general purpose of this work is thus to investigate the toxicokinetics of lipophilic pollutants during periods of negative energy balance. In particular, we aim at studying:

- their mobilisation from the adipose tissue and the impact of the physico-chemical properties of the compounds on their behaviour during adipose tissue lipolysis;
- the potential link with the release of FAs from adipocyte TGs;
- the possible biotransformation after the release from adipocytes.

In order to reach this goal, our study exploited two different experimental approaches:

- an *in vivo* approach that allows studies on the tissues of the whole living organism sampled in its natural environment;
- an *in vitro* approach that allows simplifing the model, controlling the parameters of contamination and going deeper into mechanistic interpretation.

Our *in vivo* study model was the northern elephant seal (NES) (*Mirounga angustirostris*) from the Año Nuevo State Reserve (CA, USA). This species, which is considered as a physiologically obese animal, undergoes several natural periods of fast during its life. Therefore, it can be considered as a good model to study the lipolysis within the adipose tissue. Furthermore, the NES is a marine mammal predator at the top of the food chain that is characterised by a significant contamination by lipophilic pollutants (Debier et al., 2006; Debier et al., 2012).

The first chosen *in vitro* model was a primary culture of differentiated NES adipocytes directly obtained from blubber biopsies of NES and the second *in vitro* model was a primary culture of differentiated rat adipocytes obtained from fat pads of male Wistar rats. The last model was naturally

selected as our laboratory has a good expertise in such cell cultures since the PhD project of Sophie Bourez.

Each of these models allowed achieving specific goals:

- The first objective of the present work was to study the dynamics of mobilisation of PBDEs, PCBs and OCPs from the blubber of NES pups during the post-weaning fast. Samples of blood and blubber were longitudinally analysed in order to determine the levels and patterns of these lipophilic pollutants over the period of fast.

- The second objective was to develop a functional *in vitro* model of differentiated NES adipocytes from isolated cells of blubber biopsies. Due to the complexity of the *in vivo* model, the *in vitro* scale is a good compromise to understand the behaviour of a few selected lipophilic compounds at a given concentration during a lipolytic process within fat cells. The first steps of the set-up of this new cell culture model were carried out in this present work.

- The third objective was to develop an efficient *in vitro* adipocytes model of long-term lipolysis using the primary cultures of differentiated rat adipocytes. To achieve this goal, we tested the impact of the renewal of lipolytic medium and isoproterenol, a well-known lipolytic agent, on the efficiency of the lipolytic process.

- The fourth objective was to study the influence of the number and position of chlorine atoms of PCBs on their release from adipocytes during lipolytic process as well as the potential impact of the presence of other PCB congeners on the mobilisation rate of such molecules.

- The fifth objective was to examine the profiles of FAs stored in blubber throughout the post-weaning fast of NES and to compare them with the profiles of FAs in blood. The patterns of FAs were analysed in the TG fraction from blubber, which is the lipid fraction involves in the lipolytic pathway, and in the free FA fraction from

blood, which is the reflection of the lipolytic products. The objective was then to link the dynamics of mobilisation of fatty acids from blubber to those of PBDEs, PCBs and OCPs.

- Eventually, the sixth objective of this thesis was to evaluate a potential biotransformation of PCBs by the NES pups. Hydroxylated PCB metabolites are mainly found in the circulation. In order to study the levels and patterns of hydroxylated PCBs, we thus analysed the samples of serum from the same cohort of NES pups as in the first *in vivo* experiment (i.e. the first objective).

References

Bourez, S., et al., 2012a. Accumulation capacity of primary cultures of adipocytes for PCB-126: Influence of cell differentiation stage and triglyceride levels. Toxicology Letters. 214**,** 243-250.

Bourez, S., et al., 2012b. Accumulation of polychlorinated biphenyls in adipocytes: Selective targeting to lipid droplets and role of caveolin-1. PLoS ONE. 7**,** e31834.

Bourez, S., et al., 2013. The dynamics of accumulation of PCBs in cultured adipocytes vary with the cell lipid content and the lipophilicity of the congener. Toxicology Letters. 216**,** 40-46.

Debier, C., et al., 2006. Mobilization of PCBs from blubber to blood in northern elephant seals (*Mirounga angustirostris*) during the post-weaning fast. Aquatic Toxicology. 80**,** 149-157.

Debier, C., et al., 2012. Differential changes of fat-soluble vitamins and pollutants during lactation in northern elephant seal mother–pup pairs. Comparative Biochemistry and Physiology Part A. 162**,** 323-330.

Debier, C., et al., 2003. Quantitative dynamics of PCB transfer from mother to pup during lactation in UK grey seals *Halichoerus grypus*. Marine Ecology Progress Series. 247**,** 237-248.

Kim, M. J., et al., 2011. Fate and complex pathogenic effects of dioxins and polychlorinated biphenyls in obese subjects before and after drastic weight loss. Environmental Health Perspectives. 119**,** 377-383.

Vanden Berghe, M., et al., 2013. Effects of polychlorobiphenyls, polybromodiphenylethers, organochlorine pesticides and their metabolites on vitamin A status in lactating grey seals. Environmental Research. 120**,** 18-26.

Vanden Berghe, M., et al., 2012. Selective transfer of persistent organic pollutants and their metabolites in grey seals during lactation. Environment International. 46**,** 6-15.

Chapter 3

Mobilisation of lipophilic pollutants from blubber in northern elephant seal pups (*Mirounga angustirostris*) during the post-weaning fast

Foreword

As presented in the general introduction of this thesis, a previous study from our laboratory[1] reported an increase of PCB concentrations in blubber and serum of NES pups throughout the post-weaning fast. In the present chapter, we completed this research by studying the dynamics of mobilisation of PCBs and additional POPs (PBDEs and OCPs). We assessed the changes of their concentrations and profiles within blubber and serum of a cohort of 22 free-ranging NES pups longitudinally sampled throughout the post-weaning fast. We distinguished the inner blubber layer (i.e. closed to the muscle) from the outer blubber layer (i.e. closed to the skin) in order to highlight a potential stratification of POP contamination. The present results were published in Environmental Research.

[1] Debier, C., et al., 2006. Mobilization of PCBs from blubber to blood in northern elephant seals (*Mirounga angustirostris*) during the post-weaning fast. Aquatic Toxicology. 80, 149-157.

Mobilisation of lipophilic pollutants from blubber in northern elephant seal pups (*Mirounga angustirostris*) during the pos-weaning fast

Caroline Louis, Alin C. Dirtu, Marie Stas, Yves Guiot, Govindan Malarvannan, Krishna Das, Daniel P. Costa, Daniel E. Crocker, Adrian Covaci and Cathy Debier

Published in Environmental Research, 2014, 132:438-448

Abstract

Northern elephant seals (NES) (*Mirounga angustirostris*) from the Año Nuevo State Reserve (CA, USA) were longitudinally sampled during the post-weaning fast in order to study the mobilisation and redistribution of various classes of persistent organic pollutants (POPs), such as polybrominated diphenyl ethers (PBDEs), polychlorinated biphenyls (PCBs), dichlorodiphenyldichloroethylene (*p,p'*-DDE) and hexachlorobenzene (HCB) between blubber and blood. Inner and outer blubber layers were analysed separately. Organohalogenated compounds were detected in all blubber samples in the decreasing order of their concentrations: *p,p'*-DDE > PCBs >> HCB > PBDEs. The concentrations of all studied compounds were homogeneously distributed in the blubber layer at early fast, since the concentrations of POPs were statistically not different in the inner and outer layers. With the progression of the fast, the concentrations of PBDEs, PCBs and *p,p'*-DDE increased more sharply in inner blubber than in outer blubber. As a result, their levels became significantly higher in inner blubber as compared to outer blubber at late fast. The rise of pollutant concentrations in blubber might result from a less efficient mobilisation than triglycerides and/or a reuptake by adipocytes of some of the pollutants released into the circulation. The mobilisation of pollutants from blubber was higher at late fast. An increase of pollutant concentrations was observed in serum between early and late fast. Lower halogenated congeners (i.e. tetra-CBs) were present in higher proportions in serum, whereas the higher halogenated congeners (i.e. hepta-CBs) were mainly found in the inner and outer blubber layers. The transfer ratios of both PBDEs and PCBs from inner blubber to serum decreased with the number of chlorine and bromine atoms. In addition, the distribution of both types of compounds between serum and blubber was strongly influenced by their lipophilic character (log K_{ow} values), with more lipophilic compounds being less efficiently released from blubber to serum.

Keywords

Northern elephant seal – PCBs – PBDEs – Pesticides – Blubber – Serum

3.1. Introduction

Persistent organic pollutants (POPs), such as polychlorinated biphenyls (PCBs), organochlorine pesticides (e.g. dichlorodiphenyltrichloroethane and its metabolites (DDTs), hexachlorobenzene (HCB)) and polybrominated diphenyl ethers (PBDEs), have captured the attention of scientists since several decades. They accumulate in living organisms and can biomagnify in aquatic and terrestrial food webs (Covaci et al., 2002a; Jürgens et al., 2013; Letcher et al., 2010; Vanden Berghe et al., 2012). Marine mammals are highly exposed to these fat-soluble chemicals because of their high trophic-chain position and their long life spans. POPs are preferentially accumulated in the adipose tissue (Debier et al., 2003; Debier et al., 2006; Vanden Berghe et al., 2012), but also in various compartments such as blood, liver and brain (Covaci et al., 2002b; de Wit, 2002; Mössner et al., 1994; Weijs et al., 2009). The presence of POPs might generate an insidious threat, as they are known to exert negative effects such as immunotoxicity and endocrine disruption (Darnerud, 2008; Ross, 2002; Ylitalo et al., 2005). Some POPs (e.g. PBDEs, PCBs or *p,p'*-dichlorodiphenyldichloroethylene (*p,p'*-DDE)) may interfere with the metabolism and blood transport of thyroid hormones and vitamin A (Das et al., 2006; Debier et al., 2005b; Vanden Berghe et al., 2010), which are essential to ensure proper development of the pup.

During fasting periods, which are very common in the life cycle of marine mammals, lipophilic molecules, such as POPs, are liberated from the blubber into the blood circulation (Debier et al., 2003; Debier et al., 2006; Vanden Berghe et al., 2012). Among marine mammal species, northern elephant seals (NES) exhibit some of the longest durations of natural fast (e.g. during reproduction, moulting, post-weaning and lactation). During these periods, they mobilise the triglycerides stored in the blubber in order to provide energy and to maintain homeostasis of the body. This phenomenon induces the combination of two effects: the release of lipophilic pollutants into the circulation as well as the increase of their concentration in the blubber, possibly because POPs are less efficiently mobilised from blubber than lipids (Debier et al., 2006; Vanden Berghe et al., 2012). During lactation, high

levels of POPs are transferred from the body stores of fasting females to the pups through the consumption of lipid-rich milk (Debier et al., 2006; Debier et al., 2012; Vanden Berghe et al., 2012). Upon weaning, NES pups fast and mobilise primarily lipids from their large amount of blubber. Previously, we have investigated the dynamics of mobilisation of PCBs from blubber to blood during the post-weaning fast of NES (Debier et al., 2006). PCBs appeared to concentrate in the inner part of the blubber at the beginning of the fast, before being released in high amounts in the circulation at the end of the fast. This pattern has not been investigated for other POPs (e.g. PBDEs, DDT and HCB). In general, little is known about the mobilisation of pollutants during energy deprivation stages and particularly in young and fasting animals.

In this paper, we describe the dynamics of mobilisation of POPs (PBDEs, PCBs, HCB and *p,p'*-DDE) from the blubber to the blood circulation of NES pups throughout their post-weaning fast. Blubber was differentiated into inner and outer layers. Samples were collected on free-ranging animals from the Año Nuevo colony from January to April 2010, caught four times throughout the post-weaning fast. Individuals from the same colony were already sampled in 2002 to provide information on the dynamics of PCBs throughout the post-weaning fast of NES pups (Debier et al., 2006).

3.2. Experimental procedures

3.2.1. Seal sampling

The sampling took place at Año Nuevo State Reserve, CA, USA (37°06'30''N, 122°20'10''W) from January to April 2010, under the National Marine Fisheries Service Marine Mammal Permit #87-1743-05. Twenty-two free ranging pups were sampled at 1-, 4-, 7- and 10-week post-weaning (later also assigned early, mid, late and very late fast, respectively). Each animal was specifically marked with dye and was followed by observing the colony each day. NES pups were initially immobilised with an intramuscular injection of Telazol at 1 mg/kg of estimated body mass and sedation was maintained through subsequent intravenous injections of Ketamine (all drugs were from Fort Dodge Animal Health, Fort Dodge, IA, USA) as needed. At each capture, blood was collected from the extradural vein into Vacutainer serum tubes (Becton-Dickinson, Erembodegem, Belgium). Samples were centrifuged at 1300xg for 15 min at 4°C and serum was aliquoted into microtubes and stored at -20°C until analysis. At weeks 1, 4 and 7, blubber samples were taken after subcutaneous injection of lidocaine for local anaesthesia. A blubber biopsy extending the full depth of the blubber layer was taken in the lateral pelvis area using 6-mm biopsy punches (Miltex, Help Medical, Paris, France) and stored in aluminium foil at -20°C until analysis. This biopsy is considered as a representative sample since the anatomical area chosen for blubber collection has little influence on pollutant content (Debier et al., 2006; Severinsen et al., 2000).

3.2.2. POP analyses

Blubber biopsies were cut into three equal parts. Inner (closest to the muscle) and outer (closest to the skin) layers were analysed separately. In all blubber and serum samples, 6 PBDEs (IUPAC numbers: BDE-28, -47, -99, -100, -153 and -154), 30 PCB congeners (IUPAC numbers: CB-28, -47, -49, -52, -74, -95, -99, -101, -105, -110, -118 , -128, -138, -146, -149, -151, -153, -156, -170, -171, -172, -174, -177, -180, -183, -187, -194, -199, -206 and -209), *p,p'*-DDE and HCB were targeted.

Details of the preparation, extraction, clean-up and quality control for the blubber samples are described in Covaci et al. (2008). Briefly, inner and outer blubber were weighed (approximately 150 mg), mixed with anhydrous Na_2SO_4 and spiked with internal standards (CB-143 and BDE-77) in each sample. Pollutant and lipid extractions were carried out by automated Soxhlet method with *n*-hexane/acetone (3:1, *v:v*). Samples were then loaded on acid silica (44% H_2SO_4, *w:w*) cartridge in order to clean them up and were eluted with *n*-hexane and dichloromethane. Finally, solvents were evaporated and purified extracts were reconstituted in *iso*-octane.

Serum samples were analysed as reported in Weijs et al. (2009) and Vanden Berghe et al. (2012). In brief, internal standards (CB-143, ε-HCH and BDE-77) were added at 1.5 mL serum followed by deionized water and formic acid. The mixture was sonicated for 20 min and loaded on solid-phase-extraction (SPE) cartridge (200 mg, Oasis HLB, Waters, Milford, MA). Pollutants were eluted with dichloromethane/methanol (1:1, *v:v*). Extracts were then dried and reconstituted in hexane. PBDEs, PCBs, *p,p'*-DDE and HCB were eluted with *n*-hexane from a silica SPE cartridge (500 mg, VWR, Belgium) topped with acidified silicagel (44% H_2SO_4, *w:w*). Samples were then evaporated and reconstituted in *iso*-octane.

All compounds were measured with an Agilent 6890 gas chromatograph coupled with a 5973 mass spectrometer system (GC-MS). All analytical details as well as performed quality assurance and quality control are available in Vanden Berghe et al. (2012).

3.2.3. Lipid determination

Lipid content in blubber was performed gravimetrically after the automated Soxhlet extraction (see 3.2.2) and was used to normalise contaminant data. For serum, different lipid classes (total cholesterol, phospholipids, triglycerides and free fatty acids (FAs)) were measured using *in vitro* enzymatic colorimetric method assays (Wako and Diasys, Sopachem, Eke, Belgium) following the manufacturer's instructions. The total lipids of serum correspond to the sum of the different targeted lipid classes.

3.2.4. Blubber morphometry

One blubber biopsy was taken as described above on three different animals, sampled at 1-, 4- and 7-week post-weaning, respectively. Each sample was fixed in 4% buffered paraformaldehyde solution and then routinely embedded in paraffin. Five-micrometer-thick slices were processed. Sections were counterstained with hematoxylin eosine (Sigma-Aldrich, Bornem, Belgium). The cell profile area of adipocytes was estimated by planimetry. Equipment consisted of an inverted microscope (20x magnification, Axiostar Zeiss, Zeiss, Zaventem, Belgium) and a video camera (AxioCam MRc Zeiss). Each adipocyte was manually delineated and 700 – 1200 cells per condition were assessed. The cell profile area of adipocytes (μm^2) was calculated using an image analyser software (AxioVision 4.7.1; 08-2008). Final results are expressed as distribution of cell profile area.

3.2.5. Statistical analysis

Data were log transformed to achieve normality. For pollutant concentrations below the limit of quantification (LOQ), a LOQ×detection frequency value was assigned (see Appendices). Statistical analyses were conducted using SAS 9.3 software (SAS Institute Inc., Cary, USA). Linear mixed models were used to test the differences in pollutant levels and profiles as well as lipid levels throughout the post-weaning fast periods within a same tissue. Animal ID was modelled as a random effect. Furthermore, pollutant and lipid concentrations were analysed using one-way ANOVA with a Tukey test for each capture in order to compare the levels between tissues. The level of statistical significance was set at p-values<0.05 for all analyses. Results are presented as means ± SEM.

Regarding morphometry, statistical analyses were conducted using a Kolmogorov-Smirnov test to compare two distributions of adipocyte profile area (SAS 9.3 software). Results of distribution of cell profile area are presented in percentage and by class of adipocyte size.

3.3. Results

3.3.1. Biometry of NES

At early fast, the mean mass of NES was 128 ± 3 kg with a mean body mass index (BMI) of 59 ± 1 kg/m^2. Animals lost weight throughout the fast to reach 96 ± 2 kg with a BMI of 42 ± 1 kg/m^2 after 7 weeks of fast (Table 3.1). The sex ratio of targeted NES was 1:1.

Table 3.1 – Biometry of northern elephant seals throughout the post-weaning fast period; mean ± SEM (range)

	n	Post-weaning fast day [day]	Mass [kg]	Standard length [cm]	BMI [kg/m^2]
Week 1	22	1 ± 1 (0-4)	128 ± 3 (92-148)	146 ± 1 (131-156)	59 ± 1 (48-69)
Week 4	22	23 ± 1 (22-25)	110 ± 2 (77-125)	147 ± 2 (130-159)	51 ± 1 (41-63)
Week 7	22	46 ± 2 (44-50)	96 ± 2 (66-115)	151 ± 1 (132-160)	42 ± 1 (38-50)
Week 10	14	61 ± 2 (58-66)	-	-	-

Sex ratio (female:male) = 1:1

3.3.2. Changes of lipid contents in blubber and serum

Total lipid content of outer blubber increased during the first half of the fast (p<0.001) and remained stable between weeks 4 and 7 (p=0.282) (Figure 3.1 A). In inner blubber, lipid content did not vary between weeks 1 and 4 (p=0.261) and then decreased slightly between weeks 4 and 7 (p=0.030), reaching lipid concentration similar to early fast (p=0.475) (Figure 3.1 A). The lipid percentages were significantly higher in the inner blubber than in the outer blubber (p=0.006 at week 1 and p<0.001 at week 4), except at week 7 (p=0.746).

Morphometric analysis of one blubber biopsy showed that the proportion of small adipocytes (cell area < 2800 µm^2) tended to increase during the fast in both layers, whereas the proportions of mid-size adipocytes (2800 µm^2 < cell area < 5600 µm^2) as well as large-size adipocytes (5600 µm^2 < cell area < 8400 µm^2) tended to decrease (Figure 3.1 B). The size of each class of

adipocytes is shown in Figure 3.1 C. The 2-sample Kolmogorov-Smirnov test highlighted a significant difference in the distribution of adipocyte profile area throughout the fast within the inner ($0.001<p<0.017$) and outer blubber ($0.001<p<0.036$). Furthermore, these distributions were also significantly different between the two layers for a given capture ($p<0.001$ at week 1, $p=0.007$ at week 4, $p<0.001$ at week 7) (Figure 3.1 B).

The total lipids of serum were formed by phospholipids (54 ± 3%), total cholesterol (32 ± 3%), triglycerides (9 ± 3%) and free FAs (5 ± 2%) (see Appendices; Table S1). The total lipid content in serum increased sharply between weeks 1 and 4 ($p<0.001$), then tended to stabilize between weeks 4 and 7 ($p=0.051$) and remained constant between weeks 7 and 10 ($p=0.558$) (Figure 3.2 A). Free FAs, which result from the lipolytic activity and thus, the hydrolysis of triglycerides mobilised from the blubber, doubled between weeks 1 and 10 ($p<0.001$) (Figure 3.2 B).

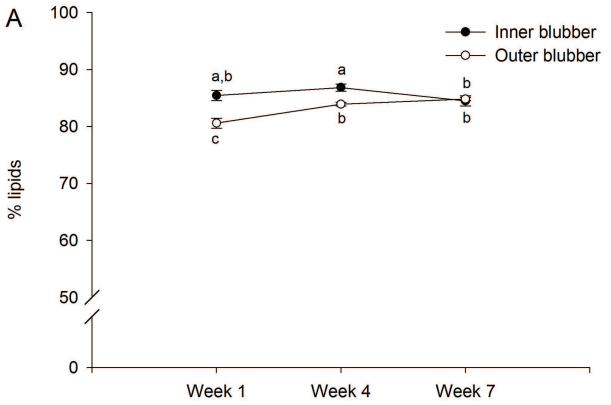
A
100
90
80
70
60
50
0
% lipids
Inner blubber
Outer blubber
a,b
a
b
c
b
b
Week 1
Week 4
Week 7

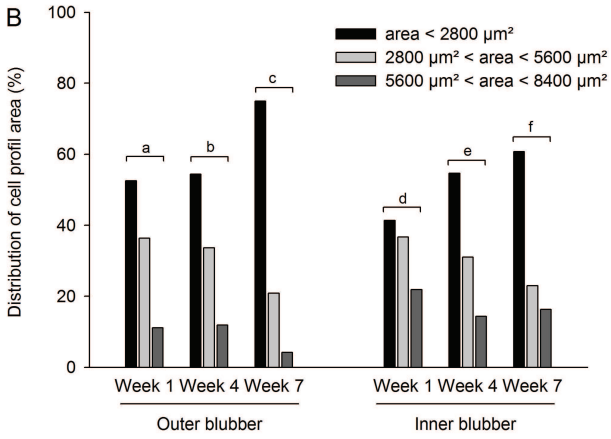
B
100
80
60
40
20
0
Distribution of cell profil area (%)
area < 2800 µm²
2800 µm² < area < 5600 µm²
5600 µm² < area < 8400 µm²
a
b
c
d
e
f
Week 1 Week 4 Week 7
Week 1 Week 4 Week 7
Outer blubber
Inner blubber

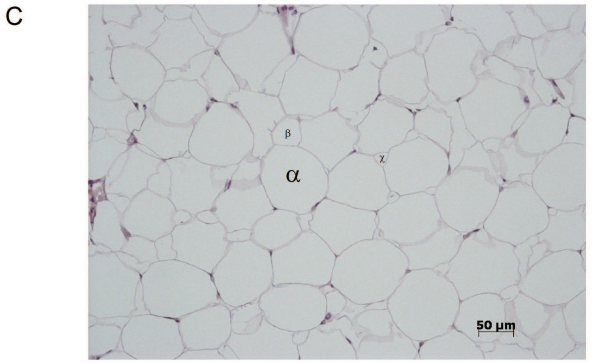
C
β
χ
α
50 µm

Figure 3.1 – Overall changes of lipids throughout the post-weaning fast of northern elephant seal pups in inner and outer blubber layers (weeks 1, 4 and 7). A. Lipid levels in blubber (mean levels ± SEM). Values with different symbols are significantly different within a defined layer as well as for a considered period ($p \leq 0.050$). B. Distribution of cell profile area arbitrarily classified in three categories of size. The area of small-size adipocytes was lower than 2800 µm^2. The area of mid-size adipocytes was between 2800 µm^2 and 5600 µm^2 and the area of large-size adipocytes, between 5600 µm^2 and 8400 µm^2. Distributions that do not share same letter show significant differences ($p \leq 0.050$). C. Histological slide of northern elephant seal adipose tissue (light microscopy). Symbols illustrate the three categories of adipocyte sizes: α for large-size class, β for mid-size class and χ for small-size class.

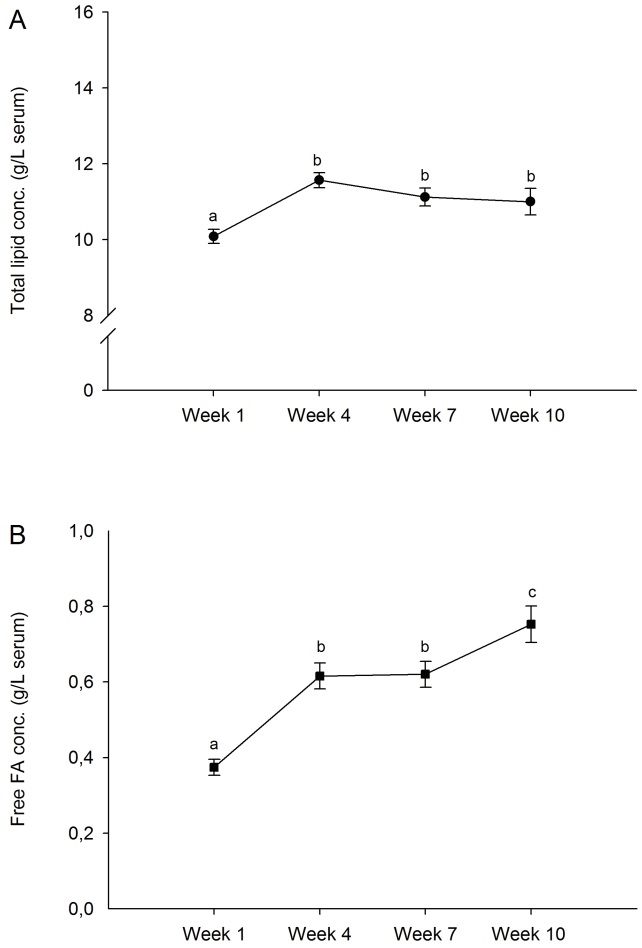

Figure 3.2 – Overall changes of lipids throughout the post-weaning fast of northern elephant seal pups in serum (weeks 1, 4, 7 and 10). Total lipid concentration (mean ± SEM) (A) and free fatty acid (FA) concentrations (mean ± SEM) (B) measured in the serum, expressed in g/L. Values with different symbols are significantly different ($p \leq 0.050$).

3.3.3. Changes of POPs in blubber

3.3.3.1. PBDEs

Total PBDE concentrations were similar in inner and outer blubber at the beginning of the fast and at mid fast (p=0.895 and p=0.155, respectively). On the other hand, concentrations became significantly higher in the inner layer as compared to the outer layer at late fast (p=0.003). The appearance of a difference at late fast resulted from variations in the dynamics of total PBDEs across the fast between both layers. Indeed, while total PBDE content increased significantly in the inner blubber throughout the fast (p<0.001), it remained stable between weeks 1 and 4 (p=0.963) and only increased between weeks 4 and 7 (p<0.001) in outer blubber. Thus, the magnitude of the increase was much greater in inner blubber than in outer blubber (Figure 3.3 A).

Among PBDE congeners that have been targeted, BDE-28 and BDE-153 were detected only in a few samples of NES pups (see Appendices; Table S2). Because of their low detection rates, no statistical test was performed on these congeners. BDE-47 was the major congener representing 82 ± 2%. Within the outer blubber, the concentrations of BDE-47 and -100 increased significantly between weeks 1 and 7 (p<0.001), while BDE-99 and -154 remained stable over the fast (0.361<p<0.647) (Table 3.2). Within the inner blubber, the concentrations of BDE-47, -99, -100 and -154 rose significantly throughout the fast (0.001<p<0.015) (Table 3.2).

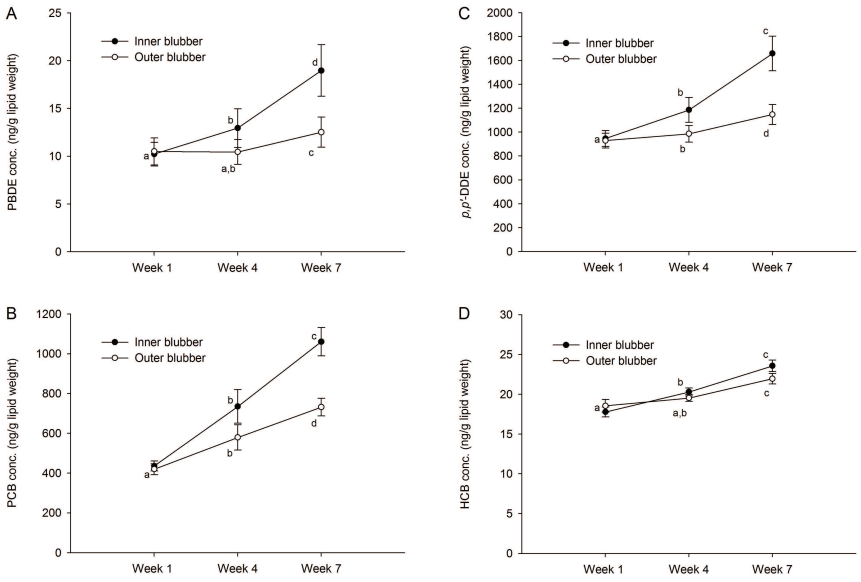

Figure 3.3 – Means ± SEM of concentrations of PBDEs (A), PCBs (B), *p,p'*-DDE (C) and HCB (D) measured in inner and outer blubber of northern elephant seals during the post-weaning fast (weeks 1, 4 and 7). Values with different symbols are significantly different within a blubber layer as well as a defined time ($p \leq 0.050$).

Table 3.2 – Means ± SEM of levels of PBDE congeners, PCB classes, *p,p'*-DDE and HCB measured in the outer and inner blubber layers as well as in serum of weaned NES pups.

	Outer blubber (ng/g lipid weight)			Inner blubber (ng/g lipid weight)			Serum (pg/mL wet weight)			
	Week 1	Week 4	Week 7	Week 1	Week 4	Week 7	Week 1	Week 4	Week 7	Week 10
BDE-47	8.4 ± 1.2^{a}	8.6 ± 1.1^{a}	10.4 ± 1.3^{b}	8.5 ± 1.0^{a}	10.7 ± 1.6^{b}	15.4 ± 2.2^{c}	66.3 ± 10.2^{a}	81.8 ± 11.2^{b}	93.3 ± 12.5^{c}	102.5 ± 12.7^{d}
BDE-99	$0.6 \pm 0.1^{a,b}$	0.4 ± 0.1^{a}	0.6 ± 0.1^{b}	0.4 ± 0.1^{a}	0.6 ± 0.1^{b}	1.0 ± 0.1^{c}	2.3 ± 1.6^{a}	0.5 ± 0.2^{b}	2.3 ± 0.3^{a}	1.3 ± 0.9^{a}
BDE-100	0.7 ± 0.1^{a}	0.8 ± 0.2^{a}	0.9 ± 0.2^{b}	0.8 ± 0.2^{a}	1.0 ± 0.3^{b}	1.5 ± 0.4^{c}	3.5 ± 1.1^{a}	1.7 ± 1.0^{b}	1.0 ± 1.6^{b}	3.0 ± 1.3^{a}
BDE-154	0.7 ± 0.1^{a}	0.6 ± 0.1^{a}	0.6 ± 0.1^{a}	0.6 ± 0.6^{a}	0.7 ± 0.1^{b}	0.9 ± 0.9^{c}	N.D	N.D	N.D	N.D
∑ PBDEs	**11 ± 1^{a}**	**10 ± 1^{a}**	**13 ± 2^{b}**	**10 ± 1^{a}**	**13 ± 2^{b}**	**19 ± 3^{c}**	**72 ± 11^{a}**	**84 ± 13^{b}**	**97 ± 14^{c}**	**107 ± 15^{d}**
∑ tri-CBs	4 ± 1^{a}	3 ± 1^{a}	4 ± 1^{a}	$3 \pm 1^{a,b}$	2 ± 0^{a}	3 ± 1^{b}	149 ± 23^{a}	173 ± 26^{a}	5 ± 3^{b}	12 ± 8^{c}
∑ tetra-CBs	5 ± 1^{a}	6 ± 2^{b}	6 ± 1^{c}	5 ± 1^{a}	7 ± 2^{b}	9 ± 2^{c}	$130 \pm 55^{a,c}$	153 ± 61^{a}	69 ± 13^{b}	90 ± 26^{c}
∑ penta-CBs	112 ± 8^{a}	154 ± 17^{b}	192 ± 12^{c}	115 ± 7^{a}	193 ± 22^{b}	273 ± 18^{c}	1033 ± 48^{a}	1392 ± 77^{b}	1644 ± 81^{c}	1934 ± 115^{d}
∑ hexa-CBs	218 ± 13^{a}	302 ± 23^{b}	380 ± 33^{c}	226 ± 12^{a}	382 ± 44^{b}	556 ± 37^{c}	1642 ± 69^{a}	1979 ± 90^{b}	2602 ± 126^{c}	2961 ± 174^{d}
∑ hepta-CBs	64 ± 5^{a}	93 ± 12^{b}	126 ± 8^{c}	68 ± 4^{a}	249 ± 93^{b}	184 ± 13^{b}	381 ± 30^{a}	363 ± 18^{a}	529 ± 33^{b}	572 ± 41^{b}
∑ octa-CBs	1.3 ± 0.3^{a}	1.9 ± 0.3^{b}	2.3 ± 0.4^{c}	1.4 ± 0.2^{a}	2.9 ± 0.8^{b}	4.5 ± 0.9^{c}	N.D	N.D	N.D	N.D
∑ PCBs	**419 ± 27^{a}**	**579 ± 63^{b}**	**732 ± 45^{c}**	**436 ± 25^{a}**	**735 ± 85^{b}**	**1060 ± 71^{c}**	**3723 ± 172^{a}**	**4533 ± 246^{b}**	**5058 ± 248^{c}**	**5851 ± 348^{d}**
***p,p'*-DDE**	**928 ± 62^{a}**	**986 ± 69^{b}**	**1147 ± 84^{c}**	**946 ± 66^{a}**	**1186 ± 104^{b}**	**1658 ± 145^{c}**	**7416 ± 636^{a}**	**10609 ± 872^{b}**	**12514 ± 979^{c}**	**14628 ± 996^{d}**
HCB	**19 ± 1^{a}**	**20 ± 1^{a}**	**22 ± 1^{b}**	**18 ± 1^{a}**	**20 ± 1^{b}**	**24 ± 1^{c}**	**168 ± 12^{a}**	**309 ± 14^{b}**	**253 ± 16^{c}**	**430 ± 29^{d}**

For a defined tissue, values within a row followed by different letters are significantly different ($p \leq 0.05$).
N.D = not detected

3.3.3.2. PCBs

Total PCB concentrations were statistically similar in inner and outer blubber at weeks 1 and 4 of fast (p=0.608 and p=0.132, respectively). On the other hand, concentrations became significantly higher at week 7 in the inner layer as compared to the outer layer (p<0.001). Similarly to PBDEs, the increase of total PCBs throughout the fast was sharper in inner blubber as compared to outer blubber (p<0.001 in inner blubber and 0.006<p<0.022 in outer blubber) (Figure 3.3 B).

Within PCB groups, PCB-206, the only nona-CB targeted in this study, and CB-209, the deca-CB, were not detected in any sample. As a result, those congeners were not included in statistical analyses (see Appendices; Table S3). In both blubber layers, the main classes were hexa-CBs (PCB-128, -138, -146, -149, -151, -153 and -156) followed by penta-CBs (PCB-95, -99, -101, -105, -110 and -118), hepta-CBs (PCB-170, -171, -172, -174, -177, -180, -183, -187), tetra-CBs (PCB-47, -49, -52, -74), tri-CBs (PCB-28) and octa-CBs (PCB-194 and -199) across the fasting period. PCB-153 formed almost one half of hexa-CB congeners (42 ± 2% in outer blubber and 42 ± 1% in inner blubber) and PCB-138, one third (32 ± 2% in outer blubber and 33 ± 2% in inner blubber). In the class of penta-CBs, two congeners were predominant: PCB-99 (30 ± 5% in outer and inner blubber layers) and PCB-118 (38 ± 4% in outer blubber and 38 ± 3% in inner blubber). Two congeners were important in the group of hepta-CBs: PCB-180 (30 ± 1% in outer blubber and 30 ± 2% in inner blubber) and PCB-187 (31 ± 3% in outer blubber and 29 ± 3% in inner blubber). Within the class of tetra-CBs, PCB-74 (59 ± 4% in outer blubber and 56 ± 1% in inner blubber) followed by PCB-52 (18 ± 5% in outer blubber and 18 ± 4% in inner blubber) were the most representative congeners. Finally, the class of octa-CBs were mainly composed of PCB-199 (93 ± 2% in outer blubber and 87 ± 3% in inner blubber).

In the outer blubber, concentrations of tri-CBs remained stable between early and late fast (p=0.216), whereas the concentrations of tetra-, penta-, hexa-, hepta- and octa-CBs increased (p<0.001) (Table 3.2). In the inner

blubber, similar dynamics were observed for tri-CBs (p=0.411) and the other congener classes (p<0.001) (Table 3.2). The magnitude of the increase of concentration between early and late fast varied among PCB classes, especially in inner blubber. Indeed, the rises were significantly higher for octa- and hepta-CBs than for hexa- and penta-CBs (0.001<p<0.018), which were themselves significantly higher than for tetra- and tri-CBs (p<0.001). On the contrary, the rises between early and late fast were similar between octa- and hepta-CBs (p=0.078), hexa- and penta-CBs (p=0.330) and tetra- and tri-CBs (p=0.648).

3.3.3.3. *p,p'*-DDE

p,p'-DDE contents were similar between both blubber layers for the first two captures (0.073<p<0.847) and became statistically higher in inner layer at week 7 (p<0.001). Here again, the increase of *p,p'*-DDE concentrations over the fast was more accentuated in inner blubber as compared to outer blubber (0.001<p<0.038) (Figure 3.3 C).

3.3.3.4. HCB

HCB concentrations did not differ between the two blubber layers at each studied time (0.132<p<0.475). The HCB concentrations increased slightly, but significantly, between early and late fast in both layers (p<0.001 for both blubber layers) (Figure 3.3 D).

Among all studied pollutants, PBDE and HCB concentrations were within the same order of magnitude in the blubber, whereas PCB and *p,p'*-DDE concentrations were between one and two orders of magnitude higher. *p,p'*-DDE concentrations were systematically the highest in all blubber samples.

3.3.4. Changes of POPs in serum

3.3.4.1. PBDEs

The concentrations of total PBDEs in serum (expressed per unit of wet weight or per unit of lipid weight) increased significantly throughout the fasting period ($p<0.001$) (Figure 3.4 A-B). The dynamics of PBDEs were also expressed per unit of circulating free FAs, as this lipid class directly reflects the lipolytic process and thus, the mobilisation of blubber triglycerides. Total serum PBDE concentrations expressed per unit of free FAs dropped between weeks 1 and 4 ($p<0.001$) before remaining constant until the end of the fast ($0.082<p<0.708$). Concentrations at week 10 did not statistically differ from those at week 1 ($p=0.145$) (Figure 3.4 C).

BDE-28, -153 and -154 were detected in only a few samples of serum (see Appendices; Table S2). No statistical test was thus performed with these congeners. BDE-47 was the major congener representing 96 ± 4%. When the results were expressed per unit of wet weight (Table 3.2), the concentrations of BDE-47 increased in the serum throughout the fast ($p<0.001$), while the concentrations of BDE-99 and -100 remained stable between early and late fast ($p=0.550$ and $p=0.452$, respectively). Similar tendencies were observed when individual PBDEs were expressed per unit of serum lipids (see Appendices; Table S4). On the other hand, when expressed per unit of circulating free FAs, levels of BDE-47, -99 and -100 decreased significantly between weeks 1 and 4 ($p<0.001$) before remaining constant (BDE-47 and -99) ($p=0.061$ and $p=0.911$, respectively) or increasing slightly (BDE-100) ($p<0.001$) until the end of the fast (see Appendices; Table S4).

3.3.4.2. PCBs

Total PCB levels (expressed per unit of wet weight or per unit of lipid weight) rose in serum throughout the studied period ($p<0.001$) (Figure 3.4 D-E). When the results were expressed per unit of circulating free FAs, total PCB concentrations dropped between weeks 1 and 4 ($p<0.001$) and then slightly increased between weeks 4 and 10 ($p=0.012$). Like for total PBDEs,

concentrations at week 10 did not statistically differ from those at week 1 (p=0.463) (Figure 3.4 F).

Within PCB groups, octa-CBs (PCB-194 and-199), nona-PCB (PCB-206) and deca-CB (PCB-209) were measured in only a few samples (see Appendices; Table S3). As a result, these congeners were not included in statistical analyses. In serum, we found mainly hexa-CBs (PCB-128, -138, -146, -149, -151, -153 and -156), followed by penta-CBs (PCB-95, -99, -101, -105, -110 and -118), tetra-CBs (PCB-47, -49, -52, -74) and hepta-CBs (PCB-170, -171, -174, -177, -180, -183, -187) for the first part of the fast and hexa-CBs followed by penta-CBs, hepta-CBs and then tetra-CBs for the second part of the fast. Similar to blubber, PCB-28 was the only congener constituting the tri-CB class. The class of tetra-CBs was composed of PCB-74 (50 ± 18%) followed by PCB-47 (27 ± 6%). The main congeners in the penta-CB class were PCB-99 (35 ± 2%) and PCB-118 (46 ± 1%). PCB-153 formed almost one half of hexa-CB congeners (44 ± 1%) and PCB-138, one third (36 ± 0%). Finally, two congeners were predominant in the group of hepta-CBs: PCB-180 (34 ± 1%) and PCB-187 (36 ± 1%).

When the results were expressed per unit of wet weight, tri-CBs decreased significantly between weeks 1 and 10 (p<0.001) and tetra-CBs remained constant (p=0.085). The concentrations of penta-, hexa- and hepta-CBs increased significantly between early and late fast (p<0.001) (Table 2). When the levels of PCBs were expressed per unit of serum lipids, tri- and tetra-CBs decreased between weeks 1 and 10 (0.001<p<0.026), whereas penta-, hexa- and hepta-CBs increased (0.001<p<0.005) (see Appendices; Table S4). When the different classes of PCBs were expressed per unit of circulating free FAs, the levels of tri- and tetra-CBs decreased between weeks 1 and 10 (p<0.001). The concentrations of penta-, hexa- and hepta-CBs dropped between weeks 1 and 4 (0.001<p<0.035), then rose significantly between weeks 4 and 7 (0.001<p<0.016) before remaining stable until week 10 (0.291<p<0.751).

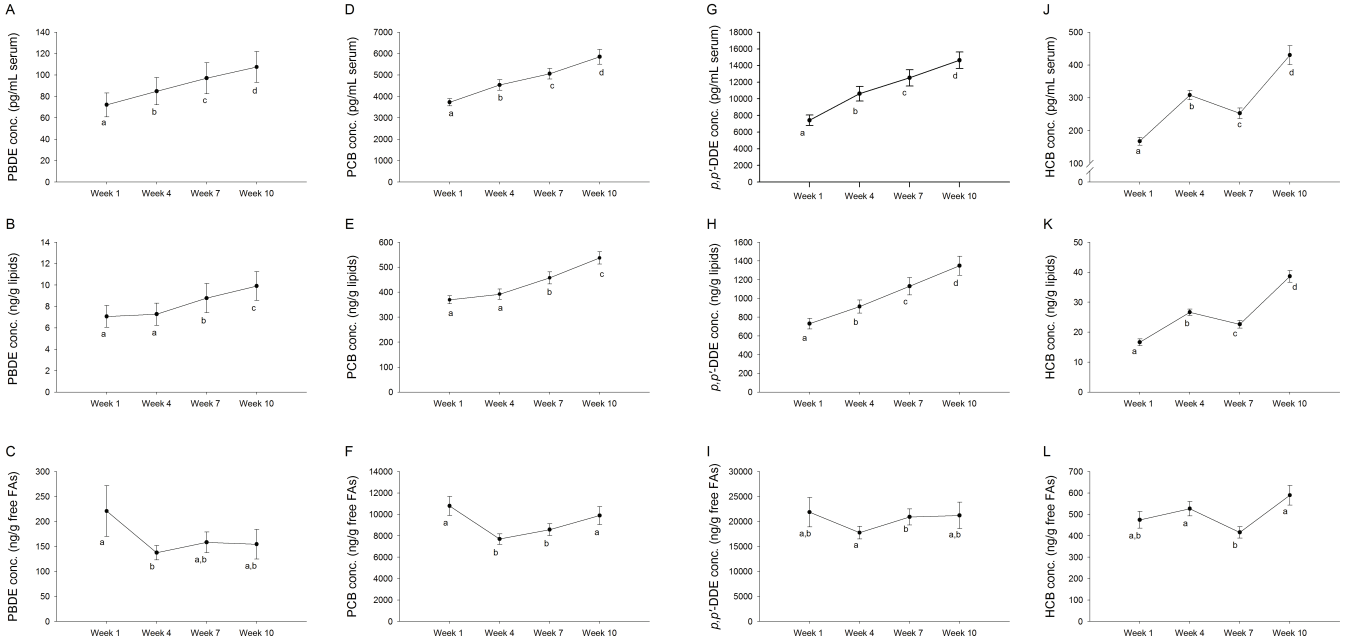

Figure 3.4 – Time course of levels of total PBDEs, total PCBs, *p,p'*-DDE and HCB in the serum of northern elephant seals during the post-weaning fast, expressed per unit of wet weight (A, D, G and J), serum lipids (B, E, H and K) and free fatty acids (FAs) (C, F, I and L). Data represent the mean concentrations ± SEM per capture (weeks 1, 4, 7 and 10). Values with different letters are significantly different ($p \leq 0.050$).

3.3.4.3. *p,p'*-DDE

Similar to previous studied pollutants, *p,p'*-DDE levels increased significantly during the fast of NES when the results were expressed per unit of wet weight and per unit of lipid weight ($p<0.001$) (Figure 3.4 G-H). *p,p'*-DDE concentrations expressed per unit of free FAs remained constant between weeks 1 and 10 ($p=0.977$) (Figure 3.4I).

3.3.4.4. HCB

The HCB levels increased significantly between early and late fast when the results were expressed either per unit of wet weight or per unit of lipid weight ($p<0.001$) (Figure 3.4 J-K). When expressed per unit of free FAs, the concentrations of HCB did not differ between weeks 1 and 10 ($p=0.070$) (Figure 3.4 L).

Similarly to blubber, serum of weaned NES pups was mainly contaminated by *p,p'*-DDE and PCBs across the fasting period. Their concentrations were two orders of magnitude higher than those of PBDEs and HCB. Here again, *p,p'*-DDE concentrations were systematically the highest in all samples.

3.3.5. Comparisons of POP profiles between tissues

3.3.5.1. PBDEs

There was no significant difference of PBDE profile between outer and inner blubber, for a considered period ($0.062<p<0.998$). The proportion of BDE-47 was lower in inner blubber than in serum at each studied period ($p<0.001$), while the proportions of BDE-100 and -154 were higher in inner blubber than in serum at each studied period ($p<0.001$). The proportions of BDE-99 were also higher in inner blubber than in serum ($p<0.001$), except at week 1 where proportions were similar between these two compartments ($p=0.723$) (Figure 3.5 A).

3.3.5.2. PCBs

For a considered period within the post-weaning fast (weeks 1, 4 or 7), no significant difference was noted in the proportions of each class of PCBs between outer and inner blubber ($0.109<p<0.998$). The percentages of tri-, tetra- and penta-CBs were lower in inner blubber compared to serum ($p<0.001$), whereas those of hexa- and hepta-CBs were higher in inner blubber compared to serum ($p<0.001$) (Figure 3.5 B).

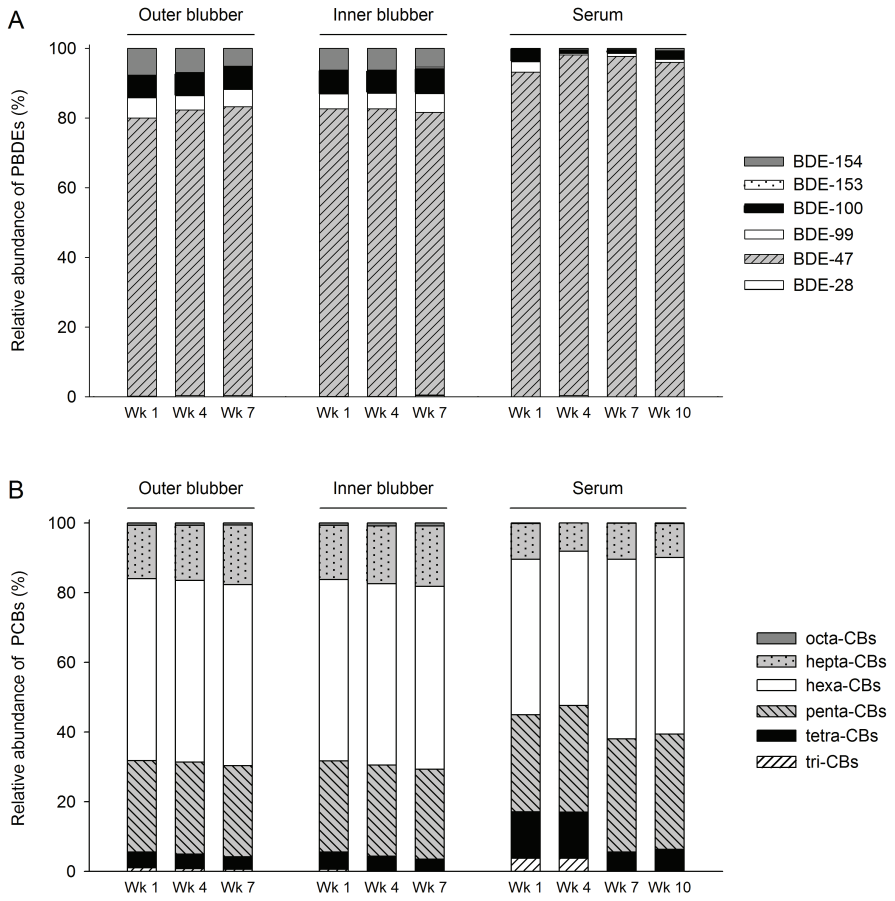

Figure 3.5 – The proportions of the different congeners of PBDEs (A) and classes of PCBs (B) in outer blubber, inner blubber and serum of NES pups during the post-weaning fast.

3.3.6. Transfer ratios of POPs from blubber to serum

The transfer ratios (TR) from inner blubber to serum, which correspond to the ratio of concentrations between the serum and inner blubber decreased with the number of chlorine and bromine atoms within a period of fast (weeks 1, 4 and 7) for studied PBDE congeners and PCB classes (Figure 3.6 A-B). Furthermore, an inverse correlation was observed between the logarithm transformation of TR from inner blubber to serum and the log K_{ow}. This was noticed at each studied period of fast (weeks 1, 4 and 7). These results suggest an exponentially decreasing relationship between TR and log K_{ow} values. No relationships were found for *p,p'*-DDE and HCB (results not shown).

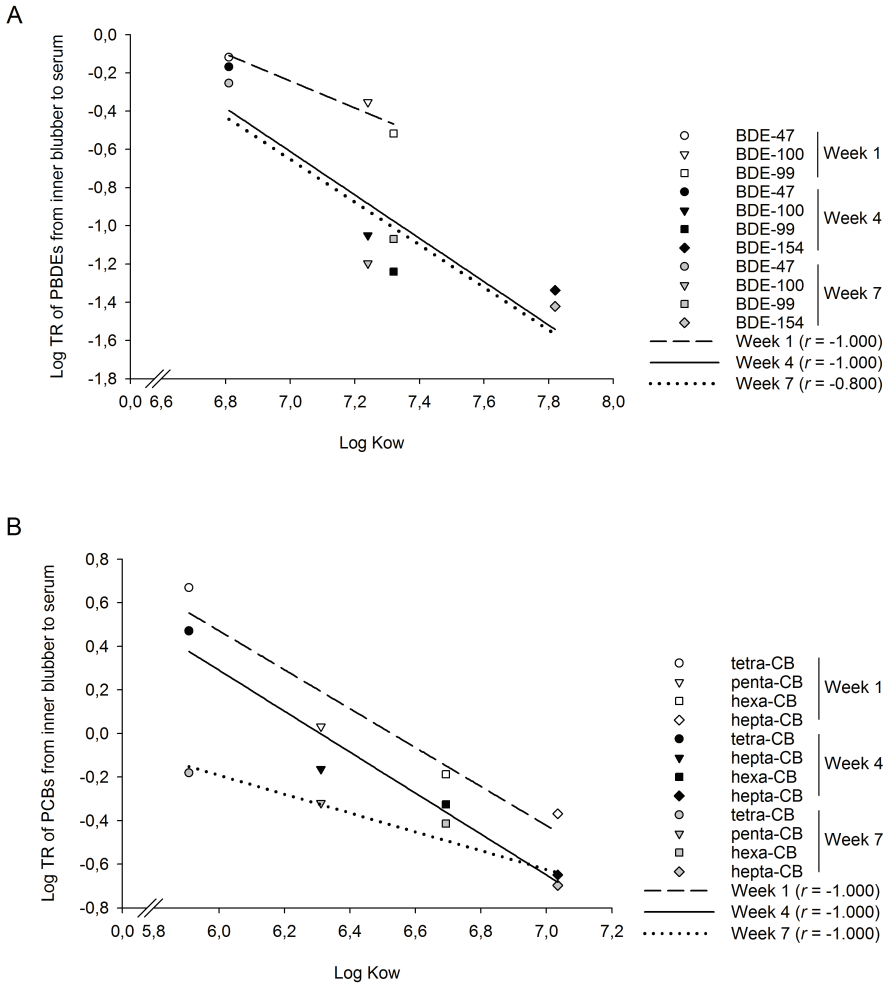

Figure 3.6 – Relationships between the octanol/water partition coefficient (log K_{ow}) values and the transfer ratios (TR) from inner blubber to serum of PBDE congeners (A) and PCB classes (B) in NES pups during the post-weaning fast (weeks 1, 4 and 7). Values of log K_{ow} were compiled from Braekevelt et al. (2003), De Bruijn et al. (1989) and Hansen et al. (1999). Log K_{ow} for the different classes of PCBs was calculated as the mean of log K_{ow} of each PCB congener present in the corresponding group.

3.4. Discussion

This is the first study that monitors and compares the levels, profiles and dynamics of PBDEs, PCBs, *p,p'*-DDE and HCB in the blubber and serum of NES pups throughout the post-weaning fast.

3.4.1. Levels and profiles of pollutants

Concentrations of targeted lipophilic groups measured in the weaned NES were in the order *p,p'*-DDE > PCBs >> HCB > PBDEs.

3.4.1.1. PBDEs

Weaned NES pups were marginally contaminated by PBDEs. The only other study investigating PBDE concentrations in NES focused on young (less than 1 year old), stranded individuals from southern California (Meng et al., 2009). The total blubber PBDE concentrations were 20 to 30 times higher than in the present study. The stranded animals used in Meng et al. (2009) were sampled from 1994 to 2006, just before they died. The cause of death and the degree of emaciation may influence the concentrations of PBDEs and thus explain, at least partly, the higher concentrations observed in their study. One must also note that 4 to 16 years separate the sampling of the two studies. The lower PBDE concentrations reported in our study might thus also be interpreted as a potential temporal trend as already observed in harbour seals near Vancouver Island (Ross et al., 2013). The drop of concentrations was explained by the withdrawal of the Penta- and Octa-BDE mixtures from the market in 2004 (Ross et al., 2013). Further investigations are however needed to confirm this hypothesis for NES.

Weaned NES pups were also less contaminated by PBDEs (one order of magnitude) than weaned harbour seal pups from central California (Greig et al., 2011). Higher levels of contamination are also reported in marine mammals from other parts of the world, such as in harbour seals from northwestern North America (one order of magnitude) (Ross et al., 2013) and from northwest Atlantic coast (one to two orders of magnitude) (Shaw

et al., 2012) and in grey seals from Scotland (one order of magnitude) (Vanden Berghe et al., 2012).

The PBDE profile of weaned NES was mainly composed of BDE-47. This congener is usually the dominant PBDE congener in marine mammals (Meng et al., 2009; Vanden Berghe et al., 2012). The high proportion of BDE-47 could be explained by different factors, such as the importance of this congener, together with BDE-99, in the Penta-BDE industrial mixture, widely used in the 1990s and 2000s (de Wit, 2002), the ability of marine mammals to debrominate BDE-99 into BDE-47 (Meng et al., 2009; Stapleton et al., 2004) and the higher bioaccumulation potential of lower brominated congeners (She et al., 2002).

3.4.1.2. PCBs

Total PCB levels reported in the present study were similar to the concentrations measured in the blubber of weaned NES pups sampled in the same colony in 2002 (Debier et al., 2005a; 2006). There was thus no temporal change of PCB concentrations in the blubber of weaned NES pups from Año Nuevo colony between 2002 and 2010. The PCB concentrations were also comparable to the data of healthy free-ranging yearling NES sampled in 1992 in California (Beckmen et al., 1997). Similar concentrations were also seen between 1997 and 2002 for NES pups along the Californian coast (Blasius and Goodmanlowe, 2008). In addition, weaned NES pups were contaminated within the range of PCB values encountered in NES lactating females from the same colony, most likely as a consequence of the efficient transfer through the milk (Debier et al., 2012).

Other data about PCBs in NES concern stranded/diseased NES pups and yearlings sampled in the 1990s and early 2000s. Levels reported in those studies are between 2 and more than 50 times higher than those reported in the present study (Beckmen et al., 1997; Blasius and Goodmanlowe, 2008; Kajiwara et al., 2001; Kannan et al., 2004). Such higher levels most probably result from the fact that those animals were not in good condition. Indeed, emaciation induces the concentration of pollutants within the remaining amount of blubber. In addition, during their first year of life, NES feed in

the polluted coastal waters and do not gain much weight, leading to a concentration of pollutants in the adipose tissue. Their contamination thus rather reflects coastal pollution as compared to weaned pups and adult females (Debier et al., 2005a). The higher levels could also come, at least in part, from a prospective temporal trend, as a consequence of the reduction of PCB input since 1976 in USA and since 1977 in Canada. Data collected from the 1970s to the 1990s indicate decreasing levels of PCBs in the blubber of pinnipeds and cetaceans from the Pacific coast (Aguilar et al., 2002). Nevertheless, the fact that the PCB concentrations reported in NES healthy yearlings in 1992 were comparable to those of the present study indicates that body condition rather than temporal trend is the main factor involved in the higher concentrations observed in stranded/diseased NES.

Higher PCB concentrations (around one order of magnitude) are usually reported in the tissues of marine mammals from the Pacific coast of North America, such as live-captured harbour seals near Vancouver Island (Ross et al., 2013) and harbour seal pups from central California (Greig et al., 2011). In general, higher PCB levels (around one order of magnitude) are also found in marine mammals from other parts of the world, such as lactating grey seals from Scotland (Vanden Berghe et al., 2012) and harbour seals from Canada (Cullon et al., 2012).

The penta-, hexa- and hepta-CBs were the major components of the PCB content, as previously observed in NES from the same colony (Debier et al., 2005a; Debier et al., 2006; Debier et al., 2012) with CB-99, -118, -138 and -153 being the biggest contributors to the burden of PCBs.

3.4.1.3. *p,p'*-DDE

The levels of *p,p'*-DDE in the blubber of weaned NES, which makes up more than 98% of total DDT (Debier et al., 2012; Greig et al., 2011; Vanden Berghe et al., 2012), were lower than the levels of total DDT previously reported in stranded yearling NES in 1990s and 2002 (Beckmen et al., 1997; Kajiwara et al., 2001; Kannan et al., 2004). As already explained for PCBs, a combination of coastal feeding habits, poor body condition and temporal trends is most probably at the origin of the higher total DDT levels reported

in those studies. On the contrary, the total DDT concentrations encountered in the blubber of lactating females from the same colony were comparable to the present results, which reflects the high transfer of *p,p'*-DDE from mother to pup through the consumption of milk (Debier et al., 2012). The high DDE/PCB ratio reported in weaned NES pups is a common pattern of contamination on the west coast of North America (Debier et al., 2005a; Debier et al., 2012). More generally, the contamination of weaned NES pups was similar to the one of adult female grey seals from Scotland (Vanden Berghe et al., 2012) and higher than adult male and female Weddell seals from Antarctica (Trumble et al., 2012).

3.4.1.4. HCB

The concentrations of HCB were in the same order of magnitude as those found in earlier investigations on stranded yearling NES in California (Kajiwara et al., 2001; Kannan et al., 2004). There are also similar to those of lactating grey seals and harp seals sampled in Canada (Frouin et al., 2012; Sørmo et al., 2003), but slightly higher than those of lactating grey seals sampled in Scotland (Vanden Berghe et al., 2012).

3.4.2. Dynamics of POPs throughout the fast

During 6 weeks of post-weaning fast, weaned NES lost more than 30 kg. Their lipid mass is reduced from 24-49% (Noren et al., 2003). Blubber lipids, which are mainly composed of triglycerides, are thus mobilised in high amounts during that period (Ryg et al., 1988). The mobilisation occurs mainly from the inner blubber layer, while the outer blubber layer remains relatively stable (Vanden Berghe et al., 2012; Wheatley et al., 2008). In the present study, constant lipid percentage per unit of weight was observed in inner blubber between early and late fast. Similar tendency was also highlighted in the blubber of NES lactating females (Crocker et al., 2001). Such results were however different from those of Vanden Berghe et al. (2012), for lactating grey seals, in which a small, but significant drop of blubber lipid percentage was seen. Adipocytes of fasting NES pups appear to shrink with the hydrolysis of triglycerides and the mobilisation of free FAs in

the circulation. Indeed, morphometric results showed an increase of small-size adipocytes as well as a decrease of mid- and large-size adipocytes in the blubber. In addition, there was a corresponding rise of circulating free FAs throughout the post-weaning fast. The proportion of connective tissue being very small in phocid seals in general (1 – 4%), it might explain the fact that the lipid percentage, expressed per unit of blubber weight, did not change significantly with the progression of the fast, despite the important triglyceride mobilisation.

At early fast, the concentrations of PBDEs, PCBs and *p,p'*-DDE were homogeneously distributed in the blubber. Similar results were already observed for PCBs in the blubber of weaned NES (Debier et al., 2006). During suckling, NES pups accumulate a large fat deposit through the lipid-rich milk and lipophilic pollutants are distributed evenly throughout the adipose tissue. The onset of pollutant stratification within the blubber column may occur during the first fasting period (i.e. the post-weaning fast) and could be maintained throughout the life of adult animals by the numerous "feeding/fasting" cycles (Debier et al., 2006). PCB and DDT concentrations of NES lactating females are indeed characterised by a stratification between inner and outer blubber (Debier et al., 2012), a pattern also observed in other phocid seal species (Debier et al., 2003; Vanden Berghe et al., 2012). The concentrations of PBDEs, PCBs and *p,p'*-DDE expressed per unit of blubber lipids of weaned NES rose throughout the fast. The phenomenon was more pronounced in inner blubber, probably because of the higher mobilisation of lipids from this layer. As a result, POP concentrations became higher in inner blubber as compared to outer blubber at late fast. This suggests a more efficient and prominent mobilisation of lipids than POPs from blubber, as already shown in weaned NES (Debier et al., 2006). It is possible that such lipophilic pollutants preferentially remain within the adipose tissue and/or are released into the circulation and then reabsorbed by adipocytes, as a result of their affinity for this lipophilic compartment (Vanden Berghe et al., 2012).

Within PCB groups, the increase of concentrations appeared to vary with the chlorination degree of the congeners, especially in inner blubber.

The rise of concentrations was indeed more pronounced for more lipophilic compounds such as octa- and hepta-CBs, followed by hexa- and penta-CBs, followed by tetra- and tri-CBs. It suggests that the mobilisation of POPs from blubber is influenced, at least in part, by the physico-chemical properties of the molecules (molecular weight, size and lipophilicity) (Vanden Berghe et al., 2012). By way of example, the mean log K_{ow} for hepta-CBs is 7.0 (range: 6.93 – 7.17), which can therefore be considered as extremely lipophilic, whereas the log K_{ow} for tri-CBs (represented by PCB-28) is 5.55, which reflects a less lipophilic character. The higher chlorinated, and thus more lipophilic, congeners concentrate more importantly in the blubber with the progression of the fast than the lower chlorinated congeners.

Furthermore, it should be noted that the behaviour of HCB was slightly different from the ones of total PBDEs, total PCBs and *p,p'*-DDE. It was homogeneously distributed in the blubber at early fast and increased slightly, over the course of fast, in both layers. It seems that HCB (log K_{ow} = 5.47; Gobas et al. (1988)) does not concentrate in inner blubber lipids as dramatically as the other POPs families. HCB dynamic could thus be compared to the behaviour of lower chlorinated PCBs, especially to tri- (log K_{ow} for PCB-28 = 5.55) and tetra-CBs (mean log K_{ow} = 5.9; range: 5.86 – 6.01). Due to their less pronounced lipophilic character, they seem to be more easily mobilised from blubber into the serum.

An increase in concentration of POPs was noted in the serum of weaned NES throughout the fast, when the results were expressed per unit of wet weight or per unit of lipid weight. Since blubber is the main storage site of POPs (Wolkers et al., 2006), it is reasonable to assume that the contamination of serum would depend in part on the mobilisation of POPs from the inner layer, which is more vascularised and metabolically active. As already noted above, POPs may be mobilised from blubber into the bloodstream together with lipids. One part of the discharged POPs might then be reabsorbed by the blubber, while the other part is put into circulation by the blood flow (Vanden Berghe et al., 2012). Serum free FAs increase significantly across the fast in weaned pups but this increase may be strongly influenced by changes in rates of re-esterification instead of

enhanced lipolysis (Viscarra and Ortiz, 2013). When the POP levels were expressed per unit of serum free FAs, the concentrations of PBDEs and PCBs dropped between weeks 1 and 4, before stabilizing until the end of the fast. These dynamics support the hypothesis that the mobilisation of POPs from adipose tissue is less important than the one of lipids especially during the first part of the fast, but rises at the end of the fast (Debier et al., 2003; Debier et al., 2006).

Within PCB groups, the dynamics of tri- and tetra-CBs differed from those of other congeners and from the general tendency discussed here above. Their levels, expressed per unit of wet weight, lipid weight and free FAs, decreased during the second part of the fast. It is possible that those congeners, once mobilised into the circulation, are efficiently taken up by other tissues such as the liver and biotransformed. Indeed, marine mammals appear to be capable of biotransforming PCBs to some extent, through the production of cytochrome P450 in the phase I biotransformation process (Nyman et al., 2001; Teramitsu et al., 2000). More investigations are needed to warrant this hypothesis on the metabolisation of tri- and tetra-CBs in NES pups.

3.4.3. Comparisons of POP composition between tissues

The PBDE and PCB profiles were fairly stable within the blubber layers. Otherwise, the pattern of the inner blubber differed from that of serum. Indeed, the lower halogenated congeners (BDE-47, a tetra-BDE, and tetra- and penta-CBs) were present in higher proportions in serum, whereas the higher halogenated congeners (two penta-BDEs: BDE-99 and -100; a hexa-BDE: BDE-154; together with hexa- and hepta-CBs) were found in higher proportions in the inner blubber. Such pattern supports the selective retention of some congeners in inner blubber. The TR of PBDE congeners and PCB classes from inner blubber to serum was indeed inversely related to their water solubility (log K_{ow}), which agreed with previous findings on the mobilisation of PCBs and PBDEs from the blubber of lactating grey seals (Vanden Berghe et al., 2012). This tendency has been also observed during weight loss in humans (Dirtu et al., 2013). The less lipophilic contaminants

(with low log K_{ow}) were more efficiently mobilised from inner blubber to serum than the more lipophilic ones (with high log K_{ow}).

It is reasonable to think that the mobilisation of POPs is affected by the lipid composition of both compartments. Phocid blubber lipids contain more than 99% of non-polar triglycerides (Wheatley et al., 2008), while circulating blood lipids consist of non-polar triglycerides, but also free FAs, cholesterol, cholesterol esters and phospholipids (Sørmo et al., 2003). The most apolar POPs would thus preferentially remain in the adipose tissue.

3.5. Conclusion

With the exception of HCB, the weaned NES pups were characterised by a relatively low contamination as compared to the levels usually found in the literature on marine mammals. Nevertheless, the significant release of POPs from blubber to serum during the post-weaning fast may cause a potential risk for the health of such young animals, which undergo a crucial period of development. We observed a homogeneous distribution of POPs throughout the blubber at early fast in weaned NES pups. At late fast, the concentrations of PBDEs, PCBs and *p,p'*-DDE were higher in inner than in outer blubber, as a result of the sharp increase of their levels in the inner layer with the progression of the fast. These findings could be explained by a more efficient mobilisation of lipids from adipose tissue as compared to POPs. The behaviour of POPs was influenced by the physico-chemical properties of the molecules: the higher halogenated POPs (i.e. the more lipophilic congeners) were preferentially kept within blubber with the progression of the fast than the lower halogenated congeners.

3.6. Appendices

Table S1. Means ± SD of the lipid fractions (g/L) measured in the serum of weaned NES pups. Within a row, values followed by different letters are significantly different ($p \leq 0.05$).

Lipid fraction	Serum			
(g/L)	Week 1	Week 4	Week 7	Week 10
Triglycerides	0.8 ± 0.2^{a}	0.9 ± 0.3^{b}	1.2 ± 0.3^{c}	1.5 ± 0.6^{c}
Cholesterol	$3.3 \pm 0.5^{a,c}$	3.8 ± 0.5^{b}	3.4 ± 0.4^{a}	3.2 ± 0.3^{c}
Free FAs	0.4 ± 0.1^{a}	0.6 ± 0.2^{b}	0.6 ± 0.2^{b}	0.8 ± 0.2^{c}
Phospholipids	5.3 ± 0.5^{a}	6.2 ± 0.6^{b}	5.9 ± 0.4^{c}	5.6 ± 0.5^{a}
Total lipids	10.1 ± 0.9^{a}	11.6 ± 1.1^{b}	11.1 ± 0.9^{b}	11.0 ± 1.3^{b}

Table S2. Mean detection frequency (f) and limit of quantification (LOQ) for each PBDE congener in the different investigated tissues.

Congeners	LOQ OB (ng/g lw)	%f OB	LOQ IB (ng/g lw)	%f IB	LOQ S (pg/mL)	%f S
BDE 28	0.2	8	0.2	9	5	1
BDE 47	0.2	100	0.2	100	5	75
BDE 99	0.2	83	0.2	94	5	7
BDE 100	0.2	100	0.2	100	5	19
BDE 153	0.2	0	0.2	8	5	0
BDE 154	0.2	86	0.2	97	5	4

OB = outer blubber; IB = inner blubber; S = serum

Table S3. Mean detection frequency (f) and limit of quantification (LOQ) for each PCB congener, *p,p'*-DDE and HCB in the different investigated tissues.

Congeners	LOQ OB (ng/g)	%f OB	LOQ IB (ng/g)	%f IB	LOQ S (pg/mL)	%f S
CB-28	5.0	35	5.0	18	5.0	25
CB-47	2.5	92	2.5	100	2.5	97
CB-49	2.5	0	2.5	2	2.5	23
CB-52	2.5	64	2.5	76	2.5	31
CB-74	2.5	100	2.5	100	2.5	100
CB-95	2.5	98	2.5	100	2.5	100
CB-99	2.5	100	2.5	100	2.5	100
CB-101	2.5	92	2.5	98	2.5	94
CB-105	2.5	95	2.5	97	2.5	100
CB-110	2.5	64	2.5	70	2.5	10
CB-118	2.5	100	2.5	100	2.5	100
CB-128	2.5	100	2.5	100	2.5	100
CB-138	2.5	100	2.5	100	2.5	100
CB-146	2.5	98	2.5	100	2.5	100
CB-149	2.5	100	2.5	100	2.5	100
CB-151	2.5	100	2.5	100	2.5	100
CB-153	2.5	100	2.5	100	2.5	100
CB-156	2.5	56	2.5	71	2.5	12
CB-170	2.5	100	2.5	100	2.5	98
CB-171	2.5	42	2.5	58	2.5	12
CB-172	2.5	26	2.5	38	2.5	0
CB-174	2.5	71	2.5	64	2.5	5
CB-177	2.5	100	2.5	100	2.5	94
CB-180	2.5	100	2.5	100	2.5	100
CB-183	2.5	100	2.5	100	2.5	99
CB-187	2.5	100	2.5	100	2.5	100
CB-194	2.5	6	2.5	27	2.5	0
CB-199	2.5	71	2.5	95	2.5	15
CB-206	2.5	0	2.5	0	2.5	0
CB-209	2.5	0	2.5	0	2.5	0
p,p'-DDE	10	100	10	100	50	100
HCB	4	100	4	100	20	100

Table S4. Means ± SEM of the concentration of PBDE congeners and PCB classes in the serum in NES pups throughout the post-weaning fast, expressed per unit of serum lipids and unit of free FAs.

	Serum (ng/g lipids)				Serum (ng/g free FAs)			
	Week 1	Week 4	Week 7	Week 10	Week 1	Week 4	Week 7	Week 10
BDE-47	6.52 ± 0.93^{a}	7.02 ± 0.91^{b}	8.44 ± 1.17^{c}	9.46 ± 1.18^{d}	201.71 ± 46.14^{a}	$133.51 \pm 12.88^{b,c}$	$153.69 \pm 18.09^{a,b}$	148.50 ± 21.39^{c}
BDE-99	0.23 ± 0.15^{a}	0.04 ± 0.02^{b}	0.09 ± 0.03^{a}	0.12 ± 0.08^{a}	6.79 ± 4.67^{a}	0.68 ± 0.27^{b}	1.47 ± 0.47^{b}	1.69 ± 0.94^{b}
BDE-100	0.33 ± 0.10^{a}	0.14 ± 0.08^{b}	0.21 ± 0.12^{b}	0.27 ± 0.15^{a}	11.25 ± 4.73^{a}	2.23 ± 1.16^{b}	3.39 ± 2.34^{b}	4.24 ± 2.46^{c}
BDE-154	N.D.	N.D.	N.D.	N.D.	N.D.	N.D.	N.D.	N.D.
∑ PBDEs	**7.08 ± 1.02^{a}**	**7.28 ± 1.04^{a}**	**8.78 ± 1.36^{b}**	**9.91 ± 1.35^{c}**	**220.96 ± 50.96^{a}**	**137.71 ± 14.45^{b}**	**$158.42 \pm 20.82^{a,b}$**	**$154.49 \pm 29.52^{a,b}$**
∑ tri-CBs	14.6 ± 2.1^{a}	14.9 ± 2.2^{a}	0.4 ± 0.2^{b}	1.0 ± 0.7^{c}	427 ± 78^{a}	274 ± 41^{a}	7 ± 3^{b}	14 ± 9^{c}
∑ tetra-CBs	50.2 ± 5.8^{a}	52.8 ± 5.3^{a}	24.8 ± 1.2^{b}	32.4 ± 2.1^{c}	1436 ± 186^{a}	992 ± 90^{b}	471 ± 32^{c}	499 ± 46^{c}
∑ penta-CBs	102.7 ± 4.8^{a}	120.5 ± 6.6^{b}	148.8 ± 8.0^{c}	176.9 ± 10.7^{d}	2998 ± 254^{a}	2373 ± 163^{b}	2804 ± 185^{a}	$2758 \pm 273^{a,b}$
∑ hexa-CBs	163.1 ± 6.6^{a}	171.2 ± 7.4^{a}	235.4 ± 12.3^{b}	273.0 ± 18.4^{c}	4740 ± 361^{a}	3399 ± 223^{b}	4434 ± 292^{a}	$4321 \pm 512^{a,b}$
∑ hepta-CBs	37.7 ± 2.7^{a}	31.4 ± 1.4^{b}	47.9 ± 3.1^{c}	53.0 ± 4.2^{c}	1100 ± 110^{a}	621 ± 40^{b}	897 ± 65^{a}	840 ± 108^{a}
∑ PCBs	**369.5 ± 16.0^{a}**	**392.1 ± 20.7^{a}**	**457.4 ± 24.2^{b}**	**537.4 ± 24.8^{c}**	**10792 ± 886^{a}**	**7694 ± 489^{b}**	**8573 ± 560^{b}**	**9890 ± 840^{a}**

For a defined tissue, values within a row followed by different letters are significantly different ($p \leq 0.05$).
N.D = not detected

3.7. References

Aguilar, A., et al., 2002. Geographical and temporal variation in levels of organochlorine contaminants in marine mammals. Marine Environmental Research. 53, 425-452.

Beckmen, K., et al., 1997. Clinical and pathological characterization of northern elephant seal skin disease. Journal of Wildlife Diseases. 33, 438-449.

Blasius, M. E., Goodmanlowe, G. D., 2008. Contaminants still high in top-level carnivores in the Southern California Bight: Levels of DDT and PCBs in resident and transient pinnipeds. Marine Pollution Bulletin. 56, 1973-1982.

Braekevelt, E., et al., 2003. Direct measurement of octanol–water partition coefficients of some environmentally relevant brominated diphenyl ether congeners. Chemosphere. 51, 563-567.

Covaci, A., et al., 2002a. Distribution of organobrominated and organochlorinated contaminants in Belgian human adipose tissue. Environmental Research. 88, 210-218.

Covaci, A., et al., 2008. Anthropogenic and naturally occurring organobrominated compounds in two deep-sea fish species from the Mediterranean Sea. Environmental Science & Technology. 42, 8654-8660.

Covaci, A., et al., 2002b. Determination of organohalogenated contaminants in liver of harbour porpoises (*Phocoena phocoena*) stranded on the Belgian North Sea coast. Marine Pollution Bulletin. 44, 1157-1165.

Crocker, D. E., et al., 2001. Maternal traits and reproductive effort in northern elephant seals. Ecology. 82, 3541-3555.

Cullon, D. L., et al., 2012. Biomagnification of polychlorinated biphenyls in a harbor seal (*Phoca vitulina*) food web from the strait of Georgia, British Columbia, Canada. Environmental Toxicology and Chemistry. 31, 2445-2455.

Darnerud, P. O., 2008. Brominated flame retardants as possible endocrine disrupters. International Journal of Andrology. 31, 152-160.

Das, K., et al., 2006. Interfollicular fibrosis in the thyroid of the harbour porpoise: An endocrine disruption? Archives of Environmental Contamination and Toxicology. 51, 720-729.

De Bruijn, J., et al., 1989. Determination of octanol/water partition coefficients for hydrophobic organic chemicals with the "slow-stirring" method. Environmental Toxicology and Chemistry. 8**,** 499-512.

de Wit, C. A., 2002. An overview of brominated flame retardants in the environment. Chemosphere. 46**,** 583-624.

Debier, C., et al., 2006. Mobilization of PCBs from blubber to blood in northern elephant seals (*Mirounga angustirostris*) during the post-weaning fast. Aquatic Toxicology. 80**,** 149-157.

Debier, C., et al., 2012. Differential changes of fat-soluble vitamins and pollutants during lactation in northern elephant seal mother–pup pairs. Comparative Biochemistry and Physiology Part A. 162**,** 323-330.

Debier, C., et al., 2005a. Polychlorinated biphenyls, dioxins, and furans in weaned, free-ranging northern elephant seal pups from central California, USA. Environmental Toxicology and Chemistry. 24**,** 629-633.

Debier, C., et al., 2003. Quantitative dynamics of PCB transfer from mother to pup during lactation in UK grey seals *Halichoerus grypus*. Marine Ecology Progress Series. 247**,** 237-248.

Debier, C., et al., 2005b. PCBs and DDT in the serum of juvenile California sea lions: associations with vitamins A and E and thyroid hormones. Environmental Pollution. 134**,** 323-332.

Dirtu, A. C., et al., 2013. Dynamics of organohalogenated contaminants in human serum from obese individuals during one year of weight loss treatment. Environmental Science & Technology. 47**,** 12441-12449.

Frouin, H., et al., 2012. Transfer of PBDEs and chlorinated POPs from mother to pup during lactation in harp seals *Phoca groenlandica*. Science of the Total Environment. 417**,** 98-107.

Gobas, F. A. P. C., et al., 1988. A novel method for measuring membrane-water partition coefficients of hydrophobic organic chemicals: Comparison with 1-octanol-water partitioning. Journal of Pharmaceutical Sciences. 77**,** 265-272.

Greig, D. J., et al., 2011. Geography and stage of development affect persistent organic pollutants in stranded and wild-caught harbor seal pups from central California. Science of the Total Environment. 409**,** 3537-3547.

Hansen, B. G., et al., 1999. QSARs for K_{OW} and K_{OC} of PCB congeners: A critical examination of data, assumptions and statistical approaches. Chemosphere. 39**,** 2209-2228.

Jürgens, M. D., et al., 2013. The presence of EU priority substances mercury, hexachlorobenzene, hexachlorobutadiene and PBDEs in wild fish from four English rivers. Science of the Total Environment. 461, 441-452.

Kajiwara, N., et al., 2001. Organochlorine pesticides, polychlorinated biphenyls, and butyltin compounds in blubber and livers of stranded California sea lions, elephant seals, and harbor seals from coastal California, USA. Archives of Environmental Contamination and Toxicology. 41, 90-99.

Kannan, K., et al., 2004. Organochlorine pesticides and polychlorinated biphenyls in California sea lions. Environmental Pollution. 131, 425-434.

Letcher, R. J., et al., 2010. Exposure and effects assessment of persistent organohalogen contaminants in arctic wildlife and fish. Science of the Total Environment. 408, 2995-3043.

Meng, X. Z., et al., 2009. Polybrominated diphenyl ethers in pinnipeds stranded along the Southern California coast. Environmental Pollution. 157, 2731-2736.

Mössner, S., et al., 1994. Determination of HCHs, PCBs, and DDTs in brain tissues of marine mammals off different age. Fresenius' Journal of Analytical Chemistry. 349, 708-716.

Noren, D. P., et al., 2003. Energy reserve utilization in northern elephant seal (*Mirounga angustirostris*) pups during the postweaning fast: size does matter. Journal of Comparative Physiology B. 173, 443-454.

Nyman, M., et al., 2001. Characterization of xenobiotic-metabolizing cytochrome P450 (CYP) forms in ringed and grey seals from the Baltic Sea and reference sites. Comparative Biochemistry and Physiology Part C. 128, 99-112.

Ross, P. S., 2002. The role of immunotoxic environmental contaminants in facilitating the emergence of infectious diseases in marine mammals. Human and Ecological Risk Assessment: An International Journal. 8, 277-292.

Ross, P. S., et al., 2013. Declining concentrations of persistent PCBs, PBDEs, PCDEs, and PCNs in harbor seals (*Phoca vitulina*) from the Salish Sea. Progress in Oceanography. 115, 160-170.

Ryg, M., et al., 1988. Thermal significance of the topographical distribution of blubber in ringed seals (*Phoca hispida*). Canadian Journal of Fisheries and Aquatic Sciences. 45, 985-992.

Severinsen, T., et al., 2000. Spatial distribution of persistent organochlorines in ringed seal (*Phoca hispida*) blubber. Marine Environmental Research. 49, 291-302.

Shaw, S. D., et al., 2012. Tissue-specific accumulation of polybrominated diphenyl ethers (PBDEs) including Deca-BDE and hexabromocyclododecanes (HBCDs) in harbor seals from the Northwest Atlantic. Environment International. 44, 1-6.

She, J., et al., 2002. PBDEs in the San Francisco Bay Area: Measurements in harbor seal blubber and human breast adipose tissue. Chemosphere. 46, 697-707.

Sørmo, E. G., et al., 2003. Partitioning of persistent organic pollutants in grey seal (*Halichoerus grypus*) mother–pup pairs. Science of the Total Environment. 302, 145-155.

Stapleton, H. M., et al., 2004. Debromination of polybrominated diphenyl ether congeners BDE 99 and BDE 183 in the intestinal tract of the common carp (*Cyprinus carpio*). Environmental Science & Technology. 38, 1054-1061.

Teramitsu, I., et al., 2000. Identification of novel cytochrome P450 1A genes from five marine mammal species. Aquatic Toxicology. 51, 145-153.

Trumble, S. J., et al., 2012. Assessment of legacy and emerging persistent organic pollutants in Weddell seal tissue (*Leptonychotes weddellii*) near McMurdo Sound, Antarctica. Science of the Total Environment. 439, 275-283.

Vanden Berghe, M., et al., 2010. Relationships between vitamin A and PCBs in grey seal mothers and pups during lactation. Environmental Pollution. 158, 1570-1575.

Vanden Berghe, M., et al., 2012. Selective transfer of persistent organic pollutants and their metabolites in grey seals during lactation. Environment International. 46, 6-15.

Viscarra, J. A., Ortiz, R. M., 2013. Cellular mechanisms regulating fuel metabolism in mammals: Role of adipose tissue and lipids during prolonged food deprivation. Metabolism. 62, 889-897.

Weijs, L., et al., 2009. Concentrations of chlorinated and brominated contaminants and their metabolites in serum of harbour seals and harbour porpoises. Environment International. 35, 842-850.

Wheatley, K. E., et al., 2008. Differential mobilization of blubber fatty acids in lactating Weddell seals: Evidence for selective use. Physiological and Biochemical Zoology. 81, 651-62.

Wolkers, H., et al., 2006. Tissue-specific accumulation and lactational transfer of polychlorinated biphenyls, chlorinated pesticides, and brominated flame retardants in hooded seals (*Cistophora cristata*) from the Gulf of St.

Lawrence: Applications for monitoring. Environmental Pollution. 142**,** 476-486.

Ylitalo, G. M., et al., 2005. The role of organochlorines in cancer-associated mortality in California sea lions (*Zalophus californianus*). Marine Pollution Bulletin. 50**,** 30-39.

Chapter 4

Development of an *in vitro* adipocyte model derived from the blubber of northern elephant seals (*Mirounga angustirostris*) as a tool for toxicological studies

Foreword

In the previous chapter, we reported an increase of POP concentrations within adipose tissue throughout the fast of weaned NES pups. It appeared that the lipophilicity of POPs influenced their dynamics of mobilisation from blubber. The most lipophilic pollutants were preferentially retained within the blubber compared to the less lipophilic ones. Nevertheless, due to the complexity of the whole organism and the large spectrum of contaminants present in the adipose tissue of weaned NES pups, we set up an *in vitro* model of adipocytes in order to simplify the *in vivo* situation and control different parameters to better understand the behaviour of given lipophilic pollutants within adipocytes during a lipolysis. We attempted to set up a primary culture of differentiated NES adipocytes from blubber biopsies. This chapter presents the preliminary results. These results have been submitted in Marine Mammal Science.

Development of an *in vitro* adipocyte model derived from the blubber of northern elephant seal pups (*Mirounga angustirostris*) as a tool for toxicological studies

Caroline Louis, Michael S. Tift, Daniel E. Crocker, David Alexander, Donald R. Smith and Cathy Debier

Submitted as a note in Marine Mammal Science

4.1. Introduction

Marine top predators are highly informative in understanding the quality and health of ocean habitats. Through bioamplification, they face a very large risk of exposure to toxic, persistent, and fat-soluble molecules such as polychlorinated biphenyls (PCBs), polybrominated diphenyl ethers (PBDEs), dichlorodimethyltrichloroethane (DDT), and methylmercury, which are preferentially stored in the adipose tissue. The life history of pinnipeds often includes extended periods of fasting on land. This is particularly true for phocid seals such as the northern elephant seal (NES) (*Mirounga angustirostris*). This species indeed exhibits one of the most extreme terrestrial fasting durations (up to 3 months) corresponding to breeding, lactation and moulting for females, post-weaning development for pups and maintaining a territory or competing for dominance rank on the breeding rookery for males (Le Boeuf et al., 1972). During such periods, individuals mobilise primarily lipids from their large adipose tissue stores (Costa et al., 1986; Noren et al., 2003). This mobilisation of blubber lipids presents a risk through the release of environmental pollutants into the circulation. Previous studies in fasting NES pups and females elucidated the mobilisation dynamics of PCBs, PBDEs, and DDT from blubber to blood and revealed that the mobilisation patterns of these pollutants were not directly related to those of lipids (Debier et al., 2006; Debier et al., 2012; Louis et al., 2014a). Indeed, during the beginning of the fast, the pollutants appeared to be less efficiently mobilised from blubber than lipids. Their concentrations thus increased in the remaining unmobilised blubber. The concentrations of pollutants into the blood circulation were more important at late fast. Similar dynamics were also observed in other phocid seal species such as the grey seal (Debier et al., 2003; Vanden Berghe et al., 2012). The health impact of the release of these toxic molecules into the circulation is unclear, but is believed to be at the origin of physiological disruptions (Ross et al., 2000; Vanden Berghe et al., 2010).

So far, the mechanisms associated with the mobilisation of fat-soluble pollutants from adipose tissue remain unknown. We investigated the

development of primary cultures of adipocytes from northern elephant seals, in order to study the biochemical aspects involved in the release of pollutants and lipids from the adipose tissue during periods of negative energy balance in large marine predators. Establishing such an *in vitro* model for NES is a critical element to understanding the molecular mechanisms for mobilisation and ultimately the toxicity of lipophilic environmental pollutants in these and other marine mammals. There is indeed a lack of simple *in vitro* model of adipocytes, available for the characterisation of accumulation kinetics, storage and release of fat-soluble pollutants. This model will also be useful to study the potential toxicological effects of pollutants on the endocrine function of adipose tissue. The present paper compiles the preliminary results concerning the *in vitro* differentiation of NES progenitor cells, collected on free-ranging animals, into adipocytes.

4.2. Experimental procedures

Sampling took place on NES weaned pups, at Año Nuevo State Reserve, CA, USA (37°06'30''N, 122°20'10''W) from January to April 2011, under the National Marine Fisheries Service Marine Mammal Permit #14636. Two animals were sampled for each primary culture in order to obtain 4-5 g of adipose tissue. This age class of animals was chosen due to the ease of catching. NES pups undergoing a post-weaning fast were initially immobilised with an intramuscular injection of Telazol at 1 mg/kg of estimated body mass and sedation was maintained through subsequent intravenous injections of 50 mg of ketamine (all drugs were from Fort Dodge Animal Health, Fort Dodge, IA, USA) as needed. Blood was collected from the extradural vein into Vacutainer serum tubes (Becton-Dickinson, Franklin Lakes, NJ, USA). Blubber biopsies were collected in the lateral pelvic area using 6-mm biopsy punches (Acu-punch, Acuderm Help Medical, France) and stored in cold sterile phosphate buffered saline (PBS) (Sigma-Aldrich, Atlanta, GA, USA). Once collected, samples were immediately kept at 4°C and transported to the laboratory. Blood samples were centrifuged at 1300xg for 15 min at 4°C in order to obtain serum, which was then heat-inactivated at 56°C for over 50 min, aliquoted and stored at -20°C until use. Progenitor

cells from the adipose tissue were isolated and put into culture using a protocol adapted from Bourez et al. (2012) and Louis et al. (2014b) for rats. This protocol is illustrated in Figure 4.1. First, blubber was minced with scissors under sterile conditions and added to Dulbecco's Modified Eagle Medium (DMEM) (Invitrogen, Carlsbad, CA, USA) supplemented with 10% (*v:v*) heat-inactivated fetal bovine serum (FBS) (PAA Laboratories Inc., Darthmouth, MA, USA), 10 mM HEPES buffer solution (Invitrogen), antibiotic and antifungal mixture (0.5 K/mL penicillin – 0.5 K/mL streptomycin – 1.25 µg/mL amphotericin B mixture (Lonza, Walkersville, MD, USA), 1 mg/mL gentamicin (Invitrogen) and 40 U/mL nystatin (Lonza)) and 1250 U/mL collagenase (Type II, Sigma-Aldrich). The minced fat was then incubated in the medium at 37°C for over 40 min under gentle agitation to allow tissue digestion. The digested tissue was then filtered through sterile 200 µm nylon mesh and the filtrate was centrifuged at 115xg for 5 min at 4°C. The supernatant was collected and centrifuged at 145xg for 5 min at 4°C. The pellets of the two centrifugations were pooled, filtered through sterile 25 µm nylon mesh and finally, centrifuged at 180xg for 5 min at 4°C. The supernatant was discarded. ACK lysis buffer composed of 150 mM NH_4Cl (Sigma-Aldrich), 1 mM $NaHCO_3$ (Sigma-Aldrich) and 1 µM EDTA (Sigma-Aldrich) was added to the final cell pellet at a ratio of 180:1 (*v:v*) and stored on ice for 30 min with gentle and regular stirring. The solution was then centrifuged at 200xg for 10 min at 4°C and the supernatant was then removed. This step was repeated twice in order to eliminate red blood cells. After the second centrifugation, the lysis buffer was removed and the isolated progenitor cells were suspended in DMEM supplemented with 10% (*v:v*) heat-inactivated FBS and antibiotic and antifungal mixture as described above. Cells were seeded at a mean density of $21x10^3$ cells/cm^2 on 6-well culture plates (Corning CellBind Surface, Corning Incorporated Life Sciences, Tewksbury, MA, USA). Plates were stored in an incubator at 37°C and 5% CO_2 for 24 h to allow cell sedimentation and adhesion. Twenty-four hours after the precursor isolation (day 1), the culture medium was removed and replaced by a new medium composed of DMEM, 0.1 K/mL penicillin – 0.1 K/mL streptomycin – 0.25 µg/mL amphotericin B mixture, 10% (*v:v*) heat-inactivated NES serum and

a differentiation cocktail composed of 10 nM dexamethasone, 0.5 mM 3-isobutyl-1-methylxanthine (IBMX), 10 nM ciglitizone and 8.6 µM insulin (Sigma-Aldrich) (adapted from Bourez et al. (2012) and Louis et al. (2014b)). The culture medium was renewed every two days and a visual monitoring was regularly performed.

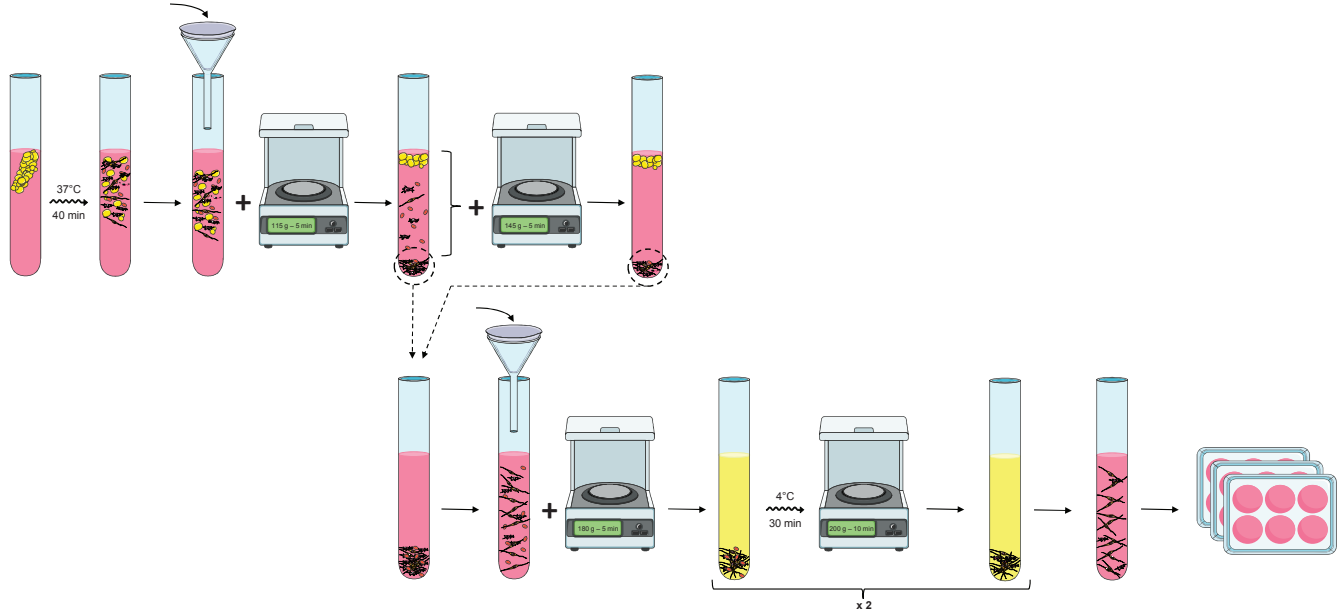

Figure 4.1 – Schematic representation of isolation of progenitor cells from northern elephant seal adipose tissue. Blubber biopsies were sampled from northern elephant seal pups. They were then digested by collagenase. Filtrations and centrifugations allowed isolating progenitor cells. Cells were treated twice with ACK lysis buffer in order to eliminate red blood cells and then, seeded on 6-well culture plates. For more details refer to the text. Figure was produced using Servier Medical Art (www.servier.com/Powerpoint-image-bank).

4.3. Results and discussion

4.3.1. Differentiation rates

The NES progenitor cells presented a typical fibroblastoid shape (Figure 4.2 A) and multiplied during the few days following the inoculation (Figure 4.2 B). After approximately 10 days, the first lipid droplets could be observed within the cells. To document the extent of adipocyte differentiation through microscopic observation, the rate of differentiation was evaluated by staining the lipids with AdipoRed (Cambrex Bio Science, Walkersville, MD, USA), a specific fluorescent staining for intracellular lipid droplets. To do this, cells were seeded on 12-well culture plates, containing a glass cover slip on the bottom, at the step of inoculation of progenitor cells. They were cultivated in culture medium that was renewed every 2 days, as described above. After 11 days, cells were stained with AdipoRed according to the manufacturer's instructions for 15 min in darkness. They were then washed with warm PBS and fixed with 4% paraformaldehyde (*v:v*) in PBS for 40 min. The cover slip was then mounted on glass slide with Vectashield (Vector Laboratories, Burlingame, CA, USA). The mounting media contained diamino-2-phenylindole (DAPI) (Sigma-Aldrich), which marked the nuclei. Cells were observed with a fluorescent microscope (excitation λ = 385 nm and emission λ = 572 nm for AdipoRed; excitation λ = 372 nm and emission λ = 454 nm for DAPI). The lipid droplets thus appeared in green and the nuclei were stained in blue. Some cells were filled with small fat droplets (Figure 4.2 C-D). After 20 days of culture in 6-well culture plates, cells were stained with Oil Red O (ORO) (Li et al., 2008). To do this, the culture medium was removed at day 20 and cells were washed twice with warm PBS before being fixed with 4% paraformaldehyde (*v:v*) (Sigma-Aldrich) in PBS for 40 min. Cells were rinsed once with deionized water and incubated with ORO solution (Sigma-Aldrich) in 60% isopropanol for 15 min. Fixed cells were kept wet with deionized water. In this staining treatment, the lipids within lipid droplets appeared red. Around 10% of the cells were considered as adipocytes after 3 weeks of culture, while around 80% of the cells kept an elongated shape but accumulated very small fat

droplets as evidenced by ORO staining on Figure 4.2 E. The cells considered as adipocytes exhibited various forms (Figure 4.2 E).

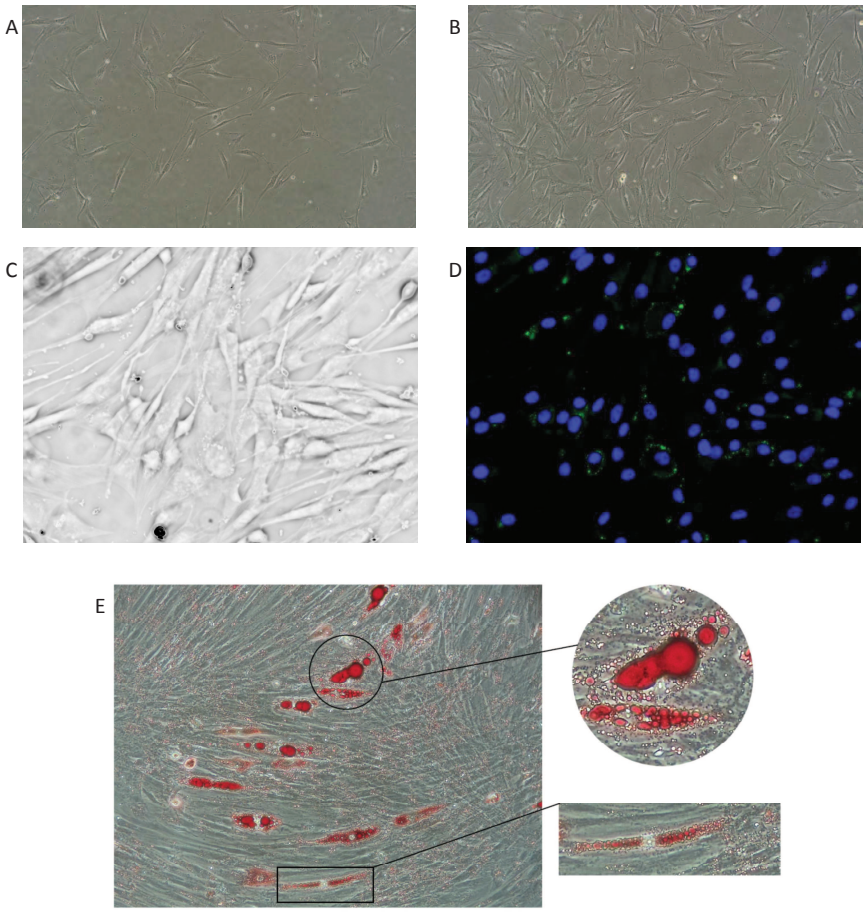

Figure 4.2 – Progenitor cells from northern elephant seals (NES) were cultivated with 10% NES serum and the differentiation cocktail during 3 days (A) and 7 days (light microscopy) (B). They were then stained with diamino-2-phenylindole and AdipoRed after 11 days of culture (light microscopy) (C). The nuclei appear in blue and lipid droplets, in green with a fluorescence microscope (D). Similarly, after 20 days of culture, cells were fixed and stained with Oil Red O. The lipid droplets then appear in red (light microscopy) (E).

4.3.2. Effect of differentiation cocktail

The differentiation cocktail used in the present study (e.g. dexamethasone, IBMX, ciglitizone and insulin) is an established cocktail for inducing adipocyte differentiation of rodent progenitor cells (Bourez et al., 2012; Louis et al., 2014b). Dexamethasone, a synthetic glucocorticoid, stimulates adipocyte differentiation in cell lines derived from mice (3T3-L1) (Yeh et al., 1995) and preadipocytes of rats, pigs and humans (Chen et al., 1995; Joyner et al., 2000; Kras et al., 1999; Shin et al., 2003). IBMX, a synthetic chemical, can induce adipocyte differentiation in 3T3-L1 cells (Birsoy et al., 2008). Both dexamethasone and IBMX induce two families of transcription factors, C/EBPs and PPAR-γ, which play major roles in the differentiation of preadipocytes (Cao et al., 1991; Shin et al., 2003). Similarly, ciglitizone, a member of thiazolidinedione family, has been shown to enhance the differentiation of murine C3H10T1/2 cell lines and human mesenchymal stem cells in adipocytes by acting as a selective ligand of PPAR-γ (Janderová et al., 2003; Lehmann et al., 1995; Rosen, 2005; Spiegelman, 1998). Insulin is known to promote differentiation of murine cell lines (3T3-L1 and 3T3-F442A) (Ailhaud, 1982), and it can indeed upregulate the transcription of C/EBPs in 3T3-L1 cell line (Klemm et al., 2001; MacDougald et al., 1995) and stimulate the PPAR-γ mRNA and protein expression in human adipocytes (*in vivo* and in mature isolated cells) (Rieusset et al., 1999). In addition, insulin induces the translocation of glucose transporter type 4 (Glut4) from the cytosol to the plasma membrane of adipocytes. As a result, the extracellular glucose may be absorbed by the cells and converted to fatty acids through the lipogenesis pathway (Cushman and Wardzala, 1980). The differentiation rate of NES progenitor cells into adipocytes obtained in the present study was lower than what is usually obtained for rodents and humans (Bourez et al., 2012; Janderová et al., 2003; Louis et al., 2014b; Pittenger et al., 1999). We believe this might be due to the fact that NES possess unique physiological specificities. For example, *in vivo* studies report different levels of insulin resistance in fasting individuals (Fowler et al., 2008; Viscarra et al., 2011). Therefore, it is possible that the differentiation cocktail used for rodents does not have the same impact on

NES progenitor cells. To address this, we investigated the effect of the presence/absence of this cocktail on the differentiation of NES progenitor cells into adipocytes. After 20 days of culture, there was no accumulation of lipids inside the cells when they were cultivated without the cocktail of differentiation (Figure 4.3 A). By microscopic observation, it appeared that without the cocktail of differentiation, cells do not have the ability to engage in the adipocyte differentiation pathway. This cocktail thus appears necessary to differentiate NES progenitor cells into adipocytes, even though its composition could be improved in order to be better adapted to NES physiology.

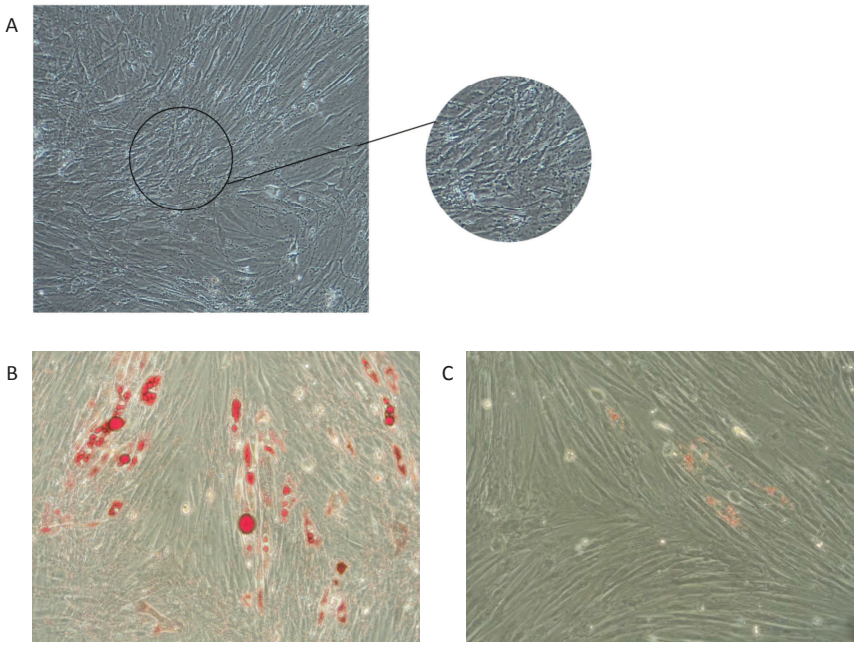

Figure 4.3 – Northern elephant seal (NES) progenitor cells were cultivated for 20 days with 10% NES serum and without the differentiation cocktail (A), with 10% NES serum and with the differentiation cocktail (B) and with 10% fetal bovine serum and with the differentiation cocktail (C). The potential accumulation of cytoplasmic triglycerides was investigated by Oil Red O staining (light microscopy).

4.3.3. Effect of NES serum

Our choice of using NES serum in the culture medium was made with the aim of getting as close as possible to the *in vivo* situation. In this section, we compared the impact of 10% (*v:v*) heat-inactivated NES serum on the rate of differentiation to the one of 10% (*v:v*) heat-inactivated FBS, which is usually used in the *in vitro* culture of rodent adipocytes (Bourez et al., 2012; Louis et al., 2014b). It appears from our visual observations that the presence of NES serum with the differentiation cocktail (Figure 4.3 B) was more favourable to the adipocyte differentiation than FBS with the differentiation cocktail (Figure 4.3 C), which might result from the specific composition of NES pup serum. This improved differentiation might be due to the high triglyceride (TG) content within the blood of NES pups, which is the result of the ingestion of highly lipid-rich milk during the nursing period (54 ± 5% lipid, Le Boeuf and Ortiz (1977)). The TG concentrations measured in the serum of suckled NES pups are elevated (2.1 ± 0.3 g TGs/L; unpublished results, permit # 87-1743-00) compared to NES adults in different physiological states (e.g. 0.67 ± 0.12 g TGs/L in fasting male serum at early breeding (Tift et al., 2011) and 0.58 ± 0.15 g TGs/L in fasting female serum at early molt (Fowler, 2012)). NES pups gain 90 ± 27 kg during the 26-day nursing period and approximately 55% of this mass gain is composed of fat (Crocker et al., 2001). The circulating TGs packed in serum lipoproteins (chylomicrons and VLDL) can be hydrolysed by lipoprotein lipase. Fatty acids are then picked up by adipose tissue and directly stored as TGs. It thus seems reasonable to think that, in the case of NES, cells accumulate lipids preferentially by direct uptake of fatty acids rather than by realising fatty acid neosynthesis from glucose as for rodents. The levels of TGs in the serum of weaned NES pups used in the present study were approximately twice as high as the TG concentrations of FBS (1.2 ± 0.3 g TGs/L in NES serum *vs.* 0.46 ± 0.01 g TGs/L in FBS). We therefore suggest that the use of NES serum may thus promote the lipid accumulation within adipocytes by direct input of fatty acids. Additionally, because most fatty acids are also agonist of PPAR-γ (Kliewer et al., 1997; Tontonoz et al., 1994), the high TG levels in NES serum may further

promote the adipogenesis. It is important to note that other molecules present in weaned NES serum (e.g. glucagon and thyroid hormones) (Kirby and Ortiz, 1994; Ortiz et al., 2001; Pucci et al., 2000) could inhibit an efficient accumulation of lipids within adipocytes. The use of serum from suckled pups might thus be preferable but requires further experiments in order to compare the lipid accretion within cells.

4.4. Conclusion

To conclude, this study represents the first attempt to isolate and differentiate *in vitro* phocid progenitor cells into adipocytes. The differentiation of isolated NES cells towards adipocytes was induced by treating them with a cocktail of differentiation including dexamethasone, IBMX, ciglitizone and insulin. The microscopic observations presented here are encouraging. The cocktail of differentiation was necessary to obtain *in vitro* adipocytes. Nevertheless, the composition of this cocktail should be further improved to adapt to the specific physiology of NES. The presence of high TG levels in the cell culture medium may enhance the accumulation of lipids in cultured NES adipocytes by direct intake of fatty acids or PPAR agonist activity. Quantifying changes in gene expression correlating with NES adipocyte differentiation may aid in refining optimal differentiation induction conditions. The ability to differentiate NES progenitor cells would provide an *in vitro* system to characterise the molecular mechanisms controlling mobilisation of lipophilic environmental pollutants in NES. Application of this innovative model to other marine mammals could then be used in physiological as well as toxicological studies to understand the behaviour and the impact of lipophilic pollutants (e.g. PCBs, PBDEs, DDT and methylmercury) and thus, directly address the risk to marine mammals from these now ubiquitous pollutants. Adipose tissue is not only used for buoyancy, insulation and energy, but it is also an endocrine organ in mammals. The availability of such tool can be indeed very useful to improve our knowledge regarding the function and metabolism of adipose tissue in marine mammals.

4.5. References

Ailhaud, G., 1982. Adipose cell differentiation in culture. Molecular and Cellular Biochemistry. 49, 17-31.

Birsoy, K., et al., 2008. Transcriptional regulation of adipogenesis by KLF4. Cell Metabolism. 7, 339-347.

Bourez, S., et al., 2012. Accumulation capacity of primary cultures of adipocytes for PCB-126: Influence of cell differentiation stage and triglyceride levels. Toxicology Letters. 214, 243-250.

Cao, Z., et al., 1991. Regulated expression of three C/EBP isoforms during adipose conversion of 3T3-L1 cells. Genes & Development. 5, 1538-1552.

Chen, N. X., et al., 1995. Glucocorticoid receptor binding in porcine preadipocytes during development. Journal of Animal Science. 73, 722-7.

Costa, D., et al., 1986. The energetics of lactation in the northern elephant seal, *Mirounga angustirostris*. Journal of Zoology. 209, 21-33.

Crocker, D. E., et al., 2001. Maternal traits and reproductive effort in northern elephant seals. Ecology. 82, 3541-3555.

Cushman, S., Wardzala, L., 1980. Potential mechanism of insulin action on glucose transport in the isolated rat adipose cell. Apparent translocation of intracellular transport systems to the plasma membrane. Journal of Biological Chemistry. 255, 4758-4762.

Debier, C., et al., 2006. Mobilization of PCBs from blubber to blood in northern elephant seals (*Mirounga angustirostris*) during the post-weaning fast. Aquatic Toxicology. 80, 149-157.

Debier, C., et al., 2012. Differential changes of fat-soluble vitamins and pollutants during lactation in northern elephant seal mother–pup pairs. Comparative Biochemistry and Physiology Part A. 162, 323-330.

Debier, C., et al., 2003. Quantitative dynamics of PCB transfer from mother to pup during lactation in UK grey seals *Halichoerus grypus*. Marine Ecology Progress Series. 247, 237-248.

Fowler, M. A., 2012. Regulation of lipid metabolism and milk lipid content in northern elephant seals.

Fowler, M. A., et al., 2008. Hormonal regulation of glucose clearance in lactating northern elephant seals (*Mirounga angustirostris*). The Journal of Experimental Biology. 211, 2943-9.

Janderová, L., et al., 2003. Human mesenchymal stem cells as an *in vitro* model for human adipogenesis. Obesity Research. 11, 65-74.

Joyner, J. M., et al., 2000. Glucocorticoid receptors in human preadipocytes: regional and gender differences. Journal of Endocrinology. 166, 145-52.

Kirby, V. L., Ortiz, C. L., 1994. Hormones and fuel regulation in fasting elephant seals. Elephant seals: Population ecology, behavior, and physiology. 374-386.

Klemm, D. J., et al., 2001. Insulin-induced adipocyte differentiation: activation of creb rescues adipogenesis from the arrest caused by inhibition of prenylation. Journal of Biological Chemistry. 276, 28430-28435.

Kliewer, S. A., et al., 1997. Fatty acids and eicosanoids regulate gene expression through direct interactions with peroxisome proliferator-activated receptors α and γ. Proceedings of the National Academy of Sciences. 94, 4318-4323.

Kras, K. M., et al., 1999. Adipocyte development is dependent upon stem cell recruitment and proliferation of preadipocytes. Obesity Research. 7, 491-497.

Le Boeuf, B. J., Ortiz, C. L., 1977. Composition of elephant seal milk. Journal of Mammalogy. 58, 683-685.

Le Boeuf, B. J., et al., 1972. Perinatal behavior of northern elephant seal females and their young. Behaviour. 43, 121-56.

Lehmann, J. M., et al., 1995. An antidiabetic thiazolidinedione is a high affinity ligand for peroxisome proliferator-activated receptor γ (PPARγ). Journal of Biological Chemistry. 270, 12953-12956.

Li, W., et al., 2008. Development of a human adipocyte model derived from human mesenchymal stem cells (hMSC) as a tool for toxicological studies on the action of TCDD. Biological Chemistry. 389, 169-77.

Louis, C., et al., 2014a. Mobilisation of lipophilic pollutants from blubber in northern elephant seal pups (*Mirounga angustirostris*) during the post-weaning fast. Environmental Research. 132, 438-448.

Louis, C., et al., 2014b. Efficient *in vitro* adipocyte model of long-term lipolysis: A tool to study the behaviour of lipophilic compounds. In Vitro Cellular & Developmental Biology - Animal. in press.

MacDougald, O. A., et al., 1995. Insulin regulates transcription of the CCAAT/Enhancer Binding Protein (C/EBP) α, β, and δ genes in fully-differentiated 3T3-L1 adipocytes. Journal of Biological Chemistry. 270, 647-654.

Noren, D. P., et al., 2003. Energy reserve utilization in northern elephant seal (*Mirounga angustirostris*) pups during the postweaning fast: size does matter. Journal of Comparative Physiology B. 173, 443-454.

Ortiz, R. M., et al., 2001. Effects of prolonged fasting on plasma cortisol and TH in postweaned northern elephant seal pups. American Journal of Physiology - Regulatory, Integrative and Comparative Physiology. 280, R790-R795.

Pittenger, M. F., et al., 1999. Multilineage potential of adult human mesenchymal stem cells. Science. 284, 143-147.

Pucci, E., et al., 2000. Thyroid and lipid metabolism. International Journal of Obesity & Related Metabolic Disorders. 24, S106-S112.

Rieusset, J., et al., 1999. Insulin acutely regulates the expression of the peroxisome proliferator-activated receptor-gamma in human adipocytes. Diabetes. 48, 699-705.

Rosen, E. D., 2005. The transcriptional basis of adipocyte development. Prostaglandins, Leukotrienes and Essential Fatty Acids. 73, 31-34.

Ross, P. S., et al., 2000. High PCB concentrations in free-ranging pacific killer whales, *Orcinus orca*: Effects of age, sex and dietary preference. Marine Pollution Bulletin. 40, 504-515.

Shin, S. M., et al., 2003. Dexamethasone reverses TGF-β-mediated inhibition of primary rat preadipocyte differentiation. FEBS Letters. 543, 25-30.

Spiegelman, B., 1998. PPAR-gamma: adipogenic regulator and thiazolidinedione receptor. Diabetes. 47, 507-514.

Tift, M. S., et al., 2011. High-density lipoprotein remains elevated despite reductions in total cholesterol in fasting adult male elephant seals (*Mirounga angustirostris*). Comparative Biochemistry and Physiology Part B. 159, 214-219.

Tontonoz, P., et al., 1994. Stimulation of adipogenesis in fibroblasts by PPAR gamma 2, a lipid-activated transcription factor. Cell. 79, 1147-56.

Vanden Berghe, M., et al., 2010. Relationships between vitamin A and PCBs in grey seal mothers and pups during lactation. Environmental Pollution. 158**,** 1570-1575.

Vanden Berghe, M., et al., 2012. Selective transfer of persistent organic pollutants and their metabolites in grey seals during lactation. Environment International. 46**,** 6-15.

Viscarra, J. A., et al., 2011. Glut4 is upregulated despite decreased insulin signaling during prolonged fasting in northern elephant seal pups. The American Journal of Physiology - Regulatory, Integrative and Comparative Physiology 300**,** R150-4.

Yeh, W.-C., et al., 1995. Cascade regulation of terminal adipocyte differentiation by three members of the C/EBP family of leucine zipper proteins. Genes & Development. 9**,** 168-181.

Chapter 5

Efficient *in vitro* adipocyte model of long-term lipolysis: A tool to study the behaviour of lipophilic compounds

Foreword

In the previous chapter, we showed the first tests that we carried out to set up an *in vitro* model of NES adipocytes. Even if the results looked promising, the rate of differentiation remained low. Additional tests would be required to continue developing the set-up of the model. It was however not possible to finalise it within the timeframe of this work, as NES weaned pups are only present on the beach during 2 to 3 months per year, limiting the amount of investigations that could be undertaken during the thesis. Despite the fact that the physiology of NES is different to the one of rat (e.g. different pathway of lipid accumulation in adipocytes), we decided to develop a protocol of lipolysis with the well-established culture of differentiated rat adipocytes[2].

[2] Bourez, S., et al., 2012. Accumulation capacity of primary cultures of adipocytes for PCB-126: Influence of cell differentiation stage and triglyceride levels. Toxicology Letters. 214, 243-250.

This chapter is devoted to the development of an *in vitro* lipolytic model. We investigated the impact of the isoproterenol, a well-known synthetic catecholamine, as well as the renewal of the extracellular lipolytic medium on the rate of triglyceride hydrolysis. During a 12-hour period, we regularly examined the triglyceride cell content and the free fatty acid extracellular content. The results obtained in this present chapter were slightly adapted from the original paper recently published in In Vitro Cellular & Developmental Biology – Animal.

Efficient *in vitro* adipocyte model of long-term lipolysis: A tool to study the behaviour of lipophilic compounds

Caroline Louis, Carine Van den Daelen, Gilles Tinant, Sophie Bourez, Jean-Pierre Thomé, Isabelle Donnay, Yvan Larondelle and Cathy Debier

Accepted for publication in In Vitro Cellular & Developmental Biology – Animal

Abstract

The triglycerides (TGs) stored in the white adipose tissue are mobilised during periods of negative energy balance. To date, there is no *in vitro* model of adipocytes imitating a long period of negative energy balance in which triglycerides are highly mobilised. Such model would allow studying the mobilisation of TGs and lipophilic compounds trapped within the adipose tissue (e.g. pollutants, vitamins). The present study aims at developing a performing long term *in vitro* lipolysis in adipocytes, resulting in a significant decrease of TG stores. Lipolysis was induced on differentiated rat adipocytes by a lipolytic medium with or without isoproterenol during 12 hours. The condition with isoproterenol was duplicated, once with medium renewal every 3 hours and once without medium renewal. Adding isoproterenol efficiently triggered lipolysis in a short time (3 hours). However, a single stimulation by isoproterenol, without medium renewal, was not sufficient to reduce the TG content during a longer term (12 hours). A re-esterification of fatty acids occurred after a few hours of lipolysis, resulting in a novel increase of cellular lipids. Regular medium renewal combined with repeated isoproterenol stimulations led to almost emptied cells after 12 hours. However, medium renewal without isoproterenol stimulation during 12 hours was as efficient is terms of lipid mobilisation. Our study demonstrates that, over a short term period, isoproterenol is required to exert a significant lipolytic effect on adipocytes. During a long term period, the presence of isoproterenol is no longer essential. Instead, medium renewal becomes the main factor involved in cell emptying. The efficiency of this protocol was demonstrated by visual tracking of the cells and by monitoring the dynamics of release of a lipophilic compound, PCB-153, from adipocytes during lipolysis.

Keywords

Adipocyte – Lipolysis – Cell culture – Lipophilic compounds

5.1. Introduction

In mammals, white adipose tissue (WAT) is the major site of energy storage. Adipocytes synthesise and accumulate massive amounts of triglycerides (TGs), which are stored within intracellular lipid droplets (LDs) (Ahmadian et al., 2010; Brasaemle et al., 2000). *In vivo*, adipocytes are unilocular and LDs fill from 90% to 99% of the cell volume (Goldrick, 1967). LDs are surrounded by a phospholipid monolayer that harbours cholesterol and several types of proteins (Brasaemle et al., 2004). The lipid core is composed of neutral lipids such as TGs for the major part, but also sterol and vitamin A esters (Chaves et al., 2011; Wang et al., 2008). Other lipophilic compounds such as toxic and persistent lipophilic pollutants are also localized in this reservoir (Bourez et al., 2012b; de Jong et al., 2004; Le Lay et al., 2004).

During period of negative energy balance (e.g. lactation, fast, disease), TGs stored in LDs can be rapidly mobilised through lipolysis. This process leads to the release of free fatty acids (FAs) and glycerol into the bloodstream so that they can be used by various tissues (Chaves et al., 2011; Large et al., 2004). Lipolysis is regulated by numerous signalling pathways. The central nervous system, hormones such as insulin and glucagon, as well as autocrine/paracrine factors are able to affect the rate of TG hydrolysis in mature adipocytes (Thompson et al., 2010). Nevertheless, the main pathway mediating lipolysis is the cAMP-dependent protein kinase A (PKA) pathway. This mechanism involves the binding of catecholamines to β-adrenergic receptors coupled to GTP-binding proteins. Adenylate cyclase is then activated by the stimulation of the α-stimulatory subunit of a G-protein. This results in an increase of intracellular cAMP levels, leading to an activation of PKA. This enzyme is then able to phosphorylate and thus activate the hormone sensitive lipase (HSL) and perilipin, which is the most abundant protein associated with lipid droplets (Belfrage et al., 1981; Chaves et al., 2011; Egan et al., 1992; Khoo et al., 1972). Phosphorylation of perilipin is required to facilitate the action of the phosphorylated HSL. It also promotes the freeing of the α/β-hydrolase domain-containing protein 5

(ABHD5 or CGI-58), which is bound to perilipin in the non-activated condition. Once released from perilipin, CGI-58 links to adipose triglyceride lipase (ATGL), which is then able to hydrolyze TGs, leading to diglycerides (DGs) production in adipocytes. Phosphorylated and thus activated HSL together with monoglyceride lipase (MGL) both contribute to the final hydrolysis of DGs and monoglycerides (MGs), respectively (Brasaemle et al., 2009; Chaves et al., 2011; Lafontan and Langin, 2009; Lass et al., 2006; Zimmermann et al., 2009). Contrary to ATGL and HSL, the activity of MGL is neither regulated by hormones nor by the energy state of the fat cells (Lass et al., 2011).

Although the adipose tissue is often considered as having a protective role by keeping toxic lipophilic organic pollutants away from target organs (Chevrier et al., 2000), it can also become a source of pollutants for the rest of the body during lipolysis. Indeed, during that metabolic process, lipophilic contaminants such as persistent organic pollutants (POPs) (e.g. polychlorinated biphenyls (PCBs), polybrominated diphenyl ethers (PBDEs)) may be mobilised from the adipose tissue to the blood circulation together with lipids. Several studies have reported an increase in circulating concentrations of POPs during periods of body weight loss in humans (Chevrier et al., 2000; Imbeault et al., 2002; Kim et al., 2011; Rogan et al., 1986), rodents (Gallenberg et al., 1987; Gallenberg and Vodicnik, 1987; Lee et al., 2002; Ring et al., 1990) and marine mammals (Debier et al., 2003; Debier et al., 2006; Debier et al., 2012; Vanden Berghe et al., 2010; Vanden Berghe et al., 2012). These molecules might cause harmful effects such as endocrine disruption, neurobehavioural alterations, hepatic- and immuno-toxicities as well as cancer developments (Faroon et al., 2000; Golden et al., 1998; Kuriyama and Chahoud, 2004; Ludewig et al., 2008). Nevertheless, the mechanisms involved in the intracellular transport of lipophilic pollutants (Bourez et al., 2012b), as well as the pathways of their mobilisation from adipocytes, have not been elucidated yet. *In vitro* models are interesting tools for such mechanistic investigations. However, up to now, no *in vitro* model of adipocytes allows studying the behaviour of lipophilic compounds trapped within adipocytes during a long-term lipolytic process.

The aim of this work was to develop a model of efficient and performing *in vitro* lipolysis in fat cells using primary cultures of rodent adipocytes. Such a model would be a proficient tool enabling not only to study the toxicokinetics of lipophilic pollutants in fat cells but also to investigate the mechanisms by which the lipophilic molecules, in general, behave in adipocytes during periods of negative energy balance. In order to achieve this, we tested (i) the effect of medium renewal and (ii) the impact of isoproterenol stimulation, on the efficiency of the lipolytic process in cultured adipocytes. Indeed, isoproterenol, a well-known synthetic catecholamine, is usually used in *in vitro* adipocytes as lipolytic factor (Bourez et al., 2012a; Nagayama et al., 2010). Nevertheless, a unique stimulation of isoproterenol only induces a limited breakdown of TG after a few hours (Nagayama et al., 2010), which does not reflect a prolonged period of negative energy balance. We thus compared three different lipolytic treatments during a period of 12 hours in order to reach the most efficient lipolytic condition for the fat cells. The first treatment involved the use of isoproterenol combined to the renewal of the lipolytic medium every 3 hours. This treatment was compared to a second treatment without isoproterenol but where the lipolytic medium was also replaced every 3 hours. Eventually, a third treatment involved the use of isoproterenol but without medium renewal. The efficiency of the lipolytic treatment was then illustrated by visual tracking of the cells. In addition, the dynamics of release of one lipophilic compound was followed throughout the lipolytic process. The targeted molecule was 2,2',4,4',5,5'-hexachlorobiphenyl (PCB-153). It was selected for its ubiquity in human and animal tissues (Covaci et al., 2008; Debier et al., 2006; Dirtu et al., 2013; Vanden Berghe et al., 2012).

5.2. Experimental procedures

5.2.1. Isolation of progenitor cells

The isolation of progenitor cells was adapted from Rodbell *et al.* (Rodbell, 1964) as described in Bourez et al. (2012a). Adipose tissue was obtained from 2-month-old male Wistar rats (Centre d'Elevage Janvier, Le

Genest Saint Isle, France). The experimental procedure was approved by the Animal Care and Use Committee of the UCLouvain. Rats were killed by decapitation and the epididymal fat pads were resected under sterile conditions. The fat tissue was then minced and digested into a Dulbecco's Modified Eagle Medium (DMEM, 4.5 g/L glucose, Gibco–Invitrogen, Merelbeke, Belgium) containing 1250 U/mL type II collagenase (Sigma-Aldrich, Bornem, Belgium), 10% (*v:v*) heat-inactivated foetal bovine serum (FBS, PAA, A&E Scientific, Marcq, Belgium), 10 mM HEPES buffer solution (Gibco–Invitrogen) and an antibiotic and antifungal mixture (100 U/mL penicillin – 100 U/mL streptomycin – 250 ng/mL amphotericin B mixture, Lonza, Verviers, Belgium; 500 ng/mL gentamicin, Gibco–Invitrogen and 40 U/mL nystatin, Lonza). The digestion was performed for 40 min at 37°C under gentle shaking. The digested tissue was then filtered through sterile 200 µm nylon mesh and the filtrate was centrifuged at 115xg for 5 min at 4°C in order to isolate the stromal-vascular fraction. The supernatant was collected and was spinned at 145xg for 5 min at 4°C. The pellets of the two centrifugations were pooled, filtered through sterile 25 µm nylon mesh and finally spinned at 180xg for 5 min at 4°C. The final pellet of stroma-vascular cells was suspended in a medium composed of DMEM, 10% (*v:v*) heat-inactivated FBS and the antibiotic and antifungal mixture (same composition as above). Cells were seeded at a mean density of 18,000 cells per cm^2 on 6-well plates (Corning CellBIND Surface, Corning, Elscolab, Kruibeke, Belgium) (day 0) and incubated at 37°C in a humidified atmosphere containing 10% CO_2 in air for 24 hours to allow cell sedimentation and adhesion.

5.2.2. Adipose differentiation of progenitor cells

Twenty-four hours after the isolation of progenitor cells (day 1), the medium was replaced by a differentiation medium composed of DMEM (4.5 g/L glucose), 10% heat-inactivated FBS, 100 U/mL penicillin – 100 U/mL streptomycin – 250 ng/mL amphotericin B mixture, 10 nM dexamethasone (Sigma-Aldrich), 10 µM ciglitizone (Sigma-Aldrich) and 5 µg/mL insulin (Sigma-Aldrich) (Bourez et al., 2012a). This medium was renewed every 48 hours until day 11 in order to obtain differentiated rat adipocytes.

5.2.3. Lipolysis experimental design

At day 11, the differentiation medium in contact with cells was removed and replaced by a lipolytic medium composed of DMEM (1.0 g/L glucose, Gibco–Invitrogen), 5% (*v:v*) heat-inactivated FBS, 2% (*w:v*) bovine albumin (Sigma-Aldrich), and supplemented or not with 1 µM isoproterenol (Sigma-Aldrich). The concentration was chosen according to Harmancey et al. (2005), Zhou et al. (2011) and Rapold et al. (2013). The condition with isoproterenol was duplicated, once with medium renewal every 3 hours and once without medium change. For the condition without isoproterenol, medium renewal was performed every 3 hours (Figure 5.1). The lipolytic experiments were carried out for 12 hours. For the condition with isoproterenol and without medium renewal some plates underwent a lipolysis during 24 hours. Cultures were frequently observed with a phase contrast microscope. Free FAs released in the extracellular medium were quantified every 3 hours in all experiments. Likewise, every 3 hours, cells from one plate (i.e. coming from the same experimental condition) were pooled in order to assess the cellular protein content and the fatty acids of cellular neutral lipids (NLs).

5.2.4. Extracellular free fatty acid assessment

Free FA concentrations were determined in the extracellular medium using an *in vitro* enzymatic colorimetric method assay (Wako NEFA HR, Sopachem, Eke, Belgium) following the manufacturer's instructions. Free FAs initially present in the lipolytic medium were quantified and subtracted of results.

5.2.5. Cellular protein assessment

After lipolytic medium removal, wells were washed once with heat up phosphate buffer saline (Sigma-Aldrich). Cells were then collected in 300 µL of lysis buffer composed of 35 mM sodium dodecyl sulfate (Merck, Darmstadt, Germany), 60 mM Tris buffer (Merck) and 10 mM ethylenediaminetetraacetic acid (Sigma-Aldrich). After homogenization, the

cellular protein content was determined by the Bicinchoninic Acid Protein Assay kit (Sigma-Aldrich) using bovine serum albumin (Sigma-Aldrich) as calibration curve (Bourez et al., 2012b).

5.2.6. Cellular neutral lipid assessment

Cells were collected as described for the determination of protein content. Total cellular lipids were extracted and assessed as detailed in Schneider et al. (2012). Briefly, after homogenization, 800 µL of cell lysate were transferred into Pyrex tubes and 5 mL of a mixture of chloroform/methanol/water (2:2:1, *v:v:v*) (Biosolve, Valkenswaard, The Netherlands) was added. Triheptadecanoin (a TG containing three C17:0 fatty acids) (Larodan, Malmö, Sweden) was used as an internal standard in order to quantify fatty acids in NLs corresponding to TGs, DGs, MGs and cholesterol esters. After spinning, the supernatant was discarded and the chloroform phase was then evaporated under a moderate nitrogen flux. Samples were then suspended into chloroform and were loaded on solid-phase extraction (SPE) columns (Bond Elut NH_2 aminopropyle 200 mg, Varian, Middelburg, The Netherlands) previously conditioned with hexane (Biosolve) in order to separate NLs from phospholipids and free FAs. After the samples were pulled through, NLs were eluted with chloroform/2-propanol (2:1, *v:v*) (Biosolve) and collected into new Pyrex tubes in order to evaporate the solvent under a moderate nitrogen flux. A methylation step was performed firstly by adding 0.1 M KOH in methanol at 70°C for 1 hour and secondly, by adding 1.2 M HCl in methanol at 70°C for 15 min. Fatty acid methyl esters (FAMEs) were then extracted by adding hexane followed by deionized water and centrifugation. FAMEs were separated by gas chromatography as described in Dang Van et al. (2011). Each peak was identified by comparison of retention times with pure methyl ester standards purchased from Larodan and from Nu-Check Prep (Elysian, MN, USA). Data processing was operated with the ChromQuest 4.2 software (ThermoFinnigan, Milan, Italy). Thereafter, results were expressed by µmol of fatty acids in cellular NLs per mg of cellular protein. For the sake of simplicity, we refer to µmol NL/mg protein in the text.

5.2.7. PCB-153 mobilisation

At day 10, some differentiated rat adipocytes were incubated with a differentiation medium supplemented with PCB-153 congener (Dr. Ehrenstorfer GmbH, Ausburg, DE) (37°C – 10% CO_2 in air). PCB-153 was added to the culture medium as an ethanolic solution (0.5% v:v) at a concentration of 300 nM, which is at the upper range of concentrations found in *in vivo* and *in vitro* studies (Bourez et al., 2012b; Meeker et al., 2011; Wassermann et al., 1979). The impact of the ethanol vehicle was tested earlier (Bourez et al., 2012b). Twelve hours later (day 11), some cells were pooled in order to quantify the intracellular accumulation of PCB-153. Simultaneously, the rest of the cells were inoculated with a PCB-153-free lipolytic medium supplemented with 1 µM isoproterenol. The medium was renewed every 3 hours. The amounts of PCB-153 were quantified every 3 hours in the extracellular medium and in the cells. Cell protein levels were also quantified every 3 hours (see 5.2.5).

5.2.8. PCB-153 quantification

Cells and extracellular medium were collected in EPA vials (Alltech, Lokeren, BE) with 5 mL of *n*-hexane (Biosolve) in order to perform a liquid-liquid extraction through a 10-minute shaking. The hexane phase was transferred into a tube and PCB-112 (Dr. Ehrenstorfer GmbH) was added as internal standard. All samples were then purified by acid and Florisil clean-up steps as described in Debier et al. (2003). Purified samples were collected in *n*-hexane. Five microliters of anhydrous nonane (Sigma-Aldrich) were added to the samples and the solvent was evaporated under gentle nitrogen flux. The purified extracts were suspended into a hexane solution of Mirex (200 pg/µL) (Dr. Ehrenstorfer GmbH) used as a standard for the injection. PCB congeners were separated and quantified with a gas chromatograph (GC Trace, ThermoFinnigan) equipped with an automatic split/splitless type injector (CTC Analytics, Zwingen, Switzerland), a fused silica capillary column (30 m x 0.25 mm internal diameter; 0.25 µm film) (Rxi-5ms, Restek, Bellefonte, PA, USA) and a mass spectrometer (Trace DSQ, ThermoFinnigan). The system used helium as carrier gas at a constant flow

rate of 1.1 mL per minute. The temperature of injector was 230°C. The oven temperature program was as follows: 2 min at 60°C, gradual heating from 60 to 140°C at the rate of 20°C per minute, 1 minute at 140°C, gradual heating from 140 to 290°C at the rate of 2.5°C per minute, 10 minutes at 290°C and gradual cooling from 290°C to 60°C at the rate of 10°C per minute. Molecules were sent to mass spectrometer by the line transfer at 290°C. The ion source of the detector was kept at 230°C. PCBs were identified according to their retention time. Data were recorded using XCalibur 1.3 software (ThermoFinnigan). Quantification was performed by comparison to an external standard composed of 28 congeners (IUPAC numbers: CB-8, -18, -28, -44, -52, -66, -77, -81, -101, -105, -114, -118, -123, -126, -128, -138, -153, -156, -157, -167, -169, -170, -180, -187, -189, -195, -206 and -209) in a certified calibration mixture (AccuStandard, New Haven, CT, USA). Five dilutions (concentration ranging from 25 to 500 pg/µL) were used in order to draw a linear calibration curve for each PCB. Blanks were run with samples series to control extraction and clean-up steps. The PCB recovery was calculated on the basis of the internal standard, PCB-112. Results were accepted only if the recoveries were between 70 and 130%. All results were corrected to obtain 100% recovery (Debier et al., 2003). The quality control was assessed through an interlaboratory comparison.

5.2.9. Cytotoxicity assessment

The potential cytotoxicities of the PCBs and the different lipolytic treatments were assessed by measuring the release of lactate dehydrogenase (LDH) in the extracellular medium. The activity of LDH was determined with the cytotoxicity detection kit (Roche Diagnostics, Vilvoorde, Belgium) according to the manufacturer's instructions in (i) the differentiation medium after 12 hours of PCB exposure and (ii) the lipolytic media collected every 3 hours during the lipolytic process. Before PCB exposure and lipolysis, some cells were lysed by exposure to 1% Triton X-100 (Sigma-Aldrich) and were used as full toxicity control (Bourez et al., 2012a). No treatment appeared toxic ($< 5\%$ of control) as compared to the full toxicity control (results not shown).

5.2.10. Lipolysis time-lapse

During the isolation of progenitor cells, some of them were seeded at a mean density of 18,000 cells per cm^2 in a tissue culture dish (Nunc, Langenselbold, Germany) (day 0). They underwent the same differentiation treatment until day 11 as previously described. The differentiation medium was then removed and replaced by the lipolytic medium described above and supplemented with 1 µM isoproterenol. The culture dish was placed inside a cinematographic chamber on the plate of an inverted microscope (20 × magnification, Leitz, Sint-Niklaas, Belgium) as described in Alomar et al. (2008). A temperature of 36.5°C – 37.5°C was maintained and a warmed and humidified air containing 10% CO_2 was frequently flushed into the chamber. The time-lapse recording equipment consisted of a colour video camera (Leica, Groot-Bijgaarden, Belgium) and a computer. This computer digitalized and recorded the frames every 2 min for 12 hours using the Leica FW 4000 software (Alomar et al., 2008). The frames from one lipolysis were used in order to make a movie. Lipolytic medium supplemented with isoproterenol was renewed every 3 hours.

5.2.11. Statistical analysis

Data are presented as mean from three independent experiments ± SEM. The statistical analysis was performed by SAS 9.3 (SAS Institute Inc., Cary, USA). Data were log transformed to achieve normality. Differences between treatments were assessed with mixed linear models and a Tukey's test. Differences were deemed significant at p-values<0.05.

5.3. Results

5.3.1. Development of a lipolytic *in vitro* model

The aim of this study was to develop a functional and performing model of *in vitro* lipolysis by comparing the efficiency of several treatments on TGs mobilisation from differentiated rat adipocytes. At day 11, the cells were incubated with a basal lipolytic medium containing only 1.0 g/L glucose and

5% heat-inactivated FBS, as compared to the differentiation medium, which was composed of 4.5 g/L glucose and 10% heat-inactivated FBS. Albumin was added to the lipolytic medium in order to bind the free FAs released in the culture medium.

5.3.1.1. Effect of isoproterenol stimulation

At day 11, differentiated rat adipocytes were incubated with a lipolytic medium supplemented (Figure 5.1 A) or not (Figure 5.1 B) with 1 µM of isoproterenol. Media from both conditions were discarded and renewed every 3 hours for 12 hours. At each time point of the experiment, (i) cells from one plate were collected and assessed for total protein and NL contents, (ii) media were collected to quantify the amounts of released free FAs.

Before lipolytic induction, adipocytes contained 4.94 ± 0.15 µmol NLs/mg protein (Figure 5.2 A – initial condition).

After 3 hours of lipolysis with isoproterenol stimulation, NLs were significantly reduced to 40% of initial level (p=0.003), whereas there was only a slight and non-significant reduction to 86% of initial level for the adipocytes incubated with the isoproterenol-free lipolytic medium (p=0.989) (Figure 5.2 A). As a consequence of the lipolytic process, the free FA levels increased in the medium. Indeed, levels of released free FAs were 1.00 ± 0.12 µmol/mL with isoproterenol supplementation and 0.22 ± 0.13 µmol/mL with the isoproterenol-free lipolytic medium (p<0.001) (Figure 5.2 B). Sums of free FAs in the medium and those present in the NLs of adipocytes after 3 hours of experiment were similar to the initial condition (p=0.336 for the stimulated condition and p=0.671 for the unstimulated condition).

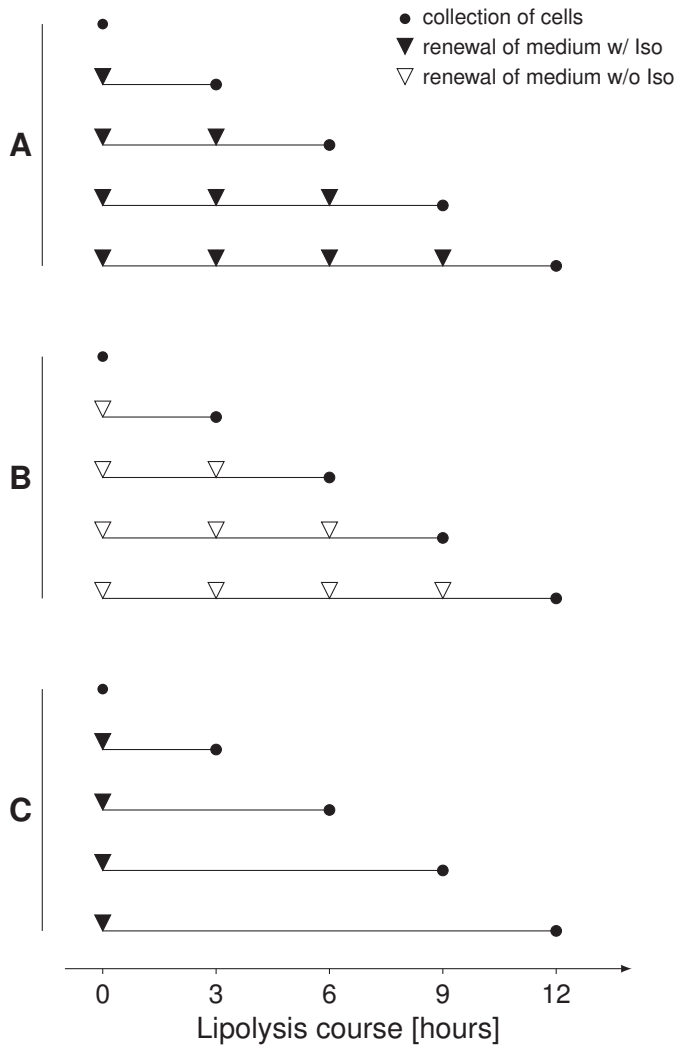

Figure 5.1 – Schematic representation of the lipolytic experiments carried out on differentiated rat adipocytes. A and B. Adipocytes were incubated with a lipolytic medium supplemented (black triangle) or not (white triangle) with 1 µM isoproterenol. Respective lipolytic media were renewed every 3 hours and old media were collected as well as cells (●). C. Adipocytes were incubated with a lipolytic medium supplemented with 1 µM isoproterenol. Cells and lipolytic media were collected every 3 hours (●).

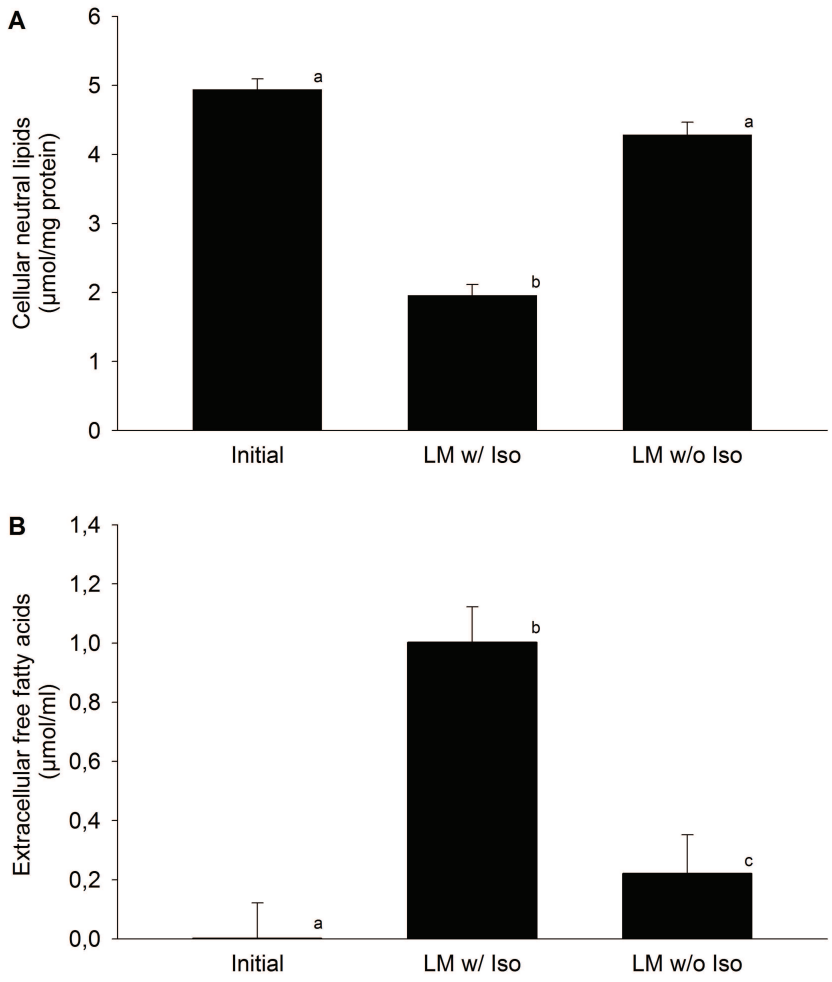

Figure 5.2 – Over a short-term period, isoproterenol showed efficient lipolytic effect. Adipocytes were incubated with a lipolytic medium (LM) containing (w/ Iso) or not (w/o Iso) 1 µM isoproterenol. After 3 hours of experiment, cellular neutral lipids (A) as well as extracellular free fatty acids (B) were quantified. These results were compared to an initial condition corresponding to differentiated rat adipocytes before the lipolytic induction. Data represent the means of three independent experiments ± SEM. Values with different symbols are significantly different ($p \leq 0.01$).

When examining the results over a longer period (up to 12 hours), the drop of NLs occurred mainly during the first half of the lipolytic process in the isoproterenol condition, whereas it was more progressive in the condition without isoproterenol (Figure 5.3 A). Levels of NLs were significantly lower in the isoproterenol-stimulated cells compared to cells without isoproterenol at each studied time ($p<0.001$ at 3, 6 and 9 hours and $p=0.002$ at 12 hours). However, the difference between the two conditions decreased as the lipolysis progressed (Figure 5.3 A). After 12 hours, we measured 0.65 ± 0.41 µmol NLs/mg protein in the stimulated condition and 0.98 ± 0.59 µmol NLs/mg protein in the unstimulated condition. It represents a reduction of lipid contents of 87% and 80% respectively as compared to the initial situation (Figure 5.3 A).

The total free FAs released by the adipocytes throughout a given period were calculated by adding the quantities measured at each period of 3 hours. For example, the amount of total free FAs released after 6 hours of lipolysis corresponds to the sum of free FAs released between 0 and 3 hours and between 3 and 6 hours (Figure 5.3 B). The free FAs released in the extracellular media increased with time in both conditions. This increase was significant during the first 6 hours of lipolysis in the stimulated condition ($p<0.001$ between 0 and 3 hours; $p=0.007$ between 3 and 6 hours; $p=0.062$ between 6 and 9 hours; $p=0.563$ between 9 and 12 hours) and during the first 9 hours of lipolysis in the condition without isoproterenol ($p<0.001$ between 0 and 3 hours; $p=0.010$ between 3 and 6 hours; $p=0.028$ between 6 and 9 hours; $p=0.914$ between 9 and 12 hours) (Figure 5.3 B). The amounts of fatty acids released in the medium were significantly higher in the stimulated condition as compared to the condition without isoproterenol during the first 9 hours of the lipolytic process ($p<0.001$ at 3 and 6 hours, $p=0.048$ at 9 hours). This difference became non-significant at 12 hours ($p=0.088$).

For a given treatment, the sums of fatty acids present in cellular NLs and in media were statistically similar between two consecutive periods ($0.194<p<0.999$).

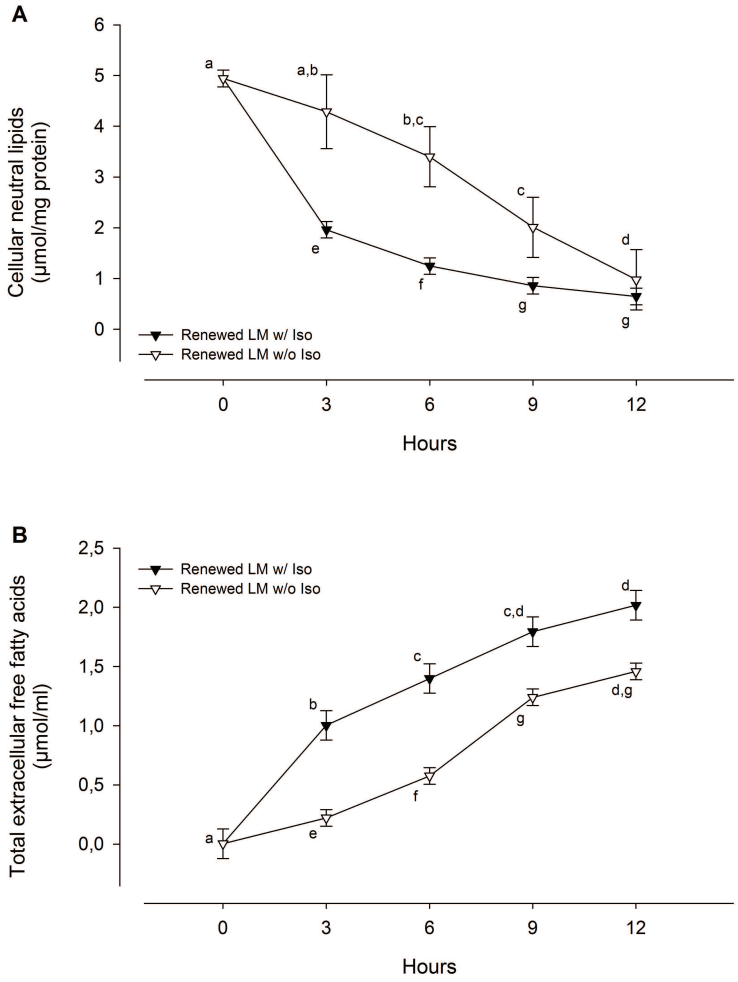

Figure 5.3 – During a long-term period, renewal of lipolytic medium is required to maintain the lipolysis. Adipocytes were incubated with a lipolytic medium (LM) containing (w/ Iso) or not (w/o Iso) 1 µM isoproterenol. The respective media were renewed every 3 hours and the assessments of cellular neutral lipids (A) and extracellular free fatty acids (B) were carried out. Data represent the means of three independent experiments ± SEM. Consecutive values with no common symbol are significantly different ($p \leq 0.05$) within a defined treatment as well as within a defined time.

5.3.1.2. Effects of medium renewal

In the present section, we compared the lipolytic efficiency of two treatments of 12 hours. In the first one, the extracellular medium supplemented with 1 µM isoproterenol was replaced every 3 hours as described previously (Figure 5.1 A). In the second one, lipolytic medium supplemented with 1 µM isoproterenol was added to the cells at the beginning of the lipolysis treatment but was not renewed during the 12 hours of the lipolytic period (Figure 5.1 C). Again, every 3 hours for both treatments, media and cells were collected for the assessment of released free FAs, as well as of cellular proteins and NLs.

During the first 3 hours of lipolysis (Figure 5.4 A), both conditions corresponded to the same treatment: addition of lipolytic medium supplemented with 1 µM isoproterenol during 3 hours. Differences between treatments started from 3 hours, with a medium renewal every 3 hours. As mentioned in the previous section, there was a drop of NLs in the condition with medium renewal. By contrast, in the condition without medium renewal, adipocytes appeared to resynthesise TGs. Indeed, levels of NLs, which are mainly composed of TGs, increased significantly with time (p=0.002 between 3 and 9 hours). After 12 hours, these cells contained 4.08 ± 0.13 µmol NLs/mg protein (corresponding to 83% of the initial content) and up to 5.96 ± 0.13 µmol NLs/mg protein (corresponding to 121% of the initial content) after 24 hours (results not shown). As a result, levels of NLs were statistically different at 6, 9 and 12 hours (p<0.001) between both conditions.

As mentioned earlier, the total free FAs released by the adipocytes throughout a given period were calculated for the medium renewal condition by adding the quantities measured at each period of 3 hours. In the condition without medium renewal, total free FAs correspond to the amounts that were quantified at the end of a given time period. Free FAs were efficiently released in the medium during the first 3 hours of lipolysis (Figure 5.4 B). The quantities released into the medium continued to increase up to 6 hours in the condition with medium renewal. By contrast,

the net release stopped in the condition without medium renewal ($0.070<p<0.995$). A slight, but non-significant drop was even visible ($p=0.197$). As a result, the amounts of free FAs measured in the medium were lower in the condition without medium renewal (i.e. single initial isoproterenol stimulation) as compared to the condition with medium renewal (i.e. repeated isoproterenol stimulation). The difference became progressively more pronounced over time ($p=0.137$ at 6 hours, $p=0.002$ at 9 hours and $p<0.001$ at 12 hours).

Eventually, as shown previously, the sums of fatty acids measured in NLs and in media were statistically similar within a given treatment ($0.194<p<0.999$).

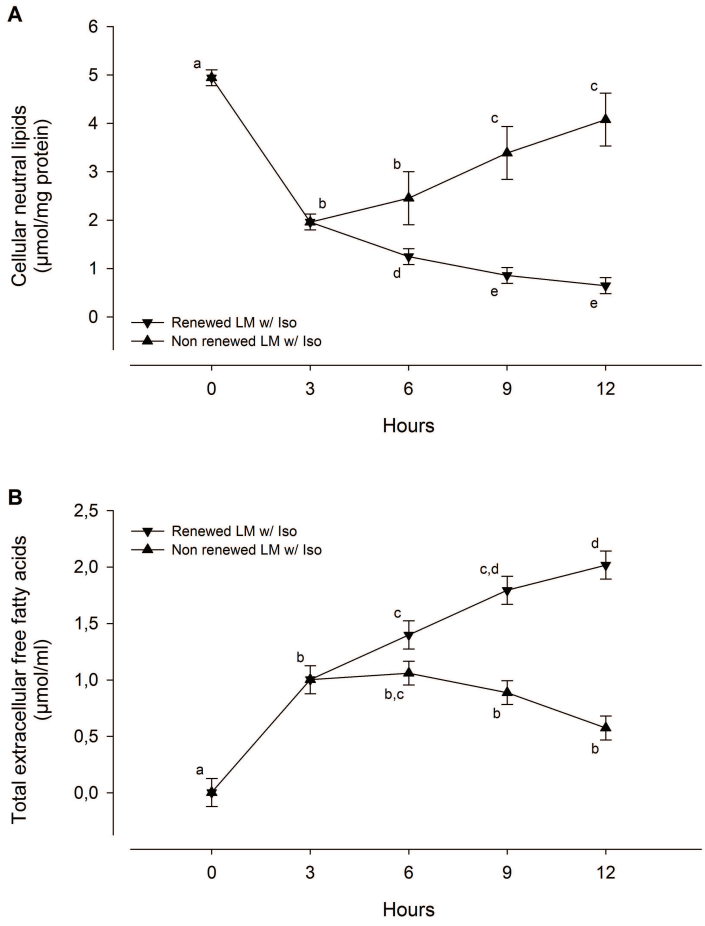

Figure 5.4 – During a long-term period, isoproterenol is not sufficient to maintain the lipolytic process. Adipocytes were incubated with a lipolytic medium (LM) supplemented with 1 µM isoproterenol (w/ Iso). We renewed the lipolytic medium with isoproterenol stimulation on half of the culture plates every 3 hours for 12 hours. The other half of the culture plates underwent the lipolysis with the initial lipolytic medium for 12 hours, without medium renewal. Cellular neutral lipids (A) and extracellular free fatty acids (B) were assessed. Data represent the means of three independent experiments ± SEM. Consecutive values with no common symbol are significantly different ($p \leq 0.05$) within a defined treatment as well as within a defined time.

5.3.2. Visual tracking of isoproterenol-stimulated lipolysis

We carried out a time course of the cells and we made a time-lapse video from the frames obtained in order to visualize the lipolytic process (Electronic Supplementary Material). This video shows the unloading of LDs during 12 hours. As for both previous experiments, the lipolysis was triggered on differentiated adipocytes at day 11 (Figure 5.5 A). The protocol used was the one with isoproterenol stimulation and medium renewal every 3 hours, as described above. After 3 hours of isoproterenol-stimulated lipolysis, the lipid content was halved (Figure 5.5 B). The mobilisation rate was however not homogeneous among the cells. Indeed, whereas some adipocytes were already completely empty (white arrow, Figure 5.5 B), others still contained significant amounts of lipids and a few of them remained with the same lipid content as the one at 0 hour (black arrow, Figure 5.5 B). After 6 (Figure 5.5 C) and 12 hours (Figure 5.5 D), adipocytes kept mobilising TGs leading to visibly emptied cells, which reflects the efficiency of the experimental protocol.

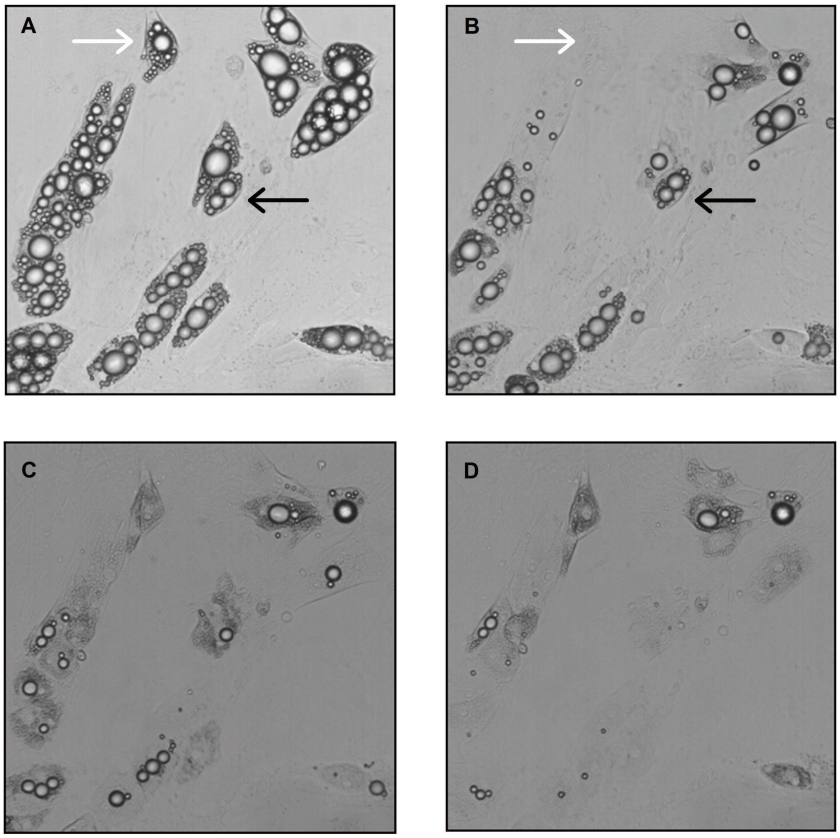

Figure 5.5 – Visual observation of the efficient emptying of cellular triglycerides during a 12-hours lipolysis. Cells were incubated with a lipolytic medium containing 1µM isoproterenol and the medium was renewed every 3 hours. A. At 0 hour, adipocytes were fully filled with lipid droplets. B. After 3 hours, more than half of the triglycerides was mobilised. Some adipocytes were almost emptied of their lipids (white arrow) while some others were still filled (black arrow). C. After 9 hours, some small lipid droplets remained observable. D. After 12 hours, only a little part of the lipids initially present in the cells was still trapped into adipocytes.

5.3.3. Dynamics of mobilisation of PCB-153 during lipolysis

At day 10, differentiated rat adipocytes were incubated with a differentiation medium supplemented with 300 nM PCB-153 during 12 hours. The congener accumulated within adipocytes, reaching a level of 1.9 ± 0.1 nmol/mg protein just before the lipolytic treatment. At day 11, lipolysis was induced with isoproterenol stimulation and medium renewal every 3 hours, as previously described. The potential presence of PCBs in the initial lipolytic medium, before being in contact with the cells, has been tested and was negligible (under the detection limit, result not shown). The amounts of PCBs in the lipolytic medium at the beginning of lipolysis (0 hour) were thus set at zero. The contents of PCB-153 were assessed in the cells and lipolytic medium at 3, 6, 9 and 12 hours of lipolysis. The PCB levels in the medium were calculated by adding the quantities measured at each period of 3 hours. For example, the amounts of PCB-153 released after 6 hours of lipolytic treatment correspond to the sum of PCB-153 released between 0 and 3 hours and between 3 and 6 hours. PCB-153 was efficiently released from adipocytes, leading to a significant reduction of its concentration in the cells and a corresponding rise in the medium between early and late lipolysis ($p<0.001$ between 0 and 12 hours) (Figure 5.6 A - B).

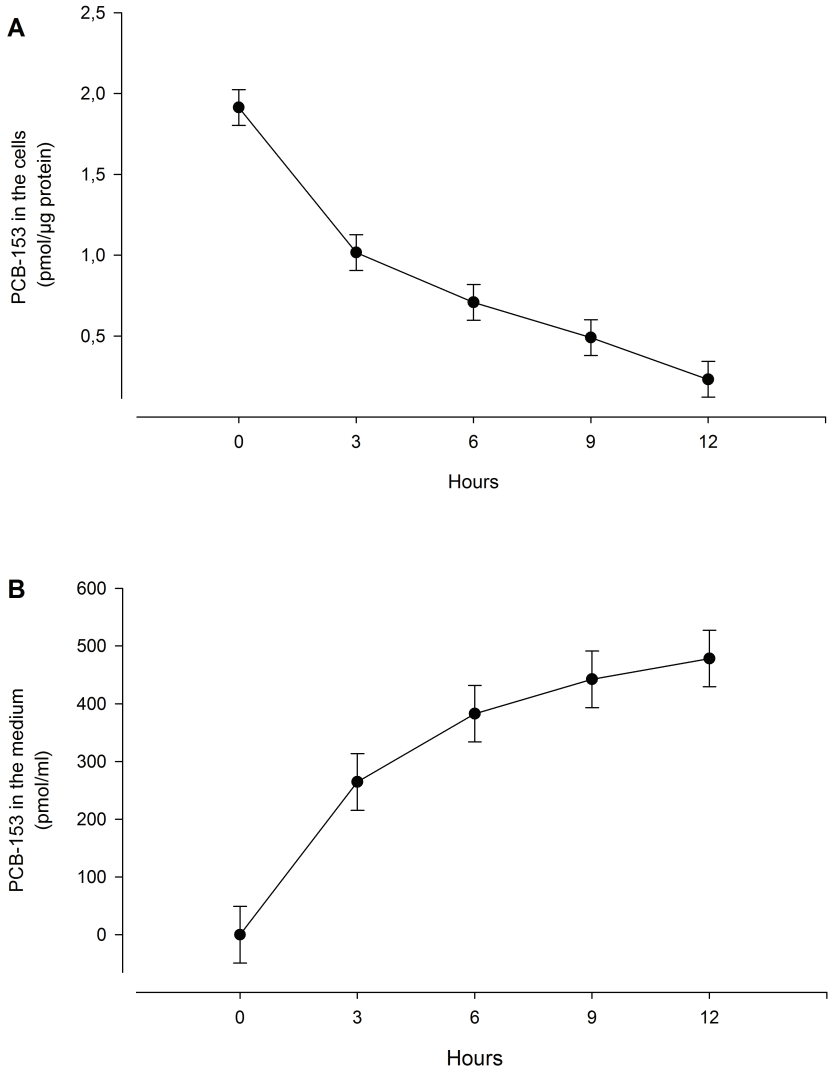

Figure 5.6 – Mobilisation of PCB-153 from adipocytes to extracellular medium throughout a 12-hour lipolytic process. Cells were previously incubated with a differentiation medium supplemented with 300 nM PCB-153. 12 hours later, a lipolysis was performed with a lipolytic medium containing 1µM isoproterenol and renewed each 3 hours. The PCB-153 levels in adipocytes and extracellular medium were evaluated. Data represent the means of three independent experiments ± SEM.

5.4. Discussion

Lipolysis in adipose tissue is a physiological process that occurs to provide fatty acids as metabolic fuel to an organism, either when the energy demand increases or when a deficiency of substrate appears (Cherel and Le Maho, 1985). In the present study, we developed a functional *in vitro* model of adipocyte lipolysis. We tested several types of treatments in order to investigate the effects of isoproterenol (acting as a non-selective β-adrenergic agonist) and medium renewal on cell discharge over short (3 hours) and longer (up to 12 hours) term lipolysis.

This study highlights a rapid and significant lipolytic action of the first isoproterenol dose for the first 3 hours. Isoproterenol was used to mimic the effects of catecholamines *in vivo*. Indeed, it activates the classic intracellular pathway of these hormones. For example, isoproterenol is known to increase the activity of HSL by the PKA pathway (Anthonsen et al., 1998) and to promote the translocation of HSL from the cytosol to the surface of the LD (Ahmadian et al., 2010). Used at a concentration of 1 µM in the medium, it markedly induced the breakdown of TGs in the present study, as observed by the significant decrease of intracellular NLs and the corresponding accumulation of free FAs in the extracellular medium. The sum of fatty acids in NLs and medium matched with the fatty acids content of NLs of initial adipocytes (i.e. at 0 hour), confirming that extracellular free FAs came from the mobilisation of TGs. These results are in accordance with the literature. Indeed, Nagayama et al. (2010) stimulated primary cultures of rat adipocytes with 0.1 µM isoproterenol and reported that phosphorylated HSL was already exclusively localized on the LD surface after only 2 hours of induction. In addition, Clifford et al. (2000) showed a significant decrease of cytosolic HSL during the first minutes after 1 µM isoproterenol stimulation in epididymal adipocytes.

During a long-term period (12 hours), the effect of isoproterenol became less obvious. Instead, the regular renewal of lipolytic medium appeared to be the overriding factor. Indeed, after 12 hours of lipolysis with medium renewal, cellular NLs were significantly reduced in both conditions (with and

without isoproterenol). Thus it seems that, even without any exogenous catecholamine stimulation, the lipolytic pathway occurs in adipocytes, provided that the medium is of lipolytic type (low levels or even absence of agents such as insulin, dexamethasone, ciglitizone and glucose) and that it is regularly renewed. Vargovic et al. (2011) demonstrated that rat adipocytes, isolated from mesenteric adipose tissue, produced catecholamines *de novo*, showing that the sympathetic innervation is not the only source of catecholamines for the adipose tissue. This production could affect the mobilisation of TGs *in vitro* as well, but further investigations using primary cultures of adipocytes are needed to confirm this hypothesis. In addition, Getty-Kaushik et al. (2005) showed that lipolysis was enhanced in primary rat adipocytes when increasing amounts of BSA were added to the medium. This growing concentration of BSA in the medium promoted the outward movement of free FAs. In the present study, a regular renewal of lipolytic medium, and thus a regular input of BSA, could also promote the lipolytic process within adipocytes. Even if the remaining cellular NLs were close in both conditions (with and without isoproterenol) after 12 hours of lipolysis with medium renewal, the dynamics of cell emptying were different. The incubation of adipocytes with repeated doses of isoproterenol induced a more rapid depletion of lipid stores than the incubation without isoproterenol. This may result in part from the fact that the use of lipolytic hormones such as catecholamines accelerates the process through the breaking down of lipid droplets into smaller ones (Brasaemle, 2007; Zechner and Madeo, 2009), in addition to the effects on HSL and ATGL. A regular use of isoproterenol could thus make TGs more available for the lipolytic enzymes.

Medium renewal allowed a regular input of BSA while avoiding extended contact between the adipocytes and the products of lipolysis, which appeared to promote the lipolytic process. Indeed, when the lipolytic media supplemented with isoproterenol remained in contact with the adipocytes throughout the experiment (condition without medium renewal), we observed that the initially significant NL mobilisation (and corresponding extracellular free FA accumulation) induced by the isoproterenol stimulation was followed by an increase of cellular NLs and a slight decrease of free FAs in the medium. These results suggest a reuptake of free FAs from the

extracellular medium by adipocytes and a re-esterification into TGs. Re-esterification of fatty acids during lipolysis appears to reach significant levels *in vivo*, particularly in situations of slow blood circulation (Raclot, 2003; Reshef et al., 2003), which is in part reflected in our condition without medium renewal, where the adipocytes remain in contact with the culture medium. The direct recycling of fatty acids is dependent on the availability of glycerol-3-phosphate (G3P) and the expression of re-esterification enzymes. In *in vivo* conditions, glycerol released during lipolysis cannot be recycled to synthetize G3P, seeing the negligible levels of adipose glycerol kinase (Gyk) in adipocytes (Jequier and Tappy, 1999; Robinson and Newsholme, 1967). When glucose is present, the G3P required for fatty acid re-esterification and TG storage is rather obtained by the reduction of dihydroxyacetonephosphate, a glycolysis intermediate. The lipolytic medium used here was composed of glucose (1 g/L) and FBS (5 %), which contained among others insulin. Serum heat inactivation at 56°C might not have altered insulin, as this protein appears to be stable at such temperature (Huus et al., 2005). As a result, without catecholamine stimulation, insulin from FBS could still promote the translocation of glucose transporter type 4 from intracellular vesicles to the adipocyte membrane. Glucose could then be able to enter the adipocytes and undergo glycolysis in order to form G3P. In addition, amino acids and pyruvate being present in the lipolytic medium (6.21 mM and 0.93 mM, respectively), they could also be at the origin of G3P by the glyceroneogenesis pathway. Indeed, during starvation, adipocytes can synthetize G3P from precursors other than glucose or glycerol by the glyceroneogenesis pathway (Duplus and Forest, 2002; Nye et al., 2008). This pathway depends on the cytosolic phosphoenolpyruvate carboxykinase (PEPCK). Several studies highlighted that in 3T3-F442A adipocytes, isoproterenol was a rapid (maximum level obtained at 4 hours) and potent (four to five folds) inducer of the PEPCK mRNA (Antras-Ferry et al., 1995; Forest et al., 1997; Tordjman et al., 2003). Likewise, Antras-Ferry et al. (1995) have shown that oleic acid can stimulate PEPCK gene transcription. This fatty acid, which represents around 25% of the fatty acid profiles of adipocyte NLs (results not shown), might thus have positively influenced PEPCK's gene transcription. A third possibility to obtain G3P is

that *in vitro* adipocytes might express Gyk in particular culture conditions. Indeed, Guan et al. (2002) reported that thiazolidinediones (TZD), acting as ligand for the nuclear receptor peroxisome proliferator-activated receptor gamma (PPARγ), induce Gyk expression. They have noted an important induction of Gyk mRNA in TZD-stimulated 3T3-L1 adipocytes after 48 hours of treatment. Lipolysis was then induced using 10 µM isoproterenol and a marked incorporation of glycerol into TGs was noticed after 5 hours of stimulation. A direct utilization of glycerol as a backbone for esterification of free FAs was suggested. The products of lipolysis (glycerol and free FAs) were thereby utilized in the futile cycle allowed by Gyk. In our conditions, we cultivated adipocytes with 10 µM ciglitizone, a class of TZD, for 11 days. Gyk activity might thus have been induced and involved in fatty acid re-esterification. Those different pathways to obtain G3P in adipocytes might also occur in the conditions with medium renewal. However, in such conditions, free FAs released in the culture medium were regularly removed and thus not available for reuptake by the cells and re-esterification into TGs.

Isoproterenol and regular lipolytic medium renewal are thus both efficient strategies to trigger the hydrolysis of cellular triglycerides in *in vitro* adipocytes. This protocol can be used a tool to study the behaviour of lipophilic molecules during lipolysis. Indeed, during periods of negative energy balance, lipophilic pollutants such as PCBs or PBDEs, which are stored in the adipose tissue (La Merrill et al., 2013; Roos et al., 2013), might be mobilised into the bloodstream. Several *in vivo* studies report increases of pollutant concentrations in the blood circulation during body weight loss episodes (Debier et al., 2006; Dirtu et al., 2013; Kim et al., 2011), raising potential toxic impacts on the individual's health. In the present study, we showed that a large amount of PCB-153, which accumulated in differentiated adipocytes, was released from the cells throughout the lipolytic process and concentrated in the extracellular medium. Further investigations could be undertaken in order to study the mechanisms involved in the mobilisation of PCBs as well as other lipophilic pollutants from adipocytes.

5.5. Conclusion

In conclusion, isoproterenol showed a fast and efficient lipolytic effect during a short term period (3 hours). However, over a longer term (12 hours), it was not sufficient to maintain the breakdown of TGs. Indeed, with a single initial dose of isoproterenol, in the absence of medium renewal, adipocytes appeared to newly synthetize TGs through the recycling of free FAs released in the medium. On the contrary, regular medium renewal appeared to be the most significant factor involved in cell discharge, whatever the presence of isoproterenol, leading to an important hydrolysis of TGs over 12 hours of lipolysis. This efficient *in vitro* model allows mimicking an important mobilisation of lipids. It is a useful tool to study the cellular mechanisms involved in the release of lipophilic compounds (lipophilic pollutants, vitamins, etc.) from adipocytes during a drastic lipolysis.

5.6. References

Ahmadian, M., et al., 2010. Lipolysis in adipocytes. International Journal of Biochemistry & Cell Biology. 42, 555-559.

Alomar, M., et al., 2008. Kinetics of fertilization and development, and sex ratio of bovine embryos produced using the semen of different bulls. Animal Reproduction Science. 107, 48-61.

Anthonsen, M. W., et al., 1998. Identification of novel phosphorylation sites in hormone-sensitive lipase that are phosphorylated in response to isoproterenol and govern activation properties *in vitro*. Journal of Biological Chemistry. 273, 215-221.

Antras-Ferry, J., et al., 1995. Fatty acids and fibrates are potent inducers of transcription of the phosphenol pyruvate carboxykinase gene in adipocytes. European Journal of Biochemistry. 234, 390-396.

Belfrage, P., et al., 1981. Regulation of adipose-tissue lipolysis by phosphorylation of hormone-sensitive lipase. International Journal of Obesity. 5, 635-41.

Bourez, S., et al., 2012a. Accumulation capacity of primary cultures of adipocytes for PCB-126: Influence of cell differentiation stage and triglyceride levels. Toxicology Letters. 214, 243-250.

Bourez, S., et al., 2012b. Accumulation of polychlorinated biphenyls in adipocytes: Selective targeting to lipid droplets and role of caveolin-1. PLoS ONE. 7, e31834.

Brasaemle, D., et al., 2009. Perilipin A and the control of triacylglycerol metabolism. Molecular and Cellular Biochemistry. 326, 15-21.

Brasaemle, D. L., 2007. Thematic review series: Adipocyte Biology. The perilipin family of structural lipid droplet proteins: stabilization of lipid droplets and control of lipolysis. Journal of Lipid Research. 48, 2547-2559.

Brasaemle, D. L., et al., 2004. Proteomic analysis of proteins associated with lipid droplets of basal and lipolytically stimulated 3T3-L1 adipocytes. Journal of Biological Chemistry. 279, 46835-46842.

Brasaemle, D. L., et al., 2000. The lipolytic stimulation of 3T3-L1 adipocytes promotes the translocation of hormone-sensitive lipase to the surfaces of lipid storage droplets. Biochimica et Biophysica Acta: Molecular and Cell Biology of Lipids. 1483, 251-262.

Chaves, V. E., et al., 2011. Several agents and pathways regulate lipolysis in adipocytes. Biochimie. 93, 1631-1640.

Cherel, Y., Le Maho, Y., 1985. Five months of fasting in king penguin chicks: body mass loss and fuel metabolism. American Journal of Physiology: Regulatory, Integrative and Comparative Physiology. 249, 387-392.

Chevrier, J., et al., 2000. Body weight loss increases plasma and adipose tissue concentrations of potentially toxic pollutants in obese individuals. International Journal of Obesity and Related Metabolic Disorders. 24, 1272-8.

Clifford, G. M., et al., 2000. Translocation of hormone-sensitive lipase and perilipin upon lipolytic stimulation of rat adipocytes. Journal of Biological Chemistry. 275, 5011-5015.

Covaci, A., et al., 2008. Polybrominated diphenyl ethers (PBDEs) and polychlorinated biphenyls (PCBs) in human liver and adipose tissue samples from Belgium. Chemosphere. 73, 170-175.

Dang Van, Q. C., et al., 2011. Influence of the diet structure on ruminal biohydrogenation and milk fatty acid composition of cows fed extruded linseed. Animal Feed Science and Technology. 169, 1-10.

de Jong, J. C., et al., 2004. Carbazates as potent inhibitors of hormone-sensitive lipase. Bioorganic & Medicinal Chemistry Letters. 14, 1741-1744.

Debier, C., et al., 2006. Mobilization of PCBs from blubber to blood in northern elephant seals (*Mirounga angustirostris*) during the post-weaning fast. Aquatic Toxicology. 80, 149-157.

Debier, C., et al., 2012. Differential changes of fat-soluble vitamins and pollutants during lactation in northern elephant seal mother–pup pairs. Comparative Biochemistry and Physiology Part A: Molecular & Integrative Physiology. 162, 323-330.

Debier, C., et al., 2003. Quantitative dynamics of PCB transfer from mother to pup during lactation in UK grey seals *Halichoerus grypus*. Marine Ecology Progress Series. 247, 237-248.

Dirtu, A. C., et al., 2013. Dynamics of organohalogenated contaminants in human serum from obese individuals during one year of weight loss treatment. Environmental Science & Technology. 47, 12441-12449.

Duplus, E., Forest, C., 2002. Is there a single mechanism for fatty acid regulation of gene transcription? Biochemical Pharmacology. 64, 893-901.

Egan, J. J., et al., 1992. Mechanism of hormone-stimulated lipolysis in adipocytes: translocation of hormone-sensitive lipase to the lipid storage droplet. Proceedings of the National Academy of Sciences of the United States of America. 89, 8537-8541.

Faroon, O., et al., 2000. Effects of polychlorinated biphenyls on the nervous system. Toxicology and Industrial Health. 16, 305-333.

Forest, C., et al., 1997. Regulation of gene transcription by fatty acids, fibrates and prostaglandins: the phosphoenolpyruvate carboxykinase gene as a model. Prostaglandins Leukotrienes and Essential Fatty Acids. 57, 47-56.

Gallenberg, L. A., et al., 1987. Influence of lipolysis on the mobilization of 2,4,5,2′4′,5′-hexachlorobiphenyl from adipocytes *in vitro*. Journal of Toxicology and Environmental Health. 20, 163-171.

Gallenberg, L. A., Vodicnik, M. J., 1987. Potential mechanisms for redistribution of polychlorinated biphenyls during pregnancy and lactation. Xenobiotica. 17, 299-310.

Getty-Kaushik, L., et al., 2005. Free fatty acid regulation of glucose-dependent intrinsic oscillatory lipolysis in perifused isolated rat adipocytes. Diabetes. 54, 629-637.

Golden, R. J., et al., 1998. Environmental endocrine modulators and human health: An assessment of the biological evidence. Critical Reviews in Toxicology. 28, 109-227.

Goldrick, R., 1967. Morphological changes in the adipocyte during fat deposition and mobilization. American Journal of Physiology. 212, 777-782.

Guan, H.-P., et al., 2002. A futile metabolic cycle activated in adipocytes by antidiabetic agents. Nature Medicine. 8, 1122-1128.

Harmancey, R., et al., 2005. The vasoactive peptide adrenomedullin is secreted by adipocytes and inhibits lipolysis through NO-mediated β-adrenergic agonist oxidation. The FASEB Journal. 19, 1045-1047.

Huus, K., et al., 2005. Thermal dissociation and unfolding of insulin. Biochemistry. 44, 11171-7.

Imbeault, P., et al., 2002. Increase in plasma pollutant levels in response to weight loss is associated with the reduction of fasting insulin levels in men but not in women. Metabolism. 51, 482-486.

Jequier, E., Tappy, L., 1999. Regulation of body weight in humans. Physiological Reviews. 79, 451-480.

Khoo, J. C., et al., 1972. Activation of hormone-sensitive lipase from human adipose tissue by cyclic AMP-dependent protein kinase. Biochemical and Biophysical Research Communications. 49, 407-413.

Kim, M. J., et al., 2011. Fate and complex pathogenic effects of dioxins and polychlorinated biphenyls in obese subjects before and after drastic weight loss. Environmental health perspectives. 119, 377-383.

Kuriyama, S. N., Chahoud, I., 2004. *In utero* exposure to low-dose 2,3′,4,4′,5-pentachlorobiphenyl (PCB 118) impairs male fertility and alters neurobehavior in rat offspring. Toxicology. 202, 185-197.

La Merrill, M., et al., 2013. Toxicological function of adipose tissue: focus on persistent organic pollutants. Environmental Health Perspectives. 121, 162-169.

Lafontan, M., Langin, D., 2009. Lipolysis and lipid mobilization in human adipose tissue. Progress in Lipid Research. 48, 275-297.

Large, V., et al., 2004. Metabolism of lipids in human white adipocyte. Diabetes & Metabolism. 30, 294-309.

Lass, A., et al., 2006. Adipose triglyceride lipase-mediated lipolysis of cellular fat stores is activated by CGI-58 and defective in Chanarin-Dorfman Syndrome. Cell Metabolism. 3, 309-319.

Lass, A., et al., 2011. Lipolysis - A highly regulated multi-enzyme complex mediates the catabolism of cellular fat stores. Progress in Lipid Research. 50, 14-27.

Le Lay, S., et al., 2004. Adipocyte cholesterol balance in obesity. Biochemical Society Transactions. 32, 103-6.

Lee, S. K., et al., 2002. Comparison of pharmacokinetic interactions and physiologically based pharmacokinetic modeling of PCB 153 and PCB 126 in nonpregnant mice, lactating mice, and suckling pups. Toxicological Sciences. 65, 26-34.

Ludewig, G., et al., 2008. Metabolic activation of PCBs to carcinogens *in vivo* - A review. Environmental Toxicology and Pharmacology. 25, 241-246.

Meeker, J. D., et al., 2011. Serum concentrations of polychlorinated biphenyls in relation to *in vitro* fertilization outcomes. Environmental Health Perspectives. 119, 1010-1016.

Nagayama, M., et al., 2010. Shrinking and development of lipid droplets in adipocytes during catecholamine-induced lipolysis. FEBS Letters. 584, 86-92.

Nye, C., et al., 2008. Reassessing triglyceride synthesis in adipose tissue. Trends in Endocrinology & Metabolism. 19, 356-361.

Raclot, T., 2003. Selective mobilization of fatty acids from adipose tissue triacylglycerols. Progress in Lipid Research. 42, 257-288.

Rapold, R. A., et al., 2013. Fas activates lipolysis in a Ca2+-CaMKII-dependent manner in 3T3-L1 adipocytes. Journal of Lipid Research. 54, 63-70.

Reshef, L., et al., 2003. Glyceroneogenesis and the Triglyceride/Fatty Acid Cycle. Journal of Biological Chemistry. 278, 30413-30416.

Ring, B. J., et al., 1990. The effect of diet and litter size on the elimination of 2,4,5,2',4',5'-[14C]hexachlorobiphenyl from lactating mice. Toxicology and Applied Pharmacology. 104, 9-16.

Robinson, J., Newsholme, E. A., 1967. Glycerol kinase activities in rat heart and adipose tissue. Biochemical Journal. 104, 2C-4C.

Rodbell, M., 1964. Metabolism of isolated fat cells. Journal of Biological Chemistry. 239, 375-380.

Rogan, W. J., et al., 1986. Polychlorinated biphenyls (PCBs) and dichlorodiphenyl dichloroethene (DDE) in human milk: effects of maternal factors and previous lactation. American Journal of Public Health. 76, 172-177.

Roos, V., et al., 2013. Circulating levels of persistent organic pollutants in relation to visceral and subcutaneous adipose tissue by abdominal MRI. Obesity. 21, 413-418.

Schneider, A.-C., et al., 2012. Conversion of t11t13 CLA into c9t11 CLA in caco-2 cells and inhibition by sterculic oil. PLoS ONE. 7, e32824.

Thompson, B. R., et al., 2010. Fatty acid flux in adipocytes: The in's and out's of fat cell lipid trafficking. Molecular and Cellular Endocrinology. 318, 24-33.

Tordjman, J., et al., 2003. Regulation of glyceroneogenesis and phosphoenolpyruvate carboxykinase by fatty acids, retinoic acids and thiazolidinediones: potential relevance to type 2 diabetes. Biochimie. 85, 1213-1218.

Vanden Berghe, M., et al., 2010. Relationships between vitamin A and PCBs in grey seal mothers and pups during lactation. Environmental Pollution. 158, 1570-1575.

Vanden Berghe, M., et al., 2012. Selective transfer of persistent organic pollutants and their metabolites in grey seals during lactation. Environment International. 46, 6-15.

Vargovic, P., et al., 2011. Adipocytes as a new source of catecholamine production. FEBS Letters. 585, 2279-2284.

Wang, S., et al., 2008. Lipolysis and the integrated physiology of lipid energy metabolism. Molecular Genetics and Metabolism. 95, 117-126.

Wassermann, M., et al., 1979. World PCBs map: Storage and effects in man and his biologic environment in the 1970s. Annals of the New York Academy of Sciences. 320, 69-124.

Zechner, R., Madeo, F., 2009. Cell biology: Another way to get rid of fat. Nature. 458, 1118-1119.

Zhou, L., et al., 2011. Berberine attenuates cAMP-induced lipolysis via reducing the inhibition of phosphodiesterase in 3T3-L1 adipocytes. Biochimica et Biophysica Acta (BBA). 1812, 527-535.

Zimmermann, R., et al., 2009. Fate of fat: The role of adipose triglyceride lipase in lipolysis. Biochimica et Biophysica Acta (BBA). 1791, 494-500.

Chapter 6

PCB-28, PCB-118 and PCB-153 show different dynamics of mobilisation from differentiated rat adipocytes during lipolysis

Foreword

Thanks to the experiments carried out in the previous chapter, we developed an inexpensive, simple and accurate procedure to induct an efficient lipolysis on *in vitro* adipocytes. Isoproterenol and regular lipolytic medium renewal were both efficient strategies to trigger the hydrolysis of cellular triglycerides in primary cultures of rodent fat cells. This tool was then used to examine the behaviour of given lipophilic pollutants within adipocytes. In the present chapter, three PCB congeners (PCB-28, -118 and -153) were selected because of their different number and position of chlorine atoms. They were added to the cell culture alone or in cocktail (i.e. a mixture of three congeners). We compared the time-course release of these congeners, alone or in cocktail, during a lipolytic treatment. This experimental design allowed estimating the impact of the number and position of chlorine atoms and the presence of other PCBs on their dynamics of release from adipocytes. These results have been submitted to PLOS One.

PCB-28, PCB-118 and PCB-153 show different dynamics of mobilisation from differentiated rat adipocytes during lipolysis

Caroline Louis, Gilles Tinant, Eric Mignolet,
Jean-Pierre Thomé and Cathy Debier

Submitted to PLOS One

Abstract

Polychlorinated biphenyls (PCBs) are persistent organic pollutants. Due to their lipophilic character, they are preferentially stored within the adipose tissue. During the mobilisation of lipids, PCBs might be released from the adipocytes into the bloodstream. However, the mechanisms associated with the release of PCBs have been poorly studied. Several *in vivo* studies followed their dynamics of release but the complexity of the *in vivo* situation, which is characterised by a large range of pollutants, does not allow understanding precisely the behaviour of individual congeners. The present *in vitro* experiment studied the impact of (i) the number and position of chlorine atoms of PCBs on their release from adipocytes and (ii) the presence of other PCB congeners on the mobilisation rate of such molecules.

Differentiated rat adipocytes were used to compare the behaviour of PCB-28, -118 and -153. Cells were contaminated with the three congeners, alone or in cocktail, and a lipolysis was then induced with isoproterenol during 12 hours. Our data indicate that the three congeners were efficiently released from adipocytes and accumulated in the medium during the lipolysis. Interestingly, for a same level of cell lipids, PCB-153, a hexa-CB with two chlorine atoms in *ortho*-position, was more slowly mobilised than PCB-28, a tri-CB, and PCB-118, a penta-CB, which are both characterised by one chlorine atom in *ortho*-position. It suggests an impact of the physico-chemical properties and the size of the molecules on their mobilisation during periods of negative energy balance. Moreover, the mobilisation of PCB congeners, taken individually, did not seem to be influenced by the presence of other congeners within adipocytes.

These results not only highlight the obvious mobilisation of PCBs from adipocytes during lipolysis, in parallel to lipids, but also demonstrate that the structure of congeners defines their rate of release from adipocytes.

Keywords

PCBs – Lipolysis – Adipocytes – Mobilisation of pollutants

6.1. Introduction

Polychlorinated biphenyls (PCBs) are a class of environmentally persistent pollutants that biomagnify throughout food chains. Ingestion of contaminated food, and especially fat-rich animal products, represents 90% of the mean uptake of humans (Djien Liem et al., 2000). Adipose tissue is then the main reservoir for the storage of these highly lipophilic molecules (La Merrill et al., 2013). The cytoplasm of adipocytes is almost exclusively composed of lipid droplets (LDs) (Sbarbati et al., 2010), which appear to be the principal target for PCBs (Bourez et al., 2012b). These cells therefore have an enormous capacity to accumulate lipophilic pollutants (Bourez et al., 2012a).

During periods of weight loss in humans, lipids from adipose tissue are mobilised, leading to an increase of PCB concentrations in this tissue (Chevrier et al., 2000; Kim et al., 2011).

Evidence from wildlife indicates same trends (Debier et al., 2003; Debier et al., 2004; Debier et al., 2006; Debier et al., 2012; Louis et al., 2014a; Vanden Berghe et al., 2010; Vanden Berghe et al., 2012). This phenomenon suggests that PCBs are less efficiently mobilised from adipocytes than fatty acids. However, a release of PCBs in the blood circulation does occur during such periods of weight loss and appears to become more important when the adipose stores are already significantly reduced (Debier et al., 2005; Dirtu et al., 2013; Hue et al., 2006; Imbeault et al., 2002; Kim et al., 2011; La Merrill et al., 2013). In addition to being a reservoir, the adipose tissue can thus also be an internal source of lipophilic pollutants for the rest of the body (La Merrill et al., 2013). Once in the bloodstream, pollutants are able to contaminate other tissues or be transferred in maternal milk. The exposure to PCBs is associated to adverse effects on human and animal health (Carpenter, 2006; Robertson and Hansen, 2001). Among others, PCBs are involved in endocrine disruption, immuno- and neuro-toxicity as well as in the development of cardiovascular diseases and type-2 diabetes (Dirinck et al., 2011; Gupta, 2000; Kester et al., 2000; Lee et al., 2011; Schantz et al., 2003). A correlation between the rise of persistent organic pollutants

(POPs), such as PCBs, in the serum and the alterations of skeletal muscle oxidative capacity has been suggested in humans (Imbeault et al., 2002). Furthermore, individuals who underwent bariatric surgery exhibited a positive association between POP serum levels and a diminished improvement of lipid values and liver markers (Kim et al., 2011).

Even if several *in vivo* studies report a release of PCBs from the adipose tissue during lipolytic process (Debier et al., 2006; Hue et al., 2006; Kim et al., 2011; Louis et al., 2014a; Vanden Berghe et al., 2012), little is known concerning the chemical and biochemical factors that govern their mobilisation and transfer into the circulation. *In vivo* studies on long-term fasting wild animals report an impact of the fasting stage as well as the degree of lipophilicity of PCB congeners on their dynamics of mobilisation from the adipose tissue (Debier et al., 2003; Debier et al., 2006; Louis et al., 2014a; Vanden Berghe et al., 2012). The transfer from the adipose tissue into the blood circulation appears to be selective and strongly dependent on the log K_{ow} value of the compounds, with less lipophilic PCBs being more efficiently released. *In vivo* models being usually complex, the *in vitro* cultures of adipocytes would be useful to precisely understand the mobilisation of PCB congeners as a function of their chemical structure. A recent study from our group investigated the dynamics of accumulation of three PCB congeners, differing in the position and number of their chlorine atoms (PCB-28, log K_{ow} = 5.71; PCB-118, log K_{ow} = 6.57 and PCB-153, log K_{ow} = 6.80) in cultured adipocytes (Bourez et al., 2013). The accumulation profile revealed significant differences between PCB congeners. Their release during lipolysis was however not investigated.

In this study, we followed and compared the dynamics of mobilisation of PCB-28, PCB-118 and PCB-153 from *in vitro* differentiated rat adipocytes. Cells were contaminated by the three congeners, added individually or in cocktail, at the same concentrations in the culture medium. Lipolysis was then triggered over 12 hours with a lipolytic medium supplemented with isoproterenol, a well-known synthetic catecholamine (Louis et al., 2014b; Zhou et al., 2011). The levels of PCBs in the extracellular medium and the adipocytes were regularly assessed. The present experiment allowed (i) to

estimate the impact of the number and position of chlorine atoms of PCBs on their release from adipocytes and (ii) to assess the impact of the presence of other PCB congeners on the mobilisation dynamics of such molecules.

6.2. Experimental procedures

6.2.1. Primary cultures of rat adipocytes

Differentiated rat adipocytes were obtained and cultured as described previously (Bourez et al., 2012a; Louis et al., 2014b). The fat tissue of the stromal-vascular fraction from 2-month-old male Wistar rats (Centre d'Elevage Janvier, Le Genest Saint Isle, France) was digested in a solution of collagenase (1250 U/mL type II; Sigma-Aldrich, Bornem, Belgium). The digested tissue underwent three filtrations and three centrifugations in order to obtain a final pellet of stromal-vascular cells, which was suspended in a medium composed of Dulbecco's Modified Eagle Medium (DMEM, 4.5 g/L glucose, Gibco-Invitrogen, Merelbeke, Belgium), 10% (*v:v*) heat-inactivated foetal bovine serum (FBS, PAA, A&E Scientific, Marcq, Belgium) and an antibiotic and antifungal mixture. Cells were seeded at a mean density of 18,000 cells per cm^2 on 6-well plates (Corning CellBIND Surface, Corning, Elscolab, Kruibeke, Belgium) (day 0) and incubated at 37°C in a humidified atmosphere containing 10% CO_2 in air for 24 hours to allow cell sedimentation and adhesion. Twenty-four hours after the isolation of progenitor cells (day 1), the medium was replaced by a differentiation medium composed of DMEM (4.5 g/L glucose), 10% heat-inactivated FBS, 100 U/mL penicillin – 100 U/mL streptomycin – 250 ng/mL amphotericin B mixture (Lonza, Verviers, Belgium), 10 nM dexamethasone (Sigma-Aldrich), 10 µM ciglitizone (Sigma-Aldrich) and 5 µg/mL insulin (Sigma-Aldrich). This medium was renewed every 48 hours until day 10 in order to obtain differentiated adipocytes.

6.2.2. Cell treatment

At day 10, adipocytes were incubated with a medium supplemented with PCB congeners (Dr. Ehrenstorfer GmbH, Ausburg, DE) during 12 hours

(37°C – 10% CO_2 in air). The PCBs were added to the culture medium as ethanolic solution and four conditions of PCB contamination were tested: (i) 2,4,4'-trichlorobiphenyl (PCB-28); (ii) 2,3',4,4',5-pentachlorobiphenyl (PCB-118); (iii) 2,2',4,4',5,5'-hexachlorobiphenyl (PCB-153); (iv) an equimolar mixture of three PCB congeners (PCB-28, -118 and -153), also called cocktail of PCBs. In all conditions of contamination, each PCB was added to the culture medium at a concentration of 300 nM, which is within the range of concentrations found in *in vivo* and *in vitro* studies (Bourez et al., 2012b; Meeker et al., 2011; Wassermann et al., 1979). Impact of the ethanol vehicle was tested earlier (Bourez et al., 2012b).

6.2.3. Lipolysis experiment

At day 11, lipolytic process was induced to differentiated adipocytes as previously described in Louis et al. (2014b). The differentiation medium in contact with adipocytes was removed and replaced by a lipolytic medium composed of DMEM (1.0 g/L glucose, Gibco–Invitrogen), 5% (*v:v*) heat-inactivated FBS, 2% (*w:v*) bovine albumin (Sigma-Aldrich) and 1 µM isoproterenol (Sigma-Aldrich). The lipolytic medium was renewed every 3 hours and the process was carried out for 12 hours. In the same way as in Louis et al. (Louis et al., 2014b), cells from one plate (i.e. cells coming from the same PCB contamination) were collected every 3 hours and pooled in order to assess the cellular PCB and protein contents as well as the levels of fatty acids of cellular neutral lipids (NLs). Likewise, free fatty acids (FAs), glycerol and PCBs released in the extracellular medium were quantified every 3 hours in all conditions.

6.2.4. Cellular protein assessment

Every 3 hours, cells were washed with phosphate-buffer saline (Sigma-Aldrich) at 37°C and then collected in an aqueous solution composed of 35 mM sodium dodecyl sulfate (Merck, Darmstadt, Germany), 60 mM Tris buffer (Merck) and 10 mM ethylenediaminetetraacetic acid (Sigma-Aldrich). After homogenization, the cellular protein content was quantified by using

the Bicinchoninic Acid Protein Assay kit (Sigma-Aldrich) with bovine serum albumin (Sigma-Aldrich) as calibration curve (Louis et al., 2014b).

6.2.5. Cellular neutral lipid assessment

Cells were collected as described for the determination of protein content. The method used for the extraction and the isolation of the NL fraction (i.e. triglycerides (TGs), diglycerides, monoglycerides and cholesterol esters) from cell lysates is described in details in Louis et al. (2014b). Briefly, the lipids were extracted with a mixture of chloroform/methanol/water (2:2:1, *v:v:v*) (Biosolve, Valkenswaard, The Netherlands) containing triheptadecanoin (Larodan, Malmö, Sweden) used as internal standard. After centrifugation, the supernatant was discarded; the chloroform phase was evaporated and samples were then suspended into 200 µL chloroform. In order to isolate NLs, samples were loaded on solid-phase extraction columns (Bond Elut NH_2, 200 mg, Varian, Middelburg, The Netherlands). The NL fraction collected with chloroform/2-propanol (2:1, *v:v*) (Biosolve) was evaporated and a methylation step was performed by adding 0.1 M KOH (Sigma-Aldrich) in methanol at 70°C for 1 hour and then, by adding 1.2 M HCl in methanol at 70°C for 15 min. The addition of hexane followed by deionized water allowed extracting the fatty acid methyl esters by a centrifugation step. Those were separated by gas chromatography (Dang Van et al., 2011). Each peak was then identified and quantified by comparison with pure methyl ester standards (Larodan and Nu-Check Prep, Elysian, MN, USA). Data were processed with the ChromQuest 4.2 software (ThermoFinnigan, Milan, Italy). Thereafter, results were expressed by moles of fatty acids in cellular NLs. For the sake of simplicity, we refer to µmol NLs/mg protein in the text (Louis et al., 2014b).

6.2.6. Extracellular free fatty acid assessment

Free FA contents in the lipolytic medium were quantified with the Wako NEFA HR kit (Sopachem, Eke, Belgium) following the manufacturer's instructions (Louis et al., 2014b).

6.2.7. Extracellular glycerol assessment

Glycerol released in the extracellular medium was measured with an *in vitro* enzymatic colorimetric test using glycerol-3-phosphate-oxidase (Diasys Free Glycerol FS kit, Sopachem) according to the manufacturer's instructions.

6.2.8. PCB assessment

At each studied time of the lipolysis, cells and extracellular medium were collected in EPA vials (Alltech, Lokeren, BE) with 5 mL of *n*-hexane (Biosolve) in order to perform a liquid-liquid extraction by a 10-min shaking. The hexane phase was transferred into a tube and PCB-112 (Dr. Ehrenstorfer GmbH) was added as internal standard. All samples were then purified by acid and Florisil clean-up steps as described in Debier et al. (2003). Purified samples were collected in *n*-hexane. Five µL anhydrous nonane (Sigma-Aldrich) were added to samples and solvent was then evaporated under a gentle steam of nitrogen. The purified extracts were suspended into a hexane solution of Mirex (200 pg/µL) (Dr. Ehrenstorfer GmbH) used as internal standard for the corrections of the extract volume injected in GC/MS. PCB congeners were separated and quantified with a gas chromatograph (GC Trace, ThermoFinnigan) equipped with an automatic split/splitless type injector (CTC Analytics, Zwingen, Switzerland), a fused silica capillary column (30 m x 0.25 mm internal diameter; 0.25 µm film) (Rxi-5ms, Restek, Bellefonte, PA, USA) and a mass spectrometer (Trace DSQ, ThermoFinnigan). The system used helium as carrier gas at a constant flow rate of 1.1 mL per minute. The temperature of injector was 230°C. The oven temperature program was as follows: 2 min at 60°C, gradual heating from 60 to 140°C at the rate of 20°C per minute, 1 minute at 140°C, gradual heating from 140 to 290°C at the rate of 2,5°C per minute, 10 minutes at 290°C and gradual cooling from 290°C to 60°C at the rate of 10°C per minute. Molecules were sent to mass spectrometer by the line transfer at 290°C. The ion source of the detector was kept at 230°C. PCBs were identified according to their retention time. Data were recorded using XCalibur 1.3 software (ThermoFinnigan). Quantification was performed by

comparison to an external standard composed of 28 congeners (IUPAC numbers: PCB-8, -18, -28, -44, -52, -66, -77, -81, -101, -105, -114, -118, -123, -126, -128, -138, -153, -156, -157, -167, -169, -170, -180, -187, -189, -195, -206 and -209) in a certified calibration mixture (AccuStandard, New Haven, CT, USA). Five dilutions (concentration ranging from 25 to 500 pg/µL) were used in order to draw a linear calibration curve for each PCB.

6.2.9. Quality control

Blanks were run with sample series to control extraction and clean-up steps. The PCB recovery was calculated on the basis of the internal standard, PCB-112. Results were accepted only if the recoveries were between 70 and 130% according to EC council (EC, 2002). All results were corrected to obtain 100% recovery (Debier et al., 2003). The quality control was assessed through an interlaboratory comparison.

6.2.10. Cytotoxicity assessment

The potential cytotoxicities of the PCBs and the lipolytic treatment were assessed by measuring the release of lactate dehydrogenase (LDH) in the extracellular medium. The activity of LDH was determined using the cytotoxicity detection kit (Roche Diagnostics, Vilvoorde, Belgium) according to the manufacturer's instructions in (i) the differentiation medium after 12 hours of PCB exposure and (ii) the lipolytic media collected every 3 hours during the lipolytic process. Before the PCB exposure and the lipolysis, some cells were lysed with 1% Triton X-100 (Sigma-Aldrich) and were used as full toxicity control (Louis et al., 2014b). No treatments appeared toxic ($< 5\%$ of control) as compared to the full toxicity control (results not shown).

6.2.11. Statistical analysis

Data are presented as means ± SEM of three independent experiments for the conditions with PCB congeners alone and means ± SEM of five independent experiments for the condition with the cocktail of PCBs. The statistical analysis was performed by SAS 9.3 software (SAS Institute Inc.,

Cary, USA). Differences between treatments were assessed with mixed linear models and a Tukey's test (Louis et al., 2014b). Differences were deemed significant at p-values<0.05.

6.3. Results

6.3.1. Incorporation of PCBs in adipocytes

At day 10, differentiated rat adipocytes were exposed to four different treatments of PCBs during a 12-hour period. Three PCB congeners (PCB-28, -118 and -153) were added to the culture medium at a concentration of 300 nM, alone or in cocktail. Assessment of PCBs within adipocytes was carried out before the induction of lipolysis. The concentration of each congener in adipocytes, expressed as nmol per unit of cellular protein, was statistically similar, whatever the kind of contamination (alone or in cocktail) ($0.328<p<1.000$) (Table 6.1). Same conclusions were drawn when the results were expressed per unit of NLs ($0.207<p<1.000$). Since the dynamics of accumulation of PCBs in cells vary with cellular lipid content (Bourez et al., 2013), the levels of NLs were quantified and no statistical difference was noted ($0.457<p<0.978$) (Table 6.1).

Table 6.1 – Efficient accumulation of PCBs in adipocytes during a 12-hour period. Quantities of PCBs accumulated in cultured adipocytes, expressed in nmol per unit of cellular protein and per unit of neutral lipids (NLs), when a dose of PCBs was added during 12 hours in the culture medium. Quantities of NLs, expressed in µmol per unit of cellular protein are also presented. Data represent the means of (i) three independent experiments ± SEM for conditions with one PCB congener alone, (ii) five independent experiments ± SEM for conditions with the cocktail of PCBs. There was no significant difference of PCB and NL concentrations between the three PCB congeners, whatever the kind of contamination, alone or in cocktail ($p<0.05$).

	Contamination by a PCB congener alone:			Contamination by a cocktail of three PCB congeners:		
	PCB-28	PCB-118	PCB-153	PCB-28	PCB-118	PCB-153
PCBs (nmol/mg protein)	1.7 ± 0.1	2.0 ± 0.1	1.8 ± 0.1	1.8 ± 0.1	2.1 ± 0.1	1.8 ± 0.1
PCBs (nmol/mg NLs)	0.47 ± 0.08	0.62 ± 0.09	0.48 ± 0.08	0.61 ± 0.08	0.70 ± 0.08	0.60 ± 0.08
NLs (µmol/mg protein)	13.6 ± 1.1	13.1 ± 1.3	15.6 ± 1.1	11.4 ± 1.1	11.4 ± 1.1	11.4 ± 1.1

6.3.2. The time-course of lipolysis

At day 11, adipocytes contaminated with PCBs (alone or in cocktail) were incubated with a lipolytic medium supplemented with 1 µM isoproterenol, which was replaced every 3 hours for 12 hours. Since the aim of this work was to study the kinetics of PCB release during the mobilisation of lipids in adipocytes, we firstly ensured of the efficiency of lipolysis. Cellular NLs as well as free FAs and glycerol released in the culture medium were quantified over 12 hours (Figure 6.1). The free FAs and glycerol initially present in the lipolytic medium, before being in contact with adipocytes, were subtracted from each result, leading to a value of 0 at 0 hour (Figure 6.1 B-C). The total free FAs and glycerol released by the adipocytes throughout a given period were calculated by adding the quantities measured at each period of 3 hours. For example, the amount of total free FAs or glycerol released after 6 hours of lipolysis corresponds to the sum of free FAs or glycerol released between 0 and 3 hours and between 3 and 6 hours (Louis et al., 2014b).

A significant decrease of cellular NLs was observed between early and late lipolysis for the conditions with the PCB-28 (p=0.005) and cocktail of PCBs (p=0.029). The cell NLs tended to decrease over 12 hours within adipocytes contaminated with PCB-118 (p=0.298) and PCB-153 (p=0.097). For all conditions, the greatest reduction occurred during the first 3 hours of the experiment (Figure 6.1 A). Indeed, a mean loss of 57 ± 3% initial NLs was noted between 0 and 12 hours, whereas after 3 hours of lipolysis, adipocytes already lost 33 ± 6% of NLs on average, compared to the initial levels ($0.372<p<0.721$ for all conditions of contamination between 0 and 3 hours). The comparison of NL levels between the four PCB treatments at a given period did not highlight any difference ($0.255<p<1.000$).

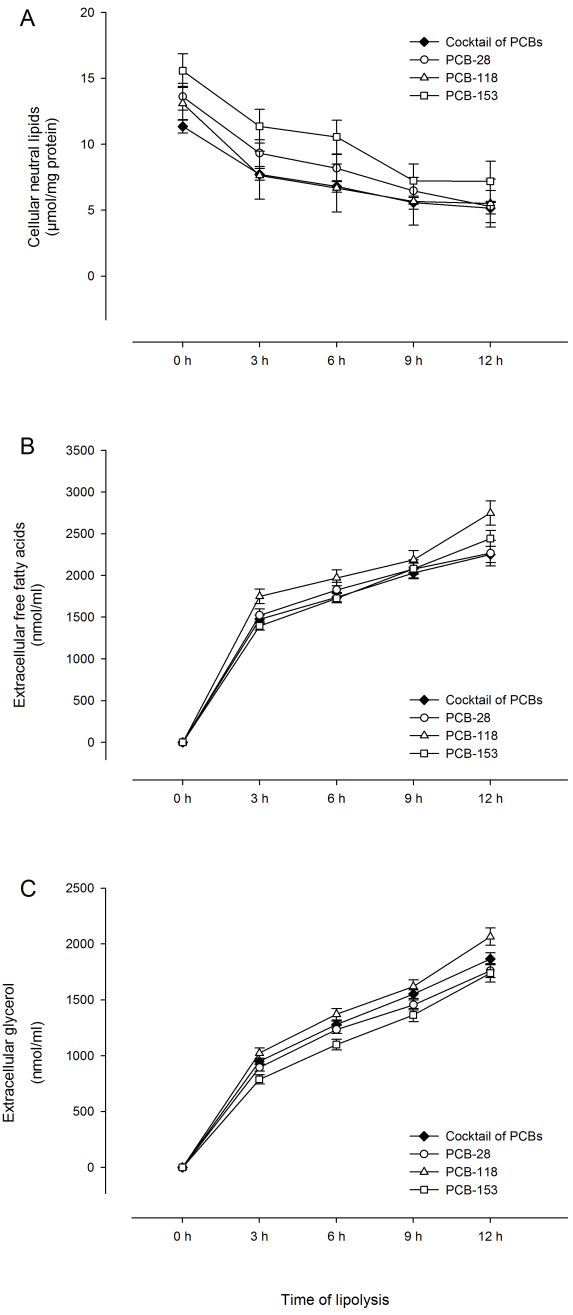
A
Cellular neutral lipids (µmol/mg protein)
20
15
10
5
0
Cocktail of PCBs
PCB-28
PCB-118
PCB-153
0 h
3 h
6 h
9 h
12 h
B
Extracellular free fatty acids (nmol/ml)
3500
3000
2500
2000
1500
1000
500
0
Cocktail of PCBs
PCB-28
PCB-118
PCB-153
0 h
3 h
6 h
9 h
12 h
C
Extracellular glycerol (nmol/ml)
2500
2000
1500
1000
500
0
Cocktail of PCBs
PCB-28
PCB-118
PCB-153
0 h
3 h
6 h
9 h
12 h
Time of lipolysis

Figure 6.1 – Lipolytic treatment decreased cellular neutral lipids and increased extracellular free fatty acids and glycerol. At day 11, differentiated rat adipocytes, which were previously contaminated with PCBs, were incubated with a lipolytic medium supplemented with 1 µM isoproterenol. We renewed the lipolytic medium every 3 hours for 12 hours. Cellular neutral lipids (corresponding to µmol of fatty acids in cellular neutral lipids) were expressed per mg of total cell protein (A). Total extracellular free fatty acids (B) and total extracellular glycerol (C) were expressed per mL of medium. Quantities of total free fatty acids and glycerol in the medium were obtained by adding the quantities released during the periods of 3 hours (e.g. total free fatty acids at 6 hours correspond to the sum of total free fatty acids released between 0 and 3 hours and between 3 and 6 hours). Data represent the means of (i) three independent experiments ± SEM for conditions with one PCB congener alone, (ii) five independent experiments ± SEM for conditions with the cocktail of PCBs.

The decrease of cellular lipid contents was accompanied by a significant increase of total free FAs in the lipolytic medium over the 12-hour period ($p<0.001$) (Figure 6.1 B). The increase of total free FAs was more pronounced during the first 3 hours of lipolysis, during which an average of 63 ± 4% released total free FAs occurred ($p<0.001$). Free FA concentrations then continued to increase slightly, but not significantly, between the subsequent consecutive periods ($0.491<p<0.985$ for all conditions of contamination between 3 and 6 hours, 6 and 9 hours, 9 and 12 hours). No difference in the release of free FAs was noted between the four conditions of contamination at a given time of the lipolytic process ($0.273<p<1.000$).

As for total free FAs, contaminated adipocytes released a significant amount of total glycerol throughout the lipolytic process ($p<0.001$ between 0 and 12 hours) (Figure 6.1 C). The major part of the release (49 ± 3%) also occurred during the first 3 hours of lipolysis for all conditions ($p<0.001$) (Figure 6.1 C). Here again, no difference in the release of glycerol was noted between the different conditions of PCB contamination over the 12-hour period ($0.119<p<0.999$).

6.3.3. Comparative dynamics of mobilisation of PCB-28, -118 and -153, present in cocktail in adipocytes

In the present section, we compared the dynamics of mobilisation of PCB-28, -118 and -153 (present in cocktail within the cells) from the same adipocytes undergoing a lipolytic process over 12-hour period. In order to strictly compare the different mobilisations between congeners, we expressed the results as percentages of the amounts initially present in adipocytes (i.e. at 0 hour). The potential presence of PCBs in the lipolytic medium, before being in contact with the cells, has been tested and was negligible (result not shown). The proportions of PCBs in the lipolytic medium at 0 hour were thus set at 0%. Regarding the subsequent studied times of the lipolysis (3, 6, 9 and 12 hours), the PCB levels in the medium were calculated by adding the quantities evaluated at each period of 3 hours. For example, the amounts of each PCB congener released after 6 hours of lipolytic treatment correspond to the sum of PCBs released between 0 and 3 hours and between 3 and 6 hours.

In parallel to the lipid mobilisation, there was a release of PCBs from the adipocytes into the culture medium (Figure 6.2). An important drop of the cellular PCB content occurred during the first half of the lipolytic process ($p<0.001$ between 0 and 6 hours for the three PCBs). It was followed by a slight, but still significant reduction of PCB-28, -118 and -153 in adipocytes during the second part of the lipolysis ($p<0.001$ between 6 and 12 hours for the three PCBs). Accordingly, a reversed trend was noted in the lipolytic medium: the proportions of PCB-28, -118 and -153 accrued during the first 6 hours ($p<0.001$ between 0 and 6 hours for the three PCBs). The PCB accumulation in the culture medium was more moderate, but still significant ($0.001<p<0.006$), during the second part of the lipolytic process.

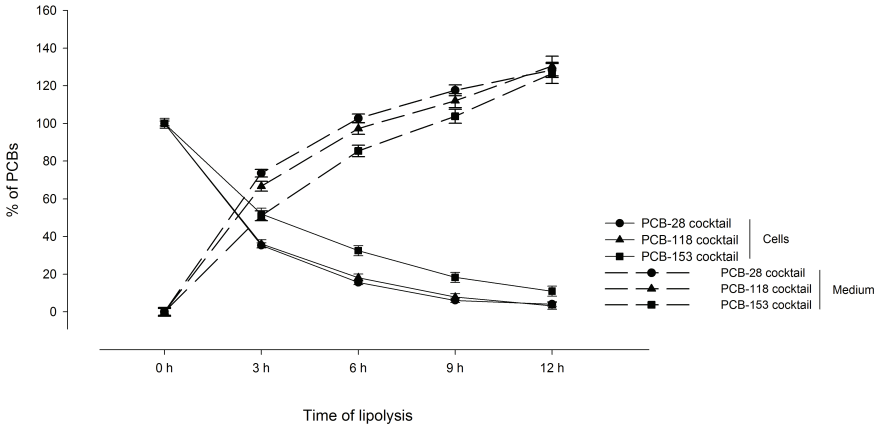

Figure 6.2 – Lipolytic treatment decontaminated the adipocytes, inducing an accumulation of PCB congeners in the extracellular medium. At day 11, contaminated adipocytes underwent a lipolytic process. The PCB contents as well as the proportions of PCBs released in the extracellular medium were assessed every 3 hours. For each PCB congener, all results were expressed in percentage of the amounts initially present in the cells. Proportions of one PCB congener in the medium were obtained by adding the amounts released during periods of 3 hours (e.g. proportion of one congener at 6 hours correspond to the sum of this congener released between 0 and 3 hours and between 3 and 6 hours). Data represent the means of (i) three independent experiments ± SEM for conditions with one PCB congener alone, (ii) five independent experiments ± SEM for conditions with the cocktail of PCBs.

Even if all congeners dropped in the cells and increased in the culture medium, the dynamics of release of PCB-153 somewhat differed from those of PCB-28 and -118. Indeed, despite the fact that the amounts of the 3 congeners within adipocytes were statistically similar before the beginning of the lipolysis (Table 6.1), the percentages of PCB-153 in adipocytes remained higher than the ones of PCB-28 and PCB-118 at 3, 6 and 9 hours of lipolysis ($0.001<p<0.032$ for PCB-28; $0.031<p<0.037$ for PCB-118). The difference disappeared at 12 hours between PCB-153 and PCB-28 ($p=0.139$), but remained significant between PCB-153 and PCB-118 ($p=0.027$). On the other hand, the cellular percentage of PCB-28 and PCB-118 did not differ between each other throughout the lipolytic process ($0.373<p<1.000$). The slower mobilisation of PCB-153 from adipocytes was reflected by a slower increase in the culture medium as compared to PCB-28 and PCB-118 after 3 hours of lipolysis ($p<0.001$ for the both comparisons). After 6 hours, the accumulation in the medium was weaker for PCB-153 than PCB-28 ($p=0.027$) and similar between PCB-153 and PCB-118 ($p=0.178$). The proportions of PCB-153 were then similar to those of PCB-28 and -118 for the subsequent hours ($0.275<p<0.986$ at 9 and 12 hours). On the other hand, the percentages of PCB-28 and -118 in the extracellular medium were similar to each other over the lipolysis ($0.429<p<1.000$).

6.3.4. Impact of the presence of other PCB congeners on the dynamics of mobilisation of PCB-28, -118 and -153

We investigated if the dynamics of mobilisation of one PCB congener was influenced by the presence of the other congeners. To achieve this goal, we contaminated adipocytes either with one of the three PCB congeners (PCB-28, -118 or -153) or with a cocktail of the three congeners. Here also, the results are expressed as percentages of the amounts initially present in adipocytes. As previously described, the proportions of PCBs just before the lipolytic process (i.e. 0 hour) was set to 0% since no PCB congener was quantified in the initial lipolytic medium. The total PCB congeners released by the adipocytes throughout a given period were calculated by adding the quantities measured at each period of 3 hours.

At each studied time throughout the 12-hour period, similar proportions of PCB-28, PCB-118 and PCB-153 (Figure 6.3 A-C) within adipocytes were quantified between both conditions of contamination (i.e. congeners alone and in cocktail) ($0.134<p<0.934$). Accordingly, no difference was noted between the percentages of PCBs released in the lipolytic medium in contact with adipocytes in both conditions of contamination ($0.122<p<0.916$), except after 3 hours of lipolysis, where the proportion of PCB-153 measured in the medium were higher when it was added in cocktail than when it was added alone ($p=0.046$).

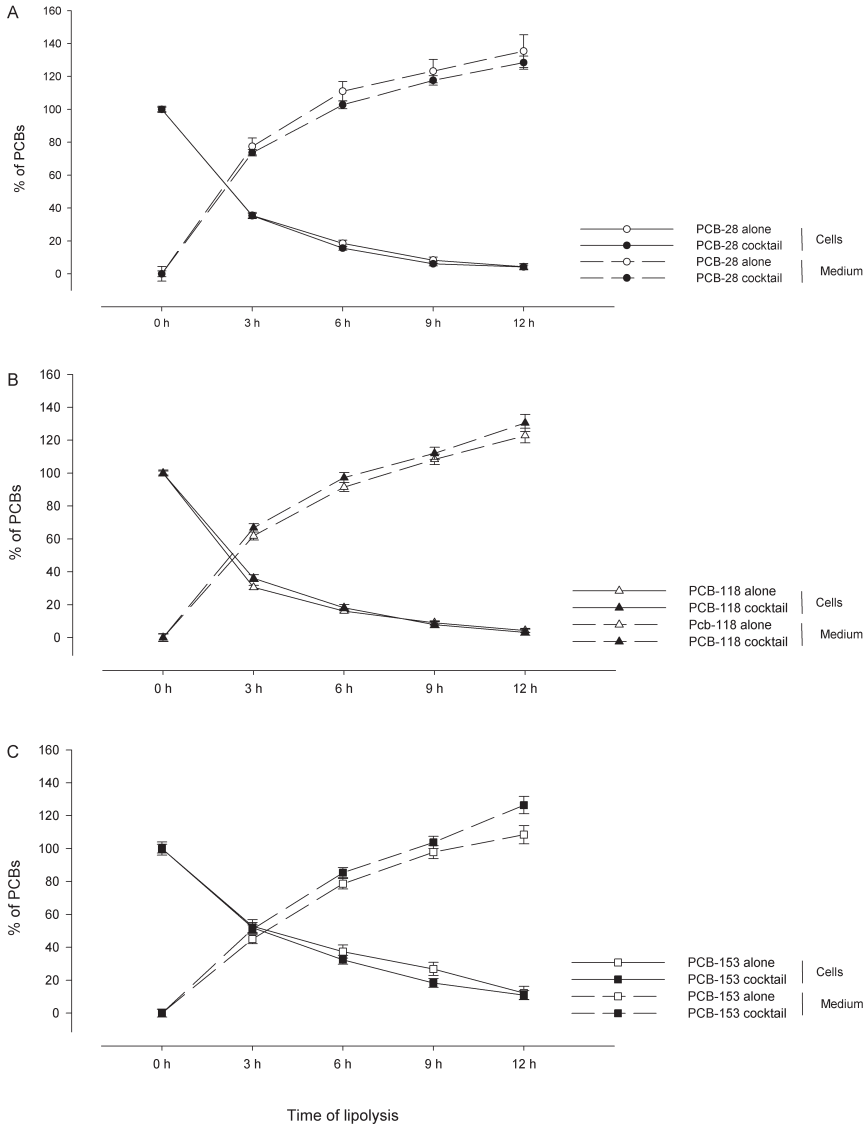
A
B
C
% of PCBs
0
20
40
60
80
100
120
140
160
0 h
3 h
6 h
9 h
12 h
PCB-28 alone
PCB-28 cocktail
PCB-28 alone
PCB-28 cocktail
Cells
Medium
PCB-118 alone
PCB-118 cocktail
Pcb-118 alone
PCB-118 cocktail
Cells
Medium
PCB-153 alone
PCB-153 cocktail
PCB-153 alone
PCB-153 cocktail
Cells
Medium
Time of lipolysis

Figure 6.3 – Presence of other congeners did not influence the dynamic of PCB mobilisation. At day 11, adipocytes, which were previously contaminated with either individual PCB congeners or with a cocktail, underwent a lipolytic process. The cellular levels of PCBs before the lipolytic process were quantified and set at 100%. During 12-hour period of lipolysis, the contents of PCB congeners within adipocytes and in the extracellular medium were assessed every 3 hours. The results for PCB-28 (A), PCB-118 (B) and PCB-153 (C) were expressed by the percentage of initial amounts of each congener. Within a condition of contamination, proportions of one PCB congener in the medium were obtained by adding the quantities released during the periods of 3 hours (e.g. proportion of one congener at 6 hours corresponds to the sum of this congener released between 0 and 3 hours and between 3 and 6 hours). Data represent the means of (i) three independent experiments ± SEM for conditions with one PCB congener alone, (ii) five independent experiments ± SEM for conditions with the cocktail of PCBs.

6.4. Discussion

Considerable accumulation of PCBs within adipocytes

Differentiated rat adipocytes were exposed to three targeted PCB congeners (PCB-28, -118 and -153), which differ by the number and the position of the chlorine atoms (Carpenter, 2006; Matthews et al., 1984). After 12 hours, similar concentrations of the PCBs were stored within adipocytes. Same observations were already drawn after 4 hours of exposure for the same congeners in 3T3-L1 cell line (Bourez et al., 2013). The different molecular structures of PCBs did thus not seem to influence their accretion within adipocytes on long term. Previous studies from our group highlighted the importance of the amount of cellular NLs, acting as a trap for the accumulation of PCBs within adipocytes (Bourez et al., 2012a; Bourez et al., 2013). The fact that cellular NL levels were similar between our experimental conditions is most probably at the origin of the identical accumulation of PCBs within adipocytes. While PCB concentrations in the culture medium were in the same range than those measured in the human serum (Meeker et al., 2011; Wassermann et al., 1979), the PCB levels found in cultured adipocytes after 12 hours of incubation (data from Table 6.1 are approximately equivalent to 175 ng PCB congeners per mg NLs) were much

higher than those measured *in vivo* in the human adipose tissue (from 0.02 to 0.66 ng total PCBs per mg lipids) (Arrebola et al., 2012; De Saeger et al., 2005; Malarvannan et al., 2013; Moon et al., 2012; Wang et al., 2010). It reflects a high propensity of differentiated rat adipocytes to store PCBs (Bourez et al., 2012b). Such differences have already been noticed previously and the reasons are discussed in details elsewhere (Bourez et al., 2012a). Briefly, the higher *in vitro* concentrations of PCBs within adipocytes could result from the extended contact between the cells and the contaminated culture medium (12 hours). On the contrary, in the *in vivo* situation, the PCB congeners, transported in the circulation by lipoproteins and plasma albumin (Becker and Gamble, 1982; Matthews et al., 1984; Spindler-Vomachka et al., 1984), are in continual movement thanks to the blood flow. In addition, the culture medium contains only a low concentration of serum (10%) (Bourez et al., 2012b), and therefore very low levels of lipoproteins and albumin, which could contribute to a smaller retention of PCBs in this hydrophilic compartment and a higher storage in the lipophilic compartment represented by adipocytes. The differentiated rat adipocytes are also organised as a monolayer, whereas *in vivo* adipose tissue shows a complex 3D-structure. Furthermore, lipolysis, which occurs regularly *in vivo*, may lead to the mobilisation of PCBs from adipocytes. Finally, the circulating PCBs may be taken up by other tissues such as the liver.

Similar dynamics of mobilisation between cellular lipids and PCBs

Once the lipolytic pathway was induced, adipocytes started to mobilise their lipid content. A decrease of the cellular NLs could be observed throughout the 12-hour experiment, with a more pronounced lipolytic action during the first 3 hours. This sharper decrease of NL content at early lipolysis was in accordance with our previous study (Louis et al., 2014b). As a result of the mobilisation of cellular NLs, free FAs and glycerol were released in the extracellular medium. The lipolytic treatment also led to the release of PCBs from adipocytes to the extracellular medium. The dynamics of mobilisation of PCBs exhibited some parallelism with those of cellular lipids, as the major part of PCB discharge occurred during the first hours of lipolysis as well. Previously, it was shown that *in vitro* epididymal

adipocytes isolated from rats also unloaded PCB-153 during a lipolytic treatment of 50 min with 0.8 µM isoproterenol (Gallenberg et al., 1987). The release of PCBs might accompany the mobilisation of cell lipids, which agrees with previous studies on the behaviour of dioxins (Irigaray et al., 2005). In addition, cellular TG content is an important parameter governing the accumulation of PCBs in adipocytes (Bourez et al., 2012a; Bourez et al., 2013). PCBs are stored almost exclusively within the LDs (Bourez et al., 2012b). As this lipophilic pool is reduced during lipolysis (Louis et al., 2014b), the capacity of storage is thus also lessened, promoting the release of PCBs in the extracellular medium, where they could be tightly associated with diverse lipoproteins (present in the 5% serum) and bovine albumin (2%).

Although an obvious release of PCBs occurred from adipocytes during the lipolytic experiment, some molecules of PCBs could be taken up again by the cells as previously suggested in *in vivo* studies (Louis et al., 2014a; Vanden Berghe et al., 2012). This phenomenon is well known for free FAs, which are partly reabsorbed by adipocytes and re-esterified into newly synthesised TGs (Edens et al., 1990; Louis et al., 2014b). Nevertheless, such a mechanism is somewhat limited in our experimental conditions, because of the renewal of the lipolytic medium every 3 hours (Louis et al., 2014b).

Studies investigating the release of POPs from adipose tissue during periods of weight loss in humans and animals usually report an increase of the concentrations of PCBs and related compounds in adipose tissue, despite their significant discharge in the blood circulation (Dirtu et al., 2013; Hue et al., 2006; Kim et al., 2011; Louis et al., 2014a). This increase suggests a less efficient mobilisation of PCBs from this tissue than lipids and a concentration of those xenobiotics in the remaining amount of fat cells. The adipose tissue is a macroscopic structure with several cell layers that is heterogeneously irrigated by blood vessels. During adipose tissue lipolysis, it is possible that PCBs are transferred to adipocyte layers that still contain significant amounts of lipids in their LDs instead of being all released into the circulation. It is also possible that PCBs are released in the bloodstream together with the lipids and then reabsorbed by the adipose tissue as a result

of their higher affinity for the remaining lipids present in the cells (Vanden Berghe et al., 2012). Our *in vitro* model differs from the *in vivo* situation among others by the fact that it is characterised by only one layer of cells, which is in direct contact with the extracellular medium that is regularly renewed. A reuptake of PCBs by the cells and/or a migration of PCBs to deeper adipocyte layers that are still filled with fat are thus not possible. Moreover, the high PCB concentrations, which are found in our cultivated adipocytes before the lipolytic induction, might also promote the massive release of congeners to the extracellular medium.

Differences of release according to the kind of PCB congener

When the three congeners were added in cocktail to the culture medium, we could observe that PCB-153 was less efficiently mobilised from adipocytes than PCB-28 and PCB-118 during the first part of the lipolytic process. This difference however disappeared at 12 hours of lipolysis. The slower mobilisation of PCB-153 from adipocytes reflects the fact that, besides the cellular lipid content, the rate of release is also governed by the physico-chemical properties of the congeners, which are defined by the number and the position of chlorine atoms on the biphenyl core (La Merrill et al., 2013). If we consider the electrostatic potentials of PCBs (Bourez et al., 2013), PCB-153 exhibits a large electron-deficient zone. This characteristic makes this congener rather lipophilic, which is reflected by the higher partition coefficient *n*-octanol/water (log K_{ow} = 6.80). On the other hand, PCB-28 and PCB-118 has a reduced electron-deficient zone, translated by lower log K_{ow} (PCB-28: log K_{ow} = 5.71 and PCB-118: log K_{ow} = 6.57). PCB-153 could thus be more trapped within LDs than PCB-28 and PCB-118 and as a consequence, be released slower.

In addition, it was previously observed that a small proportion of PCB-153 was sequestrated in the cell membranes when isolated primary adipocytes absorbed the PCB congeners present in the culture medium for 2 hours (Bourez et al., 2012b). It was not the case for PCB-28 and -118. Likewise, several studies showed that PCB-52 and -153, two di-*ortho*-substituted PCBs, intercalate between membrane phospholipids similarly to

cholesterol and have an impact on the membrane fluidity in fish, rodent and chicken cells (Campbell et al., 2008; Gonzalez et al., 2013; Katynski et al., 2004; López-Aparicio et al., 1997; Yilmaz et al., 2006). In the present study, the release of PCB-153 from adipocytes could thus be slowed down by its association with cell membranes, as compared to PCB-28 and PCB-118, two mono-*ortho*-substituted congeners. The fact that PCB-153 has two chlorine atoms in the *ortho* position on the biphenyl core induces a more perpendicular layout of the phenyl rings. It means that PCB-153 occupies a larger bulk than PCB-28 and PCB-118, which could be involved in the sequestration of PCB-153 within membranes and its slower mobilisation from adipocytes.

Similar rate of release when PCBs are present alone or in cocktail

In the *in vivo* situation, tissues are exposed to a cocktail of contaminants that might interact with each other, regarding either the toxicokinetics or the toxicodynamics of the molecules. Here, we investigated the effect of a simple combination of PCBs (three congeners) on their release by adipocytes during lipolysis. To do this, the discharge of PCB-28, -118 and -153 from adipocytes was followed either alone, or in cocktail (i.e. with two other congeners). In the two conditions of contaminations, the dynamics of PCB release were similar, meaning that the mobilisation of PCB congeners was not influenced by the presence of other congeners within adipocytes in these experimental conditions. As noted above, PCB-153 influences the properties of cell membranes. One could thus have expected that this congener could influence the dynamics of release of other PCBs from the cells.

6.5. Conclusion

Our results showed an efficient accumulation of PCB-28, -118 and -153 in adipocytes. Once lipolysis was induced, the congeners were massively mobilised from the cells into the culture medium, in parallel with the release of lipids. The dynamics of discharge however differed between the three investigated congeners. The release of PCB-153 was slightly but significantly slower than the ones of PCB-28 and -118. The phenomenon might be explained by the fact that PCB-153 is more lipophilic than the two other congeners and could thus be more trapped in LDs. In addition, PCB-153 being a di-*ortho*-substituted congener, it is more bulky, which could be involved in its partial sequestration within cell membrane (Bourez et al., 2012a) and its slower mobilisation from adipocytes. On the other hand, the dynamics of mobilisation of one congener was not influenced by the presence of the other two congeners.

6.6. References

Arrebola, J. P., et al., 2012. Concentrations of organochlorine pesticides and polychlorinated biphenyls in human serum and adipose tissue from Bolivia. Environmental Research. 112, 40-47.

Becker, M. M., Gamble, W., 1982. Determination of the binding of 2,4,5,2',4',5'-hexachlorobiphenyl by low density lipoprotein and bovine serum albumin. Journal of Toxicology and Environmental Health. 9, 225-34.

Bourez, S., et al., 2012a. Accumulation capacity of primary cultures of adipocytes for PCB-126: Influence of cell differentiation stage and triglyceride levels. Toxicology Letters. 214, 243-250.

Bourez, S., et al., 2012b. Accumulation of polychlorinated biphenyls in adipocytes: Selective targeting to lipid droplets and role of caveolin-1. PLoS ONE. 7, e31834.

Bourez, S., et al., 2013. The dynamics of accumulation of PCBs in cultured adipocytes vary with the cell lipid content and the lipophilicity of the congener. Toxicology Letters. 216, 40-46.

Campbell, A. S., et al., 2008. PCB association with model phospholipid bilayers. Environmental Science & Technology. 42, 7496-501.

Carpenter, D. O., 2006. Polychlorinated biphenyls (PCBs): routes of exposure and effects on human health. Reviews on Environmental Health. 21, 1-23.

Chevrier, J., et al., 2000. Body weight loss increases plasma and adipose tissue concentrations of potentially toxic pollutants in obese individuals. International Journal of Obesity and Related Metabolic Disorders. 24, 1272-8.

Dang Van, Q. C., et al., 2011. Influence of the diet structure on ruminal biohydrogenation and milk fatty acid composition of cows fed extruded linseed. Animal Feed Science and Technology. 169, 1-10.

De Saeger, S., et al., 2005. Monitoring of polychlorinated biphenyls in Belgian human adipose tissue samples. Chemosphere. 58, 953-960.

Debier, C., et al., 2006. Mobilization of PCBs from blubber to blood in northern elephant seals (*Mirounga angustirostris*) during the post-weaning fast. Aquatic Toxicology. 80, 149-157.

Debier, C., et al., 2012. Differential changes of fat-soluble vitamins and pollutants during lactation in northern elephant seal mother–pup pairs. Comparative Biochemistry and Physiology Part A. 162, 323-330.

Debier, C., et al., 2005. Polychlorinated biphenyls, dioxins, and furans in weaned, free-ranging northern elephant seal pups from central California, USA. Environmental Toxicology and Chemistry. 24, 629-633.

Debier, C., et al., 2003. Quantitative dynamics of PCB transfer from mother to pup during lactation in UK grey seals *Halichoerus grypus*. Marine Ecology Progress Series. 247, 237-248.

Debier, C., et al., 2004. An unexpected parallelism between Vitamin A and PCBs in seal milk. Aquatic Toxicology. 68, 179-183.

Dirinck, E., et al., 2011. Obesity and persistent organic pollutants: Possible obesogenic effect of organochlorine pesticides and polychlorinated biphenyls. Obesity. 19, 709-714.

Dirtu, A. C., et al., 2013. Dynamics of organohalogenated contaminants in human serum from obese individuals during one year of weight loss treatment. Environmental Science & Technology. 47, 12441-12449.

Djien Liem, A. K., et al., 2000. Exposure of populations to dioxins and related compounds. Food Additives & Contaminants. 17, 241-259.

EC, 2002. European Commission. Council L221/8. Official Journal of the European Communities. 262, 8-36.

Edens, N. K., et al., 1990. Mechanism of free fatty acid re-esterification in human adipocytes *in vitro*. Journal of Lipid Research. 31, 1423-1431.

Gallenberg, L. A., et al., 1987. Influence of lipolysis on the mobilization of 2,4,5,2′4′,5′-hexachlorobiphenyl from adipocytes *in vitro*. Journal of Toxicology and Environmental Health. 20, 163-171.

Gonzalez, A., et al., 2013. PCB-153 and temperature cause restructuring of goldfish membranes: Homeoviscous response to a chemical fluidiser. Aquatic Toxicology. 144–145, 11-18.

Gupta, C., 2000. Reproductive malformation of the male offspring following maternal exposure to estrogenic chemicals. Proceedings of the Society for Experimental Biology and Medicine. 224, 61-68.

Hue, O., et al., 2006. Increased plasma levels of toxic pollutants accompanying weight loss induced by hypocaloric diet or by bariatric surgery. Obesity Surgery. 16**,** 1145-1154.

Imbeault, P., et al., 2002. Weight loss-induced rise in plasma pollutant is associated with reduced skeletal muscle oxidative capacity. American Journal of Physiology. 282**,** E574-E579.

Irigaray, P., et al., 2005. Behaviour of dioxin in pig adipocytes. Food and Chemical Toxicology. 43**,** 457-460.

Katynski, A. L., et al., 2004. 3,3',4,4',5-pentachlorobiphenyl (PCB 126) impacts hepatic lipid peroxidation, membrane fluidity and β-adrenoceptor kinetics in chick embryos. Comparative Biochemistry and Physiology Part C. 137**,** 81-93.

Kester, M. H., et al., 2000. Potent inhibition of estrogen sulfotransferase by hydroxylated PCB metabolites: A novel pathway explaining the estrogenic activity of PCBs. Endocrinology. 141**,** 1897-900.

Kim, M. J., et al., 2011. Fate and complex pathogenic effects of dioxins and polychlorinated biphenyls in obese subjects before and after drastic weight loss. Environmental Health Perspectives. 119**,** 377-383.

La Merrill, M., et al., 2013. Toxicological function of adipose tissue: focus on persistent organic pollutants. Environmental Health Perspectives. 121**,** 162-169.

Lee, D. H., et al., 2011. Low dose organochlorine pesticides and polychlorinated biphenyls predict obesity, dyslipidemia, and insulin resistance among people free of diabetes. PLoS ONE. 6**,** e15977.

López-Aparicio, P., et al., 1997. Effect of Aroclor 1248 and two pure PCB congeners upon the membrane fluidity of rat renal tubular cell cultures. Pesticide Biochemistry and Physiology. 57**,** 54-62.

Louis, C., et al., 2014a. Mobilisation of lipophilic pollutants from blubber in northern elephant seal pups (*Mirounga angustirostris*) during the post-weaning fast. Environmental Research. 132**,** 438-448.

Louis, C., et al., 2014b. Efficient *in vitro* adipocyte model of long-term lipolysis: A tool to study the behaviour of lipophilic compounds. In Vitro Cellular & Developmental Biology - Animal. in press.

Malarvannan, G., et al., 2013. Distribution of persistent organic pollutants in two different fat compartments from obese individuals. Environment International. 55, 33-42.

Matthews, H. B., et al., 1984. Halogenated biphenyl transport by blood components. Fundamental and Applied Toxicology. 4, 420-428.

Meeker, J. D., et al., 2011. Serum concentrations of polychlorinated biphenyls in relation to *in vitro* fertilization outcomes. Environmental Health Perspectives. 119, 1010-1016.

Moon, H. B., et al., 2012. Polybrominated diphenyl ethers, polychlorinated biphenyls, and organochlorine pesticides in adipose tissues of Korean women. Archives of Environmental Contamination and Toxicology. 62, 176-184.

Robertson, L., Hansen, L., 2001. PCBs: Recent advances in environmental toxicology and health effects. The University Press of Kentucky, Lexington, Kentucky.

Sbarbati, A., et al., 2010. Subcutaneous adipose tissue classification. European Journal of Histochemistry. 54, e48.

Schantz, S. L., et al., 2003. Effects of PCB exposure on neuropsychological function in children. Environmental Health Perspectives. 111, 357-576.

Spindler-Vomachka, M., et al., 1984. Transport of 2,4,5,2',4',5'-hexachlorobiphenyl by lipoproteins *in vivo*. Toxicology and Applied Pharmacology. 74, 70-77.

Vanden Berghe, M., et al., 2010. Relationships between vitamin A and PCBs in grey seal mothers and pups during lactation. Environmental Pollution. 158, 1570-1575.

Vanden Berghe, M., et al., 2012. Selective transfer of persistent organic pollutants and their metabolites in grey seals during lactation. Environment International. 46, 6-15.

Wang, N., et al., 2010. Levels of polychlorinated biphenyls in human adipose tissue samples from Southeast China. Environmental Science & Technology. 44, 4334-4340.

Wassermann, M., et al., 1979. World PCBs map: Storage and effects in man and his biologic environment in the 1970s. Annals of the New York Academy of Sciences. 320, 69-124.

Yilmaz, B., et al., 2006. Effects of PCB 52 and PCB 77 on cell viability, $[Ca^{2+}]_i$ levels and membrane fluidity in mouse thymocytes. Toxicology. 217, 184-193.

Zhou, L., et al., 2011. Berberine attenuates cAMP-induced lipolysis via reducing the inhibition of phosphodiesterase in 3T3-L1 adipocytes. Biochimica et Biophysica Acta (BBA). 1812**,** 527-535.

Chapter 7

Mobilisation of blubber fatty acids of northern elephant seal pups (*Mirounga angustirostris*) during the post-weaning fast

Foreword

Chapters 3 and 6 have pointed out the selective release of POPs from *in vivo* and *in vitro* adipocytes during a lipolytic period. We reported a selective retention of higher lipophilic pollutants, whereas the less lipophilic ones tended to be more efficiently released. Since the lipophilic character of POPs seems to influence their fate within the adipose tissue, we found relevant to explore the potential link between the mobilisation of fatty acids and that of lipophilic pollutants. In the present chapter, we analyzed the pattern of fatty acids making up the triglycerides, which is the lipid fraction involved in the lipolytic process, within the blubber of weaned NES pups throughout the post-weaning fast. We also determined the concentrations and profiles of free fatty acids, which is the lipid fraction resulting from the lipolytic process, in the serum of these same animals.

Mobilisation of blubber fatty acids of northern elephant seal pups (*Mirounga angustirostris*) during the post-weaning fast

Caroline Louis, Laurent Perdaens, Stéphanie Suciu, Stephen Tavoni, Daniel E. Crocker and Cathy Debier

Abstract

Twenty northern elephant seal (NES) pups were longitudinally sampled at Año Nuevo State Reserve during the post-weaning fast, in order to evaluate the changes of fatty acid (FA) profiles in serum as well as in the inner and outer layers of blubber. The patterns of fatty acids were analyzed in the triglyceride fraction of blubber, which is the lipid fraction involved in the lipolytic pathway, and in the free fatty acid fraction of serum, which reflects the lipolytic products. The major FAs of inner and outer blubber layers were broadly similar to those found in NES maternal milk, suggesting a direct deposit of dietary FAs in the blubber during the suckling period. A stratification of FA classes was noted between inner and outer blubber. The outer blubber layer contained more medium-chain monounsaturated FAs that contribute to keep the fluidity of this tissue at cold temperatures. It was compensated by higher proportions of saturated FAs in inner blubber layer. The FA signature of inner blubber, the layer that is mainly mobilised during energy deprivation differed from the one of serum. This suggests a selective mobilisation of FAs from blubber. We demonstrated that lipophilicity is the main factor governing the mobilisation of FAs from blubber. The least lipophilic FAs were preferentially hydrolysed from blubber, leading to an enrichment of the more lipophilic FAs in this tissue with the progression of the fast.

Keywords

Northern elephant seal – Fast – Blubber – Serum – Mobilisation – Fatty acids

7.1. Introduction

Northern elephant seal (NES) has a typical life history. NES female gives birth to a single pup, which then ingests fat-rich milk (20-55% lipid) for around 26 days (Crocker et al., 2001). During this nursing period, NES pup forms a large amount of subcutaneous blubber layer. It gains about 90 kg, and approximately 55% of this mass gain is composed of fat (Crocker et al., 2001). The fat storage in the subcutaneous layer of adipose tissue mainly serves as a thermal insulation due to its low conductivity and thus reduction of heat loss (Irving et al., 1957; Strandberg et al., 2008). In addition, it contributes to buoyancy and streamlining (Strandberg et al., 2008).

The NES pup is abruptly weaned after 27 days of suckling. Its average weight is 128 ± 3 kg (Louis et al., 2014). It begins a period of fast ashore in which it grows and acquires the capabilities to swim and dive (Crocker et al., 2001). In order to prevent protein catabolism, the triglycerides stored in lipid droplets of blubber are mobilised by the lipolytic pathway to provide fatty acids (FAs), and thus energy to other tissues by β-oxidation of FAs (Ryg et al., 1988). Adipose triglyceride lipase (ATGL), hormone-sensitive lipase (HSL) and monoglyceride lipase (MGL) are the lipases involved in the lipolytic steps (Lass et al., 2011; Viscarra and Ortiz, 2013). ATGL hydrolyses triglycerides (TGs) into diglycerides (DGs) and FAs, HSL mainly hydrolyses DGs into monoglycerides (MGs) and FAs, and MGL hydrolyses MGs into free glycerol and FAs (Brasaemle et al., 2009; Viscarra and Ortiz, 2013). The central nervous system, endocrine and autocrine/paracrine factors are able to affect the rate of TG hydrolysis in adipocytes (Thompson et al., 2010). Contrary to ATGL and HSL, the activity of MGL is neither regulated by hormones nor by the energy state of the fat cells (Lass et al., 2011).

The blubber of phocid seals exhibits a typical composition of FAs, with a stratification of the FA profile between the outer (close to the skin) and inner (close to the muscle) layers (Best et al., 2003; Fowler et al., 2014; Strandberg et al., 2008). The outer blubber layer is composed of a higher proportion of medium-chain monounsaturated FAs (MC-MUFAs) (i.e. ≤ 18 carbon atoms). The inner blubber layer contains a higher proportion of

saturated FAs (SFAs) and long-chain monounsaturated FAs (LC-MUFAs). The trend for polyunsaturated FAs (PUFAs) is less clear, some studies show higher proportions in inner compared to outer blubber, while others report uniform distribution across both layers (Best et al., 2003; Fowler et al., 2014; Strandberg et al., 2008).

In vitro and *in vivo* studies on several species (e.g. human, rat, rabbit, American mink and wild racoon dog) report a selective mobilisation of FAs from adipose tissue during lipolytic periods (Conner et al., 1996; Mustonen et al., 2007; Nieminen et al., 2006a; Raclot and Groscolas, 1993, 1995; Raclot et al., 1997; Raclot, 2003). The relative mobilisation of FAs from adipose tissue increases with the degree of unsaturation for a given chain length and decreases with the chain length for a given number of unsaturation, whatever the FA composition of adipose tissue. These rules seem to be confirmed for adult phocid seals in period of fast such as lactating NES, lactating grey seals and lactating Weddell seals (Arriola-Ortiz, 2010; Fowler et al., 2014; Wheatley et al., 2008), but not for the NES pups during the post-weaning fast (Noren et al., 2013). Nevertheless, with the exception of the study of Fowler et al. (2014), these last studies did not differentiate the inner blubber layer from the outer one for the FA analysis, whereas a vertical stratification of FAs in blubber does exist.

In this paper, we describe the dynamics of FA mobilisation from blubber to blood in NES pups during the post-weaning fast. Blubber core was divided into the inner and outer layers and only FAs from TGs were analysed. On the one hand, this allowed determining the degree to which the blubber is stratified and on the other hand, considering only the lipid fraction (i.e. TG fraction) involved in the lipolytic process. In addition, we evaluated the pattern of free FAs in serum. Coming from the hydrolysed of TGs, the free fatty acid fraction of serum directly reflects the FAs released from blubber. In order to study the FA changes at best, all results were expressed per unit of wet weight, contrary to the studies mentioned above in which results were expressed in percentages of total FAs. We also investigated the relative mobilisation of FAs from both blubber layers between early and late fast. An analysis of mRNA corresponding to enzymes

involved in the lipolytic process (ATGL and HSL) was carried out in parallel in order to follow up the fast.

7.2. Materials and methods

7.2.1. Animal sampling

The sampling took place at Año Nuevo State Reserve, CA, USA (37°06'30''N, 122°20'10''W) from January to April 2012, under the National Marine Fisheries Service Marine Mammal Permit #14636-02. The technique of sampling was described elsewhere (Louis et al., 2014). Twenty free-ranging pups were specifically marked with dye and were followed by observing the colony each day. At weeks 1, 4, 7 and 10 during the post-weaning fast, blood was collected from the extradural vein into Vacutainer serum tubes (Becton-Dickinson, Erembodegem, Belgium). Samples were centrifuged at 3000xg for 15 min at 4°C and serum was aliquoted into microtubes and stored at -70°C until analysis. At weeks 1, 4 and 7 of post-weaning fast, two blubber biopsies extending the full depth of the blubber layer were taken in the lateral pelvis area using 6-mm biopsy punches (Miltex, Help Medical, Paris, France). They were cut in three equal parts. The outer (closest to the skin) and inner (closest to the muscle) layers from the first biopsy were stored separately into dried microtube at -70°C until lipid analysis. The inner and outer blubber layers from the second biopsy were stored separately into microtube with QIAzol Lysis Reagent (Qiagen, Antwerp, Belgium). Blubber tissue was minced, kept at 4°C overnight and then stored at -70°C until RNA analysis.

Body mass of animals was determined at each capture using a metal tripod and 250 kg capacity digital scale (accuracy to 0.1 kg; Measurement Systems International, Seattle, Washington, USA). Standard lengths were measured at weeks 1, 4 and 7.

7.2.2. Lipid assessment

7.2.2.1. Lipid extraction and free fatty acid isolation from serum

After thawing, 800 µL of serum were transferred into Pyrex tubes to which 5 mL of a chloroform/methanol/water (2:2:1, *v:v:v*) mixture (Biosolve, Valkenswaard, The Netherlands) was added. Tridecanoic acid (C13:0) (Sigma-Aldrich, Bornem, Belgium) was used as an internal standard to quantify the free FA fraction of the serum. After shaking, 1 mL of a solution of 0.88% KCl in deionized water was added. Samples were then centrifuged at 1450xg for 10 min. The supernatant was removed and transferred in a new Pyrex tube in order to carry out a second extraction with 2 mL chloroform. Samples were shacked and centrifuged. The supernatant of the second extraction was then removed and placed in a new Pyrex tube. A third extraction was performed, similarly to the second one. The lower phases from the three extractions were pooled in a new Pyrex tube and the solvent was evaporated under a moderate nitrogen flux. Samples were suspended into 200 µL chloroform and loaded on solid-phase extraction (SPE) columns (Bond Elut NH_2, 200 mg, Varian, Middelburg, The Netherlands) previously conditioned with hexane (Biosolve). After the samples were pulled through, neutral lipids (NLs) were eluted with 1.8 mL chloroform/2-propanol (2:1, *v:v*) (Biosolve) and discarded. The column was then loaded with 2.4 mL diethyl ether/acetic acid (98:2, *v:v*) to elute free FAs. This fraction was collected into new Pyrex tubes.

7.2.2.2. Lipid extraction and triglyceride isolation from blubber

After thawing, blubber samples were inserted in a tube with ceramic beads (MagNa Lyser Green Beads, Roche Applied Biosystem, Penzberg, Germany) and 800 µL buffer composed of 60 mM tris(hydroxymethyl)aminomethane (Sigma-Aldrich) and 10 nM ethylenediaminetetraacetic acid (Sigma-Aldrich). Samples were crushed with MagNa Lyser Instrument at 5800xg for 30 sec and then, transferred into Pyrex tubes. A mixture of chloroform/methanol/water (2:2:1, *v:v:v*) (Biosolve) was added. Triheptadecanoin (a TG formed by three C17:0 FAs)

(Larodan, Malmö, Sweden) was used as an internal standard in order to quantify FAs from TGs. Two extractions were performed as described above (see 7.2.2.1). Two hundred µL of lower phases from the two extractions were pooled in a new Pyrex tube and evaporated under a moderate nitrogen flux. Samples were then suspended in 200 µL of chloroform and loaded on SPE columns previously conditioned with hexane. After the samples were pulled through, NLs (corresponding to TGs, DGs, MGs and cholesterol esters) were eluted with chloroform/2-propanol (2:1, *v:v*) (Biosolve) and collected into Pyrex tubes. The solvent was evaporated under a moderate nitrogen flux and samples were suspended in 200 µL of chloroform. A second SPE column was conditioned with hexane and the NL fraction was loaded. After the samples in chloroform were pulled through the column, the cholesterol ester fraction was eluted with 1.2 mL hexane and discarded. The column was then loaded with 3.6 mL hexane/diethyl ether/dichloromethane in order to collect TG fraction in new Pyrex tubes.

7.2.2.3. Fatty acid analysis

The solvents of serum and blubber samples were evaporated under a moderate nitrogen flux. A methylation step was performed firstly by adding 1 mL 0.1 M KOH in methanol at 70°C for 1 hour and secondly, by adding 0.4 mL 1.2 M HCl in methanol at 70°C for 15 min. FA methyl esters (FAMEs) were then extracted by addition 2 mL of hexane followed by 1 mL of deionized water and centrifugation (1000xg for 5 min). FAMEs were separated by gas chromatography as described in Dang Van et al. (2011). Thirty-three FAMEs were analysed in the NES samples (C6:0, C8:0; C10:0; C12:0, C14:0, C14:1n-5; C16:0, C16:1n-7, C18:0, C18:1n-7, C18:1n-9, C18:2n-6, C18:3n-3, C18:3n-6, C18:4n-3, C20:0, C20:1n-9, C20:2n-6, C20:3n-3, C20:3n-6, C20:4n-3, C20:4n-6, C20:5n-3, C22:0, C22:1n-9, C22:4n-6, C22:5n-3, C22:5n-6, C22:6n-3, C24:0, C24:1n-5, C24:5n-3, C24:6n-3). Each peak was identified by comparison of retention times with pure methyl ester standards purchased from Larodan and from Nu-Check Prep (Elysian, MN, USA). Data processing was operated with the ChromQuest 4.2 software (ThermoFinnigan, Milan, Italy). Thereafter, the concentrations of FAs are expressed per unit of wet weight in serum and blubber.

7.2.2.4. Rate of mobilisation of FAs

In order to illustrate the rate of mobilisation of FAs from blubber as a function of their initial concentrations, we calculated the fractional mobilisation (FM) values as following (adapted from Mustonen et al. (2007) and Noren et al. (2013)):

$$\frac{\text{Concentrations of FAs at week 1} - \text{Concentrations of FAs at week 7}}{\text{Concentrations of FAs at week 1}}$$

FAs with a positive FM value tend to be mobilised from the blubber layer over the fast, whereas those with a negative FM tend to be conserved in the blubber layer.

Furthermore, the predicted logarithm of partition constant P (log P), which corresponds to the value of the octanol-water partitioning coefficient, were estimated for each detected FA thanks to Advanced Chemistry Development, Inc. software (ACD/Labs, Toronto, Ontario, Canada) (ACD/PhysChem Suite version 12.01).

7.2.3. Gene analysis

Total RNA was extracted from the outer and inner blubber layers with RNeasy Lipid Tissue Mini kit (Qiagen) following the manufacturer's instructions. RNA integrity was tested based on microcapillary electrophoresis with Agilent Bioanalyzer 2011 (Agilent Technologies, Diegem, Belgium). No RNA degradation was observed (data not shown). cDNAs (0.5 µg) were then synthesised with oligo(dT) (Qiagen) using Ready-To-Go You-Prime First-Strand Beads kit (GE Healthcare, Diegem, Belgium) according to the manufacturer's guidelines. Real-time reverse transcriptase polymerase chain reaction (RT-PCR) assays were performed at a final volume of 20 µL per well with the GoTaq® qPCR Master Mix (Promega, Leiden, The Netherlands) using StepOne Plus thermocycler (Applied Biosystem, Foster City, CA, USA).

Target genes were ATGL and HSL. Succinate dehydrogenase complex, subunit A (SDHA) and ribosomal protein L8 (RPL8) genes were chosen as reference genes. Because of the lack of knowledge about the sequences for the targeted transcripts in NES, consensus region between species were identified with Clustal W2 (EMBL-EBI; http://www.ebi.ac.uk/Tools/msa/clustalw2/). Primer pairs were then designed on these regions with Primer Express v2.0 (Applied Biosystem) (Table 7.1). Amplicons were then sequenced by Macrogen (Seoul, Korea) and compared with known sequences using BLAST (http://blast.ncbi.nlm.nih.gov/Blast.cgi) in order to confirm that the desired targets were amplified (results not shown).

Table 7.1 – Sequences of primer for reference genes (RPL8 and SDHA) and target genes (ATGL and HSL)

Genes	Forward primers	Reverse primers
RPL8	5'-TCGTGTACTGCGGCAAGAAA-3'	5'-TCCAGACAGCACACGATGGT-3'
SDHA	5'-AGGAATCAATGCTGCTCTGGG-3'	5'-AGCCAGTCGGAGCCCTTCA-3'
ATGL	5'-ATGGTGCCCTACACTCTGCC-3'	5'-TCCTTCATCCACCGGATGTC-3'
HSL	5'-GCTGAGTTTGAGCGGATCAT-3'	5'-TGCCATGTTTGCTAGAGACG-3'

7.2.4. Statistical analysis

Data were log transformed to achieve normality. Statistical analyses were conducted using SAS 9.3 software (SAS Institute Inc., Cary, USA). Linear mixed models were used to test the differences in FA levels throughout the post-weaning fast period within a same tissue as well as to compare the FA profiles between tissues for each capture. Animal ID was modelled as a random effect. The level of statistical significance was set at p-values<0.05 for all analyses. Results are presented as means ± SEM.

The stability of reference gene expression was tested using qBase PLUS (Biogazelle, Zwijnaarde, Belgium). The log transformation of the ratios between the expression levels of two reference genes has to be similar between two samples, whatever the experimental conditions (Vandesompele et al., 2002). Gene-stability values (M) and coefficients of variation were

calculated (Hellemans et al., 2007; Vandesompele et al., 2002) and the stability of reference genes were confirmed ($M<1$ and coefficients of variation<0.5; results not shown). The evolution of target gene expressions was evaluated using qBase PLUS in order to transform cycle threshold values into normalised relative quantities (NRQs). This method allows taking into account the use of several reference genes. The stability of NRQs was then evaluated after a log transformation with a linear mixed model. The level of statistical significance was set at p-values<0.05 for all analyses.

7.3. Results

7.3.1. Biometry of NES

At week 1, the mean mass of weaned NES pups was 122 ± 4 kg. NES pups lost weight throughout the fast until reaching 90 ± 4 kg after 10 weeks ($p<0.001$). During the 7 first weeks of fast, standard length of weaned NES pups significantly increased ($p<0.001$) and their body mass index (BMI) significantly decreased ($p<0.001$) (Table 7.2). The sex ratio of targeted NES was 1:1.

Table 7.2 – Biometry of northern elephant seals throughout the post-weaning fast period; mean ± SEM (range).

	n	Mass [kg]	Standard length [cm]	BMI [kg/m²]
Week 1	20	122 ± 4^{a} (88-154)	145 ± 2^{a} (127-156)	61 ± 2^{a} (50-75)
Week 4	20	106 ± 4^{b} (73-133)	148 ± 2^{b} (133-165)	48 ± 1^{b} (37-58)
Week 7	20	94 ± 4^{c} (60-122)	155 ± 2^{c} (143-164)	42 ± 1^{c} (37-48)
Week 10	14	90 ± 4^{d} (78-106)	-	-

Values within a column followed by different letters are significantly different ($p<0.05$).
Sex ratio (female:male) = 1:1

7.3.2. Fatty acid profiles and changes with time

Among the FAs that have been targeted, C24:0 was not detected in any sample (detection frequency = 0%) and C6:0 and C8:0 were detected only in a few samples (detection frequency < 1%). Because of their low detection rates, they were thus not included in the data analyses.

FAs were classified according to the length of carbon chain and the degree of unsaturation: MC-SFAs (C10:0, C12:0, C14:0, C16:0 and C18:0), LC-SFAs (C20:0 and C22:0), MC-MUFAs (C14:1n-5, C16:1n-7, C18:1n-7 and C18:1n-9), LC-MUFAs (C20:1n-9, C22:1n-9 and C24:1n-5), ω-3 PUFAs (C18:3n-3, C18:4n-3, C20:3n-3, C20:4n-3, C20:5n-3, C22:5n-3, C22:6n-3,

C24:5n-3 and C24:6n-3) and ω-6 PUFAs (C18:2 n-6, C18:3 n-6, C20:2 n-6, C20:3 n-6, C20:4 n-6, C22:4 n-6 and C22:5 n-6).

7.3.2.1. In blubber

The main classes of FAs were MC-MUFAs (58%), followed by MC-SFAs (20%), ω-3 PUFAs (10%), LC-MUFAs (8%), ω-6 PUFAs (4%) and LC-SFAs (0.1%) in both blubber layers across the fasting period. C18:1n-9 composed almost one half of the FA content in both blubber layers (43% for outer blubber and 42% for inner blubber). It was followed in decreasing order by C16:0 (14%), C16:1n-7 (10%), C20:1n-9 (7%) and C22:6n-3 (6%) in the outer blubber and by C16:0 (15%), C20:1n-9 (9%), C16:1n-7 (7%) and C22:6n-3 (6%) in the inner blubber.

In both blubber layers, the concentration of total FAs expressed per unit of wet weight remained similar between two consecutive periods ($0.108<p<0.653$) (Table 7.3). Even if the total FA levels did not change with time, several temporal trends were observed within the different FA classes, especially in inner blubber.

In outer blubber, the levels of MC-SFAs remained constant throughout the fast ($p=0.567$). Within this class, the concentrations of all FAs remained constant, except for C10:0, which decreased significantly ($p=0.026$). The LC-SFA content significantly increased between weeks 1 and 7 ($p=0.009$) due to the rise of C20:0 concentrations ($p=0.002$), whereas the second FA of this class, C22:0, remained constant over the fast ($p=0.504$). The concentrations of MC-MUFAs rose between weeks 1 and 7 ($p=0.007$). Within this class, C14:1n-5 and C16:1n-7 remained stable between early and late fast ($0.342<p<0.586$), whereas the concentrations of C18:1n-7 and C18:1n-9 increased significantly ($0.001<p<0.005$). The levels of LC-MUFAs rose between weeks 1 and 7 ($p=0.002$), similarly to the levels of C20:1n-9 ($p=0.002$). In contrary, the levels C22:1n-9 and C24:1n-5 were not significantly different between early and late fast ($0.106<p<0.193$). The class of ω-3 PUFAs remained constant throughout the fast ($p=0.506$). However, this trend was not followed by all FAs of this class: C18:3n-3, C22:5n-3 and C24:5n-3 significantly increased ($p<0.001$) and C20:5n-3 significantly

decreased between early and late fast (p=0.022). The levels of ω-6 PUFA class did not vary over the fast (p=0.062). This profile was followed by all individual ω-6 PUFAs, with the exception of C18:2n-6 and C22:4n-6, which significantly increased ($0.008<p<0.021$) with time (Table 7.3). Overall, FAs in outer blubber remained relatively similar with time.

Variations of FAs were more pronounced in inner blubber. The levels of MC-SFAs decreased between weeks 1 and 7 (p=0.004). This decrease was due to C10:0, C12:0, C14:0 and C16:0 ($0.001<p<0.039$), whereas C18:0 remained constant (p=0.113). The LC-SFA content increased between weeks 1 and 7 ($p<0.001$) because of the rise with time of both constitutive FAs, C20:0 and C22:0 ($0.001<p<0.005$). The concentrations of MC-MUFAs remained constant between early and late fast (p=0.083). Nevertheless, we can distinguish two groups of FAs within this class. C14:1n-5 and C16:1n-7 significantly decreased between early and late fast ($0.001<p<0.004$), while C18:1n-7 and C18:1n-9 remained constant ($0.550<p<0.907$). The class of LC-MUFAs significantly increased during the studied period ($p<0.001$), as all the constituent FAs of this group (C20:1n-9, C22:1n-9 and C24:1n-5) ($p<0.001$). The class of ω-3 PUFAs decreased between weeks 1 and 7 (p=0.006). Within this class, this tendency was followed by C18:3 n-3, C18:4 n-3, C20:4 n-3 and C20:5 n-3, with C20:5n-3 showing the most important decrease with time ($p<0.001$). On the other hand, the levels of C20:3n-3 and C24:6n-3 remained similar between weeks 1 and 7 ($0.433<p<0.960$) and C22:5n-3 and C24:5n-3 significantly increased ($0.001<p<0.004$). The class of ω-6 PUFAs remained constant throughout the studied period (p=0.339), which is mainly due to the stability of the main ω-6 PUFA, C18:2n-6 (p=0.779). The concentrations of C18:3n-6 and C20:4n-6 decreased between weeks 1 and 7 ($0.001<p<0.031$), while C20:2n-6, C22:4n-6 and C22:5n-6 increased ($0.001<p<0.008$) (Table 7.3).

Table 7.3 – Concentrations of fatty acid classes in the outer and inner blubber layers of weaned northern elephant seal pups throughout the post-weaning fast. Values were expressed in µg of fatty acids per g of wet weight ± SEM.

	Outer blubber			**Inner blubber**		
	Week 1	Week 4	Week 7	Week 1	Week 4	Week 7
C10:0	11.4 ± 0.3^{a}	11.2 ± 0.3^{a,b}	10.5 ± 0.7^{b}	11.7 ± 0.2^{a}	11.0 ± 0.4^{b}	9.2 ± 0.2^{c}
C12:0	36.8 ± 0.7^{a}	35.9 ± 0.5^{a}	35.8 ± 0.7^{a}	35.2 ± 0.6^{a}	34.6 ± 1.0^{a,b}	33.6 ± 0.8^{b}
C14:0	931.3 ± 21.2^{a}	945.5 ± 21.4^{a}	940.8 ± 25.5^{a}	981.2 ± 24.8^{a}	951.3 ± 24.5^{b}	945.3 ± 28.6^{b}
C16:0	3941.0 ± 96.1^{a}	4024.5 ± 87.1^{a}	3998.8 ± 69.2^{a}	4672.8 ± 107.9^{a}	4371.8 ± 120.2^{b}	4138.7 ± 145.5^{b}
C18:0	690.0 ± 24.9^{a}	697.4 ± 20.7^{a}	709.7 ± 15.2^{a}	1034.0 ± 31.3^{a,b}	1009.3 ± 25.3^{a}	1077.5 ± 21.6^{b}
MC-SFAs	**5597 ± 135^{a}**	**5771 ± 120^{a}**	**5805 ± 103^{a}**	**6915 ± 150^{a}**	**6631 ± 150^{b}**	**6374 ± 182^{b}**
C20:0	29.6 ± 0.9^{a}	30.6 ± 1.0^{a}	32.7 ± 0.8^{b}	34.9 ± 1.0^{a}	36.8 ± 1.4^{a}	43.4 ± 1.4^{b}
C22:0	7.8 ± 0.4^{a}	7.9 ± 0.5^{a}	8.1 ± 0.5^{a}	8.6 ± 0.6^{a}	9.9 ± 0.7^{a,b}	11.0 ± 0.6^{b}
LC-SFAs	**37 ± 1^{a}**	**39 ± 1^{a,b}**	**42 ± 1^{b}**	**44 ± 1^{a}**	**47 ± 2^{a}**	**56 ± 2^{b}**
C14:1n-5	79.8 ± 2.4^{a}	83.1 ± 2.3^{a}	82.4 ± 2.3^{a}	47.7 ± 1.9^{a}	47.1 ± 2.2^{a}	42.2 ± 1.9^{b}
C16:1n-7	2971.5 ± 223.2^{a}	3043.1 ± 236.4^{a}	2950.4 ± 227.2^{a}	2158.9 ± 57.5^{a}	2019.6 ± 89.9^{b}	1708.4 ± 87.3^{c}
C18:1n-7	1180.7 ± 25.3^{a}	1284.2 ± 23.8^{b}	1311.2 ± 21.1^{b}	1255.7 ± 23.4^{a}	1279.6 ± 33.6^{a}	1258.6 ± 38.7^{a}
C18:1n-9	12004.0 ± 260.7^{a}	12628.2 ± 350.3^{a,b}	12775.2 ± 256.8^{b}	12441.2 ± 265.9^{a}	12379.4 ± 354.9^{a}	12210.7 ± 270.2^{a}
MC-MUFAs	**16216 ± 328^{a}**	**17079 ± 458^{b}**	**17156 ± 340^{b}**	**15891 ± 266^{a}**	**15675 ± 427^{a}**	**15174 ± 349^{a}**
C20:1n-9	1999.4 ± 68.5^{a}	2034.9 ± 60.7^{a}	2165.1 ± 57.3^{b}	2311.0 ± 63.4^{a}	2401.8 ± 78.0^{b}	2720.7 ± 85.5^{c}
C22:1n-9	154.0 ± 6.7^{a,b}	145.3 ± 6.1^{a}	162.0 ± 6.8^{b}	185.7 ± 6.0^{a}	188.9 ± 8.4^{a}	225.1 ± 10.5^{b}
C24:1n-5	40.8 ± 1.1^{a,b}	39.9 ± 1.0^{a}	41.8 ± 1.2^{b}	46.2 ± 0.9^{a}	46.8 ± 1.8^{a}	54.0 ± 1.6^{b}
LC-MUFAs	**2205 ± 75^{a}**	**2229 ± 67^{a}**	**2388 ± 64^{b}**	**2555 ± 68^{a}**	**2648 ± 86^{b}**	**3036 ± 94^{c}**

For a defined tissue, values within a row followed by different letters are significantly different ($p \leq 0.05$). MC-SFAs = medium-chain (≤18C) saturated fatty acids (FAs); LC-SFAs = long-chain (>18C) saturated FAs; MC-MUFAs = medium-chain (≤18C) monounsaturated FAs; LC-MUFAs = long-chain (>18C) monounsaturated FAs; PUFAs = polyunsaturated FAs

(continued)

	Outer blubber			**Inner blubber**		
	Week 1	Week 4	Week 7	Week 1	Week 4	Week 7
C18:3n-3	173.8 ± 5.5^{a}	183.1 ± 4.5^{a,b}	195.7 ± 4.9^{b}	178.8 ± 4.3^{a}	178.0 ± 6.6^{b}	171.3 ± 6.6^{c}
C18:4n-3	66.3 ± 3.7^{a}	66.9 ± 3.0^{a}	64.2 ± 3.2^{a}	72.3 ± 3.5^{a}	66.0 ± 3.9^{b}	57.5 ± 3.7^{c}
C20:3n-3	52.2 ± 2.3^{a}	50.9 ± 1.6^{a}	53.6 ± 1.5^{a}	57.9 ± 1.6^{a}	56.6 ± 1.9^{a}	58.0 ± 2.1^{a}
C20:4n-3	126.5 ± 5.01^{a}	130.1 ± 4.5^{a}	127.3 ± 4.6^{a}	140.5 ± 5.2^{a}	132.3 ± 5.3^{b}	121.9 ± 6.2^{c}
C20:5n-3	492.6 ± 29.2^{a}	504.7 ± 26.4^{a}	465.2 ± 26.1^{b}	471.5 ± 26.2^{a}	387.4 ± 30.5^{b}	289.0 ± 28.8^{c}
C22:5n-3	437.3 ± 19.4^{a}	472.1 ± 21.6^{a,b}	483.4 ± 20.0^{b}	450.8 ± 24.9^{a}	484.3 ± 25.0^{a}	506.7 ± 25.0^{b}
C22:6n-3	1702.5 ± 51.6^{a}	1736.5 ± 41.6^{a}	1754.4 ± 42.4^{a}	1814.0 ± 58.1^{a}	1784.3 ± 57.0^{a}	1784.7 ± 60.4^{a}
C24:5n-3	8.3 ± 0.5^{a}	8.6 ± 0.4^{a}	9.1 ± 0.3^{a}	9.3 ± 0.4^{a}	9.8 ± 0.3^{a}	10.7 ± 0.4^{b}
C24:6n-3	19.5 ± 0.6^{a}	20.6 ± 0.5^{a}	20.4 ± 0.5^{a}	17.9 ± 0.7^{a}	19.3 ± 0.6^{a}	18.7 ± 0.5^{a}
ω-3 PUFAs	**3056 ± 108^{a}**	**3160 ± 93^{a}**	**3163 ± 92^{a}**	**3285 ± 114^{a}**	**3095 ± 117^{b}**	**2999 ± 123^{b}**
C18:2n-6	576.3 ± 12.5^{a}	598.1 ± 8.7^{a,b}	606.8 ± 9.7^{b}	612.8 ± 9.6^{a}	605.1 ± 10.2^{a}	610.5 ± 13.8^{a}
C18:3n-6	6.1 ± 1.1^{a}	7.6 ± 0.9^{a}	8.7 ± 0.7^{a}	8.3 ± 0.8^{a}	6.8 ± 1.1^{a}	6.3 ± 1.0^{b}
C20:2n-6	132.4 ± 4.4^{a}	135.2 ± 2.9^{a}	135.0 ± 3.0^{a}	151.8 ± 3.1^{a}	152.3 ± 3.5^{a}	162.2 ± 3.6^{b}
C20:3n-6	24.9 ± 0.7^{a}	25.8 ± 0.6^{a}	26.0 ± 0.6^{a}	27.8 ± 0.7^{a}	27.2 ± 0.6^{a}	28.5 ± 0.7^{a}
C20:4n-6	208.7 ± 4.4^{a}	214.7 ± 4.1^{a}	214.0 ± 3.5^{a}	211.4 ± 4.7^{a}	190.9 ± 6.3^{b}	171.1 ± 7.0^{c}
C22:4n-6	35.4 ± 1.0^{a}	36.9 ± 1.3^{a}	38.9 ± 1.2^{b}	36.7 ± 1.7^{a}	38.2 ± 1.7^{a}	40.9 ± 1.3^{b}
C22:5n-6	66.1 ± 1.5^{a}	65.6 ± 1.4^{a}	67.3 ± 1.5^{a}	72.4 ± 1.9^{a}	73.8 ± 2.4^{a}	82.2 ± 1.8^{b}
ω-6 PUFAs	**1049 ± 23^{a}**	**1085 ± 17^{a}**	**1098 ± 16^{a}**	**1119 ± 18^{a}**	**1092 ± 19^{a}**	**1100 ± 22^{a}**
∑ FAs	**28207 ± 462^{a}**	**29269 ± 612^{a,b}**	**29495 ± 422^{b}**	**29558 ± 458^{a}**	**29000 ± 652^{a}**	**28599 ± 599^{a}**

For a defined tissue, values within a row followed by different letters are significantly different ($p \leq 0.05$). MC-SFAs = medium-chain (≤18C) saturated fatty acids (FAs); LC-SFAs = long-chain (>18C) saturated FAs; MC-MUFAs = medium-chain (≤18C) monounsaturated FAs; LC-MUFAs = long-chain (>18C) monounsaturated FAs; PUFAs = polyunsaturated FAs

7.3.2.2. In serum

We found mainly MC-MUFAs in serum (42%), followed by MC-SFAs (33%), PUFAs (10% for ω-3 PUFAs and 11% for ω-6 PUFAs), LC-MUFAs (4%) and LC-SFAs (0.01%). Similarly to the blubber, C18:1n-9 was the major FA in the serum (33%). It was followed in the decreasing order by C16:0 (19%) > C18:0 (11%) > C20:4n-6 (7%) > C22:6n-3 (6%) ≈ C16:1n-7 (6%) > C20:1n-9 (4%).

The concentrations of total FAs expressed per unit of wet weight significantly rose until week 7 ($p<0.001$) and then remained constant until week 10 ($p=0.437$ between weeks 7 and 10) (Table 7.4).

Within the different FA classes, the concentrations of all FA classes (MC-SFAs, LC-SFAs, MC-MUFAs, LC-MUFAs, ω-3 PUFAs and ω-6 PUFAs) as well as all constituent FAs increased significantly between weeks 1 and either week 7 or week 10 ($p<0.001$) (Table 7.4). On average, the levels of individual FAs rose from 2 to 3 folds in serum over the fast.

Table 7.4 – Concentrations of fatty acid classes in serum of weaned northern elephant seal pups throughout the post-weaning fast. Values were expressed in µg of fatty acids per mL of wet weight ± SEM.

	Serum			
	Week 1	Week 4	Week 7	Week 10
C10:0	0.62 ± 0.04^{a}	0.82 ± 0.03^{b}	1.03 ± 0.06^{c}	1.23 ± 0.04^{d}
C12:0	0.7 ± 0.7^{a}	1.1 ± 1.1^{b}	1.3 ± 1.2^{b}	1.9 ± 1.9^{c}
C14:0	5.2 ± 0.5^{a}	8.7 ± 0.5^{b}	16.5 ± 1.1^{c}	16.0 ± 1.8^{c}
C16:0	50.9 ± 3.0^{a}	85.5 ± 4.2^{b}	143.3 ± 7.2^{c}	138.7 ± 11.5^{c}
C18:0	25.6 ± 1.8^{a}	49.5 ± 4.4^{b}	80.6 ± 6.7^{c}	90.0 ± 7.6^{c}
MC-SFAs	**89 ± 4^{a}**	**148 ± 8^{b}**	**266 ± 14^{c}**	**244 ± 21^{c}**
C20:0	0.1 ± 0.03^{a}	0.2 ± 0.04^{a}	0.3 ± 0.05^{b}	0.4 ± 0.06^{c}
C22:0	N.D	0.2 ± 0.03	0.4 ± 0.04	0.5 ± 0.06
LC-SFAs	**0.1 ± 0.03^{a}**	**0.4 ± 0.05^{b}**	**0.8 ± 0.07^{c}**	**1.0 ± 0.09^{d}**
C14:1n-5	0.12 ± 0.02^{a}	0.31 ± 0.03^{b}	0.78 ± 0.07^{c}	0.63 ± 0.11^{c}
C16:1n-7	12.8 ± 1.1^{a}	25.2 ± 2.0^{b}	53.5 ± 3.8^{c}	41.8 ± 5.7^{d}
C18:1n-7	9.5 ± 1.0^{a}	19.6 ± 1.3^{b}	36.5 ± 2.2^{c}	28.7 ± 2.8^{d}
C18:1n-9	73.2 ± 6.8^{a}	144.0 ± 9.3^{b}	294.1 ± 17.7^{c}	243.3 ± 23.99^{c}
MC-MUFAs	**98 ± 9^{a}**	**190 ± 12^{b}**	**386 ± 23^{c}**	**307 ± 32^{c}**
C20:1n-9	8.4 ± 0.7^{a}	14.5 ± 0.9^{b}	28.9 ± 1.8^{c}	28.5 ± 3.0^{c}
C22:1n-9	1.4 ± 0.2^{a}	1.7 ± 0.1^{b}	2.8 ± 0.2^{c}	2.9 ± 0.2^{c}
C24:1n-5	0.99 ± 0.04^{a}	1.08 ± 0.04^{a}	1.46 ± 0.08^{b}	1.59 ± 0.07^{b}
LC-MUFAs	**11 ± 1^{a}**	**17 ± 1^{b}**	**33 ± 2^{c}**	**33 ± 3^{c}**
C18:3n-3	1.1 ± 0.1^{a}	2.5 ± 0.2^{b}	5.1 ± 0.3^{c}	3.9 ± 0.4^{d}
C18:4n-3	0.34 ± 0.04^{a}	0.71 ± 0.07^{b}	1.44 ± 0.13^{c}	1.14 ± 0.16^{b,c}
C20:3n-3	0.27 ± 0.05^{a}	0.44 ± 0.03^{b}	0.91 ± 0.06^{c}	0.70 ± 0.09^{c}
C20:4n-3	0.7 ± 0.1^{a}	1.4 ± 0.1^{b}	2.5 ± 0.2^{c}	2.1 ± 0.2^{c}
C20:5n-3	4.2 ± 0.4^{a}	8.1 ± 0.7^{b}	14.9 ± 1.0^{c}	12.6 ± 1.7^{b,c}
C22:5n-3	1.5 ± 0.1^{a}	3.7 ± 0.2^{b}	7.4 ± 0.4^{c}	7.0 ± 0.6^{c}
C22:6n-3	13.4 ± 1.2^{a}	29.4 ± 2.7^{b}	50.8 ± 3.6^{c}	53.9 ± 5.7^{c}
C24:5n-3	N.D	N.D	N.D	N.D
C24:6n-3	0.5 ± 0.4	N.D	N.D	0.7 ± 0.3
ω-3 PUFAs	**23 ± 2^{a}**	**45 ± 4^{b}**	**82 ± 5^{c}**	**78 ± 8^{c}**
C18:2n-6	4.8 ± 0.3^{a}	10.3 ± 0.6^{b}	19.9 ± 1.0^{c}	21.0 ± 1.9^{c}
C18:3n-6	N.D	N.D	N.D	N.D
C20:2n-6	0.6 ± 0.1^{a}	1.2 ± 0.1^{b}	2.3 ± 0.2^{c}	2.4 ± 0.3^{c}
C20:3n-6	0.4 ± 0.1^{a}	0.8 ± 0.1^{b}	1.4 ± 0.1^{c}	1.8 ± 0.2^{d}
C20:4n-6	11.7 ± 1.5^{a}	30.8 ± 3.4^{b}	58.4 ± 5.7^{c}	77.9 ± 7.5^{c}
C22:4n-6	0.30 ± 0.02^{a}	0.54 ± 0.04^{b}	0.98 ± 0.07^{c}	1.05 ± 0.08^{c}
C22:5n-6	0.4 ± 0.1^{a}	0.5 ± 0.1^{a}	1.2 ± 0.1^{b}	1.4 ± 0.2^{b}
ω-6 PUFAs	**19 ± 1^{a}**	**42 ± 1^{b}**	**83 ± 1^{c}**	**101 ± 10^{d}**
∑ FAs	**230 ± 14^{a}**	**444 ± 25^{b}**	**830 ± 47^{c}**	**785 ± 72^{c}**

For a defined tissue, values within a row followed by different letters are significantly different ($p \leq 0.05$). N.D = not detected; MC-SFAs = medium-chain (≤18C) saturated fatty acids (FAs); LC-SFAs = long-chain (>18C) saturated FAs; MC-MUFAs = medium-chain (≤18C) monounsaturated FAs; LC-MUFAs = long-chain (>18C) monounsaturated FAs; PUFAs = polyunsaturated FAs

7.3.3. Comparison of fatty acid classes between adjacent tissues

The fatty acid profile significantly differed between two adjacent tissues (Figure 7.1). At each studied time within the post-weaning fast (weeks 1, 4 or 7), MC-SFA and LC-SFA percentages were significantly lower in the outer blubber layer compared to the inner blubber ($p<0.001$), whereas the reverse was true for MC-MUFA proportions ($p<0.001$). LC-MUFA proportions were similar between both blubber layers at each studied time ($p<0.001$). The proportions of ω-3 PUFAs were comparable between both blubber layers at week 1 ($p=0.186$). They were lower in the outer blubber layer than in the inner blubber layer at week 4 ($p=0.008$) and were higher in the outer blubber layer than in the inner blubber layer at week 7 ($p<0.001$). Finally, the percentages of ω-6 PUFAs remained stable between both blubber layers at weeks 1 and 4 ($p=0.203$ and $p=0.088$, respectively), and then were lower in the outer blubber layer relatively to the inner one at week 7 ($p=0.007$).

The differences of profiles were more pronounced between inner blubber and serum. For a considered period within the post-weaning fast (weeks 1, 4 or 7), MC-SFA proportions in the inner blubber layer were lower than in serum ($p<0.001$), while LC-SFA and MC-MUFA proportions were higher in the inner blubber layer compared to serum ($p<0.001$). The percentages of LC-MUFAs were greater in the inner blubber layer than in serum ($p<0.001$). The percentages of ω-3 PUFAs were higher in the inner blubber layer than serum at week 1 ($p=0.009$). They became similar at week 4 ($p=0.215$), and then higher in the inner blubber layer at week 7 ($p=0.027$). Eventually, the proportion of ω-6 PUFAs was lower in the inner blubber layer relatively to serum for all studied periods ($p<0.001$) (Figure 7.1).

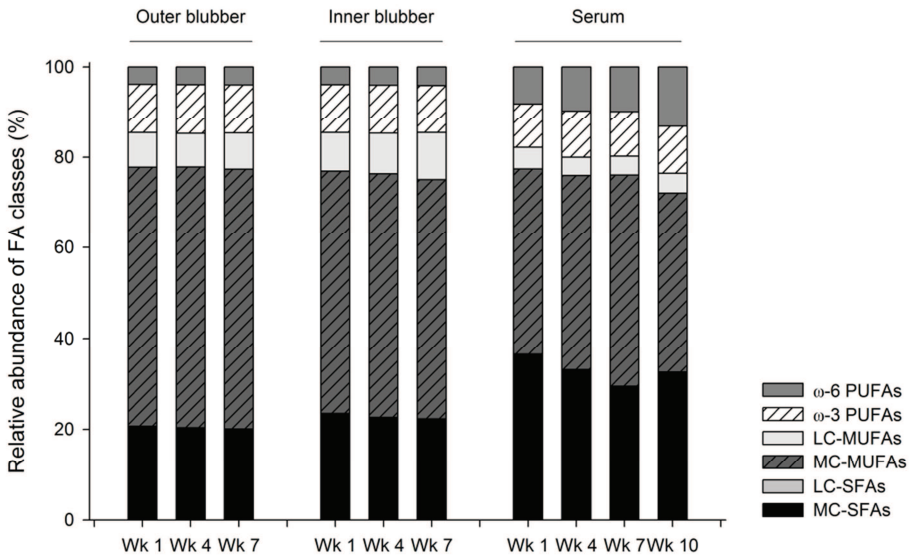

Figure 7.1 – Proportions of different fatty acid (FA) classes in the outer and inner blubber layers as well as in serum of northern elephant seals throughout the post-weaning fast period. MC-SFAs = medium-chain (≤18C) saturated FAs; LC-SFAs = long-chain (>18C) saturated FAs; MC-MUFAs = medium-chain (≤18C) monounsaturated FAs; LC-MUFAs = long-chain (>18C) monounsaturated FAs; PUFAs = polyunsaturated FAs

7.3.4. Fractional mobilisation

The results of fractional mobilisation (FM) for all targeted FAs are illustrated in Figure 7.2. The range of FM values was lower in the outer blubber ($\Delta \approx 0.22$) than in the inner blubber ($\Delta \approx 0.83$), reflecting a different amplitude of FA mobilisation between the two layers. Among the studied FAs, only 6 FAs (1 MC-MUFA, 2 SFAs and 3 ω-3 PUFAs) had positive FM values in the outer blubber layer and 16 FAs (3 ω-3 PUFAs, 4 MC-MUFAs, 4 SFAs and 5 ω-6 PUFAs), in the inner blubber layer (Figure 7.2 A-B). All studied MC-MUFAs were efficiently mobilised from the inner blubber. The FA with the greatest positive FM value was C20:5n-3 in both blubber layers. This FM value was however significantly higher in inner blubber than in outer blubber (Figure 7.2 A-B). All targeted ω-6 PUFAs were conserved in the outer blubber layer as well as all LC-MUFAs, in both blubber layers. C24:5n-3 and C22:0 had the lowest FM values in the inner and outer blubber layers, respectively.

The different molecular structures of FAs give them different degrees of lipophilicity that can be estimated by log P (Table 7.5). The predicted log P values increased with the number of carbon atoms, for a similar degree of unsaturation, and decreased with the degree of unsaturation, for a similar number of carbon atoms. The comparison of FA lipophilicity with the FM from inner blubber highlighted that the less lipophilic FAs (with a predicted log P ranging from 4.0 to 7.2) tended to be selectively mobilised from the inner blubber layer ($FM>0$), whereas the more lipophilic FAs (with a predicted log P ranging from 7.6 to 10.9) tended to be conserved ($FM<0$). An intermediate state of lipophilicity could be considered for the FAs with a predicted log P ≈ 7 and FM values close to 0 (e.g. C18:1n-7, C18:1n-9, C18:2n-6, C20:3n-3 and C20:3n-6). The rule of lipophilicity could also be applied to outer blubber layer, even if the FA mobilisation in this layer was more discreet.

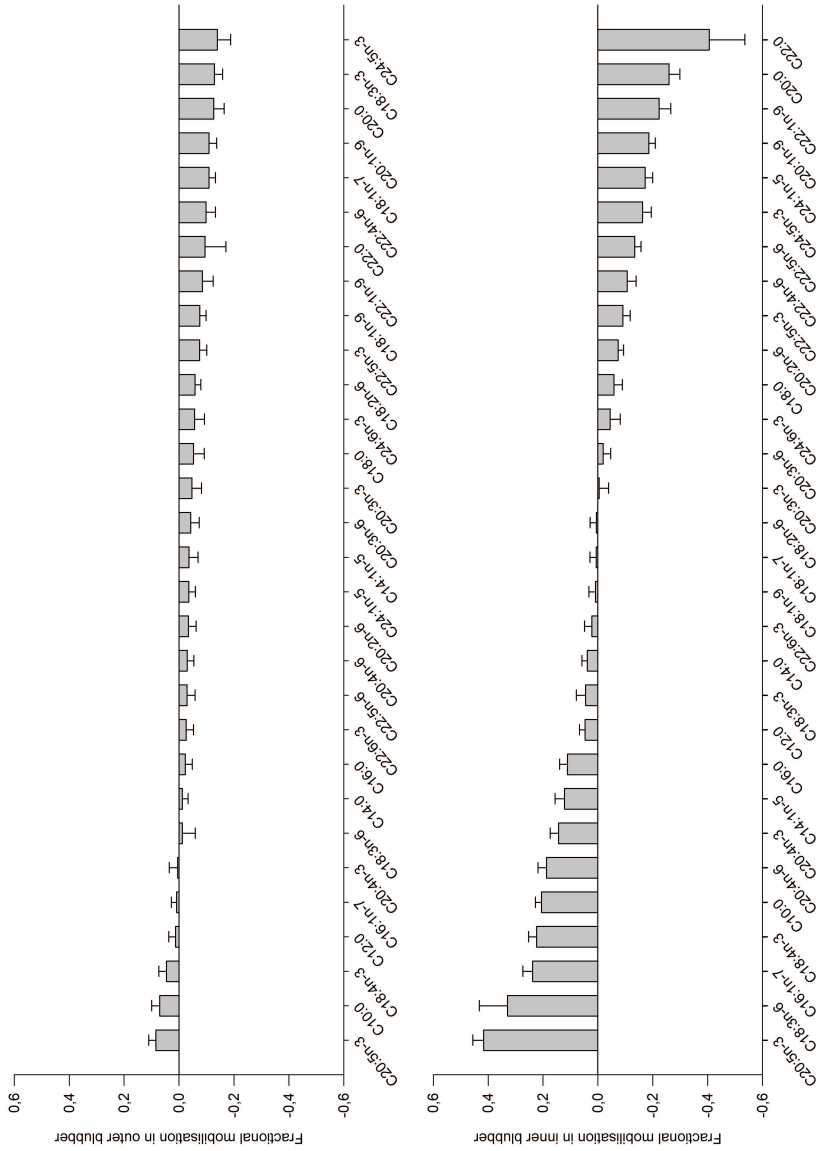

Figure 7.2 – Fractional mobilisation of fatty acids of northern elephant seal pups during the post-weaning fast in the outer and inner blubber layers.

Table 7.5 – Predicted log P values for each studied FAs, which are sorted by ascending order. Symbols "+" and "–" refer to positive and negative values of fractional mobilisation (FM) shown on Figure 7.2.

Fatty acids	Predicted log P	FM Outer blubber	FM Inner blubber
C10:0	4.0 ± 0.2	+	+
C12:0	5.0 ± 0.2	+	+
C14:1n-5	5.6 ± 0.2	-	+
C18:4n-3	5.9 ± 0.4	+	+
C14:0	6.1 ± 0.2	-	+
C20:5n-3	6.2 ± 0.5	+	+
C18:3n-3	6.5 ± 0.3	-	+
C16:1n-7	6.6 ± 0.2	+	+
C18:3n-6	6.6 ± 0.3	-	+
C22:6n-3	6.8 ± 0.5	-	+
C20:4n-3	6.9 ± 0.3	+	+
C20:4n-6	6.9 ± 0.4	-	+
C16:0	7.2 ± 0.2	-	+
C18:2n-6	7.2 ± 0.3	-	+
C20:3n-3	7.6 ± 0.3	-	-
C20:3n-6	7.6 ± 0.3	-	-
C22:5n-3	7.6 ± 0.5	-	-
C18:1n-7	7.7 ± 0.2	-	+
C18:1n-9	7.7 ± 0.2	-	+
C24:6n-3	7.7 ± 0.5	-	-
C22:5n-6	7.8 ± 0.4	-	-
C22:4n-6	8.0 ± 0.4	-	-
C18:0	8.2 ± 0.2	-	-
C20:2n-6	8.2 ± 0.3	-	-
C20:1n-9	8.8 ± 0.2	-	-
C24:5n-3	9.2 ± 0.5	-	-
C20:0	9.3 ± 0.2	-	-
C22:1n-9	9.8 ± 0.2	-	-
C22:0	10.3 ± 0.2	-	-
C24:1n-5	10.9 ± 0.2	-	-

7.3.5. Gene expression

The levels of expression of ATGL and HSL were evaluated throughout the post-weaning fast. No gene profile underwent significant change within a blubber layer between two consecutive periods of fast ($0.347<p<0.997$). In addition, there was no significant difference of expression levels between both blubber layers at each studied time ($0.064<p<0.409$) (Table 7.6).

Table 7.6 – The mean levels of expression of ATGL and HSL in the outer and inner blubber layers of northern elephant seal pups throughout the post-weaning fast (weeks 1, 4 and 7). Data are expressed in normalised relative quantities ± SEM.

	Outer blubber			Inner blubber		
	Week 1	Week 4	Week 7	Week 1	Week 4	Week 7
ATGL	1.08 ± 0.21	1.49 ± 0.43	1.26 ± 0.24	2.24 ± 0.84	1.56 ± 0.27	1.59 ± 0.29
HSL	0.94 ± 0.13	0.99 ± 0.12	1.06 ± 0.12	1.69 ± 0.33	1.33 ± 0.19	1.15 ± 0.11

7.4. Discussion

7.4.1. The patterns of fatty acids in blubber and serum

During the post-weaning fast, NES pups mobilised their lipid storage in order to meet their physiological needs. Consequently, they lost more than 30 kg for 6 weeks. In the present study, the concentrations of total FAs in TGs expressed per unit of wet weight remained stable in the blubber of NES pups with the progression of the fast. Such trends were already observed for the total lipid percentages in the blubber of weaned NES pups (Louis et al., 2014) and lactating NES females (Crocker et al., 2001). Stable levels of TG content in the blubber throughout the fast may be surprising because there is an important TG mobilisation. Indeed, the lipid mass of weaned NES pups is reduced from 24-49% (Noren et al., 2003). In our study, the mobilisation of TGs was accompanied by a net increase of free FA concentration in the NES serum between early and late fast. A morphometric study of the weaned NES pup blubber was conducted earlier (Louis et al., 2014) and showed that the proportions of small adipocytes increased in both blubber

layers, whereas the proportions of large adipocytes decreased over the fast, reflecting a reduction of lipid content in the adipocytes. The biopsy punch always samples the same amount of adipose tissue. However, it will consist of a higher number of smaller adipocytes at late fast as compared to early fast. The proportions of connective tissue being very low in the phocid blubber ($<$ 5%), it could explain the stable level of the FA concentrations expressed per unit of wet weight.

The patterns of FA classes and major individual FAs in NES pup blubber broadly followed those observed in marine mammals (MC-MUFAs $>$ SFAs $>$ PUFAs $\approx$ LC-MUFAs and C18:1n-9 $>$ C16:0 $>$ C20:1n-9 $\approx$ C16:1n-7) (Best et al., 2003; Fowler et al., 2014; Lambert et al., 2013; Noren et al., 2013). However, those studies determined the FA profiles in the blubber without distinction of FA origin, whereas it is more relevant to know the exact composition of FAs from TGs, which is the class of lipid involved in the lipolytic process. The contribution of FAs from phospholipids can indeed become more significant with the progression of the fast. Although more than 90% of blubber is composed of TGs (Best et al., 2003; Wheatley et al., 2008), the separation of different lipid fraction should help to better understanding and compare FA changes during the lipolytic period (Price and Valencak, 2012). Despite the fact that the overall fatty acid content of blubber did not change, there were variations of temporal trends within the different classes, especially in the inner blubber, as illustrated by the wide range of fractional mobilisation.

The FAs stored in the blubber may originate either by direct deposition from the circulation, or by *de novo* biosynthesis within the layers (Best et al., 2003). Iverson et al. (1995) put forth that ingested FAs are directly incorporated without modification in the blubber of marine mammals during periods of extensive fattening. In the case of NES pups, the unique dietary source of FAs was the milk transferred from the mother during the suckling period. The FA profile of NES milk is mostly formed by C18:1n-9, C16:0, C20:1n-11, C16:1n-7 and C20:1n-9 (Fowler et al., 2014), which is very similar to the FA composition of pup blubber. The FA composition of milk thus clearly determines the FA pattern of blubber in NES pups.

Data regarding FA profiles in blood of phocid seals are scare. To our knowledge, only one study reports the FA profiles in the plasma of Weddell seal pups during the post-weaning fast (Rea et al., 1997). Plasma FA pattern from the phospholipid fraction of weaned Weddell seal pups is mainly composed of C18:0 > C20:4n-6 > C16:0 > C18:1n-9 and the TG fraction mainly contains C16:0 > C20:5n-3 > C22:6n-3. In the present study, the free FA fraction in the serum of weaned NES pups was composed of C18:1n-9 > C16:0 > C18:0 > C20:4n-3 > C22:6n-3 ≈ C16:1n-7. The different FA pattern between both species may be explained by the origin of FAs. The serum free FA fraction comes mainly from the hydrolysis of TGs in adipose tissue, whereas circulating phospholipids and TGs are found in lipoproteins and do not directly represent the release of FAs from adipocytes. In order to draw strong conclusions regarding the FA pattern in the serum of weaned animals, a comparison of FAs from similar lipid fractions should be carried out.

7.4.2. Selective mobilisation of FA from blubber

Because circulating free FAs originating from hepatic synthesis are reduced during conditions of food deprivation (Aarsland and Wolfe, 1998), most of the circulating free FAs measured in fasting NES pups result from the lipolytic process in the adipose tissue. Since the inner blubber layer exhibited the highest amplitude of FM, we can expect that this layer is the most metabolically active (compared to the outer one), as already suggested elsewhere (e.g. Louis et al. (2014)) and thus, participates largely to the increase of FAs in serum. The major FAs encountered in serum (C18:1n-9 > C16:0 > C16:1n-7 ≈ C22:6n-3) were indeed similar to those of inner blubber. However, there were greater proportions of MC-SFAs and ω-6 PUFAs, and lower proportions of LC-SFAs, MC-MUFAs and LC-MUFAs in serum as compared to inner blubber. Those differences of FA profile between inner blubber and serum suggest that the hydrolysis of TGs from adipose tissue is not a homogeneous process and that some fatty acids may be more efficiently mobilised than others. Studies on fasting terrestrial carnivorous mammals evidenced differences of FA composition between plasma and adipose tissue (Nieminen et al., 2006b; Nieminen et al., 2006a). However, in those studies, the fatty acid profiles were assessed in the total lipid fraction of each tissue.

In weaned NES pups, the total lipid fraction of blood is dominated by phospholipids (52%), followed by cholesterol (31%) and TGs (10%) (Louis et al., 2014), for which the liver is the main source. The free FA fraction, which comes from the lipolytic process in blubber, represents only 5% of the total lipids of blood (Louis et al., 2014). Such data underline the importance to specifically study the free FA fraction of blood to follow the FAs mobilised from the adipose tissue.

The selective mobilisation of FAs from blubber, reflected by a wide range of FM values, may explain the differences of FA composition between inner blubber and serum. Previous *in vitro* and *in vivo* studies on terrestrial mammals have pointed out a relative mobilisation of FAs from adipose tissue according to their molecular structure (i.e. chain length and degree of unsaturation), as explained in the introduction (see 7.1.). The molecular structures of FAs give them different physico-chemical characteristics, such as different degrees of lipophilicity. It thus appears from our data that the mobilisation of FAs from adipose tissue is selective and this selection depends on the lipophilicity of FAs (estimated by log P values). TGs containing more hydrophilic FAs may thus be situated closer to the lipid-water interface, where the lipases act, and therefore be hydrolyzed first. This phenomenon leads to a modification of FA pattern in blubber layers throughout the fast through an accumulation of more lipophilic FAs. These results match the lipolytic process. Indeed, we know that the lipolytic enzymes (ATGL, HSL and MGL) are water-soluble and that their action occurs at the water-lipid interface formed by the cytosol on one hand and by the lipids on the other (Derewenda and Sharp, 1993). It is reasonable to think that the TGs containing the less lipophilic FAs are situated closer to the interface than those containing the more lipophilic FAs. Raclot (2003) put forward a similar hypothesis suggesting that the selective FA mobilisation from fat cells occurs according to their polarity, with a preferential hydrolysis TGs containing more polar FAs.

Not surprisingly, besides the impact of the physico-chemical properties of FAs on their mobilisation dynamics, the roles they play in various physiological needs seem to affect their fate in blubber. A high mobilisation

of C20:5n-3 from inner and outer blubber was observed in NES pups, as already widely described in the literature for northern elephant seals, southern elephant seals, emperor and king penguins, ringed seals and Weddell seals (Bryden and Stokes, 1969; Fowler et al., 2014; Groscolas, 1990; Noren et al., 2013; Strandberg et al., 2008; Wheatley et al., 2008). This similarity between species could be explained by the association of C20:5n-3 in many physiological processes, including neurobiological function (Innis, 2005; Kim et al., 2004). In the same way, C20:4n-6 was highly mobilised from the inner blubber layer. This FA may be the precursor of bioactive molecules, such as eicosanoids (Smith and Murphy, 2002). Furthermore, ω-3 PUFAs and ω-6 PUFAs are required for structural growth and brain (Innis, 2005). They are strong ligands of peroxisome proliferator-activated receptor (PPAR), which monitor genes involved in the lipid metabolism (Desvergne and Wahli, 1999). Eventually, the metabolism of PUFAs utilizes less oxygen than MUFAs and SFAs (Trumble and Kanatous, 2012), that may play an important role for the young animal learning to dive.

As detailed in Chapter 3, the blubber of weaned NES is contaminated by numerous lipophilic pollutants such as polybromodiphenyl ethers (PBDEs) and polychlorinated biphenyls (PCBs) (Debier et al., 2006; Louis et al., 2014). A selective mobilisation of those pollutants from the blubber of marine mammals (NES and grey seals) over the fast has been highlighted. The higher halogenated congeners (i.e. the most lipophilic congeners) were preferentially retained within the blubber, whereas the lower halogenated congeners (i.e. the less lipophilic congeners) were readily released (Debier et al., 2006; Louis et al., 2014; Vanden Berghe et al., 2012). It thus appears that less lipophilic TGs and less lipophilic pollutants are more efficiently mobilised from the blubber. It might result from the fact that they are situated closer to the interface rather than in the droplet core and, as a consequence, would be preferentially mobilised. A higher mobilisation of those more lipophilic compounds may however happen later in the fast (Debier et al., 2003; Debier et al., 2006; Raclot, 2003).

7.4.3. Stratification of FA blubber

The fatty acid profiles varied within the blubber layers. This stratification could be explained by the different roles played by the tissue (Lambert et al., 2013). The outer blubber layer was characterised by higher relative proportions of MC-MUFAs compared to the inner blubber layer. They were conserved in this layer throughout the fast. It is advantageous for NES pups to maintain this class of FAs with low melting points (Knothe and Dunn, 2009) in order to preserve the fluidity of this tissue at cold temperatures as well as insulation and streamlining (Enser, 1984; Knothe and Dunn, 2009). By way of compensation, the inner layer exhibited higher relative abundance of MC-SFAs than the outer layer. This proportion however decreased during the first half of the fast, with C10:0, C12:0, C14:0 and C16:0 showing a positive fractional mobilisation.

7.4.4. The genes involved in the lipid metabolism

Intracellular enzymes have a key role in the regulation of the breakdown of the TG storage. ATGL and HSL are indeed responsible for 95% of the lipolytic activity in mouse (Schweiger et al., 2006), but the expression of these two genes has never been quantified in weaned NES pups. Our results point out that their expression levels remained stable during the period of post-weaning fast in both blubber layers of NES. The first sampling was done during the first week of fast. We can assume that the weaned NES pups have already developed all the enzymatic mechanisms for an efficient lipolysis and thus, the maximum expression levels of ATGL and HSL were already reached at the first week of fast and maintained over the fast. Investigating the expression levels of ATGL and HSL in suckling NES pups may confirm this hypothesis.

To date, no work studied the gene expression of intracellular lipases in NES. On the other hand, Viscarra et al. (2012) reported an increase of ATGL protein levels (Viscarra et al., 2012). Nevertheless, the sampled animals did not come from a longitudinal study, but from two different cohorts of a small number of individuals (n_{early}= 5 and n_{late}=8). This

experimental design may be a source of bias. In addition, ATGL activity was stable across the fast in lactating NES females (Fowler, 2012), which supports our results. On the other hand, HSL protein levels in weaned NES pups were stable during the post-weaning fast (Viscarra et al., 2012), which corroborates the results from our study.

Otherwise, the levels of expression of lipolytic enzymes were further studied rats. Levels of ATGL and HSL mRNA in epididymal adipose tissue increased over 4 days of fast and then, remained constant during the 2-3 next fasting days for ATGL and decreased for HSL (Bertile and Raclot, 2011). In contrary, Palou et al. (2010) have shown a stability of ATGL mRNA in the mesenteric and inguinal adipose tissue of rat over 24 hours of fasting and an increase in the retroperitoneal adipose tissue. The levels of HSL mRNA in the three depots of white adipose tissue were stable over 24 h of fasting (Palou et al., 2010). These last studies show that a fast of a few days does not necessarily implied an increase of expression levels of lipolytic enzymes in rats, which are non-adapted fasting animals. NES are animals that naturally undergo extended fast periods. It is reasonable to think that they developed some physiological adaptations in order to get used to long periods of fast. This could lead to maintain of expression levels of lipolytic enzymes throughout the periods. Further longitudinal experiments coupling the study of mRNA expression and protein activity are needed to confirm this hypothesis.

To conclude, the weaned NES pups exhibit a stratification of FAs within the blubber column in terms of profiles and rates of mobilisation. It is thus primordial to distinguish the inner blubber from the outer blubber in the study of this tissue. Firstly, more MC-MUFAs made up outer blubber compared to inner blubber and by way of compensation, proportions of MC-SFAs were higher within inner blubber as compared to outer blubber. This specific pattern promotes the fluidity of the outer layer in cold temperature. Secondly, it appears from our data that the release of FAs was more important in inner blubber than outer blubber, confirming the higher metabolic activity of inner blubber. This trend was however not observed in the levels of expression of lipolytic enzymes (ATGL and HSL). Eventually,

the mobilisation of FAs was not homogeneous over the fast. The more lipophilic FAs were preferentially retained within the blubber, whereas the less lipophilic FAs were readily released. This observation could be compared to the dynamics of mobilisation of lipophilic pollutants stored in blubber, which are also influenced by the lipophilic character of the molecules.

7.5. References

Aarsland, A., Wolfe, R. R., 1998. Hepatic secretion of VLDL fatty acids during stimulated lipogenesis in men. Journal of Lipid Research. 39, 1280-1286.

Arriola-Ortiz, A., On the dynamics and selective transport of fatty acids and organochlorines in lactating grey seals (*Halichoerus grypus*). University of St Andrews, 2010.

Bertile, F., Raclot, T., 2011. ATGL and HSL are not coordinately regulated in response to fuel partitioning in fasted rats. The Journal of Nutritional Biochemistry. 22, 372-379.

Best, N. J., et al., 2003. Vertical stratification of fatty acids in the blubber of southern elephant seals (*Mirounga leonina*): Implications for diet analysis. Comparative Biochemistry and Physiology Part B. 134, 253-263.

Brasaemle, D., et al., 2009. Perilipin A and the control of triacylglycerol metabolism. Molecular and Cellular Biochemistry. 326, 15-21.

Bryden, M., Stokes, G., 1969. Metabolism of fatty acids in the southern elephant seal *Mirounga leonina* (L.). Canadian Journal of Biochemistry. 47, 757-760.

Conner, W., et al., 1996. Differential mobilization of fatty acids from adipose tissue. Journal of Lipid Research. 37, 290-298.

Crocker, D. E., et al., 2001. Maternal traits and reproductive effort in northern elephant seals. Ecology. 82, 3541-3555.

Dang Van, Q. C., et al., 2011. Influence of the diet structure on ruminal biohydrogenation and milk fatty acid composition of cows fed extruded linseed. Animal Feed Science and Technology. 169, 1-10.

Debier, C., et al., 2006. Mobilization of PCBs from blubber to blood in northern elephant seals (*Mirounga angustirostris*) during the post-weaning fast. Aquatic Toxicology. 80, 149-157.

Debier, C., et al., 2003. Quantitative dynamics of PCB transfer from mother to pup during lactation in UK grey seals *Halichoerus grypus*. Marine Ecology Progress Series. 247, 237-248.

Derewenda, Z. S., Sharp, A. M., 1993. News from the interface: the molecular structures of triacyglyceride lipases. Trends in Biochemical Sciences. 18, 20-25.

Desvergne, B., Wahli, W., 1999. Peroxisome proliferator-activated receptors: nuclear control of metabolism. Endocrine Reviews. 20**,** 649-688.

Enser, M., 1984. The chemistry, biochemistry and nutritional importance of animal fats. Fats in Animal Nutrition. 23-51.

Fowler, M. A., Regulation of lipid metabolism and milk lipid content in northern elephant seals. University of California Santa Cruz, 2012.

Fowler, M. A., et al., 2014. Fatty acid mobilization and comparison to milk fatty acid content in northern elephant seals. Journal of Comparative Physiology B. 184**,** 1-11.

Groscolas, R., 1990. Metabolic adaptations to fasting in emperor and king penguins. Penguin biology. Academic Press, San Diego. 269-296.

Hellemans, J., et al., 2007. qBase relative quantification framework and software for management and automated analysis of real-time quantitative PCR data. Genome Biology. 8**,** R19.

Innis, S., 2005. Essential fatty acid metabolism during early development. Biology of Growing Animals. 3**,** 235-274.

Irving, L., et al., 1957. On the melting points of animal fats in cold climates. Physiological Zoology. 30**,** 93-105.

Iverson, S. J., et al., 1995. Prenatal and postnatal transfer of fatty acids from mother to pup in the hooded seal. Journal of Comparative Physiology B. 165**,** 1-12.

Kim, H.-Y., et al., 2004. Substrate preference in phosphatidylserine biosynthesis for docosahexaenoic acid containing species. Biochemistry. 43**,** 1030-1036.

Knothe, G., Dunn, R., 2009. A comprehensive evaluation of the melting points of fatty acids and esters determined by differential scanning calorimetry. Journal of the American Oil Chemists' Society. 86**,** 843-856.

Lambert, A., et al., 2013. Body regional distribution and stratification of fatty acids in the blubber of New Zealand sea lions: Implications for diet predictions. Journal of Comparative Physiology B. 183**,** 145-156.

Lass, A., et al., 2011. Lipolysis - A highly regulated multi-enzyme complex mediates the catabolism of cellular fat stores. Progress in Lipid Research. 50**,** 14-27.

Louis, C., et al., 2014. Mobilisation of lipophilic pollutants from blubber in northern elephant seal pups (*Mirounga angustirostris*) during the post-weaning fast. Environmental Research. 132**,** 438-448.

Mustonen, A.-M., et al., 2007. Lipid metabolism in the adipose tissues of a carnivore, the raccoon dog, during prolonged fasting. Experimental Biology and Medicine. 232, 58-69.

Nieminen, P., et al., 2006a. Selective fatty acid mobilization in the American mink (*Mustela vison*) during food deprivation. Comparative Biochemistry and Physiology Part B. 145, 81-93.

Nieminen, P., et al., 2006b. Fatty acid profiles and relative mobilization during fasting in adipose tissue depots of the American marten (*Martes americana*). Lipids. 41, 231-240.

Noren, D. P., et al., 2013. Characterization of blubber fatty acid signatures in northern elephant seals (*Mirounga angustirostris*) over the postweaning fast. Journal of Comparative Physiology B. 138, 1065-1074.

Noren, D. P., et al., 2003. Energy reserve utilization in northern elephant seal (*Mirounga angustirostris*) pups during the postweaning fast: size does matter. Journal of Comparative Physiology B. 173, 443-454.

Palou, M., et al., 2010. Regional differences in the expression of genes involved in lipid metabolism in adipose tissue in response to short-and medium-term fasting and refeeding. The Journal of Nutritional Biochemistry. 21, 23-33.

Price, E. R., Valencak, T. G., Changes in fatty acid composition during starvation in vertebrates: Mechanisms and questions. In: Comparative Physiology of Fasting, Starvation, and Food Limitation. Springer, 2012, 237-255.

Raclot, T., 2003. Selective mobilization of fatty acids from adipose tissue triacylglycerols. Progress in Lipid Research. 42, 257-288.

Raclot, T., Groscolas, R., 1993. Differential mobilization of white adipose tissue fatty acids according to chain length, unsaturation, and positional isomerism. Journal of Lipid Research. 34, 1515-1526.

Raclot, T., Groscolas, R., 1995. Selective mobilization of adipose tissue fatty acids during energy depletion in the rat. Journal of Lipid Research. 36, 2164-2173.

Raclot, T., et al., 1997. Selective release of human adipocyte fatty acids according to molecular structure. Biochemical Journal. 324, 911-915.

Rea, L., et al., 1997. Changes in plasma fatty acids indicate change in nutritional status in developing Weddell seal pups. Polar Biology. 18, 351-357.

Ryg, M., et al., 1988. Thermal significance of the topographical distribution of blubber in ringed seals (*Phoca hispida*). Canadian Journal of Fisheries and Aquatic Sciences. 45**,** 985-992.

Schweiger, M., et al., 2006. Adipose triglyceride lipase and hormone-sensitive lipase are the major enzymes in adipose tissue triacylglycerol catabolism. Journal of Biological Chemistry. 281**,** 40236-40241.

Smith, W. L., Murphy, R. C., 2002. The eicosanoids: cyclooxygenase, lipoxygenase, and epoxygenase pathways. New Comprehensive Biochemistry. 36**,** 341-371.

Strandberg, U., et al., 2008. Stratification, composition, and function of marine mammal blubber: The ecology of fatty acids in marine mammals. Physiological and Biochemical Zoology. 81**,** 473-485.

Thompson, B. R., et al., 2010. Fatty acid flux in adipocytes: The in's and out's of fat cell lipid trafficking. Molecular and Cellular Endocrinology. 318**,** 24-33.

Trumble, S. J., Kanatous, S. B., 2012. Fatty acid use in diving mammals: More than merely fuel. Frontiers in Physiology. 3**,** 184.

Vanden Berghe, M., et al., 2012. Selective transfer of persistent organic pollutants and their metabolites in grey seals during lactation. Environment International. 46**,** 6-15.

Vandesompele, J., et al., 2002. Accurate normalization of real-time quantitative RT-PCR data by geometric averaging of multiple internal control genes. Genome Biology. 3**,** research0034.

Viscarra, J. A., Ortiz, R. M., 2013. Cellular mechanisms regulating fuel metabolism in mammals: Role of adipose tissue and lipids during prolonged food deprivation. Metabolism. 62**,** 889-897.

Viscarra, J. A., et al., 2012. Decreased expression of adipose CD36 and FATP1 are associated with increased plasma non-esterified fatty acids during prolonged fasting in northern elephant seal pups (*Mirounga angustirostris*). The Journal of Experimental Biology. 215**,** 2455-2464.

Wheatley, K. E., et al., 2008. Differential mobilization of blubber fatty acids in lactating Weddell seals: Evidence for selective use. Physiological and Biochemical Zoology. 81**,** 651-62.

Chapter 8

Bioaccumulation of hydroxylated polychlorinated biphenyls and pentachlorophenol in the serum of northern elephant seal pups (*Mirounga angustirostris*)

Foreword

We clearly demonstrated in the previous experimental chapters an important release of lipophilic pollutants from the adipose tissue during fasting periods. Once in the circulation, they can reach different tissues such as the liver and undergo reactions of biotransformation. This may result in the formation of more polar metabolites that tend to accumulate in blood. Since a few studies demonstrated the presence of biotransformation enzymes (i.e. cytochrome P450) in seals[3,4,5], we investigated the progression of the

[3] Nyman, M., et al., 2000. Expression and inducibility of members in the cytochrome P4501 (CYP1) family in ringed and grey seals from polluted and less polluted waters. Environmental Toxicology and Pharmacology. 8, 217-225.

[4] Wolkers, J., et al., 1998. Phase I and phase II enzyme activities in Ringed seals (*Phoca hispida*): characterization of hepatic cytochrome P450 by activity patterns, inhibition studies, mRNA analyses, and western blotting. Aquatic toxicology. 44, 103-115.

[5] Wolkers, H., et al., 2000. Chlorinated pesticide concentrations, with an emphasis on polychlorinated camphenes (toxaphenes), in relation to cytochrome P450 enzyme

levels of hydroxylated PCBs, which are metabolites from Phase I biotransformation reactions, in the serum of a cohort of weaned NES pups.

activities in harp seals (*Phoca groenlandica*) from the Barents Sea. Environmental toxicology and chemistry. 19, 1632-1637.

Bioaccumulation of hydroxylated polychlorinated biphenyls and pentachlorophenol in the serum of northern elephant seal pups (*Mirounga angustirostris*)

Caroline Louis, Alin C. Dirtu, Marie Stas, Daniel E. Crocker, Govindan Malarvannan, Adrian Covaci, Cathy Debier

Abstract

Northern elephant seals (NES, *n*=22) (*Mirounga angustirostris*) from the Año Nuevo State Reserve (CA, USA) were sampled at 1-, 4-, 7- and 10-week post-weaning. Concentrations of hydroxylated polychlorinated biphenyls (HO-PCBs) and their parent PCBs were measured in the serum of each individual. The total HO-PCB concentrations in the serum increased significantly between early and late fast (from 282 ± 20 to 529 ± 31 pg/mL). This increase might result from a mobilisation of HO-PCBs transferred from the mother during gestation and/or lactation and stored in the pup's liver. Food deprivation has been shown to exacerbate biotransformation capacities in mammals, birds and fish. The HO-penta-CBs was the predominant homologue group, followed by HO-hexa-CBs and HO-hepta-CBs. No preferential pathway for the metabolism of HO-PCBs (HO-direct insertion or NIH-shift of a chlorine atom) could be evidenced. The concentrations of pentachlorophenol (PCP) in the serum of weaned NES increased from 103 ± 7 pg/mL at early fast to 246 ± 41 pg/mL at late fast, which is within the range of PCP concentrations usually encountered in marine mammals.

Keywords

Northern elephant seal – Fast – HO-PCBs – Pentachlorophenol – Serum – Pup

8.1. Introduction

Polychlorinated biphenyls (PCBs) are widely spread in the marine and terrestrial biota and biomagnify throughout food chains (Covaci et al., 2002; Letcher et al., 2010). Belonging to a high trophic level, northern elephant seals (NES) (*Mirounga angustirostris*) face an important risk for exposure to environmental lipophilic pollutants. During a 25-day period, NES pups are fed with maternal milk, which contains large amounts of fat and lipophilic pollutants, such as PCBs (Debier et al., 2012). Once absorbed by the animals, PCBs tend to accumulate in lipid-rich tissues and mainly in the adipose tissue (Debier et al., 2006; Louis et al., 2014). During the post-weaning fast, pups mobilise primarily lipids from their large subcutaneous adipose stores in order to meet the needs of animals undergoing a period of developmental and to prevent protein catabolism (Noren et al., 2003). They thus undergo both fast and development, simultaneously. Although adipose tissue is considered as an internal site of storage for PCBs (La Merrill et al., 2013), they appear to be mobilised from adipocytes into the bloodstream during this period of negative energy balance (Debier et al., 2006; Louis et al., 2014). A release of such toxic pollutants in the blood stream may be problematic since they may reach target tissues and exert harmful health effects in animals (Vanden Berghe et al., 2013).

Seals appear to be capable of biotransforming PCBs, to some extent, through the phase I and II biotransformation process, resulting in the formation of more polar metabolites, such as HO-PCBs, $(HO)_2$-PCBs and methylsulfonyl-PCBs ($MeSO_2$-PCBs) (Nyman et al., 2001; Routti et al., 2008; Teramitsu et al., 2000). Several studies demonstrated the presence of different forms of cytochrome P450 (CYP) (e.g. CYP1A, CYP3A), the phase I enzymes, in ringed, harbour, harp and grey seals (Nyman et al., 2000; Ruus et al., 2002; Tilley et al., 2002; Wolkers et al., 1998; Wolkers et al., 2000). Phase II enzymes, such as UDP glucuronosyl transferase and glutathione S-transferase (GST), were shown in ringed and harbour seals (Ruus et al., 2002; Wolkers et al., 1998).

The HO-PCBs, resulting from phase I metabolism, may be obtained by (i) the direct insertion of an HO-group, or (ii) the formation of a *meta-para*-epoxide (or arene oxide) intermediate that results in a *meta*- or *para*-HO-PCB metabolite. The *meta-para*-epoxide intermediate with a *meta*-hydrogen and a *para*-chlorine can result in both *meta*- and *para*-HO-PCB metabolites, the *para*-HO-PCB metabolite being a consequence of 1,2-shift (NIH-shift) (Figure 8.1) (Daly et al., 1972; Letcher et al., 2000). The arene oxide may also conjugate with glutathione (GSH) via glutathione-S-transferase (phase II reaction; Zamek-Gliszczynski et al. (2006)). $MeSO_2$-PCBs are then formed further via cascade reactions (details not shown). HO-PCBs were detected in seal liver (Park et al., 2009), albeit they can bind to specific plasma proteins and are therefore present in the blood compartment. $MeSO_2$-PCBs have been mainly found in the liver, followed by blubber and lung (Larsson et al., 2004).

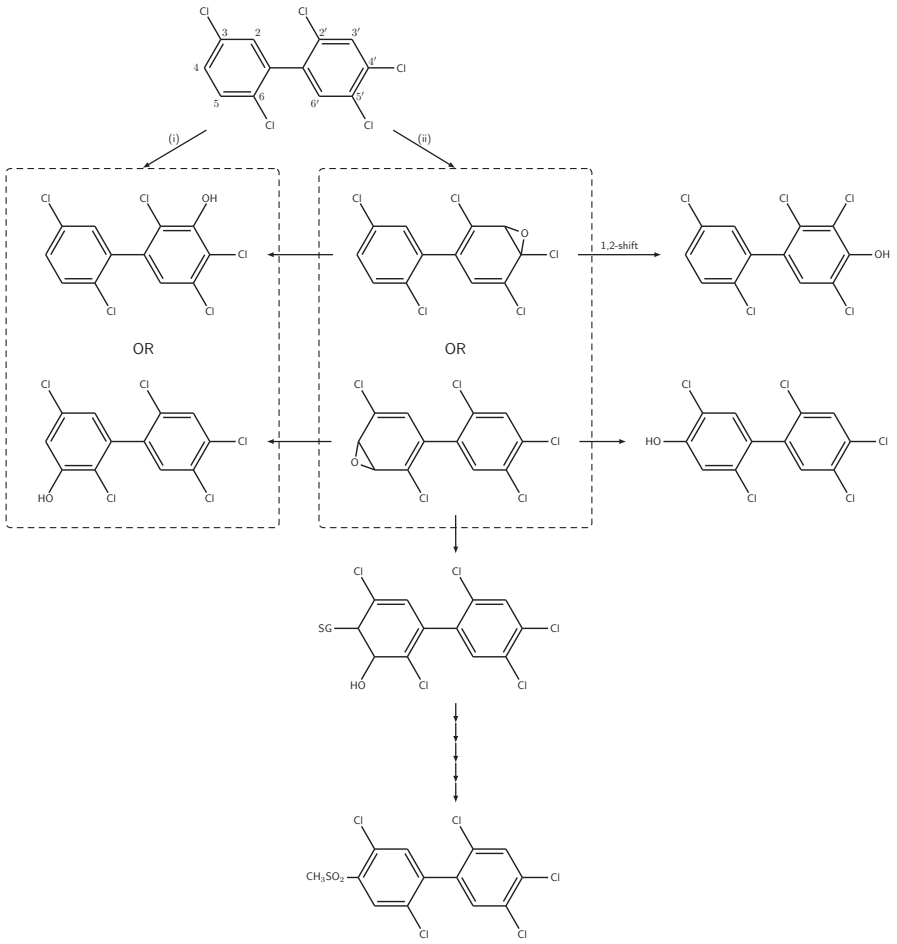

Figure 8.1 – Metabolism scheme of PCBs. PCB-101 has been chosen as an example. The formations of HO-PCBs by (i) direct HO-insertion and (ii) by NIH-shift, and $MeSO_2$-PCBs are shown. The positions 2, 2', 6 and 6' were called *ortho*. The positions 3, 3', 5 and 5' were called *meta* and the positions 4 and 4', *para* (adapted from Letcher et al. (2000)).

Biotransformation of PCBs is an important step required for their excretion. However, in numerous cases, it appears that metabolites, and especially HO-PCBs, can exert negative effects on health. Among others, they can lead to endocrine disruptions while competing with estrogens and thyroxine for the corresponding nuclear receptors (Connor et al., 1997; Lans et al., 1993; Van den Berg et al., 1991). They also affect the thyroxine (T_4) metabolism by inhibiting its sulfation (Schuur et al., 1998). HO-PCBs have been shown to disrupt the blood transport of T_4 and retinol (Van der Plas et al., 2001). They inhibit mitochondrial oxidative phosphorylation (Narasimhan et al., 1991). *In vitro* studies have also shown that some HO-PCBs exert neurotoxic effects during development leading to locomotor defects, hearing loss, and learning and memory disorders (Meerts et al., 2004).

Marine mammals are also vulnerable to other organic pollutants such as pentachlorophenol (PCP) (Dupont et al., 2013; Routti et al., 2009; Sandau et al., 2000b), a metabolite of hexachlorobenzene (HCB) (Renner, 1988). Similar to HO-PCBs, PCP binds to plasma proteins (Uhl et al., 1986) and has the capability of interacting with thyroid hormone blood transport (Van den Berg et al., 1991). Indeed, its affinity for thyroid hormone transport protein transthyretin (TTR) is twice as high as T_4. PCP is also known to affect the metabolism of thyroid hormone, which could lead to neurodevelopmental effects in newborns (Sandau et al., 2002).

The aim of the present work was to investigate the levels of HO-PCBs, which appear to be the most important metabolites present in the serum of seals (Vanden Berghe et al., 2012). Several studies have investigated HO-PCBs in young marine mammals (Bytingsvik et al., 2012; Gabrielsen et al., 2011; Weijs et al., 2009) including a study by our research group (Vanden Berghe et al., 2012), but never in NES. We compare the changes of HO-PCB contents with their potential PCB precursors in order to investigate trends in PCB metabolism pathways. The levels of PCP and HCB in the serum of NES pups were also evaluated.

8.2. Material and methods

8.2.1. NES sampling

Between January and April 2010, twenty-two free-ranging NES pups from Año Nuevo State Reserve (CA, USA) were sampled at 1-, 4-, 7- and 10-week post-weaning. All targeted animals were followed thanks to specific marks of dye during the studied period. NES pups were immobilised with an injection of Telazol at 1 mg/kg of estimated body mass and sedation was then maintained through subsequent intravenous injections of Ketamine (all drugs were from Fort Dodge Animal Health, Fort Dodge, IA, USA) as needed. Blood was collected from the extradural vein into Vacutainer serum tubes (Becton-Dickinson, Erembodegem, Belgium). Samples were centrifuged at 1300xg for 15 min at 4°C and serum was aliquoted into microtubes and stored at -20°C until analysis (Louis et al., 2014).

8.2.2. POP analyses

After thawing, serum samples were analysed as reported in Vanden Berghe et al. (2012). Briefly, internal standards (4'-HO-CB159 and CB-143) were added to 1.5 mL serum followed by deionized water and formic acid. The mixture was sonicated for 20 min and loaded on solid-phase-extraction (SPE) cartridges (200 mg/3 mL, Oasis HLB, Waters, Milford, MA). Pollutants were eluted with dichloromethane/methanol (1:1, *v:v*). Extracts were then dried and reconstituted in hexane. A fractionation step on silica SPE cartridges (500 mg/3 mL, VWR, Belgium) topped with acidified silicagel (22% H_2SO_4, *w:w*) was necessary to separate neutral compounds (PCBs and HCB) from phenolic compounds (HO-PCBs and PCP). Neutral compounds were eluted first with 6 mL *n*-hexane, evaporated and reconstituted in *iso*-octane, while phenolic compounds were eluted with 8 mL dichloromethane, evaporated and derivatized with trimethylsilyl-diazomethane for 30 min at 60°C. After solvent evaporation, residues were reconstituted in *iso*-octane. Twelve HO-PCBs (4-HO-CB107, 4-HO-CB120, 4'-HO-CB127, 4'-HO-CB130, 3-HO-CB138, 4-HO-CB146, 4-HO-CB162, 4-

HO-CB163, 4'-HO-CB172, 4-HO-CB187, 4-HO-CB193 and 4-HO-CB208; Maervoet et al. (2004)) were analysed as well as 30 PCB congeners (IUPAC numbers: CB-28, -47, -49, -52, -74, -95, -99, -101, -105, -110, -118 , -128, -138, -146, -149, -151, -153, -156, -170, -171, -172, -174, -177, -180, -183, -187, -194, -199, -206 and -209).

All compounds were measured with an Agilent 6890 gas chromatograph coupled with a 5973 mass spectrometer system (GC-MS). All analytical details as well as performed quality assurance and quality control are available in Vanden Berghe et al. (2012).

8.2.3. Statistical analysis

Data were log transformed to achieve normality. For pollutant concentrations below the limit of quantification (LOQ), a LOQ×detection frequency value was assigned. Statistical analyses were conducted using SAS 9.3 software (SAS Institute Inc., Cary, USA). Linear mixed models were used to test differences in pollutant levels and profiles throughout the post-weaning fast periods. Animal ID was modelled as a random effect. In addition, the potential correlation between HO-PCBs and their precursors were tested with a Pearson test. The level of statistical significance was set at p-values<0.05 for all analyses.

8.3. Results

8.3.1. Levels and patterns of HO-PCBs

Among the twelve HO-PCBs that were targeted, four were under the LOQ in all samples (4'-HO-CB127, 3-HO-CB138, 4-HO-CB193 and 4-HO-CB208). Congener 4'-HO-CB130 was quantified in only a few samples. Detection frequency was >50% in two HO-penta-CBs (4-HO-CB107 and 120), three HO-hexa-CBs (4-HO-CB146, 162 and 163) and two HO-hepta-CBs (4-HO-CB172 and 187) (see Appendices; Table S1).

Total HO-PCB serum concentrations remained constant during the first 3 weeks of fast (p=0.090) and then, increased significantly until week 10 (p<0.001) (Table 8.1). When looking at individual congeners, all HO-PCBs significantly increased in serum between weeks 1 and 10 (0.001<p<0.006), except 4-HO-CB162 that remained constant (p=0.492) (Table 8.1). Moreover, the rise of bioaccumulation of penta-HO-CBs between weeks 1 and 10 (i.e. 4-HO-CB-107 and 4-HO-CB-120) seems to be greater (mean factor of 2.0) than the one of hepta-HO-CBs (i.e. 4-HO-CB-172 and 4-HO-CB-187) (mean factor of 1.4) followed by the one of hexa-HO-CBs (i.e. 4-HO-CB-146, 4-HO-CB-162 and 4-HO-CB-163) (mean factor of 1.2).

Table 8.1 – Mean concentrations ± SEM of HO-PCB congeners and their potential PCB precursors, PCP and HCB in serum of weaned NES pups, expressed in pg/mL wet weight. The ratios of total measured HO-PCBs and total measured PCBs are also shown. Values within a row followed by different letters are significantly different (p≤0.05).

	Period of fast			
	Week 1	Week 4	Week 7	Week 10
4-HO-CB107	135 ± 12 [a]	147 ± 13 [a]	184 ± 17 [b]	310 ± 24 [c]
4-HO-CB120	33 ± 2 [a]	35 ± 3 [a]	38 ± 3 [b]	56 ± 4 [c]
4-HO-CB146	44 ± 2 [a]	48 ± 2 [b]	54 ± 3 [c]	77 ± 3 [d]
4-HO-CB162	46 ± 4 [a]	44 ± 4 [a,b]	43 ± 4 [b]	47 ± 4 [a,b]
4-HO-CB163	4.3 ± 0.3 [a]	3.5 ± 0.4 [b]	4.8 ± 0.4 [a]	6.7 ± 0.4 [c]
4-HO-CB172	14 ± 1 [a]	14 ± 1 [a]	15 ± 1 [a]	17 ± 1 [b]
4-HO-CB187	6.9 ± 0.4 [a,b]	6.4 ± 0.5 [a]	7.7 ± 0.5 [b,c]	8.3 ± 0.4 [c]
Σ HO-PCBs	**282 ± 20 [a]**	**299 ± 19 [a]**	**346 ± 23 [b]**	**529 ± 31 [c]**
CB-105	109 ± 9 [a]	150 ± 14 [b]	178 ± 14 [c]	191 ± 19 [d]
CB-118	470 ± 23 [a]	634 ± 37 [b]	791 ± 42 [c]	901 ± 57 [d]
CB-138	588 ± 26 [a]	722 ± 33 [b]	931 ± 45 [c]	1067 ± 61 [d]
CB-146	71 ± 4 [a]	84 ± 4 [b]	123 ± 6 [c]	141 ± 11 [c]
CB-153	739 ± 31 [a]	860 ± 37 [b]	1156 ± 58 [c]	1312 ± 79 [d]
CB-170	36 ± 3 [a]	32 ± 2 [a]	50 ± 3 [b]	50 ± 4 [b]
CB-180	131 ± 11 [a]	124 ± 7 [a]	182 ± 12 [b]	191 ± 15 [b]
CB-183	37 ± 3 [a]	37 ± 4 [a]	49 ± 4 [b]	58 ± 4 [b]
CB-187	144 ± 12 [a]	132 ± 6 [a]	182 ± 11 [b]	207 ± 13 [c]
Σ total PCBs	**3723 ± 172 [a]**	**4533 ± 246 [b]**	**5058 ± 248 [c]**	**5851 ± 348 [d]**
Σ HO-PCBs /Σ total PCBs	**0.068 ± 0.006 [a]**	**0.061 ± 0.005 [b]**	**0.064 ± 0.004 [a,b]**	**0.087 ± 0.006 [c]**
PCP	**103 ± 7 [a]**	**70 ± 9 [b]**	**146 ± 23 [a]**	**246 ± 41 [c]**
HCB	**168 ± 12 [a]**	**309 ± 14 [b]**	**253 ± 16 [c]**	**430 ±29 [d]**

Congener 4-HO-CB107 composed almost one half of total HO-PCBs (from 46.4 ± 1.5% at week 1 to 57.5 ± 1.3% at week 10). It was followed in a decreasing order by 4-HO-CB146 (from 16.7 ± 1.1% at week 1 to 15.1 ± 0.6% at week 10), 4-HO-CB162 (from 16.1 ± 0.9% at week 1 to 9.0 ± 1.0% at week 10), 4-HO-CB120 (from 10.9 ± 0.2% at week 1 to 10.5 ± 0.3% at week 10), 4-HO-CB172 (from 5.6 ± 0.5% at week 1 to 3.4 ± 0.2% at week 10), 4-HO-CB187 (from 2.7 ± 0.2% at week 1 to 1.7 ± 0.2% at week 10) and 4-HO-CB163 (from 1.6 ± 0.1% at week 1 to 1.3 ± 0.1% at week 10).

When HO-PCBs were grouped per class of chlorination degree, the main class was HO-penta-CBs followed by HO-hexa-CBs and HO-hepta-CBs (Figure 8.2).

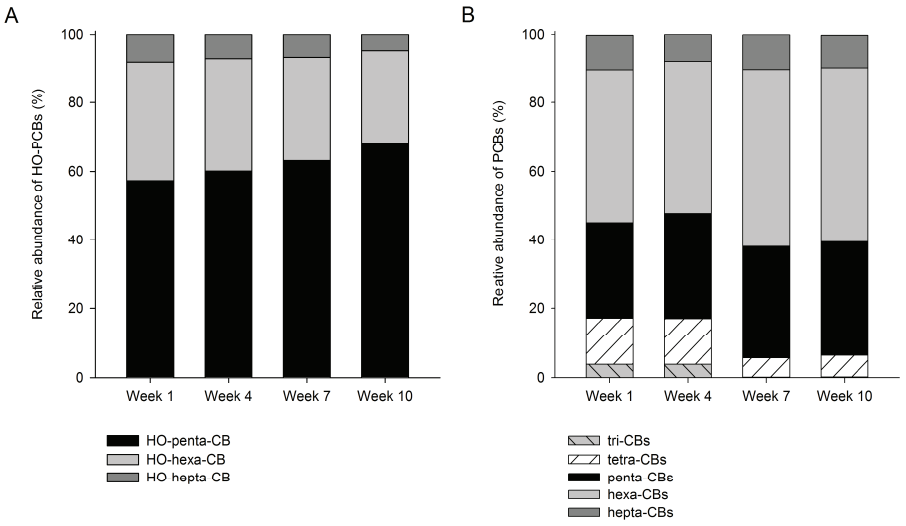

Figure 8.2 – Relative proportions of the different classes of HO-PCBs (A) and PCBs (B) in serum of NES pups during the post-weaning fast.

8.3.2. Levels and patterns of PCBs

Among the thirty PCBs analysed in the serum, CB-172 and -199 were detected in only a few samples (see Appendices; Table S1). Four congeners of PCBs (CB-174, -194, -206 and -209) were not measured in any investigated sample (see Appendices; Table S1).

Total PCB concentrations in the serum increased significantly throughout the fast ($0.001<p<0.004$) (Table 8.1). Details concerning the levels and profiles of the thirty PCBs analysed in the serum are described elsewhere (Louis et al., 2014). Some PCBs detected in serum are considered as potential precursors of HO-PCBs (Table 8.2). The concentrations of all these precursors increased significantly between early and late fast ($0.001<p<0.017$) (Table 8.1).

When the results were expressed by homologue group in percentage of total PCBs, we found mainly hexa-CBs, followed by penta-CBs , tetra-CBs, hepta-CBs and tri-CBs for the first part of the fast and hexa-CBs, followed by penta-CBs, hepta-CBs, tetra-CBs and then, tri-CBs for the second part of the fast (Figure 8.2).

8.3.3. Correlations between HO-PCBs and PCBs

The ratios between the concentrations of total HO-PCBs and total PCBs decreased significantly between weeks 1 and 4 ($p=0.018$), remained constant between weeks 4 and 7 ($p=0.651$) and rose again between weeks 7 and 10 ($p<0.001$) (Table 8.1). There was a significant positive correlation between the concentrations of total HO-PCBs and total PCBs throughout the fast (Pearson correlation coefficient $r=0.539$, $p<0.001$).

The correlations between individual HO-PCBs and their potential precursors of PCBs were also tested during the entire fasting period (Table 8.2). Regarding HO-PCBs obtained by direct HO-insertion, the concentrations of 4-HO-CB146 were positively correlated to the concentrations of CB-146 ($p<0.001$), whereas the levels of 4-HO-CB187 were not correlated to the levels of CB-187 ($p=0.227$). Regarding the metabolism

by NIH-shift, the levels of 4-HO-CB107 in the serum were positively correlated to the sum of CB-105 and CB-118 (r=0.449, p<0.001). Considering the PCB precursors separately, 4-HO-CB107 was significantly correlated to CB-118 (p<0.001), but not to CB-105 (p=0.053). The concentrations of 4-HO-CB120 were significantly correlated to the concentrations of CB-118 (p<0.001). Similar observations were drawn between 4-HO-CB146 and the sum of CB-138 and -153 (r=0.710, p<0.001) as well as between 4-HO-CB146 and the precursors taken individually (p<0.001). A significant correlation was noted between 4'-HO-CB172 and the sum of CB-170 and -180 (r=0.268, p=0.016) as well as between 4'-HO-CB172 and the precursors taken individually (p=0.028 for CB-170 and p=0.017 for CB-180). Finally, the concentration of 4-HO-CB187 was not correlated to CB-183 (p=0.139). The correlation coefficients constantly increased over time for 4-HO-CB107 and its PCB precursors. On the other hand, no trend could be highlighted for the other studied HO-PCB congeners and PCB precursors.

8.3.4. Concentrations of pentachlorophenol

The dynamics of PCP in serum differed somewhat from total HO-PCBs, with a significant decrease between weeks 1 and 4 (p<0.001), followed by an increase during the rest of the fast (p<0.001) (Table 8.1). PCP may be formed via HCB metabolism, but was also been used as wood preservative until the 1980s. HCB was analysed in these same serum samples and results are described elsewhere (Louis et al., 2014). There was a good correlation between PCP and HCB levels (r=0.334; p=0.002).

Table 8.2 – Pearson correlation coefficients (r) for individual HO-PCBs and their potential PCB precursors by direct HO-insertion (values in bold) and by the NIH-shift (values in italics) (pathways of biotransformation were compiled from Dirtu et al. (2010) and Weijs et al. (2009)). Values with a star correspond to a significant correlations (p<0.05).

	PCB precursors	r_{total}	$r_{\text{week 1}}$	$r_{\text{week 4}}$	$r_{\text{week 7}}$	$r_{\text{week 10}}$
4-HO-CB107	CB-105	*0.217*	*-0.243*	*-0.170*	*0.132*	*0.182*
	CB-107 (N.A)	\				
	CB-118	*0.493**	*0.099*	*0.263*	*0.347*	*0.411*
4-HO-CB120	CB-118	*0.445**	*0.118*	*0.278*	*0.216*	*0.297*
	CB-120 (N.A)	\				
4-HO-CB146	CB-138	*0.709**	*0.542**	*0.368*	*0.538**	*0.538**
	CB-146	**0.652***	**0.459***	**0.186**	**0.542***	**0.433**
	CB-153	*0.691**	*0.538**	*0.433**	*0.477**	*0.424*
4-HO-CB162	CB-157 (N.A)	\				
	CB-162 (N.A)	\				
	CB-167 (N.A)	\				
4-HO-CB163	CB-158 (N.A)	\				
	CB-163 (N.A)	\				
4'-HO-CB172	CB-170	*0.246**	*0.385*	*-0.015*	*0.255*	*-0.072*
	CB-172 (N.D)	\				
	CB-180	*0.267**	*0.212*	*0.082*	*0.159*	*0.125*
4-HO-CB187	CB-183	*0.171*	*-0.253*	*0.140*	*0.359*	*-0.345*
	CB-187	**0.137**	**-0.323**	**0.219**	**0.159**	**-0.046**

N.A = not analysed

N.D = not detected

8.4. Discussion

The presence of HO-PCBs in the serum of weaned NES pups may have several origins. They may come from the mother, via a placental transfer and/or the ingestion of low amounts present in the milk. Once absorbed by the pups, HO-PCBs tend to accumulate in blood, because of their high affinity for plasma proteins (Letcher et al., 2000; Vanden Berghe et al., 2012). They can also be stored in the liver, as already shown in harbour seals (Park et al., 2009). The presence of HO-PCBs in weaned NES pups may also result from an endogenous biotransformation of PCBs through the activity of CYP enzymes, which were detected in several phocid seal species (ringed, harbour, harp and grey seals) (Nyman et al., 2000; Ruus et al., 2002; Tilley et al., 2002; Wolkers et al., 1998; Wolkers et al., 2000). The concentrations of total HO-PCBs were more than one order of magnitude lower than the concentrations of total PCBs in weaned NES pups, leading to HO-PCB/PCB concentration ratios less than 0.1. Several cetacean species, such as Pacific white-sided dolphin and beluga whale, had HO-PCB/PCB concentration ratios lower than those measured in NES pups, whereas other marine mammals, including Bryde's and Minke whales, bottlenose dolphins, northern fur seals and harbour seals, showed HO-PCB/PCB concentration ratios similar to those found in weaned NES pups. Contrarily, the HO-PCB/PCB concentration ratios of killer whales, ringed seals and grey seals (lactating females and suckled pups) were much greater than in NES pups. In the same way, NES pups do not seem to easily form HO-PCBs compared to polar bears, as well as terrestrial mammals such as humans, raccoon dogs, cats and dogs (Table 8.3). These differences might be due to interspecies variation of PCB biotransformation capacity. In addition, the induction of metabolising enzymes can be influenced by the hepatic levels of PCBs (Kunisue and Tanabe, 2009; Routti et al., 2008), which can vary between species, according to their PCB exposure.

Table 8.3 – Mean HO-PCB/PCB concentration ratios in different species of mammals

Species	Age	HO-PCB/PCB ratios	References
Pacific white-sided dolphin		0.0015	Nomiyama et al. (2010)
Beluga whale		0.0045	
Bryde's whale		0.013	
Minke whale		0.069	
Bottlenose dolphin	Juveniles and adults	0.016	Houde et al. (2006)
NES	**Weaned pups**	**0.061 – 0.087**	**Present study**
Northern fur seal		0.065	Kunisue and Tanabe (2009)
Harbour seal	Juveniles and adults	0.086	Weijs et al. (2009)
Human	Adults	0.11	Sandau et al. (2000a)
Killer whale	Adults	0.170	Bennett et al. (2009)
Ringed seal	Adults	0.240	Routti et al. (2008)
Human	Adults	0.33	Sandau et al. (2000a)
Human	Adults	0.37	Kunisue and Tanabe (2009)
Grey seal	Suckled pups	0.523 – 0.742	Vanden Berghe et al. (2012)
Grey seal	Lactating females	0.515 – 1.004	
Polar bear	Juveniles and adults	1.97	Sandala et al. (2004)
Raccoon dog		4.3	Kunisue and Tanabe (2009)
Cat		5.3	
Dog		29	

The biotransformation of PCBs into HO-PCBs is a complex mechanism involving either a direct insertion of HO-group or a formation of arene oxide intermediate (Figure 8.1). Most of the HO-PCB congeners were correlated to the different parent PCBs that were analysed. It may indicate that there is no preferential pathway of biotransformation. Nevertheless, further data are needed to confirm this hypothesis, since we detected only two PCB precursors of direct HO-insertion.

HO-penta-CBs composed more than half of the total HO-PCBs in NES pup serum. The preferential accumulation of this homologue group was also noted in the circulation of grey seals from Scotland (Vanden Berghe et al., 2012), harbor seals from the Atlantic and the North Sea (Løken et al., 2008; Weijs et al., 2009) and different species of whales from the Japanese coast (melon-headed whale, Stejneger's beaked whale, Pacific white-sided dolphin, Blainville's beaked whale and killer whale) (Nomiyama et al., 2010) as well as in the liver of beluga whales from Canada (McKinney et al., 2006). The domination of HO-penta-CBs is thus common to many marine species (Nomiyama et al., 2010). Such similarity across the world most probably implies that the biotransformation of PCBs in marine mammals is catalysed by the same CYP isozymes (Gabrielsen et al., 2011). However, this accumulation pattern of HO-penta-PCBs is not comparable with terrestrial mammals, such as dogs and raccoon dogs, which accumulate larger proportions of the higher chlorinated HO-PCBs, such as HO-hepta-CBs and HO-octa-CBs (Kunisue and Tanabe, 2009). The levels of HO-hexa-CBs were higher than HO-penta-CBs in human serum (Dirtu et al., 2010; Dirtu et al., 2013). Differences in the HO-PCB accumulation patterns observed between marine and terrestrial mammals might be caused by evolutionary differences in biotransformation enzymes, but also by differences in PCB exposure.

The levels of total HO-PCBs increased significantly in the serum of weaned NES pups from mid to late fast. Similarly, there was also an increase of HO-PCB/PCB concentration ratios between early and late fast. This increase in metabolites with time might result from a mobilisation of HO-PCBs from storage tissues, such as the liver, associated with the fast. There might also be an incomplete Phase II biotransformation of PCBs, resulting in

an inefficient excretion of metabolites. Indeed, a previous study highlighted that *para* substituted HO-PCBs (like all analyzed HO-PCBs in this study) are resistant to the UGT conjugation in rat hepatic microsomes (Tampal et al., 2002), which, to some extent, could be at the origin of the rise of HO-PCB concentrations in NES blood during the fast. In addition, the *para*-HO substitution gives a similar structure to T_4, the natural substrate of TTR, to HO-PCBs (Lans et al., 1993; Letcher et al., 2000). The affinity of HO-PCBs for TTR may add to their retention and their increase in the blood. The absence of food intake for NES pups may influence the formation of HO-PCB metabolites by increasing the bioavailability of PCBs, among others through their (re)mobilisation from blubber (Debier et al., 2006; Louis et al., 2014), and by upregulating the CYP enzymes. For example, the concentrations of HO-PCBs were higher in fasting ringed seals than in non-fasting animals (Routti et al., 2010). The presence of PCBs has been shown to promote the expression of CYP1A in the liver of fasting fish (Vijayan et al., 2006). Fasting itself seems to increase the expression of genes encoding for the biotransformation enzymes in fish and rodents (Cheesman and Reilly, 1998; Ding et al., 2006). Likewise, the biotransformation capacity and the HO-PCB metabolites increase during food deprivation episodes in herring gull chicks (Routti et al., 2013). Consequently, we may suggest a positive impact of the post-weaning fast of NES on the formation of HO-PCBs and their accumulation in blood.

Eventually, the increase of HO-PCB/PCB concentration ratios of weaned NES pups from mid fast might translate an increase of metabolic capacity with age of NES. Indeed, it has been previously shown that CYP activities increase with age in humans (Milsap and Jusko, 1994) and that the age and the levels of HO-PCBs in hooded seal pups are positively correlated (Gabrielsen et al., 2011). Based on HO-PCB/PCB concentration ratios (Table 8.3), it seems that we cannot extrapolate this observation to all mammals since grey seal suckled pups had values of ratio similar to grey seal lactating females. Nevertheless, the HO-PCB/PCB concentration ratios of grey seal suckled pups can be influenced by those of the females since PCBs and, to some extent, HO-PCBs, can be transferred from mother to pup through the milk (Vanden Berghe et al., 2012). It could be interesting to

study the HO-PCB/PCB concentration ratios in fasting NES at different age stages (pups, juveniles and adults), in comparable physiological states, in order to confirm the link between age and biotransformation capacity.

It seems important to note that the increase of HO-PCBs differed between the congeners. The rise of concentration was indeed more important for the less chlorinated congeners compared to the more chlorinated ones. Louis et al. (2014) noted a more pronounced rise of penta-CBs, followed by hexa-CBs and then, hepta-CBs in the serum of weaned NES pups. It thus seems reasonable to think that the higher disponibility of less chlorinated PCBs in serum promoted their biotransformation by peripheral tissues such as the liver. Moreover, Safe (1989) reported that PCBs with more than five chlorine atoms are more resistant to biotransformation than the less chlorinated ones, leading to a higher production of less chlorinated HO-PCB congeners.

The concentrations of PCP in the serum of weaned NES pups were in the same order of magnitude as those found in the blood of harbour seals from the North Sea (Dupont et al., 2013) and northern fur seals from Japan (Kunisue and Tanabe, 2009), in the plasma of ringed seals from Canada (Sandau et al., 2000b), polar bears and ringed seals from Canada (Sandau et al., 2000b) and one captive killer whale from Canada (Bennett et al., 2009). The serum of NES weaned pups was 2-4 fold less contaminated by PCP than the plasma of ringed seals from Svalbard and the Baltic Sea (Routti et al., 2009) and one order of magnitude less contaminated than the plasma of bowhead whales from Alaska (Hoekstra et al., 2003). As a good correlation was noted between PCP and HCB, we can expect that weaned NES pups are able to biotransform the parent molecule.

The results of this study indicate that NES pups were contaminated by HO-PCBs and their concentrations in serum increased throughout the post-weaning fast. As a consequence, the increase of HO-PCB levels might have adverse effects on health of NES in full growth. It appears from our data that NES pups are able to biotransform the PCBs into HO-PCBs although HO-PCBs might also originate from placental transfer and/or ingestion of

milk. In agreement with the literature, the capacity of PCB biotransformation seems to be influenced by several factors (age, species, physiological status of the animal, PCB exposure, etc.).

8.5. Appendices

Table S1. Mean detection frequency (f) and limit of quantification (LOQ) for each HO-PCB and PCB congener in serum of northern elephant seal pups.

Congeners	LOQ (pg/mL)	%f
4-HO-CB107	20	100
4-HO-CB120	20	99
4'-HO-CB127	10	0
4'-HO-CB130	10	11
3-HO-CB138	10	0
4-HO-CB146	10	100
4-HO-CB162	5	98
4-HO-CB163	5	62
4'-HO-CB172	5	100
4-HO-CB187	5	89
4-HO-CB193	5	0
4-HO-CB208	5	0
CB-105	2.5	100
CB-107	N.A	\
CB-118	2.5	100
CB-120	N.A	\
CB-138	2.5	100
CB-146	2.5	100
CB-153	2.5	100
CB-157	N.A	\
CB-158	N.A	\
CB-162	N.A	\
CB-163	N.A	\
CB-167	N.A	\
CB-170	2.5	98
CB-172	2.5	0
CB-174	2.5	5
CB-180	2.5	100
CB-183	2.5	99
CB-187	2.5	100
CB-194	2.5	0
CB-199	2.5	15
CB-206	2.5	0
CB-209	2.5	0
PCP	20	100
HCB	20	100

N.A = not analysed

8.6. References

Bennett, E. R., et al., 2009. Chlorinated and brominated organic contaminants and metabolites in the plasma and diet of a captive killer whale (*Orcinus orca*). Marine Pollution Bulletin. 58, 1078-1083.

Bytingsvik, J., et al., 2012. PCBs and OH-PCBs in polar bear mother–cub pairs: A comparative study based on plasma levels in 1998 and 2008. Science of the Total Environment. 417, 117-128.

Cheesman, M. J., Reilly, P. E. B., 1998. Differential inducibility of specific mRNA corresponding to five CYP3A isoforms in female rat liver by RU486 and food deprivation: Comparison with protein abundance and enzymic activities. Biochemical Pharmacology. 56, 473-481.

Connor, K., et al., 1997. Hydroxylated polychlorinated biphenyls (PCBs) as estrogens and antiestrogens: structure-activity relationships. Toxicology and Applied Pharmacology. 145, 111-123.

Covaci, A., et al., 2002. Distribution of organobrominated and organochlorinated contaminants in Belgian human adipose tissue. Environmental Research. 88, 210-218.

Daly, J., et al., 1972. Arene oxides and the NIH shift: the metabolism, toxicity and carcinogenicity of aromatic compounds. Experientia. 28, 1129-1149.

Debier, C., et al., 2006. Mobilization of PCBs from blubber to blood in northern elephant seals (*Mirounga angustirostris*) during the post-weaning fast. Aquatic Toxicology. 80, 149-157.

Debier, C., et al., 2012. Differential changes of fat-soluble vitamins and pollutants during lactation in northern elephant seal mother–pup pairs. Comparative Biochemistry and Physiology Part A. 162, 323-330.

Ding, X., et al., 2006. Regulation of constitutive androstane receptor and its target genes by fasting, cAMP, hepatocyte nuclear factor α, and the coactivator peroxisome proliferator-activated receptor γ coactivator-1α. Journal of Biological Chemistry. 281, 26540-26551.

Dirtu, A. C., et al., 2013. Dynamics of organohalogenated contaminants in human serum from obese individuals during one year of weight loss treatment. Environmental Science & Technology. 47, 12441-12449.

Dirtu, A. C., et al., 2010. Distribution of PCBs, their hydroxylated metabolites, and other phenolic contaminants in human serum from two European countries. Environmental Science & Technology. 44, 2876-2883.

Dupont, A., et al., 2013. Relationships between in vitro lymphoproliferative responses and levels of contaminants in blood of free-ranging adult harbour seals (Phoca vitulina) from the North Sea. Aquatic Toxicology. 142–143, 210-220.

Gabrielsen, K. M., et al., 2011. Levels and patterns of hydroxylated polychlorinated biphenyls (OH-PCBs) and their associations with thyroid hormones in hooded seal (*Cystophora cristata*) mother-pup pairs. Aquatic Toxicology. 105, 482-491.

Hoekstra, P. F., et al., 2003. Hydroxylated and methylsulfone-containing metabolites of polychlorinated biphenyls in the plasma and blubber of bowhead whales (*Balaena mysticetus*). Environmental Toxicology and Chemistry. 22, 2650-2658.

Houde, M., et al., 2006. Polychlorinated biphenyls and hydroxylated polychlorinated biphenyls in plasma of bottlenose dolphins (*Tursiops truncatus*) from the Western Atlantic and the Gulf of Mexico. Environmental Science & Technology. 40, 5860-5866.

Kunisue, T., Tanabe, S., 2009. Hydroxylated polychlorinated biphenyls (OH-PCBs) in the blood of mammals and birds from Japan: lower chlorinated OH-PCBs and profiles. Chemosphere. 74, 950-961.

La Merrill, M., et al., 2013. Toxicological function of adipose tissue: focus on persistent organic pollutants. Environmental Health Perspectives. 121, 162-169.

Lans, M. C., et al., 1993. Structure-dependent, competitive interaction of hydroxy-polychlorobiphenyls, -dibenzo-*p*-dioxins and -dibenzofurans with human transthyretin. Chemico-Biological Interactions. 88, 7-21.

Larsson, C., et al., 2004. Enantiomeric specificity of methylsulfonyl-PCBs and distribution of bis (4-chlorophenyl) sulfone, PCB, and DDE methyl sulfones in grey seal tissues. Environmental Science & Technology. 38, 4950-4955.

Letcher, R., et al., Methyl sulfone and hydroxylated metabolites of polychlorinated biphenyls. O. Hutzinger and J. Paasivirta Eds., Springer Berlin / Heidelberg, 2000, 315-359.

Letcher, R. J., et al., 2010. Exposure and effects assessment of persistent organohalogen contaminants in arctic wildlife and fish. Science of the Total Environment. 408, 2995-3043.

Løken, K. B., et al., 2008. How important are the hydroxylated PCB metabolites in harbour seals (*Phoca vitulina*)? Organohalogen Compounds. 70, 25-8.

Louis, C., et al., 2014. Mobilisation of lipophilic pollutants from blubber in northern elephant seal pups (*Mirounga angustirostris*) during the post-weaning fast. Environmental Research. 132, 438-448.

Maervoet, J., et al., 2004. A reassessment of the nomenclature of polychlorinated biphenyl (PCB) metabolites. Environmental Health Perspectives. 112, 291-294.

McKinney, M. A., et al., 2006. Organohalogen contaminants and metabolites in beluga whale (*Delphinapterus leucas*) liver from two Canadian populations. Environmental Toxicology and Chemistry. 25, 1246-1257.

Meerts, I. A., et al., 2004. Developmental exposure to 4-hydroxy-2, 3, 3′, 4′, 5-pentachlorobiphenyl (4-OH-CB107): long-term effects on brain development, behavior, and brain stem auditory evoked potentials in rats. Toxicological Sciences. 82, 207-218.

Milsap, R. L., Jusko, W. J., 1994. Pharmacokinetics in the infant. Environmental Health Perspectives. 102 Suppl 11, 107-10.

Narasimhan, T., et al., 1991. Effects of hydroxylated polychlorinated biphenyls on mouse liver mitochondrial oxidative phosphorylation. Journal of Biochemical Toxicology. 6, 229-236.

Nomiyama, K., et al., 2010. Polychlorinated biphenyls and their hydroxylated metabolites (OH-PCBs) in the blood of toothed and baleen whales stranded along Japanese coastal waters. Environmental Science & Technology. 44, 3732-3738.

Noren, D. P., et al., 2003. Energy reserve utilization in northern elephant seal (*Mirounga angustirostris*) pups during the postweaning fast: size does matter. Journal of Comparative Physiology B. 173, 443-454.

Nyman, M., et al., 2000. Expression and inducibility of members in the cytochrome P4501 (CYP1) family in ringed and grey seals from polluted and less polluted waters. Environmental Toxicology and Pharmacology. 8, 217-225.

Nyman, M., et al., 2001. Characterization of xenobiotic-metabolizing cytochrome P450 (CYP) forms in ringed and grey seals from the Baltic Sea and reference sites. Comparative Biochemistry and Physiology Part C. 128, 99-112.

Park, J.-S., et al., 2009. Polychlorinated biphenyls (PCBs) and their hydroxylated metabolites (OH-PCBs) in livers of harbor seals (*Phoca vitulina*) from San Francisco Bay, California and Gulf of Maine. Marine Environmental Research. 67, 129-135.

Renner, G., 1988. Hexachlorobenzene and its metabolism. Toxicological & Environmental Chemistry. 18, 51-78.

Routti, H., et al., 2013. Effect of reduced food intake on toxicokinetics of halogenated organic contaminants in herring gull (*Larus argentatus*) chicks. Environmental Toxicology and Chemistry. 32, 156-164.

Routti, H., et al., 2010. Hormone, vitamin and contaminant status during the moulting/fasting period in ringed seals (*Pusa [Phoca] hispida*) from Svalbard. Comparative Biochemistry and Physiology Part A. 155, 70-76.

Routti, H., et al., 2008. Biotransformation of PCBs in Relation to Phase I and II Xenobiotic-Metabolizing Enzyme Activities in Ringed Seals (*Phoca hispida*) from Svalbard and the Baltic Sea. Environmental Science & Technology. 42, 8952-8958.

Routti, H., et al., 2009. Concentrations, patterns and metabolites of organochlorine pesticides in relation to xenobiotic phase I and II enzyme activities in ringed seals (*Phoca hispida*) from Svalbard and the Baltic Sea. Environmental Pollution. 157, 2428-2434.

Ruus, A., et al., 2002. Factors influencing activities of biotransformation enzymes, concentrations and compositional patterns of organochlorine contaminants in members of a marine food web. Aquatic toxicology. 61, 73-87.

Safe, S., 1989. Polyhalogenated aromatics: uptake, disposition and metabolism. Halogenated Biphenyls, Terphenyls, Naphthalenes, Dibenzodioxins and Related Products. 131-159.

Sandala, G. M., et al., 2004. Hydroxylated and methyl sulfone PCB metabolites in adipose and whole blood of polar bear (*Ursus maritimus*) from East Greenland. Science of the Total Environment. 331, 125-141.

Sandau, C. D., et al., 2000a. Analysis of hydroxylated metabolites of PCBs (OH-PCBs) and other chlorinated phenolic compounds in whole blood from Canadian inuit. Environmental Health Perspectives. 108, 611-616.

Sandau, C. D., et al., 2002. Pentachlorophenol and hydroxylated polychlorinated biphenyl metabolites in umbilical cord plasma of neonates from coastal populations in Quebec. Environmental Health Perspectives. 110, 411-417.

Sandau, C. D., et al., 2000b. Identification of 4-hydroxyheptachlorostyrene in polar bear plasma and its binding affinity to transthyretin: A metabolite of octachlorostyrene? Environmental Science & Technology. 34, 3871-3877.

Schuur, A. G., et al., 1998. *In vitro* inhibition of thyroid hormone sulfation by hydroxylated metabolites of halogenated aromatic hydrocarbons. Chemical Research in Toxicology. 11, 1075-1081.

Tampal, N., et al., 2002. Glucuronidation of hydroxylated polychlorinated biphenyls (PCBs). Chemical Research in Toxicology. 15, 1259-1266.

Teramitsu, I., et al., 2000. Identification of novel cytochrome P450 1A genes from five marine mammal species. Aquatic Toxicology. 51, 145-153.

Tilley, R. E., et al., 2002. Isolation of two cytochrome P450 cDNAs, CYP1A1 and CYP1A2, from harp seal (*Phoca groenlandica*) and grey seal (*Halichoerus grypus*). Comparative Biochemistry and Physiology Part C. 132, 181-191.

Uhl, S., et al., 1986. Pharmacokinetics of pentachlorophenol in man. Archives of Toxicology. 58, 182-186.

Van den Berg, K., et al., 1991. Interactions of halogenated industrial chemicals with transthyretin and effects on thyroid hormone levels *in vivo*. Archives of Toxicology. 65, 15-19.

Van der Plas, S. A., et al., 2001. Effects of subchronic exposure to complex mixtures of dioxin-like and non-dioxin-like polyhalogenated aromatic compounds on thyroid hormone and vitamin A levels in female Sprague-Dawley rats. Toxicological Sciences. 59, 92-100.

Vanden Berghe, M., et al., 2013. Effects of polychlorobiphenyls, polybromodiphenylethers, organochlorine pesticides and their metabolites on vitamin A status in lactating grey seals. Environmental Research. 120, 18-26.

Vanden Berghe, M., et al., 2012. Selective transfer of persistent organic pollutants and their metabolites in grey seals during lactation. Environment International. 46, 6-15.

Vijayan, M. M., et al., 2006. Fasting augments PCB impact on liver metabolism in anadromous Arctic char. Toxicological Sciences. 91, 431-439.

Weijs, L., et al., 2009. Concentrations of chlorinated and brominated contaminants and their metabolites in serum of harbour seals and harbour porpoises. Environment International. 35, 842-850.

Wolkers, H., et al., 2000. Chlorinated pesticide concentrations, with an emphasis on polychlorinated camphenes (toxaphenes), in relation to cytochrome P450 enzyme activities in harp seals (*Phoca groenlandica*) from the Barents Sea. Environmental Toxicology and Chemistry. 19**,** 1632-1637.

Wolkers, J., et al., 1998. Phase I and phase II enzyme activities in ringed seals (*Phoca hispida*): characterization of hepatic cytochrome P450 by activity patterns, inhibition studies, mRNA analyses, and western blotting. Aquatic Toxicology. 44**,** 103-115.

Zamek-Gliszczynski, M. J., et al., 2006. Integration of hepatic drug transporters and phase II metabolizing enzymes: Mechanisms of hepatic excretion of sulfate, glucuronide, and glutathione metabolites. European Journal of Pharmaceutical Sciences. 27**,** 447-486.

Chapter 9

General discussion and Perspectives

9.1. General discussion

The aim of this work was to investigate the behaviour of persistent lipophilic pollutants within adipose tissue during periods of negative energy balance. More particularly, we focused our study on investigating (i) the kinetics of release of lipophilic pollutants from adipocytes, (ii) the potential relationships between the mobilisation of lipophilic pollutants and the one of fatty acids, and (iii) the probable biotransformation of pollutants, after their release from the adipose tissue. For that purpose, we combined an *in vivo* approach with young NES during their post-weaning fast and *in vitro* models using rat and NES adipocytes in culture. Both approaches are complementary, as the *in vivo* model represents the "real world", whereas the *in vitro* model allows simplifying complex situations in order to get into mechanistic interpretation.

The present discussion is not structured in the same order as in the chapters of objectives and results, but rather under the form of main outcomes and "take-home" messages.

OUTCOME 1 – Within the blubber of NES, the inner and outer layers exhibited different profiles of lipophilic pollutants and FAs over the post-weaning fast.

After birth, NES pups are fed with maternal milk, as all mammals. This milk is characterised by a high content of lipid (30-60%). The excess of energy that the pup receives through the ingestion of milk is stored in large depot of adipose tissue. Lipophilic pollutants are also transferred to the offspring through the milk and preferentially stored in the blubber of the pups (Debier et al., 2006; Debier et al., 2012). After the suckling period, weaned NES pups undergo an extended fast, in which they mobilise their adipose tissue to meet the needs of the organism. Their lipid mass is reduced from 24-49% (Noren et al., 2003).

In Chapter 3, we examined the changes of concentrations of lipophilic pollutants within the blubber of NES throughout the post-weaning fast. Since several studies have shown that vertical stratification takes place within the blubber of phocid seals (e.g. Debier et al. (2012), Fowler et al. (2014) and Vanden Berghe et al. (2012)), we distinguished the inner blubber layer from the outer blubber layer. We observed that PBDEs, PCBs and OCPs were evenly distributed within the both blubber layers at early fast. A similar observation was already reported for PCBs in a previous study with weaned NES pups (Debier et al., 2006). These findings suggest that, during the suckling period, the lipophilic pollutants ingested by NES pups through the milk were homogenously spread within the fat depot. Over the fast, the concentrations of PBDEs, PCBs and OCPs, expressed per unit of lipid weight, increased in blubber, especially in the inner layer. This most probably results from the fact that there is a more important mobilisation of lipids than of lipophilic pollutants, which tend to remain and concentrate in the shrinking adipose tissue. The mobilisation of lipids from adipocytes during the fast was reflected by the decrease of adipocyte size with time, as noticed during our morphometric study. It seems important to note that the release of POPs involves only a physical process (i.e. the movement from intercellular space to extracellular space), whereas the release of lipids

implicates first a chemical process (i.e. the lipolysis of TGs) followed by a physical process.

As a result of the more pronounced increase of pollutants in inner blubber compared to outer blubber, their concentrations became greater in inner blubber than in outer blubber at late fast. The hydrolysis of TGs does not occur homogeneously within the blubber column. The inner blubber is usually considered as more metabolically active during lipolysis compared to the outer blubber and thus, submitted to a higher mobilisation of TGs, leading to a sharper increase of the concentrations of lipophilic pollutants. This hypothesis was supported by our morphometric study, in which we pointed out that the distributions of cell profile areas were different between the both layers. Moreover, we demonstrated that a large number of considered FAs was mobilised from the TGs stored in inner blubber between early and late fast, whereas most FAs tended to be conserved in outer blubber. A greater amplitude of the fractional mobilisation of FAs was also observed in inner blubber as compared to outer blubber. All these observations confirm that the lipolytic activity was higher in inner than in outer blubber, leading to sizes of adipocytes different between the layers (Figure 9.1). It seems however that these differences of FA mobilisation in the blubber layers were not inherent to the levels of expression of ATGL and HSL, two lipolytic enzymes involved in the hydrolysis of TGs. Indeed, these levels of expression remained constant over the fast within a given layer and between the both layers for a given time. However, further investigations on the activity of these enzymes are needed to clarify their involvement in the different rates of mobilisation noted between inner and outer blubber.

Figure 9.1 illustrates the changes of blubber morphology between early and late fast. Cells from the both layers are concerned by lipid mobilisation and become smaller. However, as explained here above, the phenomenon is more pronounced in inner blubber, which is more vascularised and submitted to a higher rate of lipolysis (and thus cell shrinking) than outer blubber. The mid-blubber layer has not been analysed but might constitute an intermediate situation between the inner and outer layers.

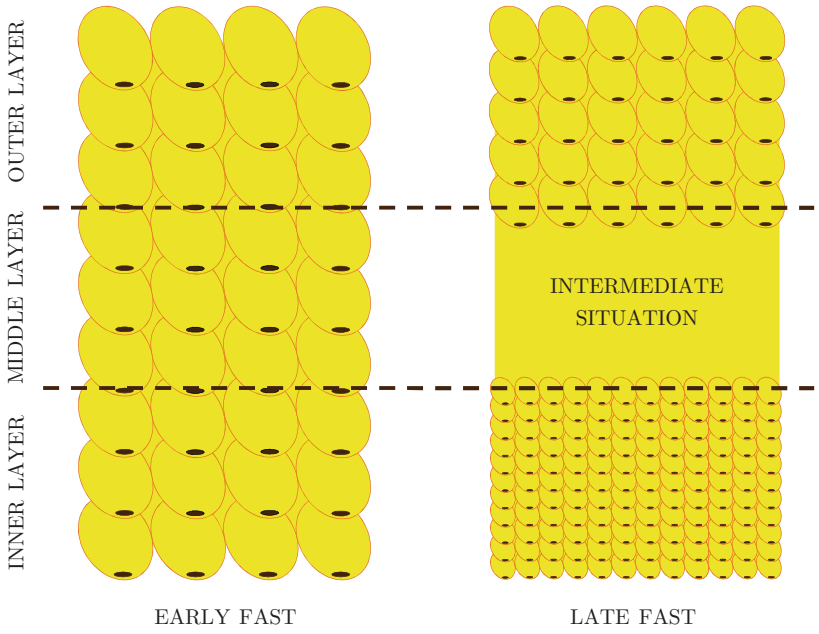

Figure 9.1 – Schematic illustration of the impact of the different metabolic activities in lipolysis over the blubber core. Over the fast, the triglyceride mobilisation seemed to be more important in the inner blubber layer than in the outer blubber layer. This leaded to a greater decrease of adipocyte size in inner blubber than in outer blubber. The middle blubber layer was not analysed but can be considered as an intermediate situation.

OUTCOME 2 – The concentrations of lipophilic pollutants increased within adipose tissue during an *in vivo* period of fast, while it decreased within adipocytes during an *in vitro* lipolytic treatment.

As already mentioned in OUTCOME 1, we noted an increase of concentrations of PBDEs, PCBs and OCPs (expressed per lipid weight but also per wet weight, as the lipid content did not change with time; see OUTCOME 3) in the blubber of NES pups between early and late fast, which most probably results from the less efficient mobilisation of lipophilic pollutants as compared to lipids. In parallel, an increase of concentrations was noted in serum over the fast. In addition to this *in vivo* study, differentiated rat adipocytes were contaminated with given lipophilic pollutants (i.e. three congeners of PCBs) and a lipolytic treatment was induced in order to mimic a situation of negative energy balance. Consequently, TGs contained in adipocytes were hydrolysed, leading to the release of FAs and glycerol into the culture medium. Following this lipid mobilisation, the concentrations of lipophilic pollutants decreased within the cells and increased in the extracellular medium. The comparison of both models indicates that the release of FAs from TGs was more effective than that of lipophilic pollutants in the *in vivo* model, leading to a partial retention of lipophilic pollutants and an increase of their concentrations. In the *in vitro* model, we observed similar dynamics of release between lipids and PCBs, as they both decreased in cells, especially during the first part of lipolysis. In addition, when the levels of PCBs were expressed per unit of cell NLs (results not shown in Chapter 6), the concentrations decreased throughout lipolysis.

At first glance, the *in vivo* and *in vitro* results seem to be contradictory, as we observed an increase of lipophilic pollutant concentrations per unit of lipids within cells *in vivo* and a decrease of lipophilic pollutant concentrations per unit of lipids within cells *in vitro*. Several explanations were already suggested in Chapter 6 to interpret these differences. Firstly, the organisation of the studied matrices is thoroughly different. *In vivo*, the blubber is a complex 3D-structure with several layers of adipocytes that are heterogeneously irrigated by blood vessels. The organisation of the *in vivo*

matrix could promote the partial retention of lipophilic pollutants and thus, lead to an increase of pollutant concentrations with time. Furthermore, the released lipophilic pollutants may be reabsorbed by neighbouring adipocytes due to the large remaining amount of fat present all around in this tissue. *In vitro*, we cultivated a simple monolayer of cells, which are continuously in contact with the lipolytic medium that is regularly renewed. The lipolysis induced *in vitro* was highly efficient, leading to an important and rapid decrease of cellular neutral lipids (a loss of 57 ± 3% in 12 hours). This large TG mobilisation could further promote the release of PCBs, as compared to the *in vivo* situation in which the TG mobilisation was more progressive and smooth (a slight decrease of cell profile areas in 7 weeks). In addition, adipocyte reuptake of FAs and PCBs, which were released in the medium of the *in vitro* model, is probably prevented through the frequent renewals of the culture medium. The initial concentrations within adipocytes also differed between the *in vivo* and *in vitro* situations. Despite the fact that the concentrations of PCBs added into the culture medium were chosen to reflect the *in vivo* situations, the concentrations found in differentiated adipocytes after 12 hours of exposure were much higher than what was found *in vivo* (525 ng PCB-28+PCB-118+PCB-153/mg neutral lipids in *in vitro* adipocytes against 0.02-0.66 ng total PCBs/mg lipids in human adipose tissue; Arrebola et al. (2012), De Saeger et al. (2005), Malarvannan et al. (2013), Moon et al. (2012) and Wang et al. (2010)). Explanations for such high differences are provided elsewhere (Bourez et al., 2012b). The high PCB concentrations in cultivated adipocytes may also exacerbate their release into the culture medium, leading to a net decrease of their concentrations within adipocytes. Finally, some physiological (e.g. pathway of lipid accumulation within adipocytes) and experimental (e.g. duration of POP exposure) differences between NES and rats could also explain the different beahaviour of lipophilic pollutants within adipocytes. The set-up and the use of the *in vitro* model of differentiate NES adipocyte should help us to bring an answer to this hypothesis.

Because of its simplicity, the *in vitro* model does not rigorously reflect the *in vivo* situation. It is however useful to work in controlled conditions, among others to investigate potential interactions between contaminants. In

the framework of this thesis, we studied the effect of the presence of other PCBs on the mobilisation of individual congeners. We did not find any significant difference between the situations in which PCBs were added alone to the cells (either PCB-28, - 118 or -153) or in cocktail (the three congeners together). However, additional investigations would be necessary as it concerns only preliminary results on a small number of molecules.

OUTCOME 3 – The massic proportions of lipids within the blubber of NES pups remained stable over the fast, despite the fact that lipids were mobilised. In the *in vitro* model, the lipid proportion decreased within adipocytes during the lipolytic treatment.

The lipid content in the blubber of weaned NES pups was assessed at the different stages of the fast in order to calculate the concentrations of lipophilic pollutants. At early fast, we analysed the proportions of lipids within a certain number of adipocytes, which were sampled by 6-mm biopsy punches. Each adipocyte contained given amounts of lipids and lipophilic pollutants. At late fast, since weaned NES pups mobilised TGs from blubber, the size of adipocytes decreased, as confirmed by the morphometric study of the blubber and the increase of FAs (i.e. the products of TG hydrolysis) in blood. The sampling at late fast was also performed with 6-mm biopsy punches. This method allows taking off blubber biopsies of same diameter. The lipid content did not change between early and late fast, despite the hydrolysis of TGs and mobilisation of FAs. Constant lipid levels were also reported in blubber of fasting NES adult females between early and late lactation (Crocker et al., 2001). The proportion of connective tissue is small in NES blubber (< 5%; D. Crocker, personal communication) and the adipocytes are the main cell type of this tissue. We most likely sampled a higher number of cells at late fast than at early fast (Figure 9.2). To confirm this, a parameter independent of the lipolytic pathway, such as DNA quantification, could be used to normalise the number of cells. The decrease of the quantity of TGs within each cell was thus not observed when expressing the lipids per unit of sample weight. Instead, expressing the lipids per unit of DNA would have most likely led to different results. Vanden Berghe et al. (2012) noticed a decrease of lipid levels in inner and outer blubber in lactating grey seals. The proportion of connective tissue might be higher in this species.

To conclude, it can be seen, through the example drawn in Figure 9.2 that, even if the quantity of TGs per cell most probably decreased throughout the fast, the fact that we sampled a higher number of cells at late fast contributed to obtain constant lipid levels per unit of sample

weight. The observed increase of POP concentrations in inner blubber, despite their mobilisation into the circulation (as reflected by the increase of POP levels with time), appears to result from a combination of two phenomena:

- the less efficient mobilisation of POPs than cell TGs and
- the sampling of a higher number of cells, which have a smaller size, at late fast.

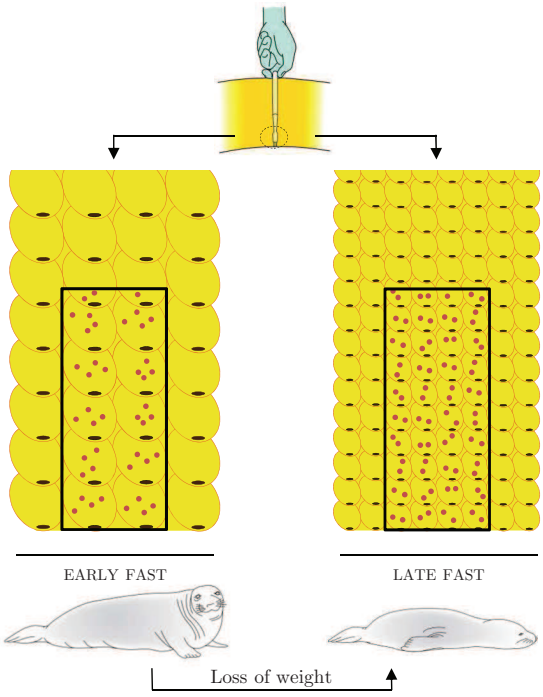

Figure 9.2 – Schematic representation of the impact of the fast on the adipocytes and lipophilic pollutants (red dots). At early and late fast, blubber biopsies were sampled with 6-mm biopsy punches. Through the fast, TGs were mobilised leading to a decrease of the size of adipocytes. Consequently, a higher amount of cells were analysed at late fast compared to early fast, preventing to observe the decrease of TG within each cell. The close-up represents adipocytes from the inner blubber layer.

The *in vitro* situation is somewhat different. Before the induction of lipolysis, the amounts of lipids and PCBs are measured per well of 6-well plates. Although cells were seeded at the same density in each well, the protein contents were determined in order to normalise the number of cells per well. The progressions of the lipid and lipophilic pollutant contents were assessed throughout the lipolytic process. As clearly disclosed by the time-lapse movie, the size of lipid droplets was lessened due to an effective mobilisation of TGs. This was confirmed by the measure of cell lipids every 3 hours, expressed per unit of protein. Through this experimental protocol, we were able to evaluate the amounts of lipids and lipophilic pollutants within a given number of cells per well over the lipolytic pathway (Figure 9.3).

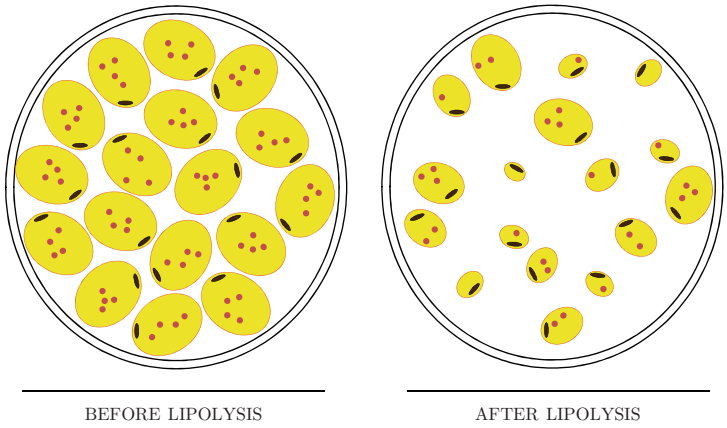

Figure 9.3 – Schematic representation of the impact of lipolytic treatment on the adipocytes in *in vitro* model. Before lipolysis, a given amount of lipophilic pollutants (red dots) were spread within a given number of cells in a well of a 6-well plate. Over the lipolytic process, TGs are mobilised leading to a decrease of the size of lipid droplets. Consequently, the lipophilic pollutants were mobilised to extracellular medium, resulting in a decrease of the concentration of lipophilic pollutants in cells.

NB: this is a simplified schematic representation as we did not detail the lipid droplets and their shrinking with time.

OUTCOME 4 – The linked destinies of lipophilic pollutants and fatty acids: their degree of lipophilicity is a major factor determining their mobilisation from adipocytes during a lipolytic process.

An important observation to be drawn from our study is the selective mobilisation of FAs from blubber during the post-weaning fast of NES. We indeed noted different fractional mobilisations between FAs. Moreover, our data showed a decrease of concentrations of certain FA classes (SFAs, MC-MUFAs and ω-3 PUFAs) within inner blubber, whereas the concentrations of other FA classes remained stable or increased (ω-6 PUFAs and LC-MUFAs, respectively). Raclot (2003) suggested that the discrimination in the released FAs that he observed in rat and human adipocytes could be linked to the molecular structure of FAs. Indeed, Raclot's study showed that the relative mobilisations of FAs increase with the number of unsaturation for a given chain length and decrease with the chain length for a given number of unsaturation. Nevertheless, such trend was not noted in the present study. The comparison between the fractional mobilisation of each FA and their log P values however highlighted that FAs with higher degree of lipophilicity (i.e. the higher values of log P) tended to be conserved within the blubber, whereas the less lipophilic FAs (i.e. with the lower values of log P) seemed to be readily mobilised from adipocytes. As discussed in Chapter 7, this agrees with the lipolytic process that involves water-soluble enzymes acting at the interphase formed by cytosol and lipid droplet. This selective mobilisation of FAs leads to a reshuffle of the FA profiles within adipocytes (especially in the inner blubber layer). Those enriched themselves with more lipophilic FAs and thus, acquired a higher lipophilic character over the fast.

A selective mobilisation from adipocytes was also noticed for lipophilic pollutants. Indeed, our study showed that the more chlorinated PCBs and more brominated PBDEs were preferentially retained within the blubber, while the less chlorinated PCBs and less brominated PBDEs were more easily released. An exponential decrease of transfer ratio from inner blubber to serum also occurred with the increase of the log K_{ow} values of the molecules. A similar relationship was also noticed for lactating grey seal females (Vanden Berghe et al., 2012).

The lipophilicity of TGs and pollutants appears to be a key factor determining their fate within adipocytes. More lipophilic TGs and more lipophilic pollutants are probably situated in the lipid droplet core, whereas less lipophilic TGs and less lipophilic pollutants are most likely situated closer to the interface, where the lipases act. Nevertheless, we have to keep in mind that, in addition to the lipophilicity, other physico-chemical parameters could also influence the mobilisation of lipophilic pollutants from adipocytes such as the bulk and the configuration of the molecules.

A selectivity of the release of PCBs from adipocytes was also noticed, however to a lower extent, in our *in vitro* model. At the beginning of lipolysis, PCB-153 (the more lipophilic congener) was less efficiently released in the culture medium than PCB-28 and -118. Nevertheless, this difference disappeared at the end of lipolysis. In our *in vitro* model, the FA profile of adipocytes is rather basic, as they result mainly from *de novo* synthesis. Three FAs (i.e. C16:0, C16:1n-7 and C18:1n-9) composed more than 85% of the TG fraction. The range of FAs with different lipophilicities is thus weak *in vitro*. This could explain the slight differences regarding the dynamics of PCB mobilisation during lipolysis. A modification of FA content to get closer to the *in vivo* situation might inform us about the involvement of FAs on the release of lipophilic pollutants.

OUTCOME 5 – The levels of hydroxylated PCBs increased in the serum of weaned NES pups over the fast.

Although the levels of PCBs were already evaluated in the serum of weaned NES pups (Debier et al., 2006), this works is the first to investigate the presence of HO-PCBs in those young animals and to find an increase of their concentrations in the serum over the fast, with a more important rise for the less chlorinated congeners compared to the more chlorinated ones. Some hypothesis can be put forward to explain this rise. NES pups could be contaminated via a placental transfer and/or through the transfer of small amounts in the milk. Once in the organism, HO-PCBs could accumulate in blood and liver as shown in grey seals and harbour seals (Park et al., 2009; Vanden Berghe et al., 2012). During the post-weaning fast, stored HO-PCBs could then be mobilised from tissues and thus, accumulate in the blood compartment due to their affinity for TTR and other transport proteins. Furthermore, biotransformation could also happen in NES pups, since it has been shown that pinnipeds synthesise different forms of CYP enzymes (e.g. Nyman et al. (2000) and Wolkers et al. (1998)). Weaned NES pups might thus be able to produce HO-PCBs from the parent molecules through the CYP enzymes. There are two different pathways to obtain HO-PCBs: either (i) by direct insertion of HO- on the biphenyl group, or (ii) by the formation of an epoxide intermediate. According to our results, a preferential biotransformation pathway does not seem to exist in weaned NES pups. The fast could promote this formation through the fact that PCBs become more available since they are mobilised from blubber and by the upregulation of genes and activity of biotransformation enzymes. Moreover, the biotransformation abilities could intensify with age. These hypotheses were supported by the increase of the HO-PCB/PCB ratio in blood circulation during the second part of the fast. Nevertheless, to date, no study has demonstrated the presence of biotransformation activity in weaned NES pups.

Outcomes 6 and 7 concern the technical achievements that have been conducted in the framework of this thesis in order to build the *in vitro* tools.

OUTCOME 6 – The cocktail of differentiation and serum of NES were essential to obtain NES adipocytes *in vitro*.

In order to obtain a functional *in vitro* model of differentiated NES adipocytes, we tested the protocol of differentiated rat adipocytes set up by Sophie Bourez (Bourez et al., 2012a). We isolated the progenitor cells from blubber biopsies taken in the field on free-ranging weaned NES pups through digestions with collagenase followed by filtrations and centrifugations. During the first days, cells exhibited a fibroblastoid phenotype. When treated with a cocktail of differentiation (i.e. dexamethasone, IBMX, ciglitizone and insulin), they began to accumulate lipids in the following days. Without the cocktail of differentiation, no lipid droplet was observed. Interestingly, the better accumulation of lipids within cells was obtained by the combination of the cocktail of differentiation and weaned NES serum. It seems that, among other factors, the high content of TGs in NES serum could promote the lipid accumulation within cells. Nevertheless, cells considered as adipocytes remained attached to the plastic of the wells rather than rounding up and sitting more on top of the adjacent cells as seen in cultures of mouse embryonic fibroblasts or in cultures of mesenchymal stem cells. In addition, the differentiation rate remained very low, as the rest of cells accumulated lipids but kept a fibroblastic shape instead of a round shape, typical of adipocytes. Our preliminary results seem to indicate that NES progenitor cells exhibit specific physiology. Indeed, even if the differentiation promoting factors had an effect, it was not as significant as for rat cells. The fact that NES are insulin resistant might be part of the explanation. Uptake and storage of fat in lipid droplets are the defining feature of adipocytes. The confirmation of the adipocyte genotype of these cells is required to consider them as differentiated NES adipocytes. Furthermore, an improvement of the differentiation rate and a control of the stability of this differentiation rate would be preferable before using as an *in vitro* model of adipocytes. Some perspectives of improvement are described in the section 9.2 of this thesis.

OUTCOME 7 – A lipolytic medium combined with isoproterenol efficiently triggered the lipolytic pathway on differentiated rat adipocytes on a short-term period. Its use was however not essential on a longer-term period since a renewal of lipolytic medium without isoproterenol was as efficient in terms of lipid mobilisation that a renewal of lipolytic medium with isoproterenol.

In order to study the behaviour of lipophilic pollutants during a period of negative energy balance within adipocytes, we set up a performing and functional model of *in vitro* lipolysis in primary cultures of rodent adipocytes. Two parameters were tested to achieve the best breakdown of TGs, i.e. the regular renewal of lipolytic medium and the use of isoproterenol, a well-known synthetic catecholamine. The condition with isoproterenol was duplicated over 12 hours, once with medium renewal every 3 hours and once without medium change. During the first 3 hours of treatment, the use of isoproterenol significantly triggered the hydrolysis of cell TGs. Over the 12 hour-period, the effect of isoproterenol was less important. Instead, the regular medium renewal became majority to unload TGs from adipocytes. After 12 hours, there was no significant difference of cell NLs between the condition with medium renewal + isoproterenol and the condition with medium renewal – isoproterenol. These results confirmed that the culture medium used in these experiments is indeed a lipolytic medium. Moreover, the regular addition of BSA could also promote the lipolytic pathway through the binding of free FAs released from adipocytes. Nevertheless, when the lipolytic medium supplemented with isoproterenol remained in contact with cells, we noted firstly a mobilisation of TGs followed by an increase of TGs, suggesting a reesterification within adipocytes. We thus highlighted the importance of the renewal of lipolytic medium to maintain the unloading of TGs from fat cells. Isoproterenol and regular lipolytic medium renewal are both efficient strategies to trigger the hydrolysis of cellular triglycerides in *in vitro* adipocytes. Such lipolytic model can be used to study the cellular mechanisms involved in the release of lipophilic compounds during a drastic lipolysis.

The major take-home messages of this thesis are:

- Because of its typical lifestyle, NES offers a good model for studies about the toxicokinetics of lipophilic pollutants from adipose tissue during periods of negative energy balance. In parallel with this *in vivo* model, we developed an efficient *in vitro* lipolytic model, which is an useful tool to study, among others, the behaviour of lipophilic pollutants during lipid mobilisation.

- During the post-weaning fast, lipophilic pollutants (PBDEs, PCBs and OCPs) were released from blubber of weaned NES pups, leading to an increase of their concentrations into the circulation. The unloading of lipids was however more efficient than the one of lipophilic pollutants, which were partially retained within the adipose tissue. This was reflected by an increase of their concentrations per unit of lipids within blubber.

- *In vivo*, the dynamics of mobilisation of lipophilic pollutants mainly depended on their degrees of lipophilicity. The most lipophilic molecules tended to be retained within adipocytes. This selectivity was also seen for the hydrolysis of TGs and mobilisation of FAs. The less lipophilic FAs were mainly released from adipocytes, leading to an enrichment of lipid droplets with the more lipophilic FAs. However, the differences of kinetic of release were less obvious in *in vitro* model since the range of FAs was narrow.

- The blubber column exhibited different properties and composition between the layers. The inner blubber layer showed a higher metabolic activity of lipolysis than the outer blubber layer. This was reflected by a larger number of FAs mobilised in higher amounts during the fast and, consequently, a greater increase of concentrations of lipophilic pollutants.

- A rise of HO-PCBs was noted in blood of weaned NES over the fast. A possible biotransformation of parent PCBs, exacerbated with the fast and growing of the animals, was suggested.

- The set-up of preliminary data regarding the *in vitro* differentiation of NES progenitor cells into adipocytes is encouraging. The presence of NES serum and the cocktail of differentiation were necessary to promote the lipid accumulation within adipocytes. Nevertheless, further improvements are needed to reach a higher and stable rate of adipocyte differentiation.

- In *in vitro* model, the use of isoproterenol combined with a lipolytic medium showed an efficient lipolytic action on a short period. Nevertheless, the renewal of lipolytic medium became more essential than isoproterenol in terms of lipid mobilisation on a longer period.

9.2. Perspectives

The findings presented all through this thesis provide interesting information regarding the behaviour of lipophilic pollutants within the adipose tissue during periods of negative energy balance. Otherwise, further investigations could help us to better understand the link between lipophilic pollutants and adipose tissue in *in vivo* and *in vitro* models. Thereafter, there is a list of non-exhaustive suggestions.

9.2.1. *In vivo* research

Our study focused on the quantification of several lipophilic pollutants. Nevertheless, more molecules currently contaminate the biota. In order to complete our study, it could be interesting to monitor the levels of contamination of other pollutants in weaned NES pups. We can cite the large family of flame retardants, in which we already studied PBDEs. The reasons for concern regarding such molecules are their persistency, their bioaccumulation and their toxicity (Law et al., 2006). A few studies have measured the concentrations of hexabromocyclododecane (HBCD) in the blubber of marine mammals (e.g. harbour porpoise, common dolphin, humpback dolphins and finless porpoises) (Lam et al., 2009; Law et al., 2006; Zegers et al., 2005). Law et al. (2006) reported a possible time trend: a sharp increase of HBCD concentrations was noted from about 2001 in the blubber of harbour porpoises. Similarly, a significant increasing trend of HBCD was observed in humpback dolphins from 1997 to 2007 (Lam et al., 2009). In addition, since the worldwide restriction on the production and use of PBDEs (Covaci et al., 2011), several halogenated flame retardants are used as alternatives for PBDEs such as 1,2-bis(2,4,6-tribromophenoxy)ethane (BTBPE), decabromodiphenyl ethane (DBDPE), bis-(2-ethylhexyl) tetrabromophtalate (TBPH), 2-ethylhexyl-2,3,4,5-tetrabromobenzoate (TBB). It thus seems important to monitor the bioaccumulation of such emergent pollutants in the blubber of NES, and more generally in marine mammals, since they have already been detected in the blubber of humpback dolphins and finless porpoises. In addition, an increasing temporal shift trend

from conventional to emerging flame retardants has been discovered in marine mammals (Zhu et al., SETAC Europe 2014, abstract book). Investigating heavy metals would be important too. A first study showed that the NES is relatively highly contaminated by mercury compared to other species (Habran et al., 2011). A thesis conducted at UCSC, in collaboration with our laboratory, is currently investigating the relationships between contaminations of NES (adults – males and females – and pups) by PBDEs, PCBs, OCPs and mercury and the feeding ecology of the individuals (migration patterns, trophic levels and feeding depths).

During the post-weaning fast, an increase of HO-PCB concentrations was observed in the circulation of weaned NES pups. We assumed that they are able to biotransform PCBs to some extent. An important progress would be to determine the activity of CYP in NES in order to confirm our hypothesis.

We suggested in the present study that at week 1 of the post-weaning fast, NES pups have already expressed all the enzymatic mechanisms for an efficient lipolysis, as the expression levels of ATGL and HSL remained constant throughout the fast. It should be interesting to compare these levels with those of suckled NES pups. Moreover, a longitudinal study of the activities of ATGL and HSL on a substantial number of animals could inform us on the regulation of lipolysis in weaned NES pups.

It would be important to pursue the histological investigations on a higher number of individuals to monitor the changes of adipocyte size and morphology with the progression of the fast. Also, expressing the levels of lipophilic pollutants and lipids per unit of cells (through DNA quantification after an adipocyte isolation) rather than per unit of lipid weight would allow to better understand the dynamics of cell emptying.

Since parameters cannot be managed with wild animals (e.g. their feeding and consequently, their levels of contamination of lipophilic pollutants), we can suggest to study the behaviour of lipophilic pollutants during periods of fast with rodent models of obesity. Indeed, the use of laboratory rodents for research is important due to their rapid and high reproductive rate, well-established breeding conditions and large availability

of molecular tools (Guerre-Millo, 2013). There are different types of rodent models of obesity such as diet-induced obesity, hypothalamic obesity and obesity induced by genetic manipulation (transgenic and knockout models). This kind of model could be used in kinetic studies in the whole animals and could contribute to enhance our knowledge in this field.

9.2.2. *In vitro* research

To better understand the mechanisms that govern the release of lipophilic pollutants, the *in vitro* model of lipolysis on differentiated rat adipocytes could be used for studies with different lipophilic pollutants such as other PCB congeners, PBDEs, DDT and HCB. In addition, the comparison of the dynamics of mobilisation using the lipolysis protocol with *vs.* without medium change every 3 hours would be interesting to investigate potential reuptake of pollutants by adipocytes, as suspected *in vivo*. In order to link the complexity of the *in vivo* model to the simplicity of the *in vitro* model, it could be planned to extract lipophilic pollutants from blubber samples of NES and add the mixture to differentiated rat adipocytes in order to study the mobilisation of lipophilic pollutants throughout an isoproterenol-induced lipolysis.

It would be interesting to enrich the differentiated rat adipocytes with a wide range of FAs exhibiting different degrees of lipophilicity in order to continue the investigations regarding the link between the mobilisations of FAs and POPs. Firstly, we could study the modifications of FA patterns throughout a 12-hour lipolysis in the cell TG fraction and the extracellular free FA fraction. Secondly, we could combine a FA modification with a contamination by lipophilic pollutants and thereby, investigate the impact of FA lipophilicity on the release of these different lipophilic pollutants by an *in vitro* approach.

As already mentioned in the previous chapter, the set-up of the primary culture of NES adipocytes is not completely achieved. Several additional tests can be suggested to improve the rate of adipocyte differentiation. During the isolation of cells from blubber biopsies, the population of cells

could be more heterogeneous than in the case of rodents. The progenitor cells, which are able to engage in the adipocyte pathway, could be in minority. Therefore, it should be interesting to sort the populations by the use of flow cytometry in order to isolate the adipocyte precursors and thus, to enhance the rate of differentiation. One of the main difficulties of the set-up of this *in vitro* model is the scarcity of the material. Indeed, we can sample weaned NES pups from early January to late April. The window of time is relatively narrow. It would thus be interesting to set up a protocol of cell freezing in order to have the opportunity to improve this cell model along the year. Similarly, we could carry out a step of cell multiplication before freezing as already undertaken in the culture of mouse embryonic fibroblasts and mesenchymal stem cells. During the culture of NES progenitor cells, the use of suckled NES serum could promote the adipocyte differentiation as well as lipid accumulation due to its high TG content. As already suggested in this work, the cocktail of differentiation usually used for the rodent culture should be improved to increase the rate of adipocyte differentiation. For example, we could try the adding of indomethacin that promotes adipogenesis by increasing C/EBPβ and PPARγ2 (Styner et al., 2010).

The next step will be to characterise this cell culture by different methods. Firstly, we could determine the population doubling time by drawing the growth curves through the measure of metabolic activity. We might assess the expression of selected adipocyte specific marker genes (e.g. PPAR-γ, C/EBPα, aP2, Glut-4, LPL, etc.) and markers of undifferentiated stem cells (e.g. preadipocyte factor-1 and metalloproteinase-1). The cell type identification may also be carried out through the use of immunohistochemistry tools as well as through the study of uptake of marked glucose and FAs. A quantitative assessment of the levels of lipid accumulation can be conducted by the extraction of lipids followed by the isolation of NL fraction (Schneider et al., 2012) throughout the adipocyte differentiation. Since the principal role of adipocytes is to store and release lipids, a lipolysis will be induced with 1 µM isoproterenol as used for the differentiated rat adipocytes. The TG content will be estimated as well as the amount of extracellular free FAs and glycerol. Eventually, the variability

of the differentiation rate between wells could be estimated. For that, the flow cytometry could be used to count cells. We would be able to see how much lipids accumulate since lipids should scatter light very differently. This method will allow us defining a population of cells with lipids as distinct from those without.

9.3. References

Arrebola, J. P., et al., 2012. Concentrations of organochlorine pesticides and polychlorinated biphenyls in human serum and adipose tissue from Bolivia. Environmental Research. 112, 40-47.

Bourez, S., et al., 2012a. Accumulation capacity of primary cultures of adipocytes for PCB-126: Influence of cell differentiation stage and triglyceride levels. Toxicology Letters. 214, 243-250.

Bourez, S., et al., 2012b. Accumulation of polychlorinated biphenyls in adipocytes: Selective targeting to lipid droplets and role of caveolin-1. PLoS ONE. 7, e31834.

Covaci, A., et al., 2011. Novel brominated flame retardants: a review of their analysis, environmental fate and behaviour. Environment International. 37, 532-556.

Crocker, D. E., et al., 2001. Maternal traits and reproductive effort in northern elephant seals. Ecology. 82, 3541-3555.

De Saeger, S., et al., 2005. Monitoring of polychlorinated biphenyls in Belgian human adipose tissue samples. Chemosphere. 58, 953-960.

Debier, C., et al., 2006. Mobilization of PCBs from blubber to blood in northern elephant seals (*Mirounga angustirostris*) during the post-weaning fast. Aquatic Toxicology. 80, 149-157.

Debier, C., et al., 2012. Differential changes of fat-soluble vitamins and pollutants during lactation in northern elephant seal mother–pup pairs. Comparative Biochemistry and Physiology Part A. 162, 323-330.

Fowler, M. A., et al., 2014. Fatty acid mobilization and comparison to milk fatty acid content in northern elephant seals. Journal of Comparative Physiology B. 184, 1-11.

Guerre-Millo, M., Animal models of obesity. In: Physiology and physiopathology of adipose tissue. J.-P. Bastard and B. Feve Eds., Springer-Verlag, France, 2013, 255-266.

Habran, S., et al., 2011. Blood dynamics of mercury and selenium in northern elephant seals during the lactation period. Environmental Pollution. 159, 2523-2529.

Lam, J. C., et al., 2009. Temporal trends of hexabromocyclododecanes (HBCDs) and polybrominated diphenyl ethers (PBDEs) and detection of two novel flame retardants in marine mammals from Hong Kong, South China. Environmental Science & Technology. 43**,** 6944-6949.

Law, R. J., et al., 2006. Levels of the flame retardants hexabromocyclododecane and tetrabromobisphenol A in the blubber of harbor porpoises (*Phocoena phocoena*) stranded or bycaught in the UK, with evidence for an increase in HBCD concentrations in recent years. Environmental Science & Technology. 40**,** 2177-2183.

Malarvannan, G., et al., 2013. Distribution of persistent organic pollutants in two different fat compartments from obese individuals. Environment International. 55**,** 33-42.

Moon, H. B., et al., 2012. Polybrominated diphenyl ethers, polychlorinated biphenyls, and organochlorine pesticides in adipose tissues of Korean women. Archives of Environmental Contamination and Toxicology. 62**,** 176-184.

Noren, D. P., et al., 2003. Energy reserve utilization in northern elephant seal (*Mirounga angustirostris*) pups during the postweaning fast: size does matter. Journal of Comparative Physiology B. 173**,** 443-454.

Nyman, M., et al., 2000. Expression and inducibility of members in the cytochrome P4501 (CYP1) family in ringed and grey seals from polluted and less polluted waters. Environmental Toxicology and Pharmacology. 8**,** 217-225.

Park, J.-S., et al., 2009. Polychlorinated biphenyls (PCBs) and their hydroxylated metabolites (OH-PCBs) in livers of harbor seals (*Phoca vitulina*) from San Francisco Bay, California and Gulf of Maine. Marine Environmental Research. 67**,** 129-135.

Raclot, T., 2003. Selective mobilization of fatty acids from adipose tissue triacylglycerols. Progress in Lipid Research. 42**,** 257-288.

Schneider, A.-C., et al., 2012. Conversion of t11t13 CLA into c9t11 CLA in caco-2 cells and inhibition by sterculic oil. PLoS ONE. 7**,** e32824.

Styner, M., et al., 2010. Indomethacin promotes adipogenesis of mesenchymal stem cells through a cyclooxygenase independent mechanism. Journal of Cellular Biochemistry. 111**,** 1042-1050.

Vanden Berghe, M., et al., 2012. Selective transfer of persistent organic pollutants and their metabolites in grey seals during lactation. Environment International. 46**,** 6-15.

Wang, N., et al., 2010. Levels of polychlorinated biphenyls in human adipose tissue samples from Southeast China. Environmental Science & Technology. 44, 4334-4340.

Wolkers, J., et al., 1998. Phase I and phase II enzyme activities in ringed seals (*Phoca hispida*): characterization of hepatic cytochrome P450 by activity patterns, inhibition studies, mRNA analyses, and western blotting. Aquatic Toxicology. 44, 103-115.

Zegers, B. N., et al., 2005. Levels of hexabromocyclododecane in harbor porpoises and common dolphins from western European seas, with evidence for stereoisomer-specific biotransformation by cytochrome P450. Environmental Science & Technology. 39, 2095-2100.